

Spring 2007

A Technique for Solving the Singular Integral Equations of Potential Theory

Brian George Burns
Old Dominion University

Follow this and additional works at: https://digitalcommons.odu.edu/mathstat_etds



Part of the [Mathematics Commons](#)

Recommended Citation

Burns, Brian G.. "A Technique for Solving the Singular Integral Equations of Potential Theory" (2007). Doctor of Philosophy (PhD), dissertation, Mathematics and Statistics, Old Dominion University, DOI: 10.25777/q9kv-0x34
https://digitalcommons.odu.edu/mathstat_etds/6

This Dissertation is brought to you for free and open access by the Mathematics & Statistics at ODU Digital Commons. It has been accepted for inclusion in Mathematics & Statistics Theses & Dissertations by an authorized administrator of ODU Digital Commons. For more information, please contact digitalcommons@odu.edu.

**A TECHNIQUE FOR SOLVING THE SINGULAR
INTEGRAL EQUATIONS OF POTENTIAL THEORY**

by

Brian George Burns
M.Sci. 1998, University of Glasgow
M.Sc. 1999, University of Stirling
M.S. 2005, Old Dominion University

A Dissertation Submitted to the Faculty of
Old Dominion University in Partial Fulfillment of the
Requirement for the Degree of

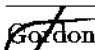
DOCTOR OF PHILOSOPHY

COMPUTATIONAL AND APPLIED MATHEMATICS

OLD DOMINION UNIVERSITY
May 2007

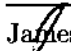
Approved by:

John Tweed (Director)

 Gordon Melrose

 John A. Adam

Richard D. Noren

 James L. Cox

ABSTRACT

A TECHNIQUE FOR SOLVING THE SINGULAR INTEGRAL EQUATIONS OF POTENTIAL THEORY

Brian George Burns

Old Dominion University, 2007

Director: Dr. John Tweed

The singular integral equations of Potential Theory are investigated using ideas from both classical and contemporary mathematics. The goal of this semi-analytic approach is to produce numerical schemes that are both general and computationally simple. Previous works based on classical methods have yielded solutions only for very special cases while contemporary methods such as finite differences, finite elements and boundary element techniques are computationally extensive. Since the two-dimensional integral equations of interest exhibit structural invariance under a wide class of conformal mappings initial emphasis is placed on circular domains. By Fourier expansion with respect to the angular variable, such two-dimensional integral equations yield simultaneous systems of one-dimensional integral equations that, in many cases, uncouple. Integral transform techniques and classical function theory are used to identify the eigenfunctions associated with the dominant parts of the one-dimensional singular equations. Hilbert spaces spanned by these eigenfunctions are then constructed and an operator theory developed for the general class of integral equations. Numerical algorithms are derived for both Galerkin and collocation solution techniques with convergence proved in the Galerkin case and collocation method verified experimentally. A generalization of the Hilbert space theory is then applied to the two-dimensional case with eigenfunctions created by combining the angular Fourier terms with the radial eigenfunctions of the dominant one-dimensional parts. Numerical algorithms based Galerkin and collocation methods are again derived and used to solve the two-dimensional equations. The techniques developed are used to solve a number of both previously known and new problems in Electrostatics and Fracture Mechanics. Simple layer potential representations yield weakly singular integral equations for the induced charge on disc shaped conductors that are placed in an electrostatic field. Similarly, double layer potentials yield hyper-singular integral equations for the crack opening displacement of penny shaped cracks in an elastic

solid under various loading conditions. Conformal mapping techniques for solving problems on non-circular domains are also briefly discussed as are extensions to fields that are governed by the Helmholtz Equation.

ACKNOWLEDGEMENTS

Thanks and appreciation go out to all of my committee members for being part of this project and taking the time to read this rather long and detailed document.

So appreciation and thanks to Professor James Cox of the Physics Department for being my external committee member. Thanks to Dr. Richard Noren for becoming the final department member. Thanks to Professor Adam for taking time from his busy schedule as a Virginian Outstanding Faculty to provide not only creditability to my thesis but also a significant source of humor. Thanks to Dr. Melrose for his service as a teacher, a supervisor and especially being the inspiration and encouragement behind my coming to the US and Old Dominion in particular. Special thanks go out to Professor Tweed who has been an inspirational advisor and mentor whose patience has held strong at all times despite being tested by my stubbornness and occasional lack of attention to detail. I could not have asked for any more in an advisor than what Professor Tweed provided.

I must also thank Professor Hideaki Kaneko and in particular Professor Mark Dorrepaal for their support in finishing my dissertation both financial and in their efforts freeing up my teaching commitments to facilitate my dissertation completion.

Special thanks too to Dr. Humberto Rocha for all his help and support both while a colleague at Old Dominion and since his return to Portugal. In particular his help with Latex and formatting was invaluable.

I would also like to thank my family for all their moral and occasional financial support through my hardships as a graduate student.

TABLE OF CONTENTS

	Page
List of Tables	ix
List of Figures	xii
 CHAPTERS	
I Introduction	1
II Preliminary Results	6
II.1 Weber-Schafheitlin Integrals	6
II.2 Layer Potential Solutions to Laplacian Boundary Value Problems	11
II.2.1 The Three-Dimensional Green's Functions	12
II.2.2 The Single Layer Potential Operator	12
II.2.3 The Double Layer Potential Operator	14
II.2.4 The Dirichlet Problem	15
II.2.5 The Neumann Problem	16
III Hilbert Spaces I	18
III.1 Introduction	18
III.2 The Hilbert Spaces $L_2^\alpha(0, 1)$	18
III.3 Operators on the $L_2^\alpha(0, 1)$ Hilbert Spaces	23
III.3.1 The L_m^α Operators	24
III.3.2 The Differential (\mathbb{D}_m) and the Hyper-Singular ($\mathbb{D}_m L_m^1$) Operators	37
III.4 The $L_{2,m}^\alpha(0, 1)$ Hilbert Spaces	40
IV A Weakly-Singular Integral Equation	49
IV.1 Introduction	49
IV.2 The Dominant Weakly-Singular Equation	49
IV.3 The General Equation	50
IV.4 Numerical Solutions	58
IV.4.1 Quadrature	58
IV.4.2 The Galerkin Method	59
IV.4.3 The Collocation Method	60
IV.4.4 Numerical Tests	61
V A Hyper-Singular Integral Equation	63
V.1 Introduction	63
V.2 The Dominant Hyper-Singular Equation	63
V.3 The General Hyper-Singular Equation	64
V.4 Numerical Solutions	68
V.4.1 Quadrature	68
V.4.2 The Galerkin Method	69
V.4.3 Collocation	70
V.4.4 Numerical tests	70
VI Hilbert Spaces II	74

VI.1	Introduction	74
VI.2	The $L_2^\alpha(\Omega)$ Hilbert Spaces	74
VI.3	Operators on $L_2^\alpha(\Omega)$	77
VI.4	The $L_{2,\omega}^\alpha(\Omega)$ Hilbert Space	85
VII	A 2-D Weakly-Singular Integral Equation	92
VII.1	Introduction	92
VII.2	The Dominant Weakly Singular Equation	93
VII.3	The General Equation	93
VII.4	Numerical Solutions	98
VII.4.1	Quadrature	98
VII.4.2	The Galerkin Method	99
VII.4.3	The Collocation Method	100
VII.4.4	Numerical Tests	100
VIII	A 2-D Hyper-Singular Integral Equation	104
VIII.1	Introduction	104
VIII.2	The Dominant Hyper-Singular Equation	105
VIII.3	The General Equation	105
VIII.4	Numerical Solutions	110
VIII.4.1	Quadrature	110
VIII.4.2	The Galerkin Method	110
VIII.4.3	The Collocation Method	111
VIII.4.4	Numerical Tests	112
IX	Applications I: Problems in Potential Theory	118
IX.1	Introduction	118
IX.2	Single Disc Problems	119
IX.2.1	General Problem	119
IX.2.2	Case 1: Circular Disc Charged to a Constant Potential	120
IX.2.3	Case 2: Earthed Circular Disc in a Parallel Field	123
IX.2.4	Case 3: Earthed Circular Disc in the Field Generated by a Point Charge	125
IX.3	Multiple Disc Problems	131
IX.3.1	The Parallel Plate Condenser	131
X	Applications II: 3-D crack problems	143
X.1	Introduction	143
X.2	Single Crack Problems	144
X.2.1	A General Problem	144
X.2.2	Case 1: Constant Pressure	148
X.2.3	Case 2: Bending Load	148
X.2.4	Case 3: Equal and Opposite Point Forces	151
X.3	Multiple Crack Problems	161
X.3.1	General Problem	161
X.3.2	Case 1: Constant Pressure	164
X.3.3	Case 2: Bending Load	166
X.3.4	Case 3: Equal and Opposite Point Forces	171

XI	Summary and Future Work	186
XI.1	Summary	186
XI.2	Extension of Laplacian Based Boundary Value Problems	187
XI.2.1	Conformal Mapping of Boussinesq's Equation	187
XI.3	Extensions to the Helmholtz Equation and Acoustics	192
	REFERENCES	193
	VITA	197

LIST OF TABLES

	Page	
1	Comparison of Galerkin and collocation results for one-dimensional hyper-singular test problem. Results shown for $p=5$, $m=3$. with the number of terms and number of collocation points both 20, with 30 quadrature points.	73
2	Comparison of results for two-dimensional hyper-singular test problem. Results are shown for the number of terms and the number of collocation points 6 for both variables, with 30 quadrature points for each variable.	117
3	Comparison of Capacitance ($C_{Sneddon}$) results for a pair of parallel plates charged to equal or opposite potentials. Source ([2],p238). . . .	135
4	The Capacitance ($C_{Sneddon}$) as the distance between two equally charged parallel discs tends towards zero can be seen to approach 0.5. Results from collocation method. Note numerical singularities appear for smaller kappa values.	136
5	The Capacitance ($C_{Sneddon}$) as the distance between two oppositely charged parallel discs tends towards infinity can be seen to approach 1. Results here are obtained from using the collocation method. . . .	137
6	Capacitance ($C_{Sneddon}$) for offset discs equally charged to a constant potential, centered at $(a,0,h)$ and $(-a,0,-h)$. Results from collocation method.	140
7	Capacitance ($C_{Sneddon}$) for offset discs equally charged to a constant potential, centered at $(a,0,h)$ and $(-a,0,-h)$. Results from Galerkin method.	141
8	Capacitance results, $C_{Sneddon}$, for offset discs oppositely charged to a constant potential, centered at $(a,0,h)$ and $(-a,0,-h)$. Results from collocation method.	142
9	A special case of the Papkovitch-Neuber solution in Cartesian Coordinates.	144
10	A special case of the Papkovitch-Neuber solution in Cylindrical Coordinates.	144

LIST OF FIGURES

	Page
1	Outline of methodology. 3
2	Some plots of the scaled charge density (σ/ϵ_0) on a lamina disc held to different F potentials. 122
3	The scaled charge density (σ/ϵ_0) on an insulated laminar disc in a parallel field of magnitude 1 oriented in the direction of the x-axis. . . 124
4	The charge density on an insulated laminar disc plotted against the radius of the disc, when a point charge of charge 5 coulombs is placed directly above at varying heights, b, above the disc. 127
5	The charge density on an insulated laminar disc when a point charge of charge 10 coulombs is placed directly above at varying heights, b, above the disc. 128
6	The charge density on an insulated laminar disc when a point charge 5 coulombs is placed in the same plane. 129
7	The charge density on an insulated laminar disc when a point charge of charge 5 coulombs is placed at varying positions. 130
8	A penny shaped crack of radius a , centered at $(0, 0, 0)$ and opened by a bending force about the line $x = b' > a$. Plots show how the scaled stress intensity factor varies with θ for several values of $b = b'/a$ 150
9	A penny shaped crack of radius a , centered at $(0, 0, 0)$ and opened by point forces $\pm P\mathbf{k}$ centered above and below the cracks at $(0, 0, \pm h')$. Plots show how the scaled stress intensity factor varies with $h = h'/a$ for several values of ν 154
10	A penny shaped crack of radius a , centered at $(0, 0, 0)$ and opened by point forces $\pm P\mathbf{k}$ at $(b, 0, \pm h')$. Plots show how the scaled stress intensity factor varies with θ for different values of $\beta = b/a$ for several values of ν with $\gamma = h/a = 1$ 157
11	A penny shaped crack of radius a , centered at $(0, 0, 0)$ and opened by point forces $\pm P\mathbf{k}$ at $(b, 0, \pm h')$. Plots show how the scaled stress intensity factor varies with θ for different small values of $\gamma = h/a$ for $\nu = 0.4$ and $\beta = b/a = 2$ 158
12	A penny shaped crack of radius a , centered at $(0, 0, 0)$ and opened by point forces $\pm P\mathbf{k}$ at $(b, 0, \pm h')$. Plots show how the scaled stress intensity factor varies with θ for different medium to large values of $\gamma = h/a$ for $\nu = 0.4$ and $\beta = b/a = 2$ 159
13	A penny shaped crack of radius a , centered at $(0, 0, 0)$ and opened by point forces $\pm P\mathbf{k}$ at $(b, 0, \pm h')$. Plot shows how the scaled maximum stress intensity factor varies with $\gamma = h/a$ and $\beta = b/a$ for $\nu = 0.4$. . . 160
14	A penny shaped crack of radius a , centered at $(0, 0, 0)$ and opened by point forces $\pm P\mathbf{k}$ at $(b, 0, \pm h')$. Contour plot shows how the scaled maximum stress intensity factor varies with $\gamma = h/a$ and $\beta = b/a$ for $\nu = 0.4$ 161

15	Coplanar penny shaped cracks of radius a , centered at $(\pm c', 0, 0)$ and opened by a constant pressure load. Plots show how the scaled stress intensity factor varies with θ for several values of $c = c'/a$	165
16	Coplanar penny shaped cracks of radius a , centered at $(\pm c', 0, 0)$ and opened by a bending force about the line $y = b'$. Plots show how the scaled stress intensity factor varies with θ for $c = c'/a = 1.4$ and several values of $b = b'/a$	168
17	Coplanar penny shaped cracks of radius a , centered at $(\pm c', 0, 0)$ and opened by a bending force about the line $y = b'$. Plots show how the scaled stress intensity factor varies with θ for $b = b'/a = 2.4$ and several values of $c = c'/a$	169
18	Coplanar penny shaped cracks of radius a , centered at $(\pm c', 0, 0)$ and opened by a bending force about the line $y = b'$. Plots show how the alternatively scaled stress intensity factor varies with θ for several values of $c = c'/a$ and $b = b'/a$	170
19	Coplanar penny shaped cracks of radius a , centered at $(\pm c', 0, 0)$ and opened by a bending force about the line $y = b'$. Plots show how the scaled maximum stress intensity factor varies with $c = c'/a$ for several values of $b = b'/a$	171
20	Coplanar penny shaped cracks of radius a , centered at $(\pm c', 0, 0)$ and opened by a bending force about the line $y = b'$. Contour plot show how the scaled maximum stress intensity factor varies with $c = c'/a$ and $b = b'/a$	172
21	Coplanar penny shaped cracks of radius a , centered at $(\pm c', 0, 0)$ and opened by point forces $\pm P\mathbf{k}$ at $(0, 0, \pm h')$. Plots show how the scaled stress intensity factor varies with θ for several values of $c = c'/a$ and $h = h'/a = 0.5$ when $\nu = 0.4$	175
22	Coplanar penny shaped cracks of radius a , centered at $(\pm c', 0, 0)$ and opened by point forces $\pm P\mathbf{k}$ at $(0, 0, \pm h')$. Plots show how the scaled stress intensity factor varies with θ for several small values of $h = h'/a$ and $c = c'/a = 1.5$ when $\nu = 0.4$	176
23	Coplanar penny shaped cracks of radius a , centered at $(\pm c', 0, 0)$ and opened by point forces $\pm P\mathbf{k}$ at $(0, 0, \pm h')$. Plots show how the scaled stress intensity factor varies with θ for several medium to large values of $h = h'/a$ and $c = c'/a = 1.5$ when $\nu = 0.4$	177
24	Coplanar penny shaped cracks of radius a , centered at $(\pm c', 0, 0)$ and opened by point forces $\pm P\mathbf{k}$ at $(0, 0, \pm h')$. Plots show how the scaled maximum stress intensity factor varies with $h = h'/a$ for several values of $c = c'/a$ when $\nu = 0.4$	178
25	Coplanar penny shaped cracks of radius a , centered at $(\pm c', 0, 0)$ and opened by point forces $\pm P\mathbf{k}$ at $(0, 0, \pm h')$. Contour plot shows how the scaled maximum stress intensity factor varies with $h = h'/a$ and $c = c'/a$ when $\nu = 0.4$	179

- 26 Coplanar penny shaped cracks of radius a , centered at $(\pm c', 0, 0)$ and opened by point forces $\pm P\mathbf{k}$ centered above and below the cracks at $(\pm c', 0, \pm h')$. Plots show how the scaled stress intensity factor varies with θ for $h = h'/a = 0.5$, $\nu = 0.4$ and several values of $c = c'/a$ 182
- 27 Coplanar penny shaped cracks of radius a , centered at $(\pm c', 0, 0)$ and opened by point forces $\pm P\mathbf{k}$ centered above and below the cracks at $(\pm c', 0, \pm h')$. Plots show how the scaled stress intensity factor varies with θ for $c = c'/a = 1.2$, $\nu = 0.4$ and several values of $h = h'/a$ 183
- 28 Coplanar penny shaped cracks of radius a , centered at $(\pm c', 0, 0)$ and opened by point forces $\pm P\mathbf{k}$ centered above and below the cracks at $(\pm c', 0, \pm h')$. Plots show how the scaled maximum stress intensity factor (for $\nu = 0.4$) varies with $h = h'/a$ for several values of $c = c'/a$. 184
- 29 Coplanar penny shaped cracks of radius a , centered at $(\pm c', 0, 0)$ and opened by point forces $\pm P\mathbf{k}$ centered above and below the cracks at $(\pm c', 0, \pm h')$. Contour plot show how the scaled maximum stress intensity factor (for $\nu = 0.4$) varies with both $h = h'/a$ and $c = c'/a$. . 185

CHAPTER I

INTRODUCTION

The objective of the research upon which this thesis is based is to solve the two types of Boundary Integral Equations shown in (I.1) and (I.2). (I.1) is weakly singular in nature, as a result of its dominant kernel $\frac{1}{|\vec{r}-\vec{\rho}|}$, while (I.2) is hyper-singular as a result of applying the Laplacian operator giving a Hadamard type singularity.

$$\frac{1}{4\pi} \int \int_{\Omega} \left\{ \frac{1}{|\vec{r}-\vec{\rho}|} + R(\vec{r}, \vec{\rho}) \right\} f(\vec{\rho}) dA(\vec{\rho}) = g(\vec{r}), \vec{r} \in \Omega \subset \mathbb{R}^2 \quad (\text{I.1})$$

$$(-\Delta_2 + \kappa) \frac{1}{4\pi} \int \int_{\Omega} \left\{ \frac{1}{|\vec{r}-\vec{\rho}|} + R(\vec{r}, \vec{\rho}) \right\} f(\vec{\rho}) dA(\vec{\rho}) = g(\vec{r}), \vec{r} \in \Omega \subset \mathbb{R}^2 \quad (\text{I.2})$$

where κ is a constant possibly zero.

Both of these equations arise from boundary value problems that model a broad range of physical problems, particularly those in or relating to potential theory. The ultimate objective is to be able to solve equations (I.1) and (I.2) for all reasonable domains $\Omega \subset \mathbb{R}^2$. The work outlined in this thesis is however almost entirely focused on domains that are circular in nature, although Chapter XI outlines future work involving conformal mappings that is geared towards dealing with the more general case. The Integral Equations, shown in (I.3) and (I.4), are those we will focus upon.

$$\int_0^1 \int_{-\pi}^{\pi} \left\{ \frac{1}{4\pi \sqrt{\rho^2 + r^2 - 2r\rho \cos(\theta - \vartheta)}} + R(\rho, \vartheta; r, \theta) \right\} f(\rho, \vartheta) w^0(\rho) d\vartheta d\rho = g(r, \theta) \quad (\text{I.3})$$

$$(-\Delta_2 + \kappa) \int_0^1 \int_{-\pi}^{\pi} \left\{ \frac{1}{4\pi \sqrt{\rho^2 + r^2 - 2r\rho \cos(\theta - \vartheta)}} + R(\rho, \vartheta; r, \theta) \right\} f(\rho, \vartheta) w^1(\rho) d\vartheta d\rho = g(r, \theta) \quad (\text{I.4})$$

$0 < r < 1$, $-\pi < \theta < \pi$, where $w^\alpha(\rho)$ are weight functions, κ a constant possibly zero, $R(\rho, \vartheta; r, \theta)$ a suitably continuous kernel and $g(r, \theta)$ a suitably smooth function.

By Fourier expansion with respect to the angular variable each of these equations

⁰This dissertation follows the style of *The Siam Journal on Optimization*

yields a simultaneous system of one dimensional integral equations. In many cases these systems uncouple to produce a weakly singular equation of the type (I.5) or a hyper-singular equation of the type (I.6) where the Hadamard singularity $\mathbb{D}_m l_m(\rho, r)$ must be considered in the proper way.

$$\int_0^1 \{l_m(\rho, r) + k(\rho, r)\} w^0(\rho) f(\rho) d\rho = g(r), 0 < r < 1 \quad (\text{I.5})$$

$$\int_0^1 \{\mathbb{D}_m l_m(\rho, r) + \kappa l_m(\rho, r) + k(\rho, r)\} w^1(\rho) f(\rho) d\rho = g(r), 0 < r < 1 \quad (\text{I.6})$$

where $m = 0, 1, 2, \dots, \kappa$, a constant possibly zero, $k(\rho, r)$ a suitably continuous kernel, $g(r)$ a suitably smooth function and \mathbb{D}_m a second order differential operator.

In each case the dominant term is derived from the weakly singular kernel

$$l_m(\rho, r) = \frac{1}{2\pi\sqrt{\rho r}} Q_{m-\frac{1}{2}} \left[\frac{\rho^2 + r^2}{2\rho r} \right], \text{ for } m = 0, 1, 2, 3, \dots \quad (\text{I.7})$$

which is defined in terms of the ring function $\{Q_{m-\frac{1}{2}}(x)\}$ or the Legendre function of the second kind (e.g. [1], section 32).

Eigenfunctions associated with the dominant parts of (I.5) and (I.6) form complete orthogonal sets that facilitate the solution of these equations and their two-dimensional counterparts (I.3) and (I.4).

The different stages involved in the processes of modeling and solving the types of physical problems that we are concerned with are outlined in Figure 1.

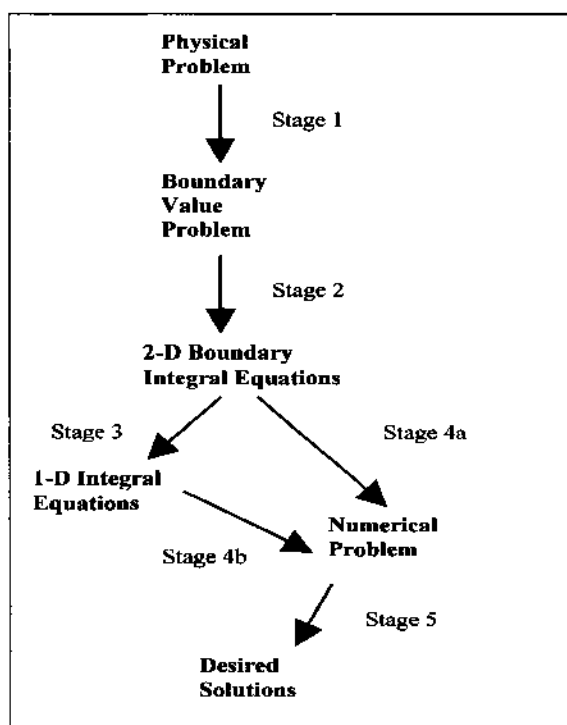


FIG. 1. *Outline of methodology.*

Stages 1 and 2 of Figure 1 are already well established but solutions to the weakly singular and especially the hyper-singular integral equations have been historically hard to find. Some particular solutions have been found for specific problems (such as those given in the Sneddon books [2, 3]) but they are generally very specific and complicated. More recently a variety of alternate methods have been employed including finite differences, finite elements and boundary element techniques all of which are computationally extensive. The approach taken here is semi-analytic and although closer in spirit to the works referenced in Sneddon [2, 3] it does produce numerical solution techniques.

Preliminary results outlined in Chapter II establish the notation to be used and introduce concepts and ideas that are needed for a proper understanding of subsequent materials.

Chapter III introduces the Hilbert spaces spanned by the eigenfunctions of the dominant integral equations associated with (I.5) and (I.6). The eigen-structure of the corresponding operators is examined in detail and the tools needed to solve (I.5) and (I.6) as operator equations in Hilbert space are developed.

In Chapters IV and V the one dimensional weakly singular (Chapter IV) and hyper-singular (Chapter V) integral equations are solved as operator equations in Hilbert Space. As well as finding solutions that exist (given set conditions) numerical algorithms are developed for both Galerkin and collocation methods. These algorithms are tested in Fortran with artificially constructed problems. In terms of Figure 1, this is considered to cover stages 4b to 5.

Attention is then focused on the two-dimensional integral equations via both Stages 3 to 4b and directly via Stage 4a of Figure 1. We are able to use the theory from the one dimensional problems to generalize and produce eigenvalues and eigenvectors for the two-dimensional dominant operators and again construct Hilbert spaces spanned by the eigenfunctions. Chapter VI builds on Chapter III and develops the Hilbert space theory required to solve the two-dimensional integral equations as operator equations in Hilbert space. Chapter VII builds on Chapter IV while Chapter VIII builds on Chapter V, solving the two-dimensional integral equations and hence dealing with Stages 3, 4 and 5 of Figure 1.

In Chapters IX and X we look at specific applications illustrating the procedures in every stage of Figure 1. Firstly in Chapter IX we look at certain Electrostatic problems using Potential Theory. Using tools developed in Chapter II, we can model the effects of placing charged discs in electrostatic fields as Boundary Value Problems (Stage 1 of Figure 1) and hence as two-dimensional weakly singular integral equations (Stage 2 of Figure 1). By looking at a variety of problems we can obtain solutions via both Stages 3 and 4b or directly via Stage 4a (of Figure 1) to get the final solution in Stage 5. We first look at simple problems with a known final solution to confirm that the solutions obtained via our method are accurate. More complicated problems with less readily known or unknown solutions are then considered to illustrate the capabilities of the method.

Some Crack Problems in Elasticity are examined in Chapter X. Using the tools developed in Chapter II we can model the stress effects of external forces on cracks as Boundary Value Problems (Stage 1 of Figure 1) and hence this time as two-dimensional hyper-singular integral equations (Stage 2 of Figure 1). We again look at a variety of problems both known and unknown, solved in various ways, to illustrate the capabilities of the methods.

In Chapter XI we summarize what has been achieved and examine possible advances and further applications for the future. Both direct continuation of the work and different directions are discussed. Two main themes are highlighted. The first being the use of conformal mappings to expand the scope of the Boundary Value Problems that can be solved. The second being an expansion on the type of Boundary Value Problems and hence Boundary Integral Equations considered.

CHAPTER II

PRELIMINARY RESULTS

II.1 WEBER-SCHAFHEITLIN INTEGRALS

The Weber-Schafheitlin Integral

$$\int_0^{\infty} t^{-\lambda} J_{\mu}(at) J_{\nu}(bt) dt, \quad a > 0, b > 0 \quad (\text{II.1})$$

is convergent if $\text{Re}(\mu + \nu + 1) > \text{Re}(\lambda) > -1$ and $a \neq b$, or if $\text{Re}(\mu + \nu + 1) > \text{Re}(\lambda) > 0$ and $a = b$.

It is discussed in great detail by Watson [4] who investigates many cases. The case of interest to us is that of Sonine and Schafheitlin which, as shown by Sneddon [2], may be expressed in the following convenient form;

The integral

$$\int_0^{\infty} t^{\alpha + \beta - \gamma} J_{\alpha - \beta}(at) J_{\gamma - 1}(bt) dt \quad (\text{II.2})$$

takes the value

$$\frac{b^{\gamma - 1} \Gamma(\alpha)}{2^{\gamma - \alpha - \beta} a^{\alpha + \beta} \Gamma(\gamma) \Gamma(1 - \beta)} {}_2F_1\left(\alpha, \beta; \gamma; \frac{b^2}{a^2}\right) \quad \text{if } 0 < b < a \quad (\text{II.3})$$

and the value

$$\frac{a^{\alpha - \beta} \Gamma(\alpha)}{2^{\gamma - \alpha - \beta} b^{2\alpha - \gamma + 1} \Gamma(\gamma - \alpha) \Gamma(\alpha - \beta + 1)} {}_2F_1\left(\alpha, \alpha - \gamma + 1; \alpha - \beta + 1; \frac{a^2}{b^2}\right) \quad (\text{II.4})$$

if $0 < a < b$.

The case $a = b$ is not covered by this result and needs to be derived independently if wanted.

Several special cases of the Sonine-Schafheitlin result will prove to be useful in our subsequent analysis. Before exhibiting these however, we will find it convenient to introduce the functions $t_n^m(\rho)$ and $u_n^m(\rho)$ which are defined for $0 \leq \rho \leq 1$ and $m, n = 0, 1, 2, \dots$. These functions are expressed in terms of the Associated Legendre

Polynomials $P_n^m(x)$ and will form orthonormal bases for the Hilbert spaces in which our analysis will be carried out.

Definition II.1

$$t_n^m(\rho) = T_n^m P_{2n+m}^m(\sqrt{1-\rho^2}), 0 \leq \rho \leq 1 \quad (\text{II.5})$$

$$u_n^m(\rho) = U_n^m \frac{P_{2n+m+1}^m(\sqrt{1-\rho^2})}{\sqrt{1-\rho^2}}, 0 \leq \rho \leq 1 \quad (\text{II.6})$$

where

$$T_n^m = \sqrt{\frac{(4n+2m+1)(2n)!}{(2n+2m)!}} \quad (\text{II.7})$$

$$U_n^m = \sqrt{\frac{(4n+2m+3)(2n+1)!}{(2n+2m+1)!}} \quad (\text{II.8})$$

and $m, n = 0, 1, 2, \dots$

Theorem II.2 $\int_0^\infty t^{1-k} J_{m+2n+k}(t) J_m(\rho t) dt =$

$$\frac{\Gamma(m+n+1) H(1-\rho^2) \rho^m (1-\rho^2)^{k-1}}{2^{k-1} \Gamma(m+1) \Gamma(n+k)} {}_2F_1(-n, m+n+k; m+1; \rho^2) \quad (\text{II.9})$$

where $k > 0; \rho > 0; m, n = 0, 1, 2, \dots$ and $H(x)$ is the Heaviside function.

Proof. Let $\alpha = m+n+1, \beta = 1-k-n, \gamma = m+1, a = 1$ and $b = \rho$ in (II.3) and (II.4). Then, if $0 < \rho < 1$, (II.3) yields

$$\begin{aligned} & \int_0^\infty t^{1-k} J_{m+2n+k}(t) J_m(\rho t) dt \\ &= \frac{\Gamma(m+n+1) \rho^m}{2^{k-1} \Gamma(m+1) \Gamma(n+k)} {}_2F_1(m+n+1, 1-k-n; m+1; \rho^2) \\ &= \frac{\Gamma(m+n+1) \rho^m (1-\rho^2)^{k-1}}{2^{k-1} \Gamma(m+1) \Gamma(n+k)} {}_2F_1(-n, m+n+k; m+1; \rho^2) \end{aligned}$$

where we have made use of the linear hypergeometric Transformation (15.3.3 of [5])

$${}_2F_1(a, b; c; z) = (1-z)^{c-a-b} {}_2F_1(c-a, c-b; c; z) \quad (\text{II.10})$$

Additionally, $\frac{1}{\Gamma(\gamma-\alpha)} = \frac{1}{\Gamma(-n)} = 0$ and hence from (II.4) we can see the integral is zero when $\rho > 1$. ■

Corollary II.3

$$\int_0^\infty t^{\frac{1}{2}} J_{m+2n+\frac{1}{2}}(t) J_m(\rho t) dt = A_{mn} \frac{H(1-\rho^2)}{\sqrt{1-\rho^2}} t_n^m(\rho) \quad (\text{II.11})$$

where

$$A_{mn} = \frac{(-1)^m (m+n)! n! 2^{2n+m+\frac{1}{2}}}{\sqrt{\pi} (2m+2n)! (2n)! (4n+2m+1)} \quad (\text{II.12})$$

Proof. Putting $k = \frac{1}{2}$ in (II.9) yields

$$\begin{aligned} & \int_0^\infty t^{\frac{1}{2}} J_{m+2n+\frac{1}{2}}(t) J_m(\rho t) dt \\ &= \frac{\sqrt{2} (m+n)! H(1-\rho^2) \rho^m}{m! \Gamma(n+\frac{1}{2}) \sqrt{1-\rho^2}} {}_2F_1\left(-n, m+n+\frac{1}{2}; m+1; \rho^2\right) \\ &= \frac{(-1)^m \sqrt{2} (m+n)! 2^{2n} n! 2^m m! (2n)! H(1-\rho^2) \rho^m}{m! \sqrt{\pi} (2n)! (2m+2n)! \rho^m} \frac{P_{2n+m}^m(\sqrt{1-\rho^2})}{\sqrt{1-\rho^2}} \\ &= \frac{(-1)^m (m+n)! n! 2^{2n+m+\frac{1}{2}} H(1-\rho^2)}{\sqrt{\pi} (2n+2m)!} \frac{P_{2n+m}^m(\sqrt{1-\rho^2})}{\sqrt{1-\rho^2}} \\ &= \frac{(-1)^m (m+n)! n! 2^{2n+m+\frac{1}{2}}}{\sqrt{\pi} (2m+2n)! (2n)! (4n+2m+1)} \frac{H(1-\rho^2)}{\sqrt{1-\rho^2}} t_n^m(\rho) \end{aligned}$$

where we have utilized the result (15.4.13 of [5]);

for $0 < x < 1$

$${}_2F_1\left(b, a; a+b+\frac{1}{2}; x\right) = 2^{a+b-\frac{1}{2}} \Gamma\left(a+b+\frac{1}{2}\right) x^{\frac{1}{2}(\frac{1}{2}-a-b)} P_{a-b-\frac{1}{2}}^{\frac{1}{2}-a-b}(\sqrt{1-x}) \quad (\text{II.13})$$

and the relationship ([1], Sect. 60, 23)

$$P_n^{-m}(x) = (-1)^m \frac{(n-m)!}{(n+m)!} P_n^m(x) \quad \blacksquare \quad (\text{II.14})$$

Corollary II.4 For $\rho > 0$,

$$\int_0^\infty t^{-\frac{1}{2}} J_{m+2n+\frac{3}{2}}(t) J_m(\rho t) dt = B_{mn} H(1-\rho^2) \sqrt{1-\rho^2} u_n^m(\rho) \quad (\text{II.15})$$

where

$$B_{mn} = \frac{(-1)^m (m+n)! n! 2^{2n+m+\frac{1}{2}}}{\sqrt{\pi} (2m+2n+1)! (2n+1)! (4n+2m+3)} \quad (\text{II.16})$$

Proof. Putting $k = \frac{3}{2}$ in (II.9) yields

$$\begin{aligned} & \int_0^\infty t^{-\frac{1}{2}} J_{m+2n+\frac{3}{2}}(t) J_m(\rho t) dt \\ &= \frac{(m+n)! H(1-\rho^2) \rho^m \sqrt{1-\rho^2}}{\sqrt{2} m! (n+\frac{1}{2}) \Gamma(n+\frac{1}{2})} {}_2F_1\left(-n, m+n+\frac{3}{2}; m+1; \rho^2\right) \\ &= \frac{(-1)^m (m+n)! n! 2^{2n+m+\frac{1}{2}}}{\sqrt{\pi} (2n+2m+1)} H(1-\rho^2) \sqrt{1-\rho^2} P_{2n+m+1}^m(\sqrt{1-\rho^2}) \\ &= \frac{(-1)^m (m+n)! n! 2^{2n+m+\frac{1}{2}}}{\sqrt{\pi} (2m+2n+1)! (2n+1)! (4n+2m+3)} H(1-\rho^2) \sqrt{1-\rho^2} u_n^m(\rho) \end{aligned}$$

where we have made use of the result (15.4.21 of [5]);

for $0 < x < 1$

$${}_2F_1\left(b, a; a+b-\frac{1}{2}; x\right) = 2^{a+b-\frac{3}{2}} \Gamma\left(a+b-\frac{1}{2}\right) \frac{x^{\frac{1}{2}(\frac{3}{2}-a-b)} P_{a-b-\frac{1}{2}}^{\frac{3}{2}-a-b}(\sqrt{1-x})}{\sqrt{1-x}} \quad (\text{II.17})$$

together with (II.14) ■

Theorem II.5 $\int_0^\infty t^{k-1} J_{m+2n+k}(t) J_m(\rho t) dt =$

$$\frac{\Gamma(m+n+k) \rho^m}{2^{1-k} \Gamma(m+1) \Gamma(n+1)} {}_2F_1(-n, m+n+k; m+1; \rho^2) \quad (\text{II.18})$$

$0 < k, 0 < \rho < 1, m, n = 0, 1, 2, \dots$

Proof. Set $\alpha = m+n+k, \beta = -n, \gamma = m+1, a = 1$ and $b = \rho$ in (II.4), then for $0 < \rho < 1$

$$\begin{aligned} & \int_0^\infty t^{k-1} J_{m+2n+k}(t) J_m(\rho t) dt \\ &= \frac{\Gamma(m+n+1) \rho^m}{2^{1-k} \Gamma(m+1) \Gamma(n+k)} {}_2F_1(m+n+k, -n; m+1; \rho^2) \\ &= \frac{\Gamma(m+n+k) \rho^m}{2^{1-k} \Gamma(m+1) \Gamma(n+1)} {}_2F_1(-n, m+n+k; m+1; \rho^2) \end{aligned}$$

where we have again made use of the hypergeometric transformation (II.10) ■

Corollary II.6 For $0 < \rho < 1$,

$$\int_0^{\infty} t^{-\frac{1}{2}} J_{m+2n+\frac{1}{2}}(t) J_m(\rho t) dt = C_{mn} t_n^m(\rho), \quad (\text{II.19})$$

where

$$C_{mn} = \frac{(-1)^m}{2^{2n+m+\frac{1}{2}} (m+n)!n!} \sqrt{\frac{\pi (2m+2n)! (2n)!}{(4n+2m+1)}} \quad (\text{II.20})$$

Proof. Put $k = \frac{1}{2}$ in (II.18), then for $0 < \rho < 1$

$$\begin{aligned} & \int_0^{\infty} t^{-\frac{1}{2}} J_{m+2n+\frac{1}{2}}(t) J_m(\rho t) dt \\ &= \frac{\Gamma(m+n+\frac{1}{2}) \rho^m}{\sqrt{2}m!n!} {}_2F_1\left(-n, m+n+\frac{1}{2}; m+1; \rho^2\right) \\ &= (-1)^m \sqrt{\frac{\pi}{2}} \frac{(2n)!}{2^{2n+m} (m+n)!n!} P_{2n+m}^m(\sqrt{1-\rho^2}) \\ & \quad \text{using (II.13) and (II.14)} \\ &= \frac{(-1)^m}{2^{2n+m+\frac{1}{2}} (m+n)!n!} \sqrt{\frac{\pi (2m+2n)! (2n)!}{(4n+2m+1)}} t_n^m(\rho) \blacksquare \end{aligned}$$

Corollary II.7 For $0 < \rho < 1$,

$$\int_0^{\infty} t^{\frac{1}{2}} J_{m+2n+\frac{3}{2}}(t) J_m(\rho t) dt = D_{mn} u_n^m(\rho) \quad (\text{II.21})$$

where

$$D_{mn} = \frac{(-1)^m}{2^{2n+m+1} n! (m+n)!} \sqrt{\frac{\pi (2n+1)! (2n+2m+1)!}{4n+2m+3}} \quad (\text{II.22})$$

Proof. Put $k = \frac{3}{2}$ into (II.18) then

$$\begin{aligned}
& \int_0^\infty t^{\frac{1}{2}} J_{m+2n+\frac{3}{2}}(t) J_m(\rho t) dt \\
&= \frac{\sqrt{2} (m+n+\frac{1}{2}) \Gamma(m+n+\frac{1}{2}) \rho^m}{m!n!} {}_2F_1\left(-n, m+n+\frac{3}{2}; m+1; \rho^2\right) \\
&= \frac{\sqrt{2\pi} (m+n+\frac{1}{2}) (2m+2n)! \rho^m (-1)^m 2^m m!}{2^{2n+2m} m!n! (m+n)! (2m+2n+1)! \sqrt{1-\rho^2} \rho^m} (2n+1)! P_{2n+2m+1}^m(\sqrt{1-\rho^2}) \\
&\quad \text{using (II.17) and (II.14)} \\
&= \frac{(-1)^m}{2^{2n+m+1} n! (m+n)!} \sqrt{\frac{\pi (2n+1)! (2n+2m+1)!}{4n+2m+3}} u_n^m(\rho) \\
&\quad \text{using (II.6), (II.8) } \blacksquare
\end{aligned}$$

II.2 LAYER POTENTIAL SOLUTIONS TO LAPLACIAN BOUNDARY VALUE PROBLEMS

Integral equations provide us with a useful formulation of the boundary value problems of potential theory. Such equations are often derived from the representation of harmonic functions by single or double surface layer potentials. The surface in question is usually the boundary of the domain in which the problem is to be solved and the resulting integral equations are then called boundary integral equations. For this reason we provide a brief summary of the necessary properties of single and double layer potentials.

We recall that a function $f(\vec{r})$ satisfies a Hölder condition in a domain $\Omega \subset \mathbb{R}^n$ if

$$|f(\vec{r}_1) - f(\vec{r}_2)| < D |\vec{r}_1 - \vec{r}_2|^\nu \quad \text{for } 0 < \nu \leq 1, D > 0 \quad (\text{II.23})$$

for any two distinct points $\vec{r}_1, \vec{r}_2 \in \Omega$.

It should be noted that Hölder continuity is stronger than continuity but not as strong as differentiability.

We will assume that the surfaces over which the layers are to be defined are Lyapunov. Recall that a surface is Lyapunov if it is smooth, possesses a normal line and tangent plane at each (non-boundary) point on it and that these vary continuously as we move from point to point on the surface. This implies the existence of local

coordinates (x, y, z) at any point p on the surface, the z -axis being along the normal and the x and y axes lying in the tangent plane. In a neighborhood of p the surface has equation $z = z(x, y)$ and the partial derivatives $z_x(x, y)$, $z_y(x, y)$ exist and are Hölder continuous.

In the remainder of the section S will denote an orientated, open, bounded Lyapunov surface. \vec{P}, \vec{Q} will be position vectors of points $P, Q \in \mathbb{R}^3$ and \vec{p}, \vec{q} the position vectors of points $p, q \in S$. The positive (outward) unit normal at a point $p \in S$ will be denoted by \vec{n}_p .

Let $\Omega \subset \mathbb{R}^3$ be a neighborhood containing S in its interior. Then if $f(\vec{P})$ is defined and continuous in $\Omega \setminus S$ we define $f^\pm(\vec{p})$ to be the limit as \vec{P} approaches \vec{p} along the normal from the positive or negative sides of S respectively.

At a point $\vec{P} \notin S$, $\frac{\partial}{\partial n_p}$ denotes differentiation in the direction of the unit vector \vec{n}_p at $\vec{p} \in S$. $\frac{\partial}{\partial n_p^\pm}$ denotes the limit of $\frac{\partial}{\partial n_p}$ as \vec{P} approaches \vec{p} from the positive or negative sides of S respectively.

The surface layer potential properties summarized below are well known, details being found in many references including [6, 7, 8, 9].

II.2.1 The Three-Dimensional Green's Functions

The potential at a point \vec{P} due to a unit source at a point \vec{Q} is given by the Green's function $G(\vec{P}, \vec{Q})$. It is well known that, in \mathbb{R}^3 , the Green's function satisfies Poisson's equation

$$\Delta_3 G = -\delta(\vec{P} - \vec{Q}) \quad (\text{II.24})$$

and takes the form

$$G(\vec{P}, \vec{Q}) = \frac{1}{4\pi R} \quad (\text{II.25})$$

where $R = R(\vec{P}, \vec{Q}) = |\vec{P} - \vec{Q}|$ is the distance between the points \vec{P} and \vec{Q} .

II.2.2 The Single Layer Potential Operator

The single layer potential operator

$$[\mathcal{S}\varphi] (\vec{P}) = \int_S \varphi(\vec{q}) G(\vec{P}, \vec{q}) dS(\vec{q}) \quad (\text{II.26})$$

gives us the potential at the point \vec{P} due to a layer of simple sources that are distributed with density $\varphi(\vec{q})$ on the surface S .

If $\varphi(\vec{q})$ is Hölder continuous on S , then;

1. $[\mathcal{S}\varphi] (\vec{P})$ satisfies Laplace's equation, $\Delta_3 V = 0$, for all $\vec{P} \in \mathbb{R}^3 \setminus S$ and approaches zero like $|\vec{P}|^{-1}$ as $|\vec{P}| \rightarrow \infty$
2. $[\mathcal{S}\varphi] (\vec{P})$ is continuous for all $\vec{P} \in \mathbb{R}^3$
3. In the neighborhood of each (non-boundary) point $\vec{p} \in S$ the tangential derivatives of $[\mathcal{S}\varphi] (\vec{p})$ exist and are continuous
4. The normal derivative $\frac{\partial}{\partial n_p} [\mathcal{S}\varphi] (\vec{p})$, is defined in the neighborhood of each (non-boundary) point $\vec{p} \in S$. At the point \vec{p} it suffers a jump discontinuity given by

$$\frac{\partial}{\partial n_p^\pm} [\mathcal{S}\varphi] (\vec{p}) = \mp \frac{1}{2} \varphi(\vec{p}) + [\mathcal{S}_{n_p} \varphi] (\vec{p}) \quad (\text{II.27})$$

where

$$\mathcal{S}_{n_p} : L_2(S) \rightarrow L_2(S) \quad (\text{II.28})$$

is a compact operator given by the improper integral;

$$[\mathcal{S}_{n_p} \varphi] (\vec{p}) = \int_S \varphi(\vec{q}) \frac{\partial}{\partial n_p} G(\vec{p}, \vec{q}) dS(\vec{q}) \quad (\text{II.29})$$

It should be noted that (II.27) can be written in the discontinuity form

$$\frac{\partial}{\partial n_p^+} [\mathcal{S}\varphi] (\vec{p}) - \frac{\partial}{\partial n_p^-} [\mathcal{S}\varphi] (\vec{p}) = -\varphi(\vec{p}) \quad (\text{II.30})$$

and

$$\frac{1}{2} \left\{ \frac{\partial}{\partial n_p^+} [\mathcal{S}\varphi] (\vec{p}) + \frac{\partial}{\partial n_p^-} [\mathcal{S}\varphi] (\vec{p}) \right\} = [\mathcal{S}_{n_p} \varphi] (\vec{p}) \quad (\text{II.31})$$

II.2.3 The Double Layer Potential Operator

The double layer potential operator

$$[\mathfrak{D}\sigma](\vec{P}) = \int_S \sigma(\vec{q}) \frac{\partial}{\partial n_q} G(\vec{P}, \vec{q}) dS(\vec{q}) \quad (\text{II.32})$$

gives us the potential at the point \vec{P} due to a layer of dipoles that are distributed over the surface S with density $\sigma(\vec{q})$.

If $\sigma(\vec{q})$ is Hölder continuously differentiable on S , then;

1. $[\mathfrak{D}\sigma](\vec{P})$ satisfies Laplace's equation, $\Delta_3 V = 0$, for all $\vec{P} \in \mathbb{R}^3 \setminus S$ and approaches zero like $|\vec{P}|^{-2}$ as $|\vec{P}| \rightarrow \infty$
2. $[\mathfrak{D}\sigma](\vec{p})$ exists in the neighborhood of each (non-boundary) point $\vec{p} \in S$ where it exhibits the discontinuity behavior

$$[\mathfrak{D}^+\sigma](\vec{p}) - [\mathfrak{D}^-\sigma](\vec{p}) = \sigma(\vec{p}) \quad (\text{II.33})$$

and

$$\frac{1}{2} \{ [\mathfrak{D}^+\sigma](\vec{p}) + [\mathfrak{D}^-\sigma](\vec{p}) \} = -[\mathfrak{D}\sigma](\vec{p}) \quad (\text{II.34})$$

In addition

$$\mathfrak{D} : L_2(S) \rightarrow L_2(S)$$

is compact and is in fact the adjoint of the operator \mathcal{S}_{n_p} defined in (II.29).

3. In the neighborhood of each (non-boundary) point $\vec{p} \in S$ the normal derivatives of $[\mathfrak{D}\sigma](\vec{p})$ exists and are continuous

$$\frac{\partial}{\partial n_p^+} [\mathfrak{D}\sigma](\vec{p}) = \frac{\partial}{\partial n_p^-} [\mathfrak{D}\sigma](\vec{p}) = \frac{\partial}{\partial n_p} [\mathfrak{D}\sigma](\vec{p}) \quad (\text{II.35})$$

4. In the neighborhood of each (non-boundary) point $\vec{p} \in S$ the tangential derivatives of $[\mathfrak{D}\sigma](\vec{p})$ exist and exhibit the discontinuity behavior

$$\frac{\partial}{\partial t_p^\pm} [\mathfrak{D}\sigma](\vec{p}) = \frac{\partial}{\partial t_p} [\mathfrak{D}\sigma](\vec{p}) \pm \frac{1}{2} \sigma(\vec{p}) \quad (\text{II.36})$$

II.2.4 The Dirichlet Problem

Let S be a region in the xy -plane. The Dirichlet problem is concerned with finding the solution $V(\vec{P})$ of Laplace's equation

$$\Delta_3 V = 0, \text{ for } \vec{P} \in \mathbb{R}^3 \setminus S \quad (\text{II.37})$$

subject to the boundary conditions;

1.

$$V(\vec{P}) \rightarrow 0 \text{ as } |\vec{P}| \rightarrow \infty \quad (\text{II.38})$$

2.

$$V(\vec{p}) = g(\vec{p}), \vec{p} \in S \quad (\text{II.39})$$

where $g(\vec{p})$ is a prescribed potential function.

In view of our discussion on the single layer potential it is clear that the desired solution is given by

$$V(\vec{P}) = [S\varphi](\vec{P}) \quad (\text{II.40})$$

provided the density $\varphi(\vec{q})$ satisfies the weakly-singular integral equation;

$$\frac{1}{4\pi} \int_S \frac{\varphi(\vec{q}) dS(\vec{q})}{R(\vec{p}, \vec{q})} = g(\vec{p}), \vec{p} \in S \quad (\text{II.41})$$

Of Particular interest is the case where S is the unit disc in the (r, θ) plane as this yields the Boussinesq Equation which motivates much of the work to follow.

$$\frac{1}{4\pi} \int_{-\pi}^{\pi} \int_0^1 \frac{\varphi(\rho, \vartheta) \rho d\rho d\vartheta}{\sqrt{r^2 + \rho^2 - 2r\rho \cos(\vartheta - \theta)}} = g(\rho, \vartheta), 0 \leq r \leq 1, -\pi < \theta \leq \pi \quad (\text{II.42})$$

It should be observed that the technique used to derive (II.41) holds also for the situation in which S is the union of non-intersecting surface elements $S_i, i = 1, 2, \dots, n$. In this case, if φ_i and g_i are the corresponding surface densities and potentials, we find that the solution takes the form

$$\varphi(\vec{P}) = \sum_{i=1}^n [S\varphi_i](\vec{P}) \quad (\text{II.43})$$

where φ_i are given by the system of n simultaneous integral equations

$$\sum_{j=1}^n \frac{1}{4\pi} \int_S \frac{\varphi_j(\vec{q}) dS(\vec{q})}{R(\vec{p}, \vec{q})} = g_i(\vec{p}), \vec{p} \in S_i, i = 1, 2, \dots, n \quad (\text{II.44})$$

each of which has one weakly singular kernel and $(n - 1)$ continuous kernels.

Symmetries of geometry and loading often enable us to reduce a system to a single equation. An example is the case for a pair of discs $0 \leq r \leq 1$, $-\pi < \theta \leq \pi$, $z = \pm h$ which are charged to equal and opposite potentials $\pm f(r, \theta)$ and thereby acquire charge densities $\pm\varphi(r, \theta)$ given by the integral equation

$$\frac{1}{4\pi} \int_{-\pi}^{\pi} \int_0^1 \left(\frac{\varphi(\rho, \vartheta)}{\sqrt{r^2 + \rho^2 - 2r\rho \cos(\vartheta - \theta)}} - \frac{\varphi(\rho, \vartheta)}{\sqrt{r^2 + \rho^2 - 2r\rho \cos(\vartheta - \theta) + 4h^2}} \right) \rho d\rho d\vartheta = g(\rho, \vartheta) \quad (\text{II.45})$$

for $0 \leq r \leq 1$, $-\pi < \theta \leq \pi$

II.2.5 The Neumann Problem

Let S be a region in the xy -plane. In the Neumann problem a solution $V(\vec{P})$ of (II.37) is again sought but this time with boundary conditions of the form;

1.

$$V(\vec{P}) \rightarrow 0 \text{ as } |\vec{P}| \rightarrow \infty \quad (\text{II.46})$$

2.

$$\frac{\partial V(\vec{P})}{\partial n} = g(\vec{p}), \vec{p} \in S \quad (\text{II.47})$$

In this case it is clear that the solution is given by the double layer potential

$$V(\vec{P}) = [\partial\sigma](\vec{P}) \quad (\text{II.48})$$

provided $\sigma(\vec{q})$ satisfies the integral equation;

$$\frac{\partial}{\partial n_p} \int_S \sigma(\vec{q}) \frac{\partial}{\partial n_q} G(\vec{p}, \vec{q}) dS(\vec{q}) = g(\vec{p}), \vec{p} \in S \quad (\text{II.49})$$

Now since G is a function of $|\vec{p} - \vec{q}|$ only, $\frac{\partial G}{\partial n_q} = -\frac{\partial G}{\partial n_p}$ yielding

$$-\frac{\partial^2}{\partial n_p^2} \int_S \sigma(\vec{q}) G(\vec{p}, \vec{q}) dS(\vec{q}) = g(\vec{p}), \vec{p} \in S \quad (\text{II.50})$$

or equivalently

$$\frac{1}{4\pi} \Delta_2 \int_S \frac{\sigma(\vec{q})}{R(\vec{p}, \vec{q})} dS(\vec{q}) = g(\vec{p}), \vec{p} \in S \quad (\text{II.51})$$

where Δ_2 is the surface Laplacian.

Note that (II.51) is a hyper-singular integral equation. The operator on its left hand side is unbounded but, as will be shown later, it has in many circumstances a compact inverse.

In the case where S is the unit disc in the (r, θ) plane, (II.51) reduces to the equation;

$$\frac{1}{4\pi} \Delta_2 \int_S \frac{\sigma(\rho, \vartheta)}{\sqrt{r^2 + \rho^2 - 2r\rho \cos(\vartheta - \theta)}} \rho d\rho d\vartheta = g(r, \theta), 0 \leq r \leq 1, -\pi < \theta \leq \pi \quad (\text{II.52})$$

As with the Dirichlet problem an extension can be made to the case where S is a union of non-intersecting surfaces, where (II.52) can be used as the prototype for developments in later chapters.

CHAPTER III

HILBERT SPACES I

III.1 INTRODUCTION

The integral equations that are to be investigated in later sections can be considered as operator equations in Hilbert Space. With the goal of solving these operator equations we construct weighted Hilbert Spaces $L_2^\alpha(0, 1)$; $\alpha = 0, 1$ and identify suitable orthonormal bases for them. By construction, these basis functions will also form a complete set of eigenfunctions for the two classes of operators which represent the dominant parts in the integral equations of interest. We will then examine these operators and in particular their eigen-structure.

III.2 THE HILBERT SPACES $L_2^\alpha(0, 1)$

The $L_2^\alpha(0, 1)$ spaces consist of all real or complex valued functions that are square integrable on the interval $(0, 1)$ with suitable weight function. An exact definition is as follows.

Definition III.1 For $\alpha = 0, 1$

$$L_2^\alpha(0, 1) = \left\{ f(\rho) : f : (0, 1) \rightarrow \mathbb{C} \text{ and } \int_0^1 |f(\rho)|^2 w^\alpha(\rho) d\rho < \infty \right\} \quad (\text{III.1})$$

where

$$w^\alpha(\rho) = \rho(1 - \rho^2)^{\alpha - \frac{1}{2}} \quad (\text{III.2})$$

with inner product

$$\langle f, g \rangle_\alpha = \int_0^1 f(\rho) \overline{g(\rho)} w^\alpha(\rho) d\rho \quad (\text{III.3})$$

and norm

$$\|f\|_\alpha = \left\{ \int_0^1 |f(\rho)|^2 w^\alpha(\rho) d\rho \right\}^{\frac{1}{2}} \quad (\text{III.4})$$

In order to construct orthonormal bases for the Hilbert spaces $L_2^\alpha(0, 1)$ we will begin by recalling that the polynomial functions $t_n^m(\rho)$, $u_n^m(\rho)$ ($m, n = 0, 1, 2, \dots$), introduced in Def. II.1, are related to the well known associated Legendre polynomials $P_n^m(x)$ as follows;

For $m, n = 0, 1, 2, \dots$

$$t_n^m(\rho) = T_n^m P_{2n+m}^m(\sqrt{1-\rho^2}), 0 \leq \rho \leq 1 \quad (\text{III.5})$$

$$u_n^m(\rho) = U_n^m \frac{P_{2n+m+1}^m(\sqrt{1-\rho^2})}{\sqrt{1-\rho^2}}, 0 \leq \rho \leq 1 \quad (\text{III.6})$$

where

$$T_n^m = \sqrt{\frac{(4n+2m+1)(2n)!}{(2n+2m)!}} \quad (\text{III.7})$$

$$U_n^m = \sqrt{\frac{(4n+2m+3)(2n+1)!}{(2n+2m+1)!}} \quad (\text{III.8})$$

are normalization constants.

The functions $t_n^m(\rho)$ and $u_n^m(\rho)$ are polynomials of degree $(2n+m)$ in ρ and contain only even powers of ρ if m is even and only odd powers if m is odd. In addition, by making a trivial change of variables in the following well known orthogonality relation for the associated Legendre polynomials (e.g. [5], 8.14.11 and 8.14.13);

$$\int_{-1}^1 P_n^m(x) P_p^m(x) dx = \frac{(n+m)!}{(n-m)!} \frac{2\delta_{np}}{2n+1} \quad (\text{III.9})$$

it is readily shown that

$$\int_0^1 w^0(\rho) t_n^m(\rho) t_p^m(\rho) d\rho = \delta_{np} \quad (\text{III.10})$$

and

$$\int_0^1 w^1(\rho) u_n^m(\rho) u_p^m(\rho) d\rho = \delta_{np} \quad (\text{III.11})$$

and hence that, for a fixed value of m , the sequences $\{t_n^m(\rho)\}_{n=0}^{\infty}$ and $\{u_n^m(\rho)\}_{n=0}^{\infty}$ are orthonormal in $L_2^0(0, 1)$ and $L_2^1(0, 1)$, respectively.

We will show that in fact these sequences are also complete and hence form orthonormal bases functions for the respective spaces.

Theorem III.2 *For any $m = 0, 1, 2, \dots$ the sequence $\{t_n^m(\rho)\}_{n=0}^{\infty}$ forms a complete orthonormal basis for $L_2^0(0, 1)$.*

Proof. We have already established that the sequence is orthonormal so we need only show completeness.

For a fixed m , let $f(\rho) \in L_2^0(0, 1)$ be orthogonal to every element of the sequence $\{t_n^m(\rho)\}_{n=0}^\infty$. Then

$$\int_0^1 f(\rho) P_{2n+m}^m(\sqrt{1-\rho^2}) w^0(\rho) d\rho = 0, n = 0, 1, 2, \dots$$

Now, by letting $x = \sqrt{1-\rho^2}$ we get

$$\int_0^1 f(\sqrt{1-x^2}) P_{2n+m}^m(x) dx = 0, n = 0, 1, 2, \dots$$

and, since $P_{n+m}^m(-x) = (-1)^n P_{n+m}^m(x)$ and $f(\sqrt{1-x^2})$ is even, we have

$$\int_{-1}^1 f(\sqrt{1-x^2}) P_{n+m}^m(x) dx = 0, n = 0, 1, 2, \dots$$

The sequence $\{P_{n+m}^m(x)\}_{n=0}^\infty$ is complete in $L_2(-1, 1)$ (e.g. [10], p123, #10) so

$$f(\sqrt{1-x^2}) = 0, \quad -1 \leq x \leq 1$$

that is

$$f(\rho) = 0, \quad 0 \leq \rho \leq 1$$

Hence $\{t_n^m(\rho)\}_{n=0}^\infty$ is complete in $L_2^0(0, 1)$ ■

Theorem III.3 For any $m = 0, 1, 2, \dots$ the sequence $\{u_n^m(\rho)\}_{n=0}^\infty$ forms a complete orthonormal basis for $L_2^1(0, 1)$.

Proof. Similar to the previous theorem we have already shown that the sequence is orthonormal so we only need show completeness.

For a fixed m , let $f(\rho) \in L_2^1(0, 1)$ be orthogonal to every element of the sequence $\{u_n^m(\rho)\}_{n=0}^\infty$. Then

$$\int_0^1 f(\rho) P_{2n+m+1}^m(\sqrt{1-\rho^2}) \rho d\rho = 0, n = 0, 1, 2, \dots \quad (\text{III.12})$$

Letting $x = \sqrt{1 - \rho^2}$ we get

$$\int_0^1 x f(\sqrt{1 - x^2}) P_{2n+m+1}^m(x) dx = 0, n = 0, 1, 2, \dots$$

and, since $P_{n+m}^m(-x) = (-1)^n P_{n+m}^m(x)$ and $x f(\sqrt{1 - x^2})$ is odd, we have

$$\int_{-1}^1 x f(\sqrt{1 - x^2}) P_{n+m}^m(x) dx = 0, n = 0, 1, 2, \dots$$

The sequence $\{P_{n+m}^m(x)\}_{m=1}^{\infty}$ is complete (e.g. [10], p123, #10) so

$$x f(\sqrt{1 - x^2}) = 0, -1 \leq x \leq 1$$

that is

$$f(\rho) = 0, 0 \leq \rho \leq 1$$

Hence $\{u_m^n\}_{n=0}^{\infty}$ is complete in $L_2^1(0, 1)$ ■

Now that we have these complete orthonormal bases functions both types of spaces are separable and hence isomorphic to the separable Hilbert space l^2 . Each element in our $L_2^s(0, 1)$ spaces can be identified with the l^2 sequence consisting of the coefficients in any basis function expansion. First let us define l^2 .

Definition III.4

$$l^2 = \left\{ x : x = \{x_n\}_{n=0}^{\infty} \text{ where } x_n \in \mathbb{C} \text{ and } \sum_{n=0}^{\infty} |x_n|^2 < \infty \right\} \quad (\text{III.13})$$

with inner product

$$\langle x, y \rangle = \sum_{n=0}^{\infty} x_n \bar{y}_n \quad (\text{III.14})$$

and norm

$$\|x\| = \left\{ \sum_{n=0}^{\infty} |x_n|^2 \right\}^{\frac{1}{2}} \quad (\text{III.15})$$

We now construct the isomorphisms between the $L_2^s(0, 1)$ spaces and l^2 to enable us to take advantage of the well known l^2 structure.

Theorem III.5 $L_2^0(0, 1)$ is a separable infinite dimensional Hilbert space isomorphic to l^2 .

Proof. Let f be the function defined as follows $f(r) = \sum_{n=0}^{\infty} f_n t_n^m(r)$, then

$$\begin{aligned} \|f\|_0^2 &= \int_0^1 |f(\rho)|^2 w^0(\rho) d\rho \\ &= \int_0^1 \left| \sum_{n=0}^{\infty} f_n t_n^m(\rho) \right|^2 w^0(\rho) d\rho \\ &= \sum_{n=0}^{\infty} |f_n|^2 \int_0^1 |t_n^m(\rho)|^2 w^0(\rho) d\rho, \text{ by orthogonality} \\ &= \sum_{n=0}^{\infty} |f_n|^2 = \|\{f_n\}_{n=0}^{\infty}\|^2 \end{aligned}$$

so $f \in L_2^0(0, 1) \Leftrightarrow \{f_n\}_{n=0}^{\infty} \in l^2$

Now define the operator $A : L_2^0(0, 1) \rightarrow l^2$ by

$$Af = \{f_n\}_{n=0}^{\infty} \tag{III.16}$$

then if

$$\begin{aligned} f(r) &= \sum_{n=0}^{\infty} f_n t_n^m(r), g(r) = \sum_{n=0}^{\infty} g_n t_n^m(r) \\ x &= \{f_n\}_{n=0}^{\infty}, y = \{g_n\}_{n=0}^{\infty}, \end{aligned}$$

we have

$$\langle Af, Ag \rangle = \langle \{f_n\}_{n=0}^{\infty}, \{g_n\}_{n=0}^{\infty} \rangle = \langle x, y \rangle$$

and it follows that A is a Hilbert space isomorphism between $L_2^0(0, 1)$ and l^2 confirming the isomorphic relationship ■

Theorem III.6 $L_2^1(0, 1)$ is a separable infinite dimensional Hilbert space isomorphic to l^2 .

Proof. Let f be the function defined as follows $f(r) = \sum_{n=0}^{\infty} f_n u_n^m(r)$, then

$$\begin{aligned} \|f\|_0^2 &= \int_0^1 |f(\rho)|^2 w^1(\rho) d\rho \\ &= \int_0^1 \left| \sum_{n=0}^{\infty} f_n u_n^m(\rho) \right|^2 w^1(\rho) d\rho \\ &= \sum_{n=0}^{\infty} |f_n|^2 \int_0^1 |u_n^m(\rho)|^2 w^1(\rho) d\rho, \text{ by orthogonality} \\ &= \sum_{n=0}^{\infty} |f_n|^2 = \|\{f_n\}_{n=0}^{\infty}\|^2 \end{aligned}$$

so $f \in L_2^1(0,1) \Leftrightarrow \{f_n\}_{n=0}^{\infty} \in l^2$

Now define the operator $B : L_2^1(0,1) \longrightarrow l^2$ by

$$Bf = \{f_n\}_{n=0}^{\infty} \tag{III.17}$$

then, if

$$\begin{aligned} f(r) &= \sum_{n=0}^{\infty} f_n t_n^m(r), g(r) = \sum_{n=0}^{\infty} g_n t_n^m(r) \\ x &= \{f_n\}_{n=0}^{\infty}, y = \{g_n\}_{n=0}^{\infty} \end{aligned}$$

we have

$$\langle Bf, Bg \rangle = \langle \{f_n\}_{n=0}^{\infty}, \{g_n\}_{n=0}^{\infty} \rangle = \langle x, y \rangle$$

and it follows that B is a Hilbert space isomorphism between $L_2^1(0,1)$ and l^2 confirming the isomorphic relationship ■

Now that we have defined the structure of our Hilbert spaces we turn our attention to operators defined on them.

III.3 OPERATORS ON THE $L_2^{\alpha}(0,1)$ HILBERT SPACES

We will now define and examine what will be the key operators for the integral equations of interest. We will first look at two weakly singular operators; \mathbb{L}_m^0 and \mathbb{L}_m^1 .

III.3.1 The L_m^α Operators

The L_m^α operators will both be defined in terms of the weakly-singular kernels $l_m(\rho, r)$ for $m = 0, 1, 2, 3, \dots$ with relevant weight functions. The definition for $l_m(\rho, r)$ now follows.

Definition III.7 For $m = 0, 1, 2, 3, \dots$

$$l_m(\rho, r) = \frac{1}{2\pi\sqrt{\rho r}} Q_{m-\frac{1}{2}} \left[\frac{\rho^2 + r^2}{2\rho r} \right] \quad (\text{III.18})$$

where $Q_{m-\frac{1}{2}}(x)$ is a ring function or a Legendre function of the second kind (e.g. [1], section 32).

It will often be convenient to represent this kernel in other ways, as allowed by the following theorem.

Theorem III.8 For $m = 0, 1, 2, 3, \dots$

$$l_m(\rho, r) = \frac{1}{\pi\rho^m r^m} \int_0^{\min(\rho, r)} \frac{t^{2m} dt}{\sqrt{(\rho^2 - t^2)(r^2 - t^2)}} \quad (\text{III.19})$$

$$= \frac{1}{2} \int_0^\infty J_m(\rho t) J_m(rt) dt \quad (\text{III.20})$$

Proof. Using the following result from ([1], p443)

$$\int_0^\pi \frac{\cos m\theta}{\sqrt{2(\cosh \vartheta - \cos \theta)}} d\theta = Q_{m-\frac{1}{2}}(\cosh \vartheta) \quad (\text{III.21})$$

and the real part of Copson's Integral ([11]) with $\vartheta = 0$;

$$\int_0^{2\pi} \frac{e^{im\theta} d\theta}{\sqrt{r^2 + \rho^2 - 2r\rho \cos(\vartheta - \theta)}} = \frac{4e^{im\vartheta}}{r^m \rho^m} \int_0^{\min(r, \rho)} \frac{t^{2m} dt}{\sqrt{(r^2 - t^2)(\rho^2 - t^2)}}$$

we can obtain with simple algebra and change of variables

$$\frac{4}{r^m \rho^m} \int_0^{\min(r, \rho)} \frac{t^{2m} dt}{\sqrt{(r^2 - t^2)(\rho^2 - t^2)}} = \frac{2}{\sqrt{r\rho}} Q_{m-\frac{1}{2}} \left(\frac{r^2 + \rho^2}{2r\rho} \right) \quad (\text{III.22})$$

from which (III.19) follows.

It is clear (III.20) follows immediately from the following result ([12], 560.04);

$$\int_0^{\infty} e^{-tz} J_m(rt) J_m(\rho t) dt = \frac{1}{\pi \sqrt{r\rho}} Q_{m-\frac{1}{2}} \left(1 + \frac{z^2 + (r-\rho)^2}{2r\rho} \right) \quad (\text{III.23})$$

by setting $z = 0$ ■

We will now define the $\mathbb{L}_m^\alpha [f(\rho)](r)$ operators using these kernels and the weight functions $w^\alpha(\rho)$ as before.

Definition III.9 For $\alpha = 0, 1$ and $m = 0, 1, 2, 3, \dots$ let

$$\mathbb{L}_m^\alpha [f(\rho)](r) = \int_0^1 l_m(\rho, r) f(\rho) w^\alpha(\rho) d\rho \quad (\text{III.24})$$

for any given $f \in L_2^\alpha(0, 1)$.

We will now go about showing that for each $m = 0, 1, 2, 3, \dots$ and for both weight functions the kernels $l_m(\rho, r)$ are square integrable on $(0, 1)$ and hence that the \mathbb{L}_m^α operators are Hilbert-Schmidt and therefore compact. We will first consider \mathbb{L}_m^0 on $L_2^0(0, 1)$ and show that for each m the basis functions t_n^m form a complete set of eigenfunctions with corresponding eigenvalues λ_{mn}^{-1} . The eigenvalues not only converge to zero but are square summable finite which is enough to establish that \mathbb{L}_m^0 is a Hilbert-Schmidt type operator (see [13], pages 59-60), meaning it is both square integrable and compact. The compactness of \mathbb{L}_m^1 will follow since $\|\mathbb{L}_m^1\|_1 < \|\mathbb{L}_m^0\|_0$, a consequence of the following facts; $w^1(0) = w^0(0)$ and $|w^1(\rho)| < |w^0(\rho)|$ for $0 < \rho \leq 1$.

The following theorem establishes the eigenvalues and eigenfunctions of \mathbb{L}_m^0 .

Theorem III.10 For $m, n = 0, 1, 2, 3, \dots, 0 \leq r \leq 1$

$$\lambda_{mn} \mathbb{L}_m^0 [t_n^m(\rho)](r) = t_n^m(r) \quad (\text{III.25})$$

where

$$\lambda_{mn} = \frac{4\Gamma(n+1)\Gamma(n+m+1)}{\Gamma(n+\frac{1}{2})\Gamma(n+m+\frac{1}{2})} = \frac{2^{4n+2m+2}n!(n+m)!}{\pi(2n)!(2n+2m)!} \quad (\text{III.26})$$

Proof.

$$\begin{aligned}
\mathbb{L}_m^0 [t_n^m(\rho)] &= \int_0^1 w^0(\rho) t_n^m(\rho) l_m(\rho, r) d\rho, \\
&= \frac{1}{2} \int_0^1 w^0(\rho) t_n^m(\rho) \int_0^\infty J_m(\rho t) J_m(rt) dt d\rho, \\
&\quad \text{by (III.20)} \\
&= \frac{1}{2} \int_0^\infty J_m(rt) \int_0^\infty w^0(\rho) H(1-\rho^2) t_n^m(\rho) J_m(\rho t) d\rho dt \\
&= \frac{1}{2A_{mn}} \int_0^\infty J_m(rt) \int_0^\infty \rho J_m(\rho t) \int_0^\infty s^{\frac{1}{2}} J_{m+2n+\frac{1}{2}}(s) J_m(\rho s) ds d\rho dt, \\
&\quad \text{by (II.11)} \\
&= \frac{1}{2A_{mn}} \int_0^\infty J_m(rt) t^{-\frac{1}{2}} J_{m+2n+\frac{1}{2}}(t) dt, \text{ by Hankel Inversion formula} \\
&= \frac{C_{mn}}{2A_{mn}} t_n^m(r), \text{ by (II.19)} \\
&= \frac{\pi(2n)!(2n+2m)!}{2^{4n+2m+2} n!(n+m)!} t_n^m(r), \text{ by (II.12) and (II.20) } \blacksquare
\end{aligned}$$

We will look at the properties of the λ_{mn} 's, in particular as n, m tend to infinity, ultimately showing that $\sum_{n=0}^\infty \frac{1}{\lambda_{mn}^2}$ is in fact bounded.

Firstly, an asymptotic result illustrating the behavior of λ_{mn} as n gets large which shows that $\frac{1}{\lambda_{mn}} \rightarrow 0$ as $n \rightarrow \infty$ at a similar rate to $\frac{1}{n}$.

Theorem III.11 For $m = 0, 1, 2, \dots$ and large n

$$\lambda_{mn} \approx 4\sqrt{n(n+m)} \tag{III.27}$$

Proof.

$$\begin{aligned}
\lambda_{mn} &= 4 \frac{\Gamma(n+1)}{\Gamma\left(n+\frac{1}{2}\right)} \frac{\Gamma(n+m+1)}{\Gamma\left(n+m+\frac{1}{2}\right)} \\
&= 4\sqrt{n} \left\{ 1 + \frac{1}{8n} + O\left(\frac{1}{n^2}\right) \right\} \sqrt{n+m} \left\{ 1 + \frac{1}{8(n+m)} + O\left(\frac{1}{(n+m)^2}\right) \right\} \\
&= 4\sqrt{n(n+m)} \left\{ 1 + \frac{1}{8n} + \frac{1}{8(n+m)} + O\left(\frac{1}{n^2}\right) \right\}
\end{aligned}$$

where we have made use of the following result ([5], 6.1.47)

$$\frac{\Gamma(z + \alpha)}{\Gamma(z + \beta)} = z^{\alpha - \beta} \left[1 + \frac{1}{2z} (\alpha - \beta) (\alpha + \beta - 1) + O\left(\frac{1}{z^2}\right) \right], |\arg(z)| < \pi \quad (\text{III.28})$$

■

Now we will establish that for a given n , $\{\lambda_{mn}\}_{m=0}^{\infty}$ is a strictly increasing sequence in m and similarly for a given m , $\{\lambda_{mn}\}_{n=0}^{\infty}$ is a strictly increasing sequence in n .

Theorem III.12 For $m = 0, 1, 2, 3, \dots$ $n = 0, 1, 2, 3, \dots$

1. $m \neq 0$

$$\lambda_{mn} > \lambda_{(m-1)n} > \dots > \lambda_{0n} \quad (\text{III.29})$$

2. $n \neq 0$

$$\lambda_{mn} > \lambda_{m(n-1)} > \dots > \lambda_{m0} \quad (\text{III.30})$$

Proof.

1.

$$\begin{aligned} \lambda_{mn} &= \frac{4\Gamma(n+1)\Gamma(n+m+1)}{\Gamma(n+\frac{1}{2})\Gamma(n+m+\frac{1}{2})} \\ &= \left(\frac{(2n+2m)}{2n+2m-1}\right)^4 \frac{\Gamma(n+1)\Gamma(n+(m-1)+1)}{\Gamma(n+\frac{1}{2})\Gamma(n+(m-1)+\frac{1}{2})} \\ &= \left(\frac{(2n+2m)}{2n+2m-1}\right) \lambda_{(m-1)n} > \lambda_{(m-1)n} \end{aligned}$$

2.

$$\begin{aligned} \lambda_{mn} &= \left(\frac{(2n)(2n+2m)}{(2n-1)(2n+2m-1)}\right)^4 \frac{\Gamma((n-1)+1)\Gamma((n-1)+m+1)}{\Gamma((n-1)+\frac{1}{2})\Gamma((n-1)+m+\frac{1}{2})} \\ &= \left(\frac{(2n)(2n+2m)}{(2n-1)(2n+2m-1)}\right) \lambda_{m(n-1)} > \lambda_{m(n-1)} \quad \blacksquare \end{aligned}$$

We wish to find a bound on $\sum_{n=0}^{\infty} \frac{1}{\lambda_{mn}^2}$ for a given m , which should exist since $\frac{1}{\lambda_{mn}^2}$ behaves similar to $\frac{1}{n^2}$ for large n . Since $\frac{1}{\lambda_{mn}}$ is strictly decreasing in m , if we establish a bound for $m = 0$ it will hold for all other values of m . Now to establish a bound for $\frac{1}{\lambda_{0n}}$.

Theorem III.13

$$\lambda_{00} = \frac{4}{\pi}, \lambda_{0n} > \frac{8n}{\pi} \quad (n \geq 1) \quad (\text{III.31})$$

Proof. The value of λ_{00} is easily computed to be

$$\lambda_{00} = 4 \frac{\Gamma(1) \Gamma(1)}{\Gamma(\frac{1}{2}) \Gamma(\frac{1}{2})} = \frac{4}{\pi}$$

The result holds for $n = 1$ since

$$\lambda_{01} = 4 \frac{\Gamma(2) \Gamma(2)}{\Gamma(\frac{3}{2}) \Gamma(\frac{3}{2})} = \frac{16}{\pi} > \frac{8}{\pi} \cdot 1$$

For $n \geq 2$ we have,

$$\begin{aligned} \lambda_{0n} &= 4 \frac{\Gamma(n+1) \Gamma(n+1)}{\Gamma(n+\frac{1}{2}) \Gamma(n+\frac{1}{2})} \\ &= \frac{4n^2}{n-\frac{1}{2}} \frac{\Gamma(n) \Gamma(n)}{\Gamma(n+\frac{1}{2}) \Gamma(n-\frac{1}{2})} \\ &= \frac{2n}{2n-1} 4n \left(\frac{2}{\pi}\right) \\ &> \frac{8n}{\pi} \end{aligned}$$

where we used the following result from ([14] page 2);

For $n = 2, 3, 4, \dots$

$$\frac{\Gamma(n+z) \Gamma(n-z)}{[(n-1)!]^2} = \frac{\pi z}{\sin \pi z} \prod_{m=1}^{n-1} \left(1 - \frac{z^2}{m^2}\right) \quad (\text{III.32})$$

■

Now we seek a bound for $\sum_{n=0}^{\infty} \frac{1}{\lambda_{0n}^2}$ and hence $\sum_{n=0}^{\infty} \frac{1}{\lambda_{mn}^2}$ for any m .

Theorem III.14 For $m = 1, 2, \dots$

$$\sum_{n=0}^{\infty} \frac{1}{\lambda_{mn}^2} < \sum_{n=0}^{\infty} \frac{1}{\lambda_{0n}^2} < \frac{\pi^2}{16} \left[1 + \frac{\pi^2}{24}\right] \quad (\text{III.33})$$

Proof. Now by (III.29) $\lambda_{mn} > \lambda_{0n}$, $m \geq 1$, so

$$\begin{aligned} \sum_{n=0}^{\infty} \frac{1}{\lambda_{mn}^2} &< \sum_{n=0}^{\infty} \frac{1}{\lambda_{0n}^2} = \frac{1}{\lambda_{00}^2} + \sum_{n=1}^{\infty} \frac{1}{\lambda_{0n}^2} \\ &< \left(\frac{\pi}{4}\right)^2 + \sum_{n=1}^{\infty} \left(\frac{\pi}{8n}\right)^2, \text{ by (III.31)} \\ &= \frac{\pi^2}{16} \left[1 + \frac{1}{4} \sum_{n=1}^{\infty} \frac{1}{n^2}\right] \\ &= \frac{\pi^2}{16} \left[1 + \frac{\pi^2}{24}\right] \blacksquare \end{aligned}$$

We can also establish a lower bound on $\frac{1}{\lambda_{mn}}$.

Theorem III.15 For $m, n = 0, 1, 2, 3, \dots$

$$\frac{1}{2(2n + 2m + 1)} \leq \frac{1}{\lambda_{mn}} \quad (\text{III.34})$$

Proof. Firstly,

for $m = n = 0$

$$\frac{1}{\lambda_{00}} = \frac{\pi}{4} \geq \frac{1}{2}$$

Now, for $m \neq 0$,

$$\begin{aligned}
\frac{1}{\lambda_{mn}} &= \frac{\Gamma\left(n + \frac{1}{2}\right) \Gamma\left(n + m + \frac{1}{2}\right)}{4\Gamma(n+1) \Gamma(n+m+1)} \\
&= \left(\frac{n+1}{n + \frac{1}{2}}\right) \frac{\Gamma\left((n+1) + \frac{1}{2}\right) \Gamma\left(n + m + \frac{1}{2}\right)}{4\Gamma((n+1)+1) \Gamma(n+m+1)} \\
&\geq \frac{\Gamma\left((n+1) + \frac{1}{2}\right) \Gamma\left(n + m + \frac{1}{2}\right)}{4\Gamma((n+1)+1) \Gamma(n+m+1)} \\
&\geq \frac{\Gamma\left((n+m) + \frac{1}{2}\right) \Gamma\left(n + m + \frac{1}{2}\right)}{4\Gamma((n+m)+1) \Gamma(n+m+1)}, \text{ by repetition} \\
&= \frac{1}{4\left(n + m + \frac{1}{2}\right)} \frac{\Gamma\left((n+m+1) + \frac{1}{2}\right) \Gamma\left((n+m+1) - \frac{1}{2}\right)}{\Gamma((n+m)+1) \Gamma(n+m+1)} \\
&= \frac{1}{2(2n+2m+1)} \frac{\pi}{2} \prod_{j=1}^{n+m} \left(1 - \frac{1}{4j^2}\right) \\
&\geq \frac{\pi}{4(2n+2m+1)} \prod_{j=1}^{\infty} \left(1 - \frac{1}{4j^2}\right) \\
&= \frac{\pi}{4(2n+2m+1)} \frac{2}{\pi} \sin \frac{\pi}{2} \\
&= \frac{1}{2(2n+2m+1)}
\end{aligned}$$

Where the following results from [14] were utilized (III.32) and ([14] page 4) with $z = \frac{1}{2}$;

$$\prod_{m=1}^{\infty} \left(1 - \frac{z^2}{m^2}\right) = \frac{\sin(\pi z)}{\pi z} = \frac{1}{\Gamma(1+z) \Gamma(1-z)} \blacksquare \quad (\text{III.35})$$

We now have upper and lower bounds on the eigenvalues as follows for $m, n = 0, 1, 2, \dots, n \neq 0$ as shown below.

$$\frac{1}{2(2n+2m+1)} \leq \frac{1}{\lambda_{mn}} < \frac{\pi}{8n} \quad (\text{III.36})$$

More importantly we have a finite bound on $\sum_{n=0}^{\infty} \frac{1}{\lambda_{mn}^2}$ so that it follows by ([15], prob. 132) that \mathbb{L}_m^0 is Hilbert-Schmidt and hence a compact self adjoint operator with a square integrable kernel.

We have then that for $m = 0, 1, 2, \dots$

$$\|\mathbb{L}_m^0\|_0 = \left\{ \int_0^1 \int_0^1 w^0(\rho) w^0(r) |t_0(\rho, r)|^2 d\rho dr \right\}^{\frac{1}{2}} < \infty \quad (\text{III.37})$$

and since $\|\mathbb{L}_m^1\|_1 < \|\mathbb{L}_m^0\|_0$ and $l_m(\rho, r)$ is real and symmetric, \mathbb{L}_m^1 is also Hilbert-Schmidt and therefore also a compact self adjoint operator.

It is now clear ([16], p63, Thm.14) that our kernel $l_m(\rho, r)$ admits the following bilinear expansion

$$l_m(\rho, r) = \sum_{n=0}^{\infty} \frac{1}{\lambda_{mn}} t_n^m(\rho) t_n^m(r) \quad (\text{III.38})$$

with convergence in the mean sense for $0 \leq r, \rho \leq 1$

We can now use this expansion to first express the norm of \mathbb{L}_m^0 in terms of its eigenvalues and hence obtain a finite bound for the norms of both operators.

Theorem III.16 For $m = 0, 1, 2, 3, \dots$

$$\|\mathbb{L}_m^0\|_0^2 = \sum_{n=0}^{\infty} \frac{1}{\lambda_{mn}^2} \quad (\text{III.39})$$

Proof.

$$\begin{aligned} \|\mathbb{L}_m^0\|_0^2 &= \int_0^1 \int_0^1 w^0(\rho) w^0(r) |l_m(\rho, r)|^2 d\rho dr \\ &= \int_0^1 \int_0^1 w^0(\rho) w^0(r) \left| \sum_{n=0}^{\infty} \frac{1}{\lambda_{mn}} t_n^m(\rho) t_n^m(r) \right|^2 d\rho dr, \text{ by (III.38)} \\ &= \sum_{n=0}^{\infty} \frac{1}{\lambda_{mn}^2}, \text{ by orthogonality of } t_n^m \blacksquare \end{aligned}$$

We can now use our bound on $\sum_{n=0}^{\infty} \frac{1}{\lambda_{mn}^2}$ (III.33), to put a bound on the norms of our operators.

For $m = 0, 1, 2, 3, \dots$

$$\|\mathbb{L}_m^1\|^2 < \|\mathbb{L}_m^0\|^2 < \frac{\pi^2}{16} \left[1 + \frac{\pi^2}{24} \right] \quad (\text{III.40})$$

We do not have a convenient eigen-structure for the \mathbb{L}_m^1 operators but we will now look at some relationships between the t_n^m and u_n^m functions that we can utilize to express $\mathbb{L}_m^1 f$ in a meaningful way using the results for \mathbb{L}_m^0 .

Let us first define some constants that will make later results more readable.

Definition III.17 For $m, n = 0, 1, 2, \dots$

$$\alpha_n^m = \sqrt{\frac{(2n+2)(2n+2m+2)}{(4n+2m+3)(4n+2m+5)}} \quad (\text{III.41})$$

$$\beta_n^m = \sqrt{\frac{(2n+1)(2n+2m+1)}{(4n+2m+1)(4n+2m+3)}} \quad (\text{III.42})$$

$$\gamma_n^m = \frac{(\alpha_n^m)^2}{\lambda_{m(n+1)}} + \frac{(\beta_n^m)^2}{\lambda_{mn}} \quad (\text{III.43})$$

$$\eta_n^m = \frac{\alpha_n^m \beta_{n+1}^m}{\lambda_{m(n+1)}} \quad (\text{III.44})$$

Let us establish some basic properties of these constants that we will utilize later. Firstly, it is clear that for all $m, n = 0, 1, 2, \dots, n \neq 0$

$$0 < \alpha_{n-1}^m < \alpha_n^m < \alpha_n^{m+1} < 1 \quad (\text{III.45})$$

and

$$0 < \beta_{n-1}^m < \beta_n^m < \beta_n^{m+1} < 1 \quad (\text{III.46})$$

We can utilize these properties to show that γ_n^m and η_n^m both converge to zero as $m, n \rightarrow \infty$.

Theorem III.18 For $m, n = 0, 1, 2, \dots$

$$\gamma_n^m < \frac{1}{\lambda_{m(n+1)}} + \frac{1}{\lambda_{mn}} \quad (\text{III.47})$$

and

$$\eta_n^m < \frac{1}{\lambda_{m(n+1)}} \quad (\text{III.48})$$

hence

$$\gamma_n^m, \eta_n^m \rightarrow 0 \text{ as } m, n \rightarrow \infty \quad (\text{III.49})$$

Proof. (III.47) and (III.48) follow directly from the definitions, (III.45) and (III.46), while (III.49) follows since $\frac{1}{\lambda_{mn}} \rightarrow 0$ as $m, n \rightarrow \infty$ ■

Now a theorem which will allow us to convert from u_n^m 's to t_n^m 's and vice versa.

Theorem III.19 For $m, n = 0, 1, 2, \dots$

$$t_n^m(\rho) = \beta_n^m u_n^m(\rho) + \alpha_{n-1}^m u_{n-1}^m(\rho) \quad (\text{III.50})$$

and

$$(1 - \rho^2) u_n^m(\rho) = \alpha_n^m t_{n+1}^m(\rho) + \beta_n^m t_n^m(\rho) \quad (\text{III.51})$$

$$= \alpha_n^m \beta_{n+1}^m u_{n+1}^m(\rho) + [(\alpha_n^m)^2 + (\beta_n^m)^2] u_n^m(\rho) + \alpha_{n-1}^m \beta_n^m u_{n-1}^m(\rho) \quad (\text{III.52})$$

Proof. Using the following result from ([17], P161, #12)

$$(2n + 1) x P_n^m(x) = (n - m + 1) P_{n+1}^m(x) + (n + m) P_{n-1}^m(x) \quad (\text{III.53})$$

(III.50) and (III.51) are easily obtained by simple algebra and the definitions of t_n^m and u_n^m while (III.52) follows from the combination of (III.50) and (III.51) ■

Some results for the inner product of t_n^m 's in $L_2^1(0, 1)$ now follow.

Theorem III.20 For $m, i, j = 0, 1, 2, \dots$

$$\langle u_i^m, t_j^m \rangle_1 = \int_0^1 u_i^m(r) t_j^m(r) w^1(r) dr = \alpha_{j-1}^m \delta_{(i+1)j} + \beta_j^m \delta_{ij} \quad (\text{III.54})$$

$$= \alpha_i^m \delta_{i(j-1)} + \beta_i^m \delta_{ij} \quad (\text{III.55})$$

Proof. $\langle u_i^m, t_j^m \rangle_1$

$$\begin{aligned} &= \int_0^1 u_i^m(r) t_j^m(r) w^1(\rho) dr \\ &= \alpha_i^m \int_0^1 t_{i+1}^m(r) t_j^m(r) w^0(r) dr + \beta_i^m \int_0^1 t_i^m(r) t_j^m(r) w^0(r) dr \\ &\quad \text{by (III.51)} \\ &= \alpha_{j-1}^m \delta_{(i+1)j} + \beta_j^m \delta_{ij}, \text{ by orthogonality} \blacksquare \end{aligned}$$

Theorem III.21 For $m, i, j = 0, 1, 2, \dots$

$$\begin{aligned}
& \langle t_i^m, t_j^m \rangle_1 \\
&= \int_0^1 t_i^m(r) t_j^m(r) w^1(r) dr \\
&= \beta_{j-1}^m \alpha_{j-1}^m \delta_{(i+1)j} + \left[(\beta_j^m)^2 + (\alpha_{j-1}^m)^2 \right] \delta_{ij} + \alpha_j^m \beta_j^m \delta_{(i-1)j} \quad (\text{III.56})
\end{aligned}$$

$$= \alpha_i^m \beta_i^m \delta_{i(j-1)} + \left[(\beta_i^m)^2 + (\alpha_{i-1}^m)^2 \right] \delta_{ij} + \alpha_{i-1}^m \beta_{i-1}^m \delta_{(i-1)j} \quad (\text{III.57})$$

Proof. $\langle t_i^m, t_j^m \rangle_1$

$$\begin{aligned}
&= \beta_i^m \langle u_i^m, t_j^m \rangle_1 + \alpha_{i-1}^m \langle u_{i-1}^m, t_j^m \rangle_1 \text{ by (III.50)} \\
&= \alpha_i^m \beta_i^m \delta_{i(j-1)} + \left[(\beta_i^m)^2 + (\alpha_{i-1}^m)^2 \right] \delta_{ij} + \alpha_{i-1}^m \beta_{i-1}^m \delta_{(i-1)j} \text{ by (III.54)} \\
&= \beta_{j-1}^m \alpha_{j-1}^m \delta_{(i+1)j} + \left[(\beta_j^m)^2 + (\alpha_{j-1}^m)^2 \right] \delta_{ij} + \alpha_j^m \beta_j^m \delta_{(i-1)j} \blacksquare
\end{aligned}$$

The \mathbb{L}_m^1 operators are not quite as nicely behaved in $L_2^1(0, 1)$ as the \mathbb{L}_m^0 are in $L_2^0(0, 1)$, in that we do not have convenient eigenvectors. The following theorems will however be important in letting us numerically evaluate $\mathbb{L}_m^1 f$ without numerically integrating this weakly-singular operator. Firstly, we can express $\mathbb{L}_m^1 u_n^m$ in terms of the t_n^m functions and hence as a tri-diagonal operator by converting to the u_n^m 's.

Theorem III.22 For $m, n = 0, 1, 2, \dots$

$$\mathbb{L}_m^1 u_n^m = \frac{\alpha_n^m}{\lambda_{m(n+1)}} t_{n+1}^m(r) + \frac{\beta_n^m}{\lambda_{mn}} t_n^m(r) \quad (\text{III.58})$$

$$= \eta_{n-1}^m u_{n-1}^m(r) + \gamma_n^m u_n^m(r) + \eta_n^m u_{n+1}^m(r) \quad (\text{III.59})$$

Proof. $\mathbb{L}_m^1 u_n^m$

$$\begin{aligned}
&= \int_0^1 u_n^m(\rho) l_m(r, \rho) w^1(\rho) d\rho \\
&= \int_0^1 l_m(r, \rho) u_n^m(\rho) (1 - \rho^2) w^0(\rho) d\rho \\
&= \alpha_n^m \int_0^1 l_m(r, \rho) t_{n+1}^m(\rho) w^0(\rho) d\rho + \beta_n^m \int_0^1 l_m(r, \rho) t_n^m(\rho) w^0(\rho) d\rho, \text{ by (III.51)} \\
&= \frac{\alpha_n^m}{\lambda_{m(n+1)}} t_{n+1}^m(r) + \frac{\beta_n^m}{\lambda_{mn}} t_n^m(r) \\
&= \frac{\alpha_n^m}{\lambda_{m(n+1)}} (\beta_{n+1}^m u_{n+1}^m(r) + \alpha_n^m u_n^m(r)) + \frac{\beta_n^m}{\lambda_{mn}} (\beta_n^m u_n^m(r) + \alpha_{n-1}^m u_{n-1}^m(r)), \\
&\quad \text{by (III.50)} \\
&= \frac{\alpha_{n-1}^m \beta_n^m}{\lambda_{mn}} u_{n-1}^m(r) + \left[\frac{(\beta_n^m)^2}{\lambda_{mn}} + \frac{(\alpha_n^m)^2}{\lambda_{m(n+1)}} \right] u_n^m(r) + \frac{\alpha_n^m \beta_{n+1}^m}{\lambda_{m(n+1)}} u_{n+1}^m(r) \\
&= \eta_{n-1}^m u_{n-1}^m(r) + \gamma_n^m u_n^m(r) + \eta_n^m u_{n+1}^m(r) \blacksquare
\end{aligned}$$

Since \mathbb{L}_m^1 is Hilbert-Schmidt it will be bounded; the next couple of results deal with the norms associated with the operator, which are of course bounded.

Theorem III.23 For $m, n = 0, 1, 2, \dots$

$$\|\mathbb{L}_m^1 u_n^m\|_1^2 = H(n-1) (\eta_{n-1}^m)^2 + (\gamma_n^m)^2 + (\eta_n^m)^2 \quad (\text{III.60})$$

Proof.

$$\begin{aligned}
\|\mathbb{L}_m^1 u_n^m\|_1^2 &= \|\eta_{n-1}^m u_{n-1}^m(r) + \gamma_n^m u_n^m(r) + \eta_n^m u_{n+1}^m(r)\|_1^2 \\
&= \int_0^1 |\eta_{n-1}^m u_{n-1}^m(r) + \gamma_n^m u_n^m(r) + \eta_n^m u_{n+1}^m(r)|^2 w^1(r) dr \\
&= H(n-1) (\eta_{n-1}^m)^2 + (\gamma_n^m)^2 + (\eta_n^m)^2 \blacksquare
\end{aligned}$$

Theorem III.24 For a given $m = 0, 1, 2, \dots$, let

$$f(\rho) = \sum_{n=0}^{\infty} f_n u_n^m(\rho)$$

then

$$\|\mathbb{L}_m^1 f\|_1^2 = \sum_{n=0}^{\infty} |\eta_{n-1}^m f_{n+1} + \gamma_n^m f_n + \eta_n^m f_{n-1} H(n-1)|^2 \quad (\text{III.61})$$

Proof. For

$$\begin{aligned}
\|\mathbb{L}_m^1 f\|_1^2 &= \left\| \sum_{n=0}^{\infty} f_n \mathbb{L}_m^1 u_n^m(\rho) \right\|_1^2 \\
&= \left\| \sum_{n=0}^{\infty} f_n \{H(n-1)\eta_{n-1}^m u_{n-1}^m(r) + \gamma_n^m u_n^m(r) + \eta_n^m u_{n+1}^m(r)\} \right\|_1^2 \\
&= \int_0^1 \left| \sum_{n=0}^{\infty} \{\eta_{n-1}^m f_{n+1} + \gamma_n^m f_n + \eta_n^m f_{n-1} H(n-1)\} u_n^m(r) \right|^2 w^1(r) dr \\
&= \sum_{n=0}^{\infty} |\eta_{n-1}^m f_{n+1} + \gamma_n^m f_n + \eta_n^m f_{n-1} H(n-1)|^2 \blacksquare
\end{aligned}$$

The next theorems give some important inner product results for $\mathbb{L}_m^1 u_n^m$ in $L_{\frac{1}{2}}^1(0, 1)$.

Theorem III.25 For $m, n, i = 0, 1, 2, \dots$

$$\langle \mathbb{L}_m^1 u_n^m, u_i^m \rangle_1 = \gamma_i^m \delta_{in} + \eta_{i-1}^m \delta_{i(n+1)} + \eta_i^m \delta_{i(n-1)} \quad (\text{III.62})$$

Proof. $\langle \mathbb{L}_m^1 u_n^m, u_i^m \rangle_1$

$$\begin{aligned}
&= \int_0^1 w^1(\rho) [\mathbb{L}_m^1 u_n^m](\rho) u_i^m(\rho) d\rho \\
&= \int_0^1 w^1(\rho) \left(\frac{\alpha_n^m}{\lambda_{m(n+1)}} t_{n+1}^m(\rho) + \frac{\beta_n^m}{\lambda_{mn}} t_n^m(\rho) \right) u_i^m(\rho) d\rho, \text{ by (III.58)} \\
&= \left(\frac{(\alpha_n^m)^2}{\lambda_{m(n+1)}} + \frac{(\beta_n^m)^2}{\lambda_{mn}} \right) \delta_{in} + \frac{\alpha_n^m \beta_{n+1}^m}{\lambda_{m(n+1)}} \delta_{i(n+1)} + \frac{\alpha_{n-1}^m \beta_n^m}{\lambda_{mn}} \delta_{i(n-1)}, \text{ by (III.54)} \\
&= \gamma_n^m \delta_{in} + \eta_n^m \delta_{i(n+1)} + \eta_{n-1}^m \delta_{i(n-1)} \blacksquare
\end{aligned}$$

Theorem III.26 For $m, n, i = 0, 1, 2, \dots$

$$\begin{aligned}
&\langle \mathbb{L}_m^1 u_n^m, t_i^m \rangle_1 \\
&= (\beta_n^m \gamma_n^m + \alpha_{n-1}^m \eta_{n-1}^m) \delta_{in} + (\alpha_n^m \gamma_n^m + \beta_{n+1}^m \eta_n^m + \beta_{n-1}^m \eta_{n-1}^m) \delta_{i(n+1)} \\
&\quad + \alpha_{n+1}^m \eta_n^m \delta_{i(n+2)} \quad (\text{III.63})
\end{aligned}$$

Proof.

$$\langle \mathbb{L}_m^1 u_n^m, t_i^m \rangle_1 = \frac{\alpha_n^m}{\lambda_{m(n+1)}} \langle t_{n+1}^m, t_i^m \rangle_1 + \frac{\beta_n^m}{\lambda_{mn}} \langle t_n^m, t_i^m \rangle_1 \text{ by (III.58)}$$

$$\begin{aligned}
&= \frac{\alpha_n^m}{\lambda_{m(n+1)}} \left(\beta_n^m \alpha_n^m \delta_{in} + [(\beta_{n+1}^m)^2 + (\alpha_n^m)^2] \delta_{i(n+1)} + \alpha_{n+1}^m \beta_{n+1}^m \delta_{(i-1)(n+1)} \right) \\
&\quad + \frac{\beta_n^m}{\lambda_{mn}} \left(\beta_{n-1}^m \alpha_{n-1}^m \delta_{(i+1)n} + [(\beta_n^m)^2 + (\alpha_{n-1}^m)^2] \delta_{in} + \alpha_n^m \beta_n^m \delta_{(i-1)n} \right) \\
&\quad \text{by (III.56)} \\
&= \left(\frac{\beta_n^m (\alpha_n^m)^2}{\lambda_{m(n+1)}} + \frac{\beta_n^m [(\beta_n^m)^2 + (\alpha_{n-1}^m)^2]}{\lambda_{mn}} \right) \delta_{in} + \frac{\alpha_n^m \alpha_{n+1}^m \beta_{n+1}^m}{\lambda_{m(n+1)}} \delta_{i(n+2)} \\
&\quad + \left(\frac{\alpha_n^m [(\beta_{n+1}^m)^2 + (\alpha_n^m)^2]}{\lambda_{m(n+1)}} + \frac{\beta_n^m [\beta_{n-1}^m \alpha_{n-1}^m + \alpha_n^m \beta_n^m]}{\lambda_{mn}} \right) \delta_{i(n+1)} \\
&= (\beta_n^m \gamma_n^m + \alpha_{n-1}^m \eta_{n-1}^m) \delta_{in} + (\alpha_n^m \gamma_n^m + \beta_{n+1}^m \eta_n^m + \beta_{n-1}^m \eta_{n-1}^m) \delta_{i(n+1)} \\
&\quad + \alpha_{n+1}^m \eta_n^m \delta_{i(n+2)} \blacksquare
\end{aligned}$$

The \mathbb{L}_m^1 operator will primarily form part of our dominant hyper-singular operator. In the next section we look at that hyper-singular operator and the differential operator used to produce it.

III.3.2 The Differential (\mathbb{D}_m) and the Hyper-Singular ($\mathbb{D}_m \mathbb{L}_m^1$) Operators

We will primarily be interested in the eigen-structure of the hyper-singular operator $\mathbb{D}_m \mathbb{L}_m^1$ but first we define \mathbb{D}_m and establish a couple of required properties.

Theorem III.27 *If \mathbb{D}_m is the following differential operator*

$$\mathbb{D}_m = -\frac{d^2}{dr^2} - \frac{1}{r} \frac{d}{dr} + \frac{m^2}{r^2} \quad (\text{III.64})$$

then;

$$\mathbb{D}_m J_m(r) = J_m(r) \quad (\text{III.65})$$

and

$$\mathbb{D}_m J_m(rt) = t^2 J_m(rt) \quad (\text{III.66})$$

Proof. *Since Bessel's Equation of order m*

$$\frac{d^2 y}{dr^2} + \frac{1}{r} \frac{dy}{dr} + \left(1 - \frac{m^2}{r^2}\right) y = 0 \quad (\text{III.67})$$

has the solution $J_m(r)$ and can be written

$$(1 - \mathbb{D}_m) y = 0 \quad (\text{III.68})$$

(III.65) follows immediately.

$$\begin{aligned}
 \mathbb{D}_m J_m(rt) &= - \left(\frac{d^2}{dr^2} + \frac{1}{r} \frac{d}{dr} - \frac{m^2}{r^2} \right) J_m(rt) \\
 &= -t^2 \left(\frac{d^2}{dx^2} + \frac{1}{x} \frac{d}{dx} - \frac{m^2}{x^2} \right) J_m(x) \\
 &= t^2 J_m(x), \text{ by (III.65)} \\
 &= t^2 J_m(rt) \blacksquare
 \end{aligned}$$

Now we establish that the u_n^m functions are eigenfunctions for $\mathbb{D}_m \mathbb{L}_m^1$;

Theorem III.28 For $0 \leq r \leq 1$ $m = 0, 1, 2, \dots$, the hyper-singular operator $\mathbb{D}_m \mathbb{L}_m^1$ has the property

$$\mu_{mn} \mathbb{D}_m \mathbb{L}_m^1 [u_n^m(\rho)](r) = u_n^m(r) \text{ for } n = 0, 1, 2, \dots \quad (\text{III.69})$$

where

$$\mu_{mn} = \frac{\Gamma(n+1) \Gamma(n+m+1)}{\Gamma(n+\frac{3}{2}) \Gamma(n+m+\frac{3}{2})} = \frac{2^{4n+2m+2} n! (n+m)!}{\pi (2n+1)! (2n+2m+1)!} \quad (\text{III.70})$$

Proof. $\mathbb{D}_m \mathbb{L}_m^1 [u_n^m(\rho)](r)$

$$\begin{aligned}
&= \mathbb{D}_m \int_0^1 u_n^m(\rho) l_m(\rho, r) w^1(\rho) d\rho \\
&= \frac{1}{2} \mathbb{D}_m \int_0^1 w^1(\rho) u_n^m(\rho) \int_0^\infty J_m(\rho t) J_m(rt) dt d\rho \\
&= \frac{1}{2} \mathbb{D}_m \int_0^\infty J_m(rt) \int_0^1 \rho J_m(\rho t) u_n^m(\rho) \sqrt{1-\rho^2} d\rho dt \\
&= \frac{\mathbb{D}_m}{2B_{mn}} \int_0^\infty J_m(rt) \int_0^\infty \rho J_m(\rho t) \int_0^\infty s^{-\frac{1}{2}} J_{m+2n+\frac{3}{2}}(s) J_m(\rho s) ds H(1-\rho^2) d\rho dt \\
&\quad \text{by (II.15)} \\
&= \frac{\mathbb{D}_m}{2B_{mn}} \int_0^\infty J_m(rt) \int_0^\infty \rho J_m(\rho t) \int_0^\infty s^{-\frac{3}{2}} J_{m+2n+\frac{3}{2}}(s) s J_m(\rho s) ds H(1-\rho^2) d\rho dt \\
&= \frac{1}{2B_{mn}} \mathbb{D}_m \int_0^\infty J_m(rt) \left[t^{-\frac{3}{2}} J_{m+2n+\frac{3}{2}}(t) \right] dt, \text{ by Hankel inversion formula} \\
&= \frac{1}{2B_{mn}} \int_0^\infty J_m(rt) t^{\frac{1}{2}} J_{m+2n+\frac{3}{2}}(t) dt, \text{ by (III.66)} \\
&= \frac{D_{mn} u_n^m(\rho)}{2B_{mn}} \text{ by (II.21)} \\
&= \frac{1}{\mu_{mn}} u_n^m(\rho)
\end{aligned}$$

where

$$\mu_{mn} = \frac{2B_{mn}}{D_{mn}} = \frac{\Gamma(n+1)\Gamma(n+m+1)}{\Gamma(n+\frac{3}{2})\Gamma(n+m+\frac{3}{2})}, \text{ by (II.20), (II.22) } \blacksquare$$

Now let's look at some properties of the eigenvalues μ_{mn} . Firstly, since $\Gamma(x)$ is monotone increasing for $x \geq 2$ and $\Gamma(1) = 1$, it is readily seen that for m and n not both zero that

$$\mu_{mn} = \frac{\Gamma(n+1)\Gamma(n+m+1)}{\Gamma(n+\frac{3}{2})\Gamma(n+m+\frac{3}{2})} < 1 \quad (\text{III.71})$$

A simple gamma function manipulation allows the μ_{mn} 's to be expressed in terms of the λ_{mn} 's as follows

$$\mu_{mn} = \frac{\lambda_{mn}}{(2n+2m+1)(2n+1)} \text{ for } m, n = 0, 1, 2, 3, \dots \quad (\text{III.72})$$

which enables the properties of μ_{mn} to be obtained from those of λ_{mn} .

The asymptotic result (III.27) shows that, for large n

$$\mu_{mn} \approx \frac{2}{\sqrt{(2n+2m+1)(2n+1)}} \quad (\text{III.73})$$

and hence, $\frac{1}{\mu_{mn}} \rightarrow \infty$ similar to n .

We can also readily see from (III.29), (III.30) that μ_{mn} is strictly decreasing in both m and n .

A bound can now be established on $\sum_{n=0}^{\infty} \mu_{mn}^2$ which will later be used to show that the inverse of $\mathbb{D}_m \mathbb{L}_m^1$ is Hilbert-Schmidt.

Theorem III.29 For $m, n = 0, 1, 2, \dots$

$$\sum_{n=0}^{\infty} \mu_{mn}^2 \leq \frac{\pi^2}{2} < \infty \quad (\text{III.74})$$

Proof.

$$\begin{aligned} \sum_{n=0}^{\infty} \mu_{mn}^2 &= \sum_{n=0}^{\infty} \left(\frac{\lambda_{mn}}{(2n+2m+1)(2n+1)} \right)^2 \text{ by (III.72)} \\ &\leq \sum_{n=0}^{\infty} \left(\frac{2(2n+2m+1)}{(2n+2m+1)(2n+1)} \right)^2 \text{ by Thm. (III.15)} \\ &= 4 + \sum_{n=1}^{\infty} \frac{4}{(2n+1)^2} \\ &= 4 \left(1 + \sum_{n=1}^{\infty} \frac{1}{(2n+1)^2} \right) = 4 \left(\frac{\pi^2}{8} \right) = \frac{\pi^2}{2} \blacksquare \end{aligned}$$

We have now established that the operator $\mathbb{D}_m \mathbb{L}_m^1$ has unbounded eigenvalues so will not be Hilbert-Schmidt or compact. To invert this operator we shall need to put tighter restrictions on its domain than simply being $L_2^1(0, 1)$. The next section will define a new space which will provide these tighter restrictions.

III.4 THE $L_{2,M}^\alpha(0, 1)$ HILBERT SPACES

We now define another two classes of Hilbert spaces $L_{2,m}^\alpha(0, 1)$ for $\alpha = 0, 1$. These spaces are going to be subsets of $L_2^\alpha(0, 1)$ for corresponding α values but not subspaces since they are not complete under the L_2^α norm. The new spaces are however

complete under their own norms, associated with new inner products based on the old ones. For solutions to our weakly-singular problem to exist, the right hand side functions will be required to belong to the $L_{2,m}^0(0,1)$ space, while the $L_{2,m}^1(0,1)$ space will form the solution space for our hyper-singular problem. The existence of the $L_{2,m}^1(0,1)$ space is far more important as its completeness is required to guarantee convergence of solution. Although they are defined for different purposes these spaces have exactly the same structure and are therefore considered at the same time. They both define the domain for an unbounded operator to map one-to-one into a Hilbert space.

To reduce repetition we introduce the following temporary notation.

Definition III.30 For $m, n = 0, 1, 2, 3, \dots$, define ω_{mn}^α and $r_{mn}^\alpha(\rho)$ for $\alpha = 0, 1$ as follows

$$\omega_{mn}^0 = \lambda_{mn} \quad (\text{III.75})$$

$$\omega_{mn}^1 = \frac{1}{\mu_{mn}} \quad (\text{III.76})$$

and

$$r_{mn}^0(\rho) = t_n^m(\rho) \quad (\text{III.77})$$

$$r_{mn}^1(\rho) = u_n^m(\rho) \quad (\text{III.78})$$

An important property of the ω_{mn}^α for $\alpha = 0, 1$ is that, for a given m and α , $\{\omega_{mn}^\alpha\}_{n=0}^\infty$ is a strictly increasing sequence with $\omega_{mn}^\alpha > 1$ (except $w_{00}^1 = \frac{4}{\pi}$). Now to define the spaces.

Definition III.31 For $m = 0, 1, 2, 3, \dots$ $\alpha = 0, 1$ let us define the inner product space, $L_{2,m}^\alpha(0,1)$ by

$$L_{2,m}^\alpha(0,1) = \left\{ f \in L_2^\alpha(0,1) : \sum_{n=0}^{\infty} (\omega_{mn}^\alpha)^2 |\langle f, r_{mn}^\alpha \rangle_\alpha|^2 < \infty \right\} \quad (\text{III.79})$$

with inner product

$$\langle f, g \rangle_{\alpha,m} = \sum_{n=0}^{\infty} (\omega_{mn}^\alpha)^2 \langle f, r_{mn}^\alpha \rangle_\alpha \overline{\langle g, r_{mn}^\alpha \rangle_\alpha} \quad (\text{III.80})$$

and Norm

$$\|f\|_{\alpha,m} = \sqrt{\langle f, f \rangle_{\alpha,m}} \quad (\text{III.81})$$

The sequence of functions s_{mn}^α for $n = 0, 1, 2, \dots$ is then defined by;

$$s_{mn}^\alpha(r) = \frac{r_{mn}^\alpha(r)}{\omega_{mn}^\alpha} \quad (\text{III.82})$$

and can be easily shown to form orthonormal bases for $L_{2,m}^\alpha(0, 1)$.

An Alternate notation to be used later is;

$$r_n^m(r) = \frac{t_n^m(r)}{\lambda_{mn}} = s_{mn}^0(r) \quad (\text{III.83})$$

$$s_n^m(r) = \mu_{mn} u_n^m(r) = s_{mn}^1(r) \quad (\text{III.84})$$

We can relate the inner product of $L_{2,m}^\alpha(0, 1)$ to that of $L_2^\alpha(0, 1)$ by using the easily established result;

For $m, n = 0, 1, 2, \dots$

$$\langle f, s_{mn}^\alpha \rangle_{\alpha,m} = \omega_{mn}^\alpha \langle f, r_{mn}^\alpha \rangle_\alpha \quad (\text{III.85})$$

Let us now define the operators \mathbb{S}_m^α that will be the inverses' of the \mathbb{L}_m^0 and $\mathbb{D}_m \mathbb{L}_m^1$ operators. The \mathbb{S}_m^0 operator will have domain $L_{2,m}^0(0, 1)$ while the \mathbb{S}_m^1 operator will map into the $L_{2,m}^1(0, 1)$ space.

Definition III.32 For a given $m = 0, 1, 2, \dots$,

$$g(r) = \sum_{n=0}^{\infty} g_n s_{mn}^0(r) \in L_{2,m}^0(0, 1)$$

and

$$f(\rho) = \sum_{n=0}^{\infty} f_n r_{mn}^1(\rho) \in L_2^1(0, 1)$$

we define the operators

$$\mathbb{S}_m^0 : L_{2,m}^0(0, 1) \rightarrow L_2^0(0, 1) \quad (\text{III.86})$$

$$\mathbb{S}_m^1 : L_2^1(0, 1) \rightarrow L_{2,m}^1(0, 1) \quad (\text{III.87})$$

by

$$\mathbb{S}_m^0 [g(r)](\rho) = \sum_{n=0}^{\infty} g_n r_{mn}^0(\rho) \quad (\text{III.88})$$

$$\mathbb{S}_m^1 [f(\rho)](r) = \sum_{n=0}^{\infty} f_n s_{mn}^1(r) \quad (\text{III.89})$$

We wish to show the completeness of the $L_{2,m}^\alpha(0,1)$ spaces, to do this we first introduce a lemma relating Cauchy sequences in these spaces with those in the $L_2^\alpha(0,1)$ spaces.

Lemma III.33 *If $\{f^{(i)}\}$ is a Cauchy sequence in $L_{2,m}^\alpha(0,1)$ for a given $m = 0, 1, 2, \dots$, then*

1. $\{f^{(i)}\}$ is also a Cauchy sequence in $L_2^\alpha(0,1)$
2. $\{g^{(i)}\} = \left\{ \begin{array}{ll} \{\mathbb{S}_m^0 f^{(i)}\} & , \alpha = 0 \\ \{\mathbb{D}_m \mathbb{L}_m^1 f^{(i)}\} & , \alpha = 1 \end{array} \right\}$ is a Cauchy sequence in $L_2^\alpha(0,1)$

Proof.

1. For $i = 0, 1, 2, \dots$

$$f^{(i)} = \sum_{n=0}^{\infty} f_n^{(i)} s_{mn}^\alpha(r) = \sum_{n=0}^{\infty} \frac{f_n^{(i)}}{\omega_{mn}^\alpha} r_{mn}^\alpha(r)$$

Now since $\{f^{(i)}\}$ is a Cauchy sequence in $L_{2,m}^\alpha(0,1)$ for any given integer $p \geq 1$ and $\epsilon > 0$, there exists an $M > 0$ such that

$$i > M \implies \|f^{(i+p)} - f^{(i)}\|_{\alpha,m}^2 < \epsilon$$

or that

$$i > M \implies \sum_{n=0}^{\infty} |f_n^{(i+p)} - f_n^{(i)}|^2 < \epsilon$$

Now

$$\|f^{(i+p)} - f^{(i)}\|_\alpha^2 = \sum_{n=0}^{\infty} \frac{1}{(\omega_{mn}^\alpha)^2} |f_n^{(i+p)} - f_n^{(i)}|^2 \leq \sum_{n=0}^{\infty} |f_n^{(i+p)} - f_n^{(i)}|^2 < \epsilon$$

Hence $\{f^{(i)}\}$ is a Cauchy sequence in $L_2^\alpha(0,1)$ ■

2. For $i = 0, 1, 2, \dots$

$$g^{(i)}(r) = \sum_{n=0}^{\infty} f_n^{(i)} r_{mn}^{\alpha}(r)$$

Now for any integer $p \geq 1$

$$\|g^{(i+p)} - g^{(i)}\|_{\alpha}^2 = \sum_{n=0}^{\infty} |f_n^{(i+p)} - f_n^{(i)}|^2 = \|f^{(i+p)} - f^{(i)}\|_{\alpha, m}^2 < \epsilon$$

Hence $\{g^{(i)}\}$ is Cauchy in $L_2^{\alpha}(0, 1)$ ■

We now establish the completeness of the $L_{2,m}^{\alpha}(0, 1)$ space and note the useful property that if a Cauchy sequence $\{f^{(i)}\} \in L_{2,m}^{\alpha}(0, 1)$ has a limit $f \in L_{2,m}^{\alpha}(0, 1)$ then it is not only Cauchy in $L_2^{\alpha}(0, 1)$ but has the same limit $f \in L_2^{\alpha}(0, 1)$.

Theorem III.34 Every Cauchy sequence $\{f^{(i)}\}$ in $L_{2,m}^{\alpha}(0, 1)$ (for a given $m = 0, 1, 2, \dots$) converges to a unique limit in $L_{2,m}^{\alpha}(0, 1)$ and hence the space is complete

Proof. By above Lemma for, $f^{(i)} = \sum_{n=0}^{\infty} f_n^{(i)} s_{mn}^{\alpha}$, the sequence $\{g^{(i)}\}$, given by

$$g^{(i)} = \sum_{n=0}^{\infty} f_n^{(i)} r_{mn}^{\alpha}$$

is Cauchy in $L_2^{\alpha}(0, 1)$ and has a unique limit

$$g = \sum_{n=0}^{\infty} g_n r_{mn}^{\alpha} \in L_2^{\alpha}(0, 1)$$

Now, there exists an $M > 0$ such that

$$i > M \implies \|g - g^{(i)}\|_{\alpha}^2 = \sum_{n=0}^{\infty} |g_n - f_n^{(i)}|^2 < \epsilon$$

Let us consider $f = \sum_{n=0}^{\infty} g_n s_{mn}^{\alpha}$ then

$$\|f\|_{\alpha, m}^2 = \sum_{n=0}^{\infty} |g_n|^2 = \|g\|_{\alpha}^2 < \infty$$

and hence $f \in L_{2,m}^{\alpha}(0, 1)$.

Let $i > M$ then

$$\|f - f^{(i)}\|_{\alpha, m}^2 = \sum_{n=0}^{\infty} |g_n - f_n^{(i)}|^2 < \epsilon$$

This shows that $L_{2, m}^{\alpha}(0, 1)$ is complete.

Now note that

$$\begin{aligned} \|f - f^{(i)}\|_{\alpha}^2 &= \sum_{n=0}^{\infty} \frac{1}{(\omega_{mn}^{\alpha})^2} |g_n - f_n^{(i)}|^2 \\ &\leq \sum_{n=0}^{\infty} |g_n - f_n^{(i)}|^2 < \epsilon \end{aligned}$$

So f is the limit of the Cauchy sequence $\{f^{(i)}\}$ in both spaces ■

Now a similar result regarding weakly-convergent sequences.

Lemma III.35 For a given $m = 0, 1, 2, \dots$, let $\{f^{(i)}\}$ be a sequence in $L_{2, m}^{\alpha}(0, 1)$ weakly convergent to $f \in L_{2, m}^{\alpha}(0, 1)$ then $\{f^{(i)}\}$ is also a weakly convergent sequence in $L_2^{\alpha}(0, 1)$ converging to the same limit $f \in L_2^{\alpha}(0, 1)$

Proof. Let

$$h = \sum_{n=0}^{\infty} h_n r_{mn}^{\alpha} \in L_2^{\alpha}(0, 1)$$

then

$$g = \sum_{n=0}^{\infty} h_n s_{mn}^{\alpha} \in L_{2, m}^{\alpha}(0, 1)$$

and by definition

$$\lim_{i \rightarrow \infty} \langle f^{(i)} - f, g \rangle_{\alpha, m} \rightarrow 0$$

so that

$$\begin{aligned}
\langle f^{(i)} - f, h \rangle_\alpha &= \sum_{n=0}^{\infty} \langle f^{(i)} - f, r_{mn}^\alpha \rangle_\alpha \langle h, r_{mn}^\alpha \rangle_\alpha \text{ by Parseval's Formula} \\
&< \sum_{n=0}^{\infty} \omega_{mn}^\alpha \langle f^{(i)} - f, r_{mn}^\alpha \rangle_\alpha \langle h, r_{mn}^\alpha \rangle_\alpha \\
&= \sum_{n=0}^{\infty} (\omega_{mn}^\alpha)^2 \langle f^{(i)} - f, r_{mn}^\alpha \rangle_\alpha \frac{h_n}{\omega_{mn}^\alpha} \\
&= \sum_{n=0}^{\infty} (\omega_{mn}^\alpha)^2 \langle f^{(i)} - f, r_{mn}^\alpha \rangle_\alpha \langle g, r_{mn}^\alpha \rangle_\alpha \\
&= \langle f^{(i)} - f, g \rangle_{\alpha, m} \rightarrow 0 \text{ as } i \rightarrow \infty
\end{aligned}$$

meaning

$$\lim_{i \rightarrow \infty} \langle f^{(i)} - f, h \rangle_\alpha \rightarrow 0, \forall h \in L_2^\alpha(0, 1)$$

and hence result ■

Theorem III.36 For any given $m = 0, 1, 2, \dots$ the operator

$$\mathbb{L}_m^0 : L_2^0(0, 1) \rightarrow L_{2,m}^0(0, 1) \quad (\text{III.90})$$

is a Hilbert space isomorphism with inverse

$$\mathbb{S}_m^0 : L_{2,m}^0(0, 1) \rightarrow L_2^0(0, 1) \quad (\text{III.91})$$

Proof. The sequence $\{t_n^m\}_{n=0}^\infty$ is a basis for $L_2^0(0, 1)$ and the sequence $\{r_n^m\}_{n=0}^\infty = \left\{ \frac{t_n^m}{\lambda_{mn}} \right\}_{n=0}^\infty$ is a basis for $L_{2,m}^0(0, 1)$ since

$$\mathbb{L}_m^0 t_n^m = r_n^m$$

it follows that \mathbb{L}_m^0 is a Hilbert space isomorphism.

We also have

$$\mathbb{S}_m^0 r_n^m = t_n^m$$

which implies that \mathbb{S}_m^0 is not only a Hilbert space isomorphism but the inverse of \mathbb{L}_m^0 ■

Theorem III.37 For any given $m = 0, 1, 2, \dots$ the operator

$$\mathbb{D}_m \mathbb{L}_m^1 : L_{2,m}^1(0,1) \rightarrow L_2^1(0,1) \quad (\text{III.92})$$

is a Hilbert space isomorphism with inverse

$$\mathbb{S}_m^1 : L_2^1(0,1) \rightarrow L_{2,m}^1(0,1) \quad (\text{III.93})$$

Proof. The sequence $\{u_n^m\}_{n=0}^\infty$ is a basis for $L_2^1(0,1)$ and the sequence $\{s_n^m\}_{n=0}^\infty = \left\{ \frac{u_n^m}{\mu_{mn}} \right\}_{n=0}^\infty$ is a basis for $L_{2,m}^1(0,1)$ since

$$\mathbb{D}_m \mathbb{L}_m^1 s_n^m = u_n^m$$

it follows that $\mathbb{D}_m \mathbb{L}_m^1$ is a Hilbert space isomorphism.

We also have that

$$\mathbb{S}_m^1 u_n^m = s_n^m$$

which implies that \mathbb{S}_m^1 is not only a Hilbert space isomorphism but the inverse of $\mathbb{D}_m \mathbb{L}_m^1$ ■

We can now see that the isomorphism \mathbb{S}_m^0 has unbounded eigenvalues (λ_{mn}) and will hence be unbounded and not compact, while the isomorphism \mathbb{S}_m^1 has bounded eigenvalues (μ_{mn}). Since \mathbb{S}_m^1 has strictly decreasing eigenvalues that are all less than 1 and converge to zero similarly to $\frac{1}{n}$ we are able to define it as an integral operator with the following well defined kernel.

Theorem III.38 For any given $m = 0, 1, 2, \dots$

$$\mathbb{S}_m^1 g = \int_0^1 w^1(\rho) g(\rho) S(r, \rho) d\rho \quad (\text{III.94})$$

where

$$S(r, \rho) = \sum_{n=0}^{\infty} \mu_{mn} u_n^m(r) u_n^m(\rho) \quad (\text{III.95})$$

Proof.

$$\begin{aligned}
& \int_0^1 w^1(\rho) g(\rho) S(r, \rho) d\rho \\
&= \int_0^1 w^1(\rho) \left(\sum_{i=0}^{\infty} g_i u_i^m(\rho) \right) \left(\sum_{n=0}^{\infty} \mu_{mn} u_n^m(r) u_n^m(\rho) \right) d\rho \\
&= \sum_{n=0}^{\infty} \sum_{i=0}^{\infty} g_i \mu_{mn} u_n^m(r) \int_0^1 w^1(\rho) u_i^m(\rho) u_n^m(\rho) d\rho \\
&= \sum_{n=0}^{\infty} g_n \mu_{nn} u_n^m(r) = \mathbb{S}_m^1 g \blacksquare
\end{aligned}$$

We can now use this integral operator definition to put a bound on the operator norm.

Theorem III.39 For $m = 0, 1, 2, \dots$

$$\|\mathbb{S}_m^1\|_1^2 = \sum_{n=0}^{\infty} \mu_{nn}^2 \leq \frac{\pi^2}{2} < \infty \quad (\text{III.96})$$

Proof. $\|\mathbb{S}_m^1\|_1^2$

$$\begin{aligned}
&= \int_0^1 w^1(r) \int_0^1 w^1(\rho) \left| \sum_{n=0}^{\infty} \mu_{nn} u_n^m(r) u_n^m(\rho) \right|^2 d\rho dr \\
&= \sum_{n=0}^{\infty} \mu_{nn}^2 \text{ by orthogonality} \\
&\leq \frac{\pi^2}{2} \text{ by (III.74)} \blacksquare
\end{aligned}$$

Here we have established that \mathbb{S}_m^1 is Hilbert-Schmidt and hence a self adjoint Compact Operator. We now have all the basic tools to proceed to solving the integral equations themselves.

CHAPTER IV

A WEAKLY-SINGULAR INTEGRAL EQUATION

IV.1 INTRODUCTION

In this chapter we will focus on solving the following one-dimensional weakly-singular integral equation

$$\int_0^1 \{l_m(\rho, r) + k(\rho, r)\} w^0(\rho) f(\rho) d\rho = g(r), 0 < r < 1 \quad (\text{IV.1})$$

where $m = 0, 1, 2, \dots$; and $k(\rho, r) \in L_2^0(0, 1) \times L_2^0(0, 1)$ is a continuous kernel.

By introducing the $L_2^0(0, 1)$ integral operator \mathbb{K}^0 with continuous kernel $k(\rho, r)$

$$[\mathbb{K}^0 f(\rho)](r) = \int_0^1 k(\rho, r) f(\rho) w^0(\rho) d\rho \quad (\text{IV.2})$$

and making use of the weakly-singular integral operator \mathbb{L}_m^0 , discussed in Chapter III, we can represent the integral equation by the operator equation

$$[(\mathbb{L}_m^0 + \mathbb{K}^0) f(\rho)](r) = g(r) \in L_{2,m}^0(0, 1) \quad (\text{IV.3})$$

for $m = 0, 1, 2, \dots$, with solutions to f being sought in $L_2^0(0, 1)$.

As a first step to developing a solution we begin by examining the case where the \mathbb{K}^0 operator is absent (i.e. the dominant equation).

IV.2 THE DOMINANT WEAKLY-SINGULAR EQUATION

The dominant weakly-singular integral equation takes the form

$$[\mathbb{L}_m^0 f(\rho)](r) = g(r) \in L_{2,m}^0(0, 1) \quad (\text{IV.4})$$

where $m = 0, 1, 2, \dots$

We have already looked at the eigen-structure of the integral operator \mathbb{L}_m^0 and have established it is a compact self adjoint operator with eigenvalues λ_{mn}^{-1} and eigenfunctions $t_n^m(\rho)$. We showed in Chapter III that the operator \mathbb{L}_m^0 :

$L_2^0(0, 1) \rightarrow L_{2,m}^0(0, 1)$ can be considered a Hilbert space isomorphism with inverse $\mathbb{S}_m^0 : L_{2,m}^0(0, 1) \rightarrow L_2^0(0, 1)$. The following theorem restates this in a form more meaningful to this chapter.

Theorem IV.1 For a given $m = 0, 1, 2, \dots$, let

$$g(r) = \sum_{n=0}^{\infty} g_n r_n^m(r) \in L_{2,m}^0(0, 1)$$

then the integral equation

$$\mathbb{L}_m^0[f(\rho)](r) = g(r) \in L_{2,m}^0(0, 1) \quad (\text{IV.5})$$

has a unique solution $f \in L_2^0(0, 1)$ given by

$$f(\rho) = \mathbb{S}_m^0[g(r)](\rho) = \sum_{n=0}^{\infty} g_n t_n^m(\rho) \quad (\text{IV.6})$$

Proof. By Thm. III.36 we can apply the isomorphic inverse (\mathbb{S}_m^0) of \mathbb{L}_m^0 to get the following unique solution for f

$$\begin{aligned} [\mathbb{L}_m^0 f(\rho)](r) &= g(r) \Leftrightarrow \mathbb{S}_m^0 \mathbb{L}_m^0 f = \mathbb{S}_m^0 g \\ \Leftrightarrow f(\rho) &= \mathbb{S}_m^0[g(r)](\rho) = \sum_{n=0}^{\infty} g_n t_n^m(\rho) \quad \blacksquare \end{aligned}$$

IV.3 THE GENERAL EQUATION

We will now investigate the circumstances under which we are able to invert the operator $(\mathbb{L}_m^0 + \mathbb{K}^0)$ and hence find a solution to (IV.3). The following theorem will give us a sufficient condition.

Theorem IV.2 For a given $m = 0, 1, 2, \dots$ the integral equation

$$[(\mathbb{L}_m^0 + \mathbb{K}^0)f(\rho)](r) = g(r) \in L_{2,m}^0(0, 1) \quad (\text{IV.7})$$

has the unique solution

$$f = (\mathbb{I} + \mathbb{S}_m^0 \mathbb{K}^0)^{-1} \mathbb{S}_m^0 g \quad (\text{IV.8})$$

provided $\mathbb{S}_m^0 \mathbb{K}^0$ is compact and the null-space of $(\mathbb{I} + \mathbb{S}_m^0 \mathbb{K}^0)$ is trivial.

Proof. By Thm. IV.1, (IV.7) is equivalent to

$$(\mathbb{I} + \mathbb{S}_m^0 \mathbb{K}^0) f = \mathbb{S}_m^0 g \in L_2^0(0, 1) \quad (\text{IV.9})$$

By the Fredholm theorems [16], this equation will have the unique solution

$$f = (\mathbb{I} + \mathbb{S}_m^0 \mathbb{K}^0)^{-1} \mathbb{S}_m^0 g$$

provided $\mathbb{S}_m^0 \mathbb{K}^0$ is compact and the null-space of $(\mathbb{I} + \mathbb{S}_m^0 \mathbb{K}^0)$ is trivial. ■

We now have conditions that enable us to tell when our integral equation (IV.1) has a unique $L_2^0(0, 1)$ solution. Next we look for conditions on the kernel of \mathbb{K}^0 that will guarantee compactness of the operator $\mathbb{S}_m^0 \mathbb{K}^0$ and hence the existence of the unique solution exhibited in Thm. IV.2.

We begin by looking at some matrix representations for $L_2^0(0, 1)$ kernels, introducing some notation as we go.

Definition IV.3 For a $L_2^0(0, 1)$ integral operator \mathbb{K}^0 with continuous kernel $k(\rho, r)$ we can define the matrices $K^{mn} = (K_{ij}^{mn})$ and $K^m = K^{mm}$ as follows

$$K_{ij}^{mn} = \langle \mathbb{K}^0 t_i^m, t_j^n \rangle_0 \quad (\text{IV.10})$$

$$= \int_0^1 \int_0^1 k(\rho, r) t_i^m(\rho) t_j^n(r) w^0(\rho) w^0(r) d\rho dr \quad (\text{IV.11})$$

We will show that the kernel of such an operator can be expanded in terms of the basis functions $\{t_i^m\}_{i=1}^\infty$, $m = 0, 1, 2, \dots$

Theorem IV.4 For $m, n = 0, 1, 2, 3, \dots$ and \mathbb{K}^0 an $L_2^0(0, 1)$ integral operator with continuous kernel $k(\rho, r)$, then

$$k(\rho, r) = \sum_{i=0}^{\infty} \sum_{j=0}^{\infty} K_{ij}^{mn} t_i^m(\rho) t_j^n(r) \quad (\text{IV.12})$$

and

$$\|\mathbb{K}^0\|_0^2 = \sum_{i=0}^{\infty} \sum_{j=0}^{\infty} |K_{ij}^{mn}|^2 \quad (\text{IV.13})$$

Proof. Since $k(\rho, r)$ is a bounded $L_2^0(0, 1)$ kernel and the $t_n^m(r)$ functions are real;

$$\begin{aligned} k(\rho, r) &= \sum_{i=0}^{\infty} t_i^m(\rho) \int_0^1 k(x, r) t_i^m(x) w^0(x) dx \\ &= \sum_{i=0}^{\infty} t_i^m(\rho) [\mathbb{K}^0 t_i^m](r) \\ &= \sum_{i=0}^{\infty} t_i^m(\rho) \sum_{j=0}^{\infty} \langle \mathbb{K}^0 t_i^m, t_j^n \rangle_0 t_j^n(r) \\ &= \sum_{i=0}^{\infty} \sum_{j=0}^{\infty} K_{ij}^{mn} t_i^m(\rho) t_j^n(r) \end{aligned}$$

Hence,

$$\begin{aligned} \|\mathbb{K}^0\|_0^2 &= \int_0^1 \int_0^1 w^0(r) w^0(\rho) |k(\rho, r)|^2 d\rho dr \\ &= \sum_{i=0}^{\infty} \sum_{j=0}^{\infty} |K_{ij}^{mn}|^2 \blacksquare \end{aligned}$$

The above kernel expansion can now be used to find an expansion of $\mathbb{K}^0 f$ for any function $f \in L_2^0(0, 1)$.

Theorem IV.5 If \mathbb{K}^0 is an $L_2^0(0, 1)$ integral operator with continuous kernel $k(\rho, r)$ and

$$f(\rho) = \sum_{k=0}^{\infty} f_k t_k^m(\rho) \in L_2^0(0, 1)$$

then

$$\mathbb{K}^0 f = \sum_{i=0}^{\infty} \sum_{j=0}^{\infty} K_{ij}^{mn} f_i t_j^n(r) \quad (\text{IV.14})$$

Proof.

$$\begin{aligned} \mathbb{K}^0 f &= \int_0^1 k(r, \rho) f(\rho) w^0(\rho) d\rho \\ &= \sum_{i=0}^{\infty} \sum_{j=0}^{\infty} \sum_{k=0}^{\infty} f_k K_{ij}^{mn} t_j^n(r) \int_0^1 t_i^m(\rho) t_k^m(\rho) w^0(\rho) d\rho \\ &= \sum_{i=0}^{\infty} \sum_{j=0}^{\infty} K_{ij}^{mn} f_i t_j^n(r) \blacksquare \end{aligned}$$

To correctly apply \mathbb{S}_m^0 to $\mathbb{K}^0 f$ we need to ensure that $\mathbb{K}^0 f$ belongs to the $L_{2,m}^0(0,1)$ space. The following theorem establishes a condition that guarantees this will be true and the theorem thereafter shows that the same condition guarantees compactness of $\mathbb{S}_m^0 \mathbb{K}^0$.

Theorem IV.6 *If \mathbb{K}^0 is an $L_2^0(0,1)$ integral operator with continuous kernel $k(\rho, r)$ such that*

$$\sum_{i=0}^{\infty} \sum_{j=0}^{\infty} \lambda_{nj}^2 |K_{ij}^{mn}|^2 < \infty \quad (\text{IV.15})$$

and

$$f(\rho) = \sum_{k=0}^{\infty} f_k t_k^n(\rho) \in L_2^0(0,1)$$

then

$$g(r) = [\mathbb{K}^0 f(\rho)](r) \in L_{2,m}^0(0,1) \quad (\text{IV.16})$$

Proof.

$$\begin{aligned} [\mathbb{K}^0 f(\rho)](r) &= \sum_{i=0}^{\infty} \sum_{j=0}^{\infty} K_{ij}^{mn} f_i t_j^n(r) \\ &= \sum_{j=0}^{\infty} g_j t_j^n(r) \end{aligned}$$

where

$$g_j = \sum_{i=0}^{\infty} K_{ij}^{mn} f_i$$

By the Cauchy-Schwartz inequality we then have

$$|g_j|^2 \leq \sum_{i=0}^{\infty} |K_{ij}^{mn}|^2 \cdot \sum_{i=0}^{\infty} |f_i|^2$$

So that

$$\begin{aligned} \|g\|_{0,m}^2 &= \sum_{j=0}^{\infty} \lambda_{nj}^2 |g_j|^2 \\ &\leq \sum_{i=0}^{\infty} \sum_{j=0}^{\infty} \lambda_{nj}^2 |K_{ij}^{mn}|^2 \cdot \|f\|_0^2 < \infty \end{aligned}$$

and result follows ■

The easiest way to show compactness of $\mathbb{S}_m^0 \mathbb{K}^0$ is to show it is an $L_2^0(0, 1)$ integral operator with the continuous kernel

$$\mathbb{S}_m^0 k(\rho, r) = \sum_{i=0}^{\infty} \sum_{j=0}^{\infty} \lambda_{mj} K_{ij}^m t_i^m(\rho) t_j^m(r) \quad (\text{IV.17})$$

i.e. that it is Hilbert-Schmidt.

The following theorem establishes the conditions for this to be true.

Theorem IV.7 *If \mathbb{K}^0 is an $L_2^0(0, 1)$ integral operator with continuous kernel $k(\rho, r)$ such that*

$$\sum_{i=0}^{\infty} \sum_{j=0}^{\infty} \lambda_{mj}^2 |K_{ij}^m|^2 < \infty \quad (\text{IV.18})$$

then $\mathbb{S}_m^0 \mathbb{K}^0$ is Hilbert-Schmidt and hence compact and additionally

$$\|\mathbb{S}_m^0 \mathbb{K}^0\|_0^2 = \sum_{i=0}^{\infty} \sum_{j=0}^{\infty} \lambda_{mj}^2 |K_{ij}^m|^2$$

Proof. *By Thm. IV.6, for each $i = 0, 1, 2, \dots$,*

$$\mathbb{K}^0 t_i^m \in L_{2,m}^0(0, 1)$$

and hence by Thm. III.37, $\mathbb{S}_m^0 \mathbb{K}^0 t_i^m$ is both defined and belongs to $L_2^0(0, 1)$.

The matrix of $\mathbb{S}_m^0 \mathbb{K}^0$ is given by

$$\begin{aligned} \langle \mathbb{S}_m^0 \mathbb{K}^0 t_i^m, t_j^m \rangle_0 &= \left\langle \mathbb{S}_m^0 \left[\sum_{q=0}^{\infty} K_{iq}^m t_q^m \right], t_j^m \right\rangle_0 \quad \text{by (IV.14)} \\ &= \left\langle \sum_{q=0}^{\infty} \lambda_{mq} K_{iq}^m t_q^m, t_j^m \right\rangle_0 \\ &= \lambda_{mj} K_{ij}^m \end{aligned}$$

So that by Thm. IV.4

$$\|\mathbb{S}_m^0 \mathbb{K}^0\|_0^2 = \sum_{i=0}^{\infty} \sum_{j=0}^{\infty} \lambda_{mj}^2 |K_{ij}^m|^2 < \infty$$

which implies $\mathbb{S}_m^0 \mathbb{K}^0$ is an $L_2^0(0,1)$ operator, Hilbert-Schmidt and compact ■

The previous theorem provides a sufficient condition for the compactness of $\mathbb{S}_m^0 \mathbb{K}^0$ but not one that is easily verified. We therefore look for simpler conditions on the kernel, $k(\rho, r)$, that will also prove to be sufficient.

Definition IV.8 For the $L_2^0(0,1)$ integral operator \mathbb{K}^0 with the continuous kernel, $k(\rho, r)$ and a given $m = 0, 1, 2, \dots$ define the integral operator

$$[\mathbb{V}_m^0 f(\rho)](r) = \int_0^1 V_m(\rho, r) f(\rho) w^0(\rho) d\rho \quad (\text{IV.19})$$

with kernel

$$V_m(\rho, r) = r^m \frac{d}{dr} \left(\frac{1}{r^m} k(\rho, r) \right) \quad (\text{IV.20})$$

Definition IV.9 For a given $m = 0, 1, 2, \dots$ the continuous kernel, $k(\rho, r)$ of the integral operator \mathbb{K}^0 , is called a V_m - bounded kernel if the following conditions are satisfied:

1. $k(\rho, r)$ is self adjoint,

$$k(\rho, r) = \overline{k(r, \rho)} \quad (\text{IV.21})$$

2. $k(\rho, r)$ is an $L_2^0(0,1)$ square integrable kernel, i.e.

$$\|\mathbb{K}^0\|_0 < \infty \quad (\text{IV.22})$$

3. $V_m(\rho, r)$ is also an $L_2^0(0,1)$ square integrable kernel, that is

$$\|\mathbb{V}_m^0\|_0 < \infty \quad (\text{IV.23})$$

Before we establish the properties of V_m and V_m - bounded kernels we investigate the behavior of the t_n^m functions under the action of the differential operator $r^m \frac{d}{dr} \left(\frac{1}{r^m} \cdot \right)$.

Lemma IV.10

$$\rho^m \frac{d}{d\rho} (\rho^{-m} t_n^m(\rho)) = \sqrt{2n(2n+2m+1)} u_{n-1}^{m+1}(\rho) \quad (\text{IV.24})$$

Proof. By making use of the well known identity ([5], 8.6.6, p334)

$$P_n^m(x) = (-1)^m (1-x^2)^{\frac{m}{2}} \frac{d^m}{dx^m} P_n(x), m \geq 0 \quad (\text{IV.25})$$

and the definition t_n^m of we get

$$\begin{aligned} \rho^m \frac{d}{d\rho} (\rho^{-m} t_n^m(\rho)) &= T_n^m \frac{P_{2n+m}^{m+1}(\sqrt{1-\rho^2})}{\sqrt{1-\rho^2}} \\ &= T_n^m \frac{P_{2(n-1)+(m+1)+1}^{m+1}(\sqrt{1-\rho^2})}{\sqrt{1-\rho^2}} \\ &= \frac{T_n^m}{U_{n-1}^{m+1}} u_{n-1}^{m+1}(\rho), \text{ by (III.6)} \\ &= \sqrt{2n(2n+2m+1)} u_{n-1}^{m+1}(\rho), \text{ by (III.7, III.8)} \blacksquare \end{aligned}$$

From the above lemma, we can see that \mathbb{V}_m^0 can be expressed in terms of the u_{n-1}^{m+1} functions a property which is exploited in the following Lemma along with the ability to express these functions in terms of the t_i^{m+1} functions using (III.51).

Lemma IV.11 For a fixed non-negative integer m , let $k(r, \rho)$ be a V_m - bounded kernel then

$$\sum_{i=1}^{\infty} \sum_{j=0}^{\infty} 2i(2i+2m+1) |K_{ji}^m|^2 \leq 4 \|\mathbb{V}_m^0\|_0^2 < \infty \quad (\text{IV.26})$$

Proof.

$$\begin{aligned} V_m(\rho, r) &= r^m \frac{d}{dr} \left(\frac{1}{r^m} k(\rho, r) \right) \\ &= \sum_{i=0}^{\infty} \sum_{j=0}^{\infty} K_{ji}^m r^m \frac{d}{dr} \left(\frac{1}{r^m} t_i^m(r) \right) t_j^m(\rho) \\ &= \sum_{i=1}^{\infty} \sum_{j=0}^{\infty} K_{ji}^m \sqrt{2i(2i+2m+1)} u_{i-1}^{m+1}(r) t_j^m(\rho), \text{ by (IV.24)} \end{aligned}$$

we can then see and that

$$\begin{aligned}
& K_{ji}^m \sqrt{2i(2i+2m+1)} \\
&= \int_0^1 w^0(r) \int_0^1 w^1(\rho) V_m(\rho, r) u_{i-1}^{m+1}(\rho) t_j^m(r) dr d\rho \\
&= \int_0^1 w^0(r) \int_0^1 w^0(\rho) V_m(\rho, r) [\alpha_i^m t_i^{m+1}(\rho) + \beta_i^m t_{i-1}^{m+1}(\rho)] t_j^m(r) dr d\rho, \\
&\quad \text{by (III.51)} \\
&= \alpha_i^m (V_m)_{ij}^{(m+1)m} + \beta_i^m (V_m)_{(i-1)j}^{(m+1)m} \tag{IV.27}
\end{aligned}$$

Where for, $i = 1, 2, 3, \dots$,

$$0 < \alpha_i^m = \sqrt{\frac{(2i)(2i+2m+2)}{(4i+2m+1)(4i+2m+3)}} < 1$$

and

$$0 < \beta_i^m = \sqrt{\frac{(2i-1)(2i+2m+1)}{(4i+2m-1)(4i+2m+1)}} < 1$$

We therefore have that

$$\begin{aligned}
|K_{ji}^m|^2 2i(2i+2m+1) &= \left| \alpha_i^m (V_m)_{ij}^{(m+1)m} + \beta_i^m (V_m)_{(i-1)j}^{(m+1)m} \right|^2 \\
&\leq 2 \left| (V_m)_{ij}^{(m+1)m} \right|^2 + 2 \left| (V_m)_{(i-1)j}^{(m+1)m} \right|^2 \tag{IV.28}
\end{aligned}$$

and hence

$$\begin{aligned}
& \sum_{i=1}^{\infty} \sum_{j=0}^{\infty} 2i(2i+2m+1) |K_{ji}^m|^2 \\
&\leq 2 \sum_{i=1}^{\infty} \sum_{j=0}^{\infty} \left| (V_m)_{ij}^{(m+1)m} \right|^2 + 2 \sum_{i=1}^{\infty} \sum_{j=0}^{\infty} \left| (V_m)_{(i-1)j}^{(m+1)m} \right|^2 \\
&\leq 4 \|V_m^0\|_0^2 < \infty
\end{aligned}$$

as required ■

Theorem IV.12 For a fixed non-negative integer m , \mathbb{K}^0 an $L_2^0(0,1)$ integral operator with the V_m -bounded kernel $k(r, \rho)$ then $\mathbb{S}_m^0 \mathbb{K}^0$ is Hilbert-Schmidt.

Proof. Since $k(\rho, r)$ is a Hermitian kernel, $K_{ij}^m = K_{ji}^m$ and therefore

$$\begin{aligned} \|\mathbb{S}_m^0 \mathbb{K}^0\|_0^2 &= \sum_{i=0}^{\infty} \sum_{j=0}^{\infty} \lambda_{mi}^2 |K_{ji}^m|^2 = \lambda_{m0}^2 \sum_{j=0}^{\infty} |K_{ji}^m|^2 + \sum_{i=1}^{\infty} \sum_{j=0}^{\infty} \lambda_{mi}^2 |K_{ji}^m|^2 \\ &\leq \lambda_{m0}^2 \|\mathbb{K}\|_0^2 + \sum_{i=1}^{\infty} \sum_{j=0}^{\infty} 4(2i + 2m + 1) |K_{ji}^m|^2 \text{ by (III.34)} \\ &\leq \lambda_{m0}^2 \|\mathbb{K}\|_0^2 + 4 \|\mathbb{V}_m^0\|_0^2 < \infty \end{aligned}$$

which implies that $\mathbb{S}_m^0 \mathbb{K}^0$ is an $L_2^0(0, 1)$ operator and the result follows ■

A potentially more verifiable way of establishing that $\mathbb{S}_m^0 \mathbb{K}^0$ is compact is given in the next theorem.

Theorem IV.13 If $k(\rho, r)$ is an Hermitian continuous kernel and is such that $\frac{1}{r}k(\rho, r)$ and $\frac{\partial}{\partial r}k(\rho, r)$ are $L_2^0(0, 1)$ kernels then $\mathbb{S}_m^0 \mathbb{K}^0$ is Hilbert-Schmidt.

Proof. Since $\frac{1}{r}k(\rho, r)$ and $\frac{\partial}{\partial r}k(\rho, r)$ are $L_2^0(0, 1)$ kernels then so are $k(\rho, r)$ and $V_m(\rho, r) = r^m \frac{\partial}{\partial r} \left[\frac{1}{r^m} k(\rho, r) \right]$. The result follows by Thm. IV.12 ■

IV.4 NUMERICAL SOLUTIONS

IV.4.1 Quadrature

We will now identify the quadrature scheme we will use throughout for integrating over the region $[0, 1]$, the quadrature points are also the points that will be used as collocation points for the collocation method. We start by defining these quadrature points and their associated weight functions.

Definition IV.14

M : Number of Quadrature points used

x_p : The Gaussian abscissae

$$P_{2M}(x_p) = 0, p = 1, 2, 3, \dots, 2M \quad (\text{IV.29})$$

w_p : The Gaussian weights

$$w_p = \frac{2}{\left[(1 - x_p^2)^2 P'_{2M}(x_p) \right]} \quad (\text{IV.30})$$

q : The redefined indices;

$$q = p - M \text{ for } p = M + 1, M + 2, M + 3, \dots, 2M \quad (\text{IV.31})$$

r_q : The points used

$$r_q = \sqrt{1 - x_q^2}, q = 1, 2, \dots, M \quad (\text{IV.32})$$

Lemma IV.15

$$\int_0^1 w^0(r) f(r) dr \simeq \sum_{q=1}^M w_q f(r_q) \quad (\text{IV.33})$$

Proof. By making the change of variable

$$r = \sqrt{1 - x^2} \quad (\text{IV.34})$$

and using the evenness of $g(\sqrt{1 - x^2})$ we can apply Gauss' Formula ([5], 25.4.29) giving;

$$\int_0^1 w^0(r) g(r) dr = \frac{1}{2} \sum_{i=1}^{2M} w_i g(r_i) \quad (\text{IV.35})$$

Now since $w_i = w_j$ and $\rho_i = \rho_j$ whenever $|x_i| = |x_j|$ this formula would be using the same points twice, using only the non-negative x_i values, by using just the r_q points as in (IV.31), we obtain the given result ■

IV.4.2 The Galerkin Method

For the Galerkin method the solution of (IV.9) and hence (IV.1), is approximated by the finite sum

$$f^{(N)}(\rho) = \sum_{j=0}^N f_j t_j^m(\rho) \quad (\text{IV.36})$$

where the coefficients f_j are obtained by requiring that

$$\langle (\mathbb{I} + \mathbb{S}_m^0 \mathbb{K}^0) f^{(N)} - \mathbb{S}_m^0 g, t_i^m \rangle_0 = 0 \quad (\text{IV.37})$$

for $i = 0, 1, 2, \dots, N$.

This leads us to the $(N + 1) \times (N + 1)$ linear algebraic system

$$\sum_{j=0}^N f_j \{ \delta_{ji} + \lambda_{mi} K_{ji}^m \} = \lambda_{mi} g_i, i = 0, 1, 2, \dots, N \quad (\text{IV.38})$$

where

$$g_i = \int_0^1 w^0(r) g(r) t_i^m(r) dr \quad (\text{IV.39})$$

$$\simeq \sum_{q=1}^M w_q g(r_q) t_i^m(r_q) \quad (\text{IV.40})$$

and

$$K_{ji}^m = \int_0^1 \int_0^1 w^0(r) w^0(\rho) k(\rho, r) t_j^m(\rho) t_i^m(r) d\rho dr \quad (\text{IV.41})$$

$$\simeq \sum_{p=1}^M \sum_{q=1}^M w_p w_q k(r_p, r_q) t_j^m(r_p) t_i^m(r_q) \quad (\text{IV.42})$$

According to Kress ([18], Thm. 13.21) the Galerkin method will converge if $\mathbb{S}_m^0 \mathbb{K}^0$ is compact and the null-space of $\mathbb{I} + \mathbb{S}_m^0 \mathbb{K}^0$ is trivial, convergence will be in the sense that;

$$\lim_{N \rightarrow \infty} \|f - f^{(N)}\|_0 = 0 \quad (\text{IV.43})$$

We can then be sure that solving (IV.38) by continuous techniques will give a solution to a required accuracy should N and M be chosen large enough and the accuracy of the linear system solver used is sufficient.

IV.4.3 The Collocation Method

As an alternative to the Galerkin method we can use the method of collocation. For collocation points we will use the quadrature points r_q ($q = 0, 1, 2, \dots, N$) given by (IV.32).

To solve (IV.1) we will again approximate the solution by the finite expansion,

$$f^{(N)}(\rho) = \sum_{n=0}^N f_n t_n^m \rho$$

which leads to the equation

$$\sum_{n=0}^N f_n \{r_n^m(r) + k_n(r)\} = g(r), 0 < r < 1 \quad (\text{IV.44})$$

where

$$k_n(r) = \int_0^1 w^0(\rho) t_n^m(\rho) k(\rho, r) d\rho \simeq \sum_{q=1}^M w_q t_n^m(r_q) k(r_q, r) \quad (\text{IV.45})$$

The coefficients f_n are then determined by insisting that this equation be satisfied at the collocation points r_q . We thus obtain the $(N + 1) \times (N + 1)$ linear algebraic system

$$\sum_{n=0}^N f_n \{r_n^m(r_q) + k_n(r_q)\} = g(r_q), q = 1, 2, \dots, N + 1 \quad (\text{IV.46})$$

which can be solved for the required $(f_n)_{n=0}^N$ by standard techniques.

The convergence of the collocation method is verified experimentally by solving known problems and/or comparing with the Galerkin method.

IV.4.4 Numerical Tests

All programming was done in Fortran. When constructing subroutines and functions, various tests were carried out to verify and build confidence in the codes. Details of these are not included here. Instead we offer a sample test problem, with known solution, that was used to test the codes and to compare the Galerkin and Collocation techniques.

For the test problem we considered the equation

$$\int_0^1 \{l_m(\rho, r) + k(\rho, r)\} w^0(\rho) f(\rho) d\rho = g(r), 0 < r < 1, m \in \mathbb{Z} \quad (\text{IV.47})$$

with continuous kernel

$$k(\rho, r) = t_1^m(r) t_2^m(\rho) + t_2^m(r) t_1^m(\rho) \quad (\text{IV.48})$$

and right hand side function

$$g(r) = \frac{t_p^m(r)}{\lambda_{mp}} + \delta_{1p} t_2^m(r) + \delta_{2p} t_1^m(r), p \in \mathbb{Z}^+ \quad (\text{IV.49})$$

with the following easily verified unique solution

$$f(\rho) = \sum_{n=0}^{\infty} \delta_{pn} t_n^m(\rho) \quad (\text{IV.50})$$

This test is a very simple one as any m value can be used, and may therefore be used to verify our computer procedures. The parameter p can be also be varied and the correct solution is readily verified by checking that the coefficients are all zero except for $f_p = 1$. For select values of m we can also use the explicit forms for the t_n^m functions when imputing the kernels as an extra check that the function and or subroutines calling them work accurately. The details for $m = 0, p = 0$ are outlined below:

$$k(r, \rho) = t_1^0(r) t_2^0(\rho) + t_2^0(r) t_1^0(\rho) \quad (\text{IV.51})$$

$$= \sqrt{5} \left(1 - \frac{3}{2}r^2\right) 3 \left(1 - 5\rho^2 + \frac{35}{8}\rho^4\right) + \sqrt{5} \left(1 - \frac{3}{2}\rho^2\right) 3 \left(1 - 5r^2 + \frac{35}{8}r^4\right) \quad (\text{IV.52})$$

$$g(r) = \frac{t_0^0(r)}{\lambda_{00}} = \frac{1}{\lambda_{00}} = \frac{\pi}{4} \quad (\text{IV.53})$$

So that (IV.47) becomes

$$\sum_{n=0}^{\infty} f_n \left(\frac{t_n^0(\rho)}{\lambda_{0n}} + \delta_{2n} t_1^0(r) + \delta_{1n} t_2^0(r) \right) = \frac{t_0^0(r)}{\lambda_{00}} \quad (\text{IV.54})$$

and hence $f_0 = 1$, and $f_n = 0$ otherwise; in other words

$$f(\rho) = t_0^0(r) = 1 \quad (\text{IV.55})$$

Both collocation and Galerkin methods quickly produced accurate results for various different values of all parameters.

CHAPTER V

A HYPER-SINGULAR INTEGRAL EQUATION

V.1 INTRODUCTION

In this chapter we focus on solving the one-dimensional hyper-singular integral equation

$$\int_0^1 \{(\mathbb{D}_m + \kappa) l_m(\rho, r) + k(\rho, r)\} w^1(\rho) f(\rho) d\rho = g(r), 0 < r < 1 \quad (\text{V.1})$$

where $m = 0, 1, 2, \dots$, κ is a constant possibly zero and $k(\rho, r) \in L_2^1(0, 1) \times L_2^1(0, 1)$ is a continuous kernel.

By introducing the $L_2^1(0, 1)$ integral operator \mathbb{K}^1 with continuous kernel $k(\rho, r)$

$$[\mathbb{K}^1 f(\rho)](r) = \int_0^1 k(\rho, r) f(\rho) w^1(\rho) d\rho \quad (\text{V.2})$$

and making use of both the weakly singular operator, \mathbb{L}_m^1 and the hyper-singular operator, $\mathbb{D}_m \mathbb{L}_m^1$, discussed in Chapter III, we can represent the integral equation by the operator equation

$$[(\mathbb{D}_m \mathbb{L}_m^1 + \kappa \mathbb{L}_m^1 + \mathbb{K}^1) f(\rho)](r) = g(r) \in L_2^1(0, 1) \quad (\text{V.3})$$

for $m = 0, 1, 2, \dots$, with solutions to f being sought in $L_{2,m}^1(0, 1)$.

We will first look at solving the dominant hyper-singular equation;

$$\mathbb{D}_m [\mathbb{L}_m^1 f(\rho)](r) = g(r) \quad (\text{V.4})$$

V.2 THE DOMINANT HYPER-SINGULAR EQUATION

We will look for solutions in $L_{2,m}^1(0, 1)$ of the form

$$f(\rho) = \sum_{n=0}^{\infty} f_n s_n^m(\rho) \quad (\text{V.5})$$

The eigen-structure of both $\mathbb{D}_m \mathbb{L}_m^1$ and \mathbb{L}_m^1 was examined in Chapter III, \mathbb{L}_m^1 was

shown to be a compact $L_2^1(0, 1)$, tri-diagonal operator while $\mathbb{D}_m \mathbb{L}_m^1$ an unbounded operator on $L_2^1(0, 1)$ with eigenvalues μ_{mn}^{-1} and eigenfunctions u_n^m . When considered on $L_{2,m}^1(0, 1)$, $\mathbb{D}_m \mathbb{L}_m^1$ was shown to be a Hilbert space isomorphism onto $L_2^1(0, 1)$ with inverse \mathbb{S}_m^1 as in Thm. III.96. The dominant integral equation can then be solved as follows.

Theorem V.1 *For a given $m = 0, 1, 2, \dots$ and*

$$g(r) = \sum_{n=0}^{\infty} g_n u_n^m(r)$$

the integral equation

$$\mathbb{D}_m \mathbb{L}_m^1 [f(\rho)](r) = g(r) \in L_2^1(0, 1) \quad (\text{V.6})$$

has the unique solution $f \in L_{2,m}^1(0, 1)$ given by

$$f(\rho) = \mathbb{S}_m^1 [g(r)](\rho) = \sum_{n=0}^{\infty} g_n s_n^m(\rho) \quad (\text{V.7})$$

Proof. *By Thm. III.37 we can apply the isomorphic inverse \mathbb{S}_m^1 , of $\mathbb{D}_m \mathbb{L}_m^1$*

$$\begin{aligned} [\mathbb{D}_m \mathbb{L}_m^1 f(\rho)](r) &= g(r) \Leftrightarrow \mathbb{S}_m^1 \mathbb{D}_m \mathbb{L}_m^1 f = \mathbb{S}_m^1 g \\ &\Leftrightarrow f(\rho) = \mathbb{S}_m^1 g = \sum_{n=0}^{\infty} g_n s_n^m(\rho) \quad \blacksquare \end{aligned}$$

V.3 THE GENERAL HYPER-SINGULAR EQUATION

Now we can go back and look at the general equation. First a result which shows that compactness on $L_2^1(0, 1)$ implies compactness on $L_{2,m}^1(0, 1)$.

Lemma V.2 *If \mathbb{K}^1 is an $L_2^1(0, 1)$ integral operator then \mathbb{K}^1 is compact when considered on $L_{2,m}^1(0, 1)$ such that*

$$\mathbb{K}^1 : L_{2,m}^1(0, 1) \rightarrow L_2^1(0, 1)$$

Proof. *By Lem. III.35 every weakly convergent sequence in $L_{2,m}^1(0, 1)$ is also a weakly convergent sequence in $L_2^1(0, 1)$ with both sequences converging to the same*

unique limit. Since \mathbb{K}^1 is Hilbert-Schmidt it is compact on $L_2^1(0, 1)$ and hence maps weakly convergent sequences in $L_2^1(0, 1)$ (and hence those in $L_{2,m}^1(0, 1)$) into strongly convergent ones in $L_2^1(0, 1)$, so the result follows ■

Theorem V.3 *If \mathbb{K}^1 is an $L_2^1(0, 1)$ integral operator with continuous kernel and the null-space of $\mathbb{I} + \mathbb{S}_m^1(\kappa\mathbb{L}_m^1 + \mathbb{K}^1)$ is trivial, then $[\mathbb{D}_m\mathbb{L}_m^1 + \kappa\mathbb{L}_m^1 + \mathbb{K}^1]^{-1}$ exists and is given by*

$$[\mathbb{D}_m\mathbb{L}_m^1 + \kappa\mathbb{L}_m^1 + \mathbb{K}^1]^{-1} = (\mathbb{I} + \mathbb{S}_m^1(\kappa\mathbb{L}_m^1 + \mathbb{K}^1))^{-1}\mathbb{S}_m^1 \quad (\text{V.8})$$

therefore the operator equation

$$[(\mathbb{D}_m\mathbb{L}_m^1 + \kappa\mathbb{L}_m^1 + \mathbb{K}^1) f(\rho)](r) = g(r) \in L_2^1(0, 1) \quad (\text{V.9})$$

has a unique solution given by

$$f = (\mathbb{I} + \mathbb{S}_m^1(\kappa\mathbb{L}_m^1 + \mathbb{K}^1))^{-1}\mathbb{S}_m^1 g \in L_{2,m}^1(0, 1) \quad (\text{V.10})$$

Proof. *By Thm. V.1, (V.9) is equivalent to*

$$[(\mathbb{I} + \mathbb{S}_m^1[\kappa\mathbb{L}_m^1 + \mathbb{K}^1]) f(\rho)](r) = \mathbb{S}_m^1 g(r) \in L_{2,m}^1(0, 1) \quad (\text{V.11})$$

$\mathbb{S}_m^1, \mathbb{L}_m^1$ and \mathbb{K}^1 are compact on $L_2^1(0, 1)$ and therefore also on $L_{2,m}^1(0, 1)$ (by Lem. V.2) so that $\mathbb{S}_m^1(\kappa\mathbb{L}_m^1 + \mathbb{K}^1)$ is also compact.

Hence, if the null-space of $\mathbb{I} + \mathbb{S}_m^1(\kappa\mathbb{L}_m^1 + \mathbb{K}^1)$ is trivial, then $(\mathbb{I} + \mathbb{S}_m^1(\kappa\mathbb{L}_m^1 + \mathbb{K}^1))^{-1}$ exists by the Fredholm theorems [16] ■

We choose for convenience to consider our operator matrix in the $L_2^1(0, 1)$ space.

Definition V.4 *For $m, n = 0, 1, 2, 3, \dots$ and for the $L_2^1(0, 1)$ integral operator \mathbb{K}^1 with kernel $k(\rho, r)$ we can define the matrices $K^{mn} = (K_{ij}^{mn})$ and $K^m = K^{mm}$ as follows*

$$K_{ij}^{mn} = \langle \mathbb{K}^1 u_i^m, u_j^n \rangle_0 \quad (\text{V.12})$$

$$= \int_0^1 \int_0^1 K(\rho, r) u_i^m(\rho) u_j^n(r) w^1(\rho) w^1(r) d\rho dr \quad (\text{V.13})$$

Using this notation we now obtain the following expansion for an $L_2^1(0, 1)$ kernel.

Theorem V.5 For \mathbb{K}^1 an $L_2^1(0, 1)$ integral operator with kernel $k(\rho, r)$, then

$$k(\rho, r) = \sum_{i=0}^{\infty} \sum_{j=0}^{\infty} K_{ij}^{mn} u_i^m(\rho) u_j^n(r) \quad (\text{V.14})$$

and

$$\|\mathbb{K}^1\|_1^2 = \sum_{i=0}^{\infty} \sum_{j=0}^{\infty} |K_{ij}^{mn}|^2 \quad (\text{V.15})$$

Proof. Since $k(\rho, r)$ is an $L_2^1(0, 1)$ kernel it is bounded and since the $u_n^m(r)$ functions are also real, we have that

$$\begin{aligned} k(\rho, r) &= \sum_{i=0}^{\infty} \langle K(\rho, r), u_i^m(\rho) \rangle_1 u_i^m(\rho) \\ &= \sum_{i=0}^{\infty} [\mathbb{K}^1 u_i^m](r) u_i^m(\rho) \\ &= \sum_{i=0}^{\infty} \sum_{j=0}^{\infty} \langle \mathbb{K}^1 u_i^m, u_j^n(r) \rangle_1 u_j^n(r) u_i^m(\rho) \\ &= \sum_{i=0}^{\infty} \sum_{j=0}^{\infty} K_{ij}^{mn} u_i^m(\rho) u_j^n(r) \end{aligned}$$

Hence

$$\begin{aligned} \|\mathbb{K}^1\|_1^2 &= \int_0^1 \int_0^1 w^1(r) w^1(\rho) |k(r, \rho)|^2 d\rho dr \\ &= \sum_{i=0}^{\infty} \sum_{j=0}^{\infty} |K_{ij}^{mn}|^2 \blacksquare \end{aligned}$$

Theorem V.6 For \mathbb{K}^1 an $L_2^1(0, 1)$ integral operator with continuous kernel $k(\rho, r)$ and

$$f(\rho) = \sum_{k=0}^{\infty} f_k u_k^m(\rho) \in L_2^0(0, 1)$$

then

$$\mathbb{K}^1 f = \sum_{i=0}^{\infty} \sum_{j=0}^{\infty} K_{ij}^{mn} f_i u_j^n(r)$$

Proof.

$$\begin{aligned}
\mathbb{K}^1 f &= \int_0^1 k(r, \rho) f(\rho) w^1(\rho) d\rho \\
&= \sum_{i=0}^{\infty} \sum_{j=0}^{\infty} \sum_{k=0}^{\infty} K_{ij}^{mn} f_k u_j^n(r) \int_0^1 u_i^m(\rho) u_k^m(\rho) w^1(\rho) d\rho \\
&= \sum_{i=0}^{\infty} \sum_{j=0}^{\infty} K_{ij}^{mn} f_i u_j^n(r) \blacksquare
\end{aligned}$$

We finish the section with some results in $L_{2,m}^1(0, 1)$ concerning the \mathbb{L}_m^1 operator, that will be required for our numerical schemes.

Theorem V.7 For $m, n, i = 0, 1, 2, \dots$

$$\langle \mathbb{L}_m^1 s_n^m, s_i^m \rangle_{1,m} = \delta_{ni} \gamma_i^m + \delta_{(n+1)i} \frac{\mu_{m(i-1)}}{\mu_{mi}} \eta_{i-1}^m + \delta_{(n-1)i} \frac{\mu_{m(i+1)}}{\mu_{mi}} \eta_i^m \quad (\text{V.16})$$

Proof. $\langle \mathbb{L}_m^1 s_n^m, s_i^m \rangle_{1,m}$

$$\begin{aligned}
&= \frac{1}{\mu_{mi}} \langle \mathbb{L}_m^1 s_n^m, u_i^m \rangle_1 = \frac{\mu_{mn}}{\mu_{mi}} \langle \mathbb{L}_m^1 u_n^m, u_i^m \rangle_1 \\
&= \frac{\mu_{mn}}{\mu_{mi}} (\gamma_i^m \delta_{ni} + \eta_{i-1}^m \delta_{(n+1)i} + \eta_i^m \delta_{(n-1)i}) \text{ by (III.59)} \\
&= \delta_{ni} \gamma_i^m + \delta_{(n+1)i} \frac{\mu_{m(i-1)}}{\mu_{mi}} \eta_{i-1}^m + \delta_{(n-1)i} \frac{\mu_{m(i+1)}}{\mu_{mi}} \eta_i^m \text{ by (III.25)} \blacksquare
\end{aligned}$$

Lemma V.8 For $m, n = 0, 1, 2, \dots$

$$[\mathbb{S}_m^1 t_n^m(\rho)](r) = \alpha_{n-1}^m s_{n-1}^m(r) + \beta_n^m s_n^m(r) \quad (\text{V.17})$$

Proof.

$$\begin{aligned}
[\mathbb{S}_m^1 t_n^m(\rho)](r) &= \sum_{p=0}^{\infty} s_p^m(r) \int_0^1 w^1(\rho) t_n^m(\rho) u_p^m(\rho) d\rho \\
&= \sum_{p=0}^{\infty} s_p^m(r) \int_0^1 w^0(\rho) t_n^m(\rho) (\alpha_p^m t_{p+1}^m(\rho) + \beta_p^m t_p^m(\rho)) d\rho \text{ by (III.51)} \\
&= \sum_{p=0}^{\infty} s_p^m(r) [\alpha_p^m \delta_{n(p+1)} + \beta_p^m \delta_{np}] \\
&= \alpha_{n-1}^m s_{n-1}^m(r) H(n-1) + \beta_n^m s_n^m(r) \blacksquare
\end{aligned}$$

Theorem V.9 For $m, n = 0, 1, 2, \dots$

$$\begin{aligned} & [\mathbb{S}_m^1 \mathbb{L}_m^1 s_n^m(r)](r) \\ &= \mu_{mn} (\gamma_n^m s_n^m(r) + \eta_{n-1}^m s_{n-1}^m(r) + \eta_n^m s_{n+1}^m(r)) \end{aligned} \quad (\text{V.18})$$

Proof. $\mathbb{S}_m^1 \mathbb{L}_m^1 s_n^m$

$$\begin{aligned} &= \mu_{mn} \left(\frac{\alpha_n^m}{\lambda_{m(n+1)}} \mathbb{S}_m^1 t_{n+1}^m(r) + \frac{\beta_n^m}{\lambda_{mn}} \mathbb{S}_m^1 t_n^m(r) \right) \text{ by (III.58)} \\ &= \frac{\mu_{mn} \alpha_n^m}{\lambda_{m(n+1)}} (\alpha_n^m s_n^m(r) + \beta_{n+1}^m s_{n+1}^m(r)) + \frac{\mu_{mn} \beta_n^m}{\lambda_{mn}} (\alpha_{n-1}^m s_{n-1}^m(r) + \beta_n^m s_n^m(r)) \\ & \quad \text{by (V.17)} \\ &= \mu_{mn} \left(\frac{(\alpha_n^m)^2}{\lambda_{m(n+1)}} + \frac{(\beta_n^m)^2}{\lambda_{mn}} \right) s_n^m(r) + \mu_{mn} \frac{\alpha_{n-1}^m \beta_n^m}{\lambda_{mn}} s_{n-1}^m(r) + \mu_{mn} \frac{\alpha_n^m \beta_{n+1}^m}{\lambda_{m(n+1)}} s_{n+1}^m(r) \\ &= \mu_{mn} \gamma_n^m s_n^m(r) + \mu_{mn} \eta_{n-1}^m s_{n-1}^m(r) + \mu_{mn} \eta_n^m s_{n+1}^m(r) \quad \blacksquare \end{aligned}$$

Theorem V.10 For $m, n, i = 0, 1, 2, \dots$

$$\begin{aligned} & \langle \mathbb{S}_m^1 \mathbb{L}_m^1 s_n^m, s_i^m \rangle_{1,m} \\ &= \delta_{ni} \mu_{mi} \gamma_i^m + \delta_{(n-1)i} \mu_{m(i+1)} \eta_i^m + \delta_{(n+1)i} \mu_{m(i-1)} \eta_{i-1}^m \end{aligned} \quad (\text{V.19})$$

Proof. $\langle \mathbb{S}_m^1 \mathbb{L}_m^1 s_n^m, s_i^m \rangle_{1,m}$

$$\begin{aligned} &= \frac{\mu_{mn}}{\mu_{mi}} \langle \gamma_n^m s_n^m(r), u_i^m \rangle_1 + \frac{\mu_{mn}}{\mu_{mi}} \langle \eta_{n-1}^m s_{n-1}^m(r), u_i^m \rangle_1 + \frac{\mu_{mn}}{\mu_{mi}} \langle \eta_n^m s_{n+1}^m(r), u_i^m \rangle_1 \\ & \quad \text{by (V.18)} \\ &= \frac{\gamma_n^m \mu_{mn} \mu_{mn}}{\mu_{mi}} \delta_{ni} + \frac{\eta_{n-1}^m \mu_{m(n-1)} \mu_{mn}}{\mu_{mi}} \delta_{(n-1)i} + \frac{\eta_n^m \mu_{m(n+1)} \mu_{mn}}{\mu_{mi}} \delta_{(n+1)i} \\ &= \gamma_n^m \mu_{mn} \delta_{ni} + \eta_{n-1}^m \mu_{mn} \delta_{(n-1)i} + \eta_n^m \mu_{mn} \delta_{(n+1)i} \quad \blacksquare \end{aligned}$$

V.4 NUMERICAL SOLUTIONS

V.4.1 Quadrature

The quadrature points will again be those defined in Def. IV.14 the points will again also be used as collocation points for the collocation method. The quadrature method will be the same as in Lem. IV.14, adapted as follows for the different weight

function

$$\int_0^1 w^1(r) g(r) dr \simeq \sum_{q=1}^M w_q g(r_q) [1 - r_q^2] \quad (\text{V.20})$$

V.4.2 The Galerkin Method

For the Galerkin method we will approximate the solution to (V.11) and hence (V.1) by the finite sum

$$f^{(N)}(\rho) = \sum_{j=0}^N f_j s_j^m(\rho) \quad (\text{V.21})$$

where the coefficients f_j are obtained by requiring that

$$\langle (\mathbb{I} + \mathbb{S}_m^1(\kappa \mathbb{L}_m^1 + \mathbb{K}^1)) f^{(N)} - \mathbb{S}_m^1 g, s_i^m \rangle_{1,m} = 0 \quad (\text{V.22})$$

for $i = 0, 1, 2, \dots, N$

This leads us to the $(N + 1) \times (N + 1)$ linear algebraic system

$$\sum_{j=0}^N f_j \left\{ \begin{array}{l} \delta_{ji} [1 + \kappa \mu_{mi}(\gamma_i^m)] + \delta_{j(i+1)} \kappa \mu_{m(i+1)} \eta_i^m \\ + \delta_{j(i-1)} \kappa \mu_{m(i-1)} \eta_{i-1}^m + \mu_{mj} K_{ji}^m \end{array} \right\} = g_i \text{ for } i = 0, 1, 2, \dots, N \quad (\text{V.23})$$

where

$$g_i = \int_0^1 w^1(r) g(r) u_i^m(r) dr \quad (\text{V.24})$$

$$\simeq \sum_{q=1}^M w_q g(r_q) u_i^m(r_q) [1 - r_q^2] \quad (\text{V.25})$$

and

$$K_{ji}^m = \int_0^1 \int_0^1 w^1(r) w^1(\rho) [k(\rho, r)] u_j^m(\rho) u_i^m(r) d\rho dr \quad (\text{V.26})$$

$$\simeq \sum_{p=1}^M \sum_{q=1}^M w_p w_q k(r_q, r_p) u_i^m(r_p) u_j^m(r_q) [1 - r_p^2] [1 - r_q^2] \quad (\text{V.27})$$

V.4.3 Collocation

We will again use the quadrature points r_q ($q = 0, 1, 2, \dots, N + 1$) given by (IV.32) as collocation points. We will approximate the solution to (V.1) by the finite sum

$$f^{(N)}(\rho) = \sum_{j=0}^N f_j s_j^m(\rho) \quad (\text{V.28})$$

which leads to the equation

$$\sum_{n=0}^N f_n \left\{ u_n^m(r) + \kappa \mu_{mn} \left(\frac{\alpha_n^m}{\lambda_{m(n+1)}} t_{n+1}^m(r) + \frac{\beta_n^m}{\lambda_{mn}} t_n^m(r) \right) + k_n^m(r) \right\} = g(r), \quad 0 < r < 1 \quad (\text{V.29})$$

or

$$\sum_{n=0}^N f_n \left\{ u_n^m(r) + \kappa \mu_{mn} \left(\eta_{n-1}^m u_{n-1}^m(r) + \gamma_n^m u_n^m(r) + \eta_n^m u_{n+1}^m(r) \right) + k_n^m(r) \right\} = g(r)$$

for $0 < r < 1$ where

$$k_n^m(r) = \int_0^1 w^1(\rho) s_n^m(\rho) k(\rho, r) d\rho \simeq \sum_{q=1}^M w_q k(r_q, r) s_n^m(r_q) [1 - r_q^2] \quad (\text{V.30})$$

The coefficients f_n are then determined by insisting that this equation be satisfied at the collocation points r_q . We thus obtain the $(N + 1) \times (N + 1)$ linear algebraic system

$$\sum_{n=0}^N f_n \left\{ u_n^m(r_q) + \kappa \mu_{mn} \left(\frac{\alpha_n^m}{\lambda_{m(n+1)}} t_{n+1}^m(r_q) + \frac{\beta_n^m}{\lambda_{mn}} t_n^m(r_q) \right) + k_n^m(r_q) \right\} = g(r_q) \quad (\text{V.31})$$

where $q = 1, 2, \dots, N + 1$.

V.4.4 Numerical tests

A couple of sample test problem are shown below. The problems are similar in style to the one illustrated for the weakly singular problem in Chapter IV.

For the first test problem we considered the equation (the Hadamard singularity

is assumed to exist only in the appropriate context)

$$\int_0^1 \{(\mathbb{D}_m + \kappa) l_m(\rho, r) + k(\rho, r)\} w^1(\rho) f(\rho) d\rho = g(r), 0 < r < 1, m \in \mathbb{Z} \quad (\text{V.32})$$

where

$$k(r, \rho) = u_1^m(r) u_2^m(\rho) + u_2^m(r) u_1^m(\rho) \quad (\text{V.33})$$

and for

$$g(r) = \frac{u_p^m(r)}{\lambda_{mp}} + \delta_{1p} u_2^m(r) + \delta_{2p} u_1^m(r), p \in \mathbb{Z}^+ \quad (\text{V.34})$$

For $\kappa = 0$ the solution is readily verified as

$$f(\rho) = \sum_{n=0}^{\infty} \delta_{pn} u_n^m(\rho) \quad (\text{V.35})$$

Both methods gave fast and accurate results.

As a test for the weakly-singular part we can use the equation

$$\int_0^1 l_m(\rho, r) w^1(\rho) f(\rho) d\rho = g(r), 0 < r < 1, m \in \mathbb{Z} \quad (\text{V.36})$$

where

$$g(r) = \mu_{mp} (H(p-1) \eta_{p-1}^m u_{p-1}^m(r) + \gamma_p^m u_p^m(r) + \eta_p^m u_{p+1}^m(r)) \quad (\text{V.37})$$

$$= \mu_{mp} \left(\frac{\beta_p^m}{\lambda_{mp}} t_p^m(r) + \frac{\alpha_p^m}{\lambda_{m(p+1)}} t_{p+1}^m(r) \right) \quad (\text{V.38})$$

with solution

$$f(\rho) = s_p^m(\rho) \quad (\text{V.39})$$

Both methods give accurate and fast solutions.

To test the full equation we used the following problem comparing the results from the two methods;

$$\int_0^1 \{(\mathbb{D}_m + 1) l_m(\rho, r) + k(\rho, r)\} w^1(\rho) f(\rho) d\rho = g(r), 0 < r < 1, m \in \mathbb{Z} \quad (\text{V.40})$$

where

$$k(r, \rho) = u_1^m(r) u_2^m(\rho) + u_2^m(r) u_1^m(\rho) \quad (\text{V.41})$$

and for

$$g(r) = \frac{u_p^m(r)}{\lambda_{mp}} + \delta_{1p} u_2^m(r) + \delta_{2p} u_1^m(r), p \in \mathbb{Z}^+ \quad (\text{V.42})$$

Table (1) shows the output coefficients from both collocation and Galerkin methods, illustrating that both give the same output.

TABLE 1

Comparison of Galerkin and collocation results for one-dimensional hyper-singular test problem. Results shown for $p=5$, $m=3$. with the number of terms and number of collocation points both 20, with 30 quadrature points.

fn	Collocation	Galerkin
0	0.00000000	0.00000000
1	0.00000000	0.00000000
2	0.00000002	0.00000002
3	0.00000444	0.00000444
4	0.00175410	0.00175410
5	1.00277028	1.00277028
6	0.00111636	0.00111636
7	0.00000097	0.00000097
8	0.00000000	0.00000000
9	0.00000000	0.00000000
10	0.00000000	0.00000000
11	0.00000000	0.00000000
12	0.00000000	0.00000000
13	0.00000000	0.00000000
14	0.00000000	0.00000000
15	0.00000000	0.00000000
16	0.00000000	0.00000000
17	0.00000000	0.00000000
18	0.00000000	0.00000000
19	0.00000000	0.00000000

CHAPTER VI

HILBERT SPACES II

VI.1 INTRODUCTION

In this chapter we will construct and examine two weighted L_2 spaces of functions defined on the unit disc. The purpose of these spaces, which are extensions of those developed in Chapter III, is to enable the representation of certain classes of two-dimensional integral equations as operator equations within these Hilbert space. These integral equations, which will be solved in the next two chapters, can under certain conditions be reduced to the solving of our one-dimensional equations discussed previously. The new spaces are however needed if we wish to investigate non-reducible problems.

VI.2 THE $L_2^\alpha(\Omega)$ HILBERT SPACES

With Ω the unit disc, and for $\alpha = 0, 1$ we define the $L_2^\alpha(\Omega)$ Hilbert spaces to be the direct product of the $L_2^\alpha(0, 1)$ space and the $L_2(-\pi, \pi)$ space, which is well known to have a trigonometric basis. A product basis for the new spaces will be constructed in the usual way.

Definition VI.1 For $\alpha = 0, 1$ the $L_2^\alpha(\Omega)$ spaces are the set of all functions

$$L_2^\alpha(\Omega) = \left\{ f(\rho, \vartheta) : f : (\Omega) \rightarrow \mathbb{C} \text{ and } \int_{-\pi}^{\pi} \int_0^1 |f(\rho, \vartheta)|^2 w^\alpha(\rho) d\rho d\vartheta < \infty \right\} \quad (\text{VI.1})$$

with inner product

$$\langle\langle f, g \rangle\rangle_\alpha = \int_{-\pi}^{\pi} \int_0^1 f(\rho, \vartheta) \overline{g(\rho, \vartheta)} w^\alpha(\rho) d\rho d\vartheta \quad (\text{VI.2})$$

and norm

$$\| \| f(\rho, \vartheta) \| \|_\alpha = \left\{ \int_{-\pi}^{\pi} \int_0^1 |f(\rho, \vartheta)|^2 w^\alpha(\rho) d\rho d\vartheta \right\}^{\frac{1}{2}} \quad (\text{VI.3})$$

Definition VI.2 For $m = 0, \pm 1, \pm 2, \pm 3, \dots$, $n = 0, 1, 2, 3, \dots$ and $\alpha = 0, 1$ we define the functions

$$e_{mn}^{\alpha}(\rho, \vartheta) = \frac{1}{\sqrt{2\pi}} \exp(im\vartheta) \begin{cases} t_n^{|\alpha|}(\rho) & , \alpha = 0 \\ u_n^{|\alpha|}(\rho) & , \alpha = 1 \end{cases} \quad (\text{VI.4})$$

Definition VI.3 For $m, n = 0, 1, 2, 3, \dots$ and $\alpha = 0, 1$ we define the functions

$$c_{mn}^{\alpha}(\rho, \vartheta) = \frac{1}{\sqrt{\pi(1+\delta_{m0})}} \cos(m\vartheta) \begin{cases} t_n^m(\rho) & , \alpha = 0 \\ u_n^m(\rho) & , \alpha = 1 \end{cases} \quad (\text{VI.5})$$

and for $m \neq 0$

$$s_{mn}^{\alpha}(\rho, \vartheta) = \frac{1}{\sqrt{\pi}} \sin(m\vartheta) \begin{cases} t_n^m(\rho) & , \alpha = 0 \\ u_n^m(\rho) & , \alpha = 1 \end{cases} \quad (\text{VI.6})$$

The following theorems establish that the spaces $L_2^{\alpha}(\Omega)$ are separable by showing they have countable sets of basis functions.

Theorem VI.4 For $m = 0, \pm 1, \pm 2, \pm 3, \dots$, $n, p = 0, 1, 2, 3, \dots$ and $\alpha = 0, 1$ the sequences

$$\{e_{mn}^{\alpha}(\rho, \vartheta)\}$$

and

$$\{c_{mn}^{\alpha}(\rho, \vartheta), s_{mn}^{\alpha}(\rho, \vartheta)\}$$

form orthonormal bases for $L_2^{\alpha}(\Omega)$.

Proof. Since

$$\left\{ \frac{1}{\sqrt{2\pi}} \exp(im\vartheta) \right\}_{m=-\infty}^{\infty}$$

and

$$\left\{ \frac{1}{\sqrt{\pi(1+\delta_{m0})}} \cos(m\vartheta), \frac{1}{\sqrt{\pi}} \sin(m\vartheta) \right\}_{m=0}^{\infty}$$

are orthonormal bases for $L_2(-\pi, \pi)$ and for any given $m = 0, 1, 2, 3, \dots$, the sequences

$$\{t_n^m(\rho)\}_{n=0}^{\infty}$$

and

$$\{u_n^m(\rho)\}_{n=0}^{\infty}$$

form orthonormal bases for $L_2^0(0, 1)$ and for $L_2^1(0, 1)$ respectively.

The results follows automatically by the definitions of $e_{mn}^\alpha(\rho, \vartheta)$, $c_{mn}^\alpha(\rho, \vartheta)$ and $s_{mn}^\alpha(\rho, \vartheta)$ ■

Since $L_2^\alpha(\Omega)$ is a separable Hilbert space we can show it is isomorphic to both l^2 and $l^2 \times l^2$ which are of course isomorphic to one another. For our purposes we will consider a double sum to be a single sum split in two i.e. an l^2 sum.

Theorem VI.5 $L_2^\alpha(\Omega)$ is a separable infinite dimensional Hilbert space isomorphic to l^2 .

Proof. Let f be the function defined as follows

$$f(\rho, \vartheta) = \sum_{m=-\infty}^{\infty} \sum_{n=0}^{\infty} f_{mn} e_{mn}^\alpha(\rho, \vartheta)$$

then

$$\begin{aligned} \|f\|_\alpha^2 &= \int_{-\pi}^{\pi} \int_0^1 |f(\rho, \vartheta)|^2 w^\alpha(\rho) d\rho d\vartheta \\ &= \int_{-\pi}^{\pi} \int_0^1 \left| \sum_{m=-\infty}^{\infty} \sum_{n=0}^{\infty} f_{mn} e_{mn}^\alpha(\rho, \vartheta) \right|^2 w^\alpha(\rho) d\rho d\vartheta \\ &= \sum_{m=-\infty}^{\infty} \sum_{n=0}^{\infty} |f_{mn}|^2 = \left\| \{f_{mn}\}_{m=-\infty, n=0}^{\infty} \right\|^2 \end{aligned}$$

so

$$f \in L_2^\alpha(\Omega) \Leftrightarrow \{f_{mn}\}_{m=-\infty, n=0}^{\infty} \in l^2$$

Define the operator $A^\alpha : L_2^\alpha(0, 1) \rightarrow l^2$ by

$$A^\alpha f = \{f_{mn}\}_{m=-\infty, n=0}^{\infty} \tag{VI.7}$$

then if

$$\begin{aligned} f(r, \theta) &= \sum_{m=-\infty}^{\infty} \sum_{n=0}^{\infty} f_{mn} e_{mn}^\alpha(r, \theta), \quad g(r, \theta) = \sum_{m=-\infty}^{\infty} \sum_{n=0}^{\infty} g_{mn} e_{mn}^\alpha(r, \theta) \\ x &= \{f_{mn}\}_{m=-\infty, n=0}^{\infty} \quad \text{and} \quad y = \{g_{mn}\}_{m=-\infty, n=0}^{\infty} \end{aligned}$$

we have

$$\langle A^\alpha f, A^\alpha g \rangle = \left\langle \{f_{mn}\}_{m=-\infty, n=0}^\infty, \{g_{mn}\}_{m=-\infty, n=0}^\infty \right\rangle = \langle x, y \rangle$$

and it follows that A^α is a Hilbert space isomorphism between $L_2^\alpha(0, 1)$ and l^2 as required ■

VI.3 OPERATORS ON $L_2^\alpha(\Omega)$

We are first going to define some operators which we will use to represent our integral equations. We will establish some results for these operators a number of which have already been seen in a different context.

Definition VI.6 Let us define the kernel $L_m(\rho, r; z)$ for $m = 0, \pm 1, \pm 2, \dots$, as follows

$$L_m(\rho, r; z) = \frac{1}{2\pi\sqrt{r\rho}} Q_{|m|-\frac{1}{2}} \left[\frac{z^2 + r^2 + \rho^2}{2r\rho} \right] \quad (\text{VI.8})$$

and the associated operators $\mathbb{L}_{m;h}^\alpha$, for $\alpha = 0, 1$, as follows

$$\mathbb{L}_{m;h}^\alpha[\sigma(\rho)](r) = \int_0^1 \sigma(\rho) L_m(\rho, r; 2h) w^\alpha(\rho) d\rho \quad (\text{VI.9})$$

observe that

$$l_m(\rho, r) = L_m(\rho, r; 0), \mathbb{L}_m^\alpha = \mathbb{L}_{m;0}^\alpha \quad (\text{VI.10})$$

For $z \neq 0$ the kernel $L_m(\rho, r; z)$ will be continuous and square integrable with both weight functions, while for $z = 0$ it will reduce to the weakly-singular kernel $l_m(\rho, r)$ that was studied in depth in Chapter III. Using the result from Hobson, (III.21), algebraic manipulation and change of variables we can see that

$$\frac{1}{4\pi} \int_{-\pi}^{\pi} \frac{e^{im\theta} d\theta}{\sqrt{z^2 + r^2 + \rho^2 - 2r\rho \cos(\theta - \vartheta)}} = e^{im\vartheta} L_m(\rho, r; z) \quad (\text{VI.11})$$

and using (III.23) we can write $L_m(\rho, r; z)$ as follows;

$$L_m(\rho, r; z) = \frac{1}{2} \int_0^\infty e^{-tz} J_m(rt) J_m(\rho t) dt \quad (\text{VI.12})$$

The next class of operators we will consider is what we will call Boussinesq and extended Boussinesq type operators. The Boussinesq type operators are closely related to Boussinesq's integral;

$$\frac{1}{4\pi} \int_0^1 \int_{-\pi}^{\pi} \frac{\rho \sigma(\rho, \vartheta)}{\sqrt{\rho^2 + r^2 - 2r\rho \cos(\theta - \vartheta)}} d\vartheta d\rho \quad (\text{VI.13})$$

and are weakly singular in nature with kernel

$$B(\rho, \vartheta; r, \theta) = \frac{1}{4\pi} \frac{1}{\sqrt{\rho^2 + r^2 - 2r\rho \cos(\theta - \vartheta)}} \quad (\text{VI.14})$$

The extended Boussinesq operators are continuous with kernel

$$B_h(\rho, \vartheta; r, \theta) = \frac{1}{4\pi} \frac{1}{\sqrt{\rho^2 + r^2 - 2r\rho \cos(\theta - \vartheta) + 4h^2}}, h \neq 0 \quad (\text{VI.15})$$

clearly $B(\rho, \vartheta; r, \theta) = B_0(\rho, \vartheta; r, \theta)$.

The operators are defined as follows with the relevant weight function.

Definition VI.7 For $\alpha = 0, 1$ let \mathbb{B}^α (Boussinesq type operators) and \mathbb{B}_h^α (Extended Boussinesq type operators) be defined on $L_2^\alpha(\Omega)$, with kernels $B(\rho, \vartheta; r, \theta)$ and $B_h(\rho, \vartheta; r, \theta)$ respectively, for $0 \leq r \leq 1$, $-\pi \leq \theta \leq \pi$ and $h > 0$, by

$$\mathbb{B}^\alpha[\sigma(\rho, \vartheta)](r, \theta, h) = \int_0^1 \int_{-\pi}^{\pi} B(\rho, \vartheta; r, \theta) \sigma(\rho, \vartheta) w^\alpha(\rho) d\vartheta d\rho \quad (\text{VI.16})$$

and

$$\mathbb{B}_h^\alpha[\sigma(\rho, \vartheta)](r, \theta, h) = \int_0^1 \int_{-\pi}^{\pi} B_h(\rho, \vartheta; r, \theta) \sigma(\rho, \vartheta) w^\alpha(\rho) d\vartheta d\rho \quad (\text{VI.17})$$

The dominant parts of the integral equations to be considered will involve the weakly-singular operator \mathbb{B}^0 or the hyper-singular operator $-\Delta_2 \mathbb{B}^1$. The \mathbb{B}_h^α operators have non-singular continuous kernels and will appear as the non-singular parts of the operator equations occurring in the applications discussed in Chapters VIII and IX. For notational simplicity we will often consider the Boussinesq type operators as

$$\mathbb{B}_0^\alpha = \mathbb{B}^\alpha, \text{ for } \alpha = 0, 1 \quad (\text{VI.18})$$

The following result allows us to expand our two-dimensional kernels in Fourier series and thereby recover their one-dimensional counterparts.

Theorem VI.8 For $\alpha = 0, 1$ and $m = 0, 1, 2, \dots$

$$\mathbb{B}_h^\alpha [f_m(\rho) \exp(im\vartheta)](r, \theta) = \exp(im\theta) \mathbb{L}_{m;h}^\alpha [f_m(\rho)](r) \quad (\text{VI.19})$$

Proof. $\mathbb{B}_h^\alpha [f_m(\rho) \exp(im\vartheta)](r, \theta)$

$$\begin{aligned} &= \int_0^1 f_m(\rho) w^\alpha(\rho) \frac{1}{4\pi} \int_{-\pi}^{\pi} \frac{\exp(im\vartheta) d\vartheta}{\sqrt{\rho^2 + r^2 - 2r\rho \cos(\theta - \vartheta) + 4h^2}} d\rho \\ &= \exp(im\theta) \int_0^1 f_m(\rho) w^\alpha(\rho) L_m(r, \rho; h) d\rho, \text{ by (VI.11)} \\ &= \exp(im\theta) \mathbb{L}_{m;h}^\alpha [f_m(\rho)](r) \blacksquare \end{aligned}$$

In dealing with the hyper-singular case we will use the following result to develop Fourier expansions for those terms involving the Laplacian operator.

Theorem VI.9

$$-\Delta_2(\exp(im\vartheta) f_m(r)) = \exp(im\theta) \mathbb{D}_m f_m(r) \quad (\text{VI.20})$$

Proof.

$$\begin{aligned} -\Delta_2(\exp(im\vartheta) f_m(r)) &= -\left(\frac{\partial^2}{\partial r^2} + \frac{1}{r} \frac{\partial}{\partial r} + \frac{1}{r^2} \frac{\partial^2}{\partial \vartheta^2}\right) \exp(im\vartheta) f_m(r) \\ &= -\exp(im\vartheta) \left(\frac{d^2 f_m}{dr^2} + \frac{1}{r} \frac{df_m}{dr} - \frac{m^2}{r^2} f_m\right) \\ &= \exp(im\theta) \mathbb{D}_m f_m(r) \blacksquare \end{aligned}$$

We now have all the results needed to show that \mathbb{B}^0 has eigenvalues λ_{mn}^{-1} and eigenfunctions e_{mn}^0 or c_{mn}^0 and s_{mn}^0 .

Theorem VI.10 For $0 \leq r \leq 1$, $-\pi \leq \theta \leq \pi$, $m = 0, \pm 1, \pm 2, \pm 3, \dots$, $n = 0, 1, 2, 3, \dots$

$$\lambda_{|m|n} \mathbb{B}^0 [e_{mn}^0(\rho, \vartheta)](r, \theta) = e_{mn}^0(r, \theta) \quad (\text{VI.21})$$

Proof.

$$\begin{aligned}
\lambda_{|m|n} \mathbb{B}^0 [e_{mn}^0(\rho, \vartheta)](r, \theta) &= \lambda_{|m|n} \mathbb{B}^0 \left[t_n^{|m|}(\rho) \frac{\exp(im\vartheta)}{\sqrt{2\pi}} \right] (r, \theta) \\
&= \frac{\lambda_{|m|n} \exp(im\theta)}{\sqrt{2\pi}} \mathbb{L}_m^0 [t_n^{|m|}(\rho)](r), \text{ by (VI.19)} \\
&= \frac{\lambda_{|m|n}}{\sqrt{2\pi}} \exp(im\theta) \frac{t_n^{|m|}(r)}{\lambda_{|m|n}}, \text{ by (III.10)} \\
&= e_{mn}^0(r, \theta) \blacksquare
\end{aligned}$$

The sine and cosine equivalents are as follows.

Theorem VI.11 For $0 \leq r \leq 1$, $-\pi \leq \theta \leq \pi$, $m, n = 0, 1, 2, 3, \dots$

1.

$$\lambda_{mn} \mathbb{B}^0 [c_{mn}^0(\rho, \vartheta)](r, \theta) = c_{mn}^0(r, \theta) \quad (\text{VI.22})$$

2.

$$\lambda_{mn} \mathbb{B}^0 [s_{mn}^0(\rho, \vartheta)](r, \theta) = s_{mn}^0(r, \theta) \quad (\text{VI.23})$$

Proof. Take real and imaginary parts of (VI.21) \blacksquare

In the case of the hyper-singular operator $-\Delta_2 \mathbb{B}^1$ we have similar results shown below.

Theorem VI.12 For $0 \leq r \leq 1$, $-\pi \leq \theta \leq \pi$, $m = 0, \pm 1, \pm 2, \pm 3, \dots$, $n = 0, 1, 2, 3, \dots$

$$\mu_{|m|n} (-\Delta_2 \mathbb{B}^1) [e_{mn}^1(\rho, \vartheta)](r, \theta) = e_{mn}^1(r, \theta) \quad (\text{VI.24})$$

Proof. $\mu_{|m|n} (-\Delta_2 \mathbb{B}^1) [e_{mn}^1(\rho, \vartheta)](r, \theta)$

$$\begin{aligned}
&= \frac{\mu_{|m|n}}{\sqrt{2\pi}} (-\Delta_2) \exp(im\theta) \mathbb{L}_m^1 [u_n^{|m|}(\rho)](r) d\rho, \text{ by (VI.19)} \\
&= \frac{\mu_{|m|n}}{\sqrt{2\pi}} \exp(im\theta) \mathbb{D}_m \mathbb{L}_m^1 [u_n^{|m|}(\rho)](r), \text{ by (VI.20)} \\
&= \frac{\mu_{|m|n}}{\sqrt{2\pi}} \exp(im\theta) \frac{u_n^{|m|}(r)}{\mu_{|m|n}} \\
&= \frac{1}{\sqrt{2\pi}} \exp(im\theta) u_n^{|m|}(r) \text{ by (III.28)} \\
&= e_{mn}^1(r, \theta) \blacksquare
\end{aligned}$$

The sine and cosine equivalents are then as follows.

Theorem VI.13 For $0 \leq r \leq 1$, $-\pi \leq \theta \leq \pi$, $m, n = 0, 1, 2, 3, \dots$

1.

$$\mu_{mn}(-\Delta_2 \mathbb{B}^1) [c_{mn}^1(\rho, \vartheta)](r, \theta) = c_{mn}^1(r, \theta) \quad (\text{VI.25})$$

2.

$$\mu_{mn}(-\Delta_2 \mathbb{B}^1) [s_{mn}^1(\rho, \vartheta)](r, \theta) = s_{mn}^1(r, \theta) \quad (\text{VI.26})$$

Proof. Take real and imaginary parts of (VI.24) ■

The Boussinesq type operator \mathbb{B}^0 is a weakly-singular operator which we can show is compact but not Hilbert-Schmidt. In other words the operator is compact and hence bounded but the kernel is not square-integrable with regards to the norm. This means that we will not have a mean convergent bilinear expansion for the kernel but since we already have the eigenvalues this does not represent a significant problem.

Theorem VI.14 The operator \mathbb{B}^0 is Compact and Self Adjoint on $L_2^0(\Omega)$.

Proof. Since by (VI.21) for $m = 0, \pm 1, \pm 2, \pm 3, \dots$, and $n = 0, 1, 2, 3, \dots$

$$\mathbb{B}^0 e_{mn}^0 = \frac{e_{mn}^0}{\lambda_{|m|n}}$$

we can, by renumbering the eigenfunctions, represent \mathbb{B}^0 as an infinite diagonal matrix, with diagonal entries convergent to zero, since $\frac{1}{\lambda_{mn}} \rightarrow 0$ as both $m, n \rightarrow \infty$, the result will follow from ([15], prob. 132) ■

The \mathbb{B}^1 weakly-singular operator is also compact, we will prove this by showing that it has a tri-diagonal matrix representation whose entries converge to zero. We will now consider the eigen-structure of the \mathbb{B}^1 operator. The structure is a generalization of that considered in Chapter III for the \mathbb{L}_m^1 operator and likewise will be tri-diagonal.

First some relationships between the $e_{mn}^1(r, \theta)$ and $e_{mn}^0(r, \theta)$ functions which will be an extension of those between the t_n^m and u_n^m functions in Chapter III.

Theorem VI.15 For $m = 0, \pm 1, \pm 2, \dots$, $n = 0, 1, 2, \dots$

$$e_{mn}^0(r, \theta) = \beta_n^{|m|} e_{mn}^1(r, \theta) + \alpha_{n-1}^{|m|} e_{m(n-1)}^1(r, \theta) \quad (\text{VI.27})$$

and

$$(1 - r^2) e_{mn}^1(r, \theta) = \alpha_n^{|m|} e_{m(n+1)}^0(r, \theta) + \beta_n^{|m|} e_{mn}^0(r, \theta) \quad (\text{VI.28})$$

$$= \alpha_n^{|m|} \beta_{n+1}^{|m|} e_{m(n+1)}^1(r, \theta) + \left[(\alpha_n^{|m|})^2 + (\beta_n^{|m|})^2 \right] e_{mn}^1(r, \theta) + \alpha_{n-1}^{|m|} \beta_n^{|m|} e_{m(n-1)}^1(r, \theta) \quad (\text{VI.29})$$

Proof. Follows from Thm. III.19 and the definitions of e_{mn}^α for $\alpha = 0, 1$ ■

Theorem VI.16

$$\langle \langle e_{mi}^1(r, \theta), e_{pj}^0(r, \theta) \rangle \rangle_1 = \delta_{mp} \left(\alpha_{j-1}^{|m|} \delta_{(i+1)j} + \beta_j^{|m|} \delta_{ij} \right) \quad (\text{VI.30})$$

Proof. $\langle \langle e_{mi}^1(r, \theta), e_{pj}^0(r, \theta) \rangle \rangle_1$

$$= \beta_j^{|m|} \langle \langle e_{mi}^1(r, \theta), e_{pj}^1(r, \theta) \rangle \rangle_1 + \alpha_{j-1}^{|m|} \langle \langle e_{mi}^1(r, \theta), e_{p(j-1)}^1(r, \theta) \rangle \rangle_1 \quad (\text{VI.27})$$

$$= \delta_{mp} \left(\alpha_{j-1}^{|m|} \delta_{(i+1)j} + \beta_j^{|m|} \delta_{ij} \right) \text{ by orthonormality} \blacksquare$$

The next result illustrates the tri-diagonal nature of \mathbb{B}^1 .

Theorem VI.17 For $0 \leq r \leq 1$, $-\pi \leq \theta \leq \pi$, $m = 0, \pm 1, \pm 2, \pm 3, \dots$, $n = 0, 1, 2, 3, \dots$

$$\mathbb{B}^1 [e_{mn}^1(\rho, \vartheta)](r, \theta) = \frac{\alpha_n^{|m|}}{\lambda_{|m|(n+1)}} e_{m(n+1)}^0(r, \theta) + \frac{\beta_n^{|m|}}{\lambda_{|m|n}} e_{mn}^0(r, \theta) \quad (\text{VI.31})$$

$$= \eta_n^{|m|} e_{m(n+1)}^1(r, \theta) + \gamma_n^{|m|} e_{mn}^1(r, \theta) + \eta_{n-1}^{|m|} e_{m(n-1)}^1(r, \theta) \quad (\text{VI.32})$$

Proof. $\mathbb{B}^1 [e_{mn}^1(\rho, \vartheta)](r, \theta)$

$$\begin{aligned}
&= \frac{1}{\sqrt{2\pi}} \exp(im\theta) L_m^1 [u_n^{|m|}(\rho)](r) d\rho, \text{ by (VI.19)} \\
&= \frac{1}{\sqrt{2\pi}} \exp(im\theta) \left(\frac{\alpha_n^{|m|}}{\lambda_{|m|(n+1)}} t_{n+1}^{|m|}(r) + \frac{\beta_n^{|m|}}{\lambda_{|m|n}} t_n^{|m|}(r) \right) \text{ by (III.58)} \\
&= \frac{\alpha_n^{|m|}}{\lambda_{|m|(n+1)}} e_{m(n+1)}^0(r, \theta) + \frac{\beta_n^{|m|}}{\lambda_{|m|n}} e_{mn}^0(r, \theta) \\
&= \frac{\alpha_n^{|m|} \beta_{n+1}^{|m|}}{\lambda_{|m|(n+1)}} e_{m(n+1)}^1(r, \theta) + \left[\frac{(\alpha_n^{|m|})^2}{\lambda_{|m|(n+1)}} + \frac{(\beta_n^{|m|})^2}{\lambda_{|m|n}} \right] e_{mn}^1(r, \theta) + \frac{\alpha_{n-1}^{|m|} \beta_n^{|m|}}{\lambda_{|m|n}} e_{m(n-1)}^1(r, \theta) \\
&\quad \text{by (VI.27)} \\
&= \eta_n^{|m|} e_{m(n+1)}^1(r, \theta) + \gamma_n^{|m|} e_{mn}^1(r, \theta) + \eta_{n-1}^{|m|} e_{m(n-1)}^1(r, \theta) \blacksquare
\end{aligned}$$

The above results can be combined to give the following inner product result for \mathbb{B}^1 which gives us the tri-diagonal matrix representation for the weakly singular part of our system.

Theorem VI.18 For $m, p = 0, \pm 1, \pm 2, \dots$ and $n, i = 0, 1, 2, \dots$ then

$$\langle \langle \mathbb{B}^1 e_{mn}^1, e_{pi}^1 \rangle \rangle_1 = \delta_{mp} \left(\gamma_i^{|m|} \delta_{in} + \eta_{i-1}^{|m|} \delta_{i(n+1)} + \eta_i^{|m|} \delta_{i(n-1)} \right) \quad (\text{VI.33})$$

Proof. $\langle \langle \mathbb{B}^1 e_{mn}^1, e_{pi}^1 \rangle \rangle_1$

$$\begin{aligned}
&= \frac{\alpha_n^{|m|}}{\lambda_{|m|(n+1)}} \langle \langle e_{m(n+1)}^0, e_{pi}^1 \rangle \rangle_1 + \frac{\beta_n^{|m|}}{\lambda_{|m|n}} \langle \langle e_{mn}^0, e_{pi}^1 \rangle \rangle_1 \text{ by (VI.31)} \\
&= \frac{\alpha_n^{|m|}}{\lambda_{|m|(n+1)}} \left(\delta_{mp} \left(\alpha_n^{|m|} \delta_{ni} + \beta_{n+1}^{|m|} \delta_{i(n+1)} \right) \right) + \frac{\beta_n^{|m|}}{\lambda_{|m|n}} \left(\delta_{mp} \left(\alpha_{n-1}^{|m|} \delta_{(i+1)n} + \beta_n^{|m|} \delta_{in} \right) \right) \\
&\quad \text{by (III.58)} \\
&= \delta_{mp} \left(\gamma_i^{|m|} \delta_{in} + \eta_{i-1}^{|m|} \delta_{i(n+1)} + \eta_i^{|m|} \delta_{i(n-1)} \right) \text{ by (III.54)} \blacksquare
\end{aligned}$$

Theorem VI.19 \mathbb{B}^1 is a Compact and Self-adjoint operator on $L_2^1(\Omega)$.

Proof. From (VI.33) we can see that \mathbb{B}^1 can be represented as a tri-diagonal matrix with γ_n^m , η_{n-1}^m and η_n^m on the diagonals and since by (III.49), $\gamma_n^m, \eta_n^m \rightarrow 0$ as $m, n \rightarrow \infty$, it follows by ([13] page 57-58) that \mathbb{B}^1 is compact \blacksquare

Some additional results involving the \mathbb{B}^1 operator in the $L_2^1(\Omega)$ Hilbert space finish off the section.

Theorem VI.20 $\langle\langle e_{mi}^0(r, \theta), e_{pj}^0(r, \theta) \rangle\rangle_1$

$$= \delta_{mp} \left(\beta_{j-1}^{[m]} \alpha_{j-1}^{[m]} \delta_{(i+1)j} + \left[\left(\beta_j^{[m]} \right)^2 + \left(\alpha_{j-1}^{[m]} \right)^2 \right] \delta_{ij} + \alpha_j^{[m]} \beta_j^{[m]} \delta_{(i-1)j} \right) \quad (\text{VI.34})$$

Proof. $\langle\langle e_{mi}^0(r, \theta), e_{pj}^0(r, \theta) \rangle\rangle_1$

$$\begin{aligned} &= \int_{-\pi}^{\pi} \frac{\exp(im\theta) \exp(ip\theta)}{\pi \sqrt{(1 + \delta_{m0})(1 + \delta_{p0})}} d\theta \int_0^1 t_i^{[m]}(r) t_j^{[m]}(r) w^1(r) dr \\ &= \delta_{mp} \left(\beta_{j-1}^{[m]} \alpha_{j-1}^{[m]} \delta_{(i+1)j} + \left[\left(\beta_j^{[m]} \right)^2 + \left(\alpha_{j-1}^{[m]} \right)^2 \right] \delta_{ij} + \alpha_j^{[m]} \beta_j^{[m]} \delta_{(i-1)j} \right) \\ &\quad \text{by orthonormality and (III.56)} \quad \blacksquare \end{aligned}$$

Theorem VI.21

$$\langle\langle \mathbb{B}^1 e_{mn}^1, e_{pi}^0 \rangle\rangle_1 = \delta_{mp} \left(\gamma_i^{[m]} \delta_{in} + \eta_{i-1}^{[m]} \delta_{i(n+1)} + \eta_i^{[m]} \delta_{i(n-1)} \right) \quad (\text{VI.35})$$

Proof. $\langle\langle \mathbb{B}^1 e_{mn}^1, e_{pi}^0 \rangle\rangle_1$

$$\begin{aligned} &= \frac{\alpha_n^{[m]}}{\lambda_{|m|(n+1)}} \langle\langle e_{m(n+1)}^0, e_{pi}^0 \rangle\rangle_1 + \frac{\beta_n^{[m]}}{\lambda_{|m|n}} \langle\langle e_{mn}^0, e_{pi}^0 \rangle\rangle_1 \quad \text{by (VI.31)} \\ &= \frac{\alpha_n^{[m]}}{\lambda_{|m|(n+1)}} \left(\delta_{mp} \left(\beta_{i-1}^{[m]} \alpha_{i-1}^{[m]} \delta_{(n+2)i} + \left[\left(\beta_i^{[m]} \right)^2 + \left(\alpha_{i-1}^{[m]} \right)^2 \right] \delta_{(n+1)i} + \alpha_i^{[m]} \beta_i^{[m]} \delta_{ni} \right) \right) \\ &\quad + \frac{\beta_n^{[m]}}{\lambda_{|m|n}} \left(\delta_{mp} \left(\beta_{i-1}^{[m]} \alpha_{i-1}^{[m]} \delta_{(n+1)i} + \left[\left(\beta_i^{[m]} \right)^2 + \left(\alpha_{i-1}^{[m]} \right)^2 \right] \delta_{ni} + \alpha_i^{[m]} \beta_i^{[m]} \delta_{(n-1)i} \right) \right) \\ &\quad \text{by (III.56)} \end{aligned}$$

$$= \delta_{mp} \left\{ \begin{aligned} &\frac{\alpha_{i-2}^{[m]} \beta_{i-1}^{[m]} \alpha_{i-1}^{[m]}}{\lambda_{|m|(i-1)}} \delta_{(n+2)i} + \frac{\beta_{i+1}^{[m]} \alpha_i^{[m]} \beta_i^{[m]}}{\lambda_{|m|(i+1)}} \delta_{(n-1)i} \\ &+ \left[\frac{\alpha_{i-1}^{[m]} \left(\left(\beta_i^{[m]} \right)^2 + \left(\alpha_{i-1}^{[m]} \right)^2 \right)}{\lambda_{|m|i}} + \frac{\alpha_{i-1}^{[m]} \left(\beta_{i-1}^{[m]} \right)^2}{\lambda_{|m|(i-1)}} \right] \delta_{(n+1)i} \\ &+ \left[\frac{\beta_i^{[m]} \left(\alpha_i^{[m]} \right)^2}{\lambda_{|m|(i+1)}} + \frac{\beta_i^{[m]} \left(\left(\beta_i^{[m]} \right)^2 + \left(\alpha_{i-1}^{[m]} \right)^2 \right)}{\lambda_{|m|i}} \right] \delta_{ni} \end{aligned} \right\}$$

$$= \delta_{mp} \left\{ \begin{array}{l} \alpha_{i-1}^{||m|} \eta_{i-2}^{||m|} \delta_{(n+2)i} + \left[\alpha_{i-1}^{||m|} \gamma_{i-1}^{||m|} + \beta_i^{||m|} \eta_{i-1}^{||m|} \right] \delta_{(n+1)i} \\ + \left[\beta_i^{||m|} \gamma_i^{||m|} + \beta_i^{||m|} \eta_{i-1}^{||m|} \right] \delta_{ni} + \beta_i^{||m|} \eta_i^{||m|} \delta_{(n-1)i} \end{array} \right\} \blacksquare$$

Theorem VI.22 *If*

$$f(\rho, \vartheta) = \sum_{m=-\infty}^{\infty} \sum_{n=0}^{\infty} f_{mn} e_{mn}^{\alpha}(\rho, \vartheta) \in L_2^{\alpha}(\Omega)$$

for $0 \leq r \leq 1$, $-\pi \leq \theta \leq \pi$, $m = 0, \pm 1, \pm 2, \pm 3, \dots$, $n = 0, 1, 2, 3, \dots$, then

$$\| \mathbb{B}^1 f \|_1^2 = \sum_{m=-\infty}^{\infty} \sum_{n=0}^{\infty} |f_{m(n+1)} \eta_{n+1}^m + f_{mn} \gamma_n^m + f_{m(n+1)} \eta_n^m|^2 \quad (\text{VI.36})$$

Proof. $\| \mathbb{B}^1 f \|_1^2$

$$\begin{aligned} &= \left\| \sum_{m=-\infty}^{\infty} \sum_{n=0}^{\infty} f_{mn} \left[\eta_n^m e_{m(n-1)}^1(r, \theta) + \gamma_n^m e_{mn}^1(r, \theta) + \eta_{n-1}^m e_{m(n-1)}^1(r, \theta) \right] \right\|_1^2 \\ &= \int_{-\pi}^{\pi} \int_0^1 \left| \sum_{m=-\infty}^{\infty} \sum_{n=0}^{\infty} \{ f_{m(n+1)} \eta_{n+1}^m + f_{mn} \gamma_n^m + f_{m(n+1)} \eta_n^m \} e_{mn}^1(r, \theta) \right|^2 w^1(r) dr d\theta \\ &= \sum_{m=-\infty}^{\infty} \sum_{n=0}^{\infty} |f_{m(n+1)} \eta_{n+1}^m + f_{mn} \gamma_n^m + f_{m(n+1)} \eta_n^m|^2 \quad \blacksquare \end{aligned}$$

The $-\Delta_2 \mathbb{B}^1$ hyper-singular operator has unbounded eigenvalues so will not be compact. We will again define a new space that will act as the solution space for our two-dimensional hyper-singular integral equations and as the space for the right hand side equations of our weakly-singular problem as in Chapter III. The new spaces will again allow us to consider our operators as Hilbert space isomorphisms.

VI.4 THE $L_{2,\omega}^{\alpha}(\Omega)$ HILBERT SPACE

We will follow the procedures almost exactly as in Chapter III. Neither compact operator will be Hilbert-Schmidt so we will not have mean bilinear expansions. We will construct the two-dimensional analogues of the $L_{2,m}^{\alpha}(0, 1)$ spaces which are this time not dependent on a given m (basically all m 's are grouped together to form the

space). We adopt the subscript ω instead of the m to discriminate from $L_2^\alpha(\Omega)$ and to represent the fact we will again use the ω_{mn}^α definitions (III.75) and (III.76) as scaling factors, shown below with a modification for negative values of m .

$$\omega_{mn}^\alpha = \begin{cases} \lambda_{|m|n} & \alpha = 0 \\ \frac{1}{\mu_{|m|n}} & \alpha = 1 \end{cases} \quad (\text{VI.37})$$

Definition VI.23 For $\alpha = 0, 1$ let us define the inner product space of functions, $L_{2,\omega}^1(\Omega)$ as follows

$$L_{2,\omega}^1(\Omega) = \left\{ f : \sum_{m=-\infty}^{\infty} \sum_{n=0}^{\infty} (\omega_{mn}^\alpha)^2 \langle\langle f, e_{mn}^\alpha \rangle\rangle_\alpha^2 < \infty \right\} \quad (\text{VI.38})$$

with inner product

$$\langle\langle f, g \rangle\rangle_{\alpha,\omega} = \sum_{m=-\infty}^{\infty} \sum_{n=0}^{\infty} (\omega_{mn}^\alpha)^2 \langle\langle f, e_{mn}^\alpha \rangle\rangle_\alpha \overline{\langle\langle g, e_{mn}^\alpha \rangle\rangle_\alpha} \quad (\text{VI.39})$$

and norm

$$\|f\|_{\alpha,\omega} = \sqrt{\langle\langle f, f \rangle\rangle_{\alpha,\omega}} \quad (\text{VI.40})$$

The sequence of functions E_{mn}^α for $n = 0, 1, 2, \dots$ defined as follows can be easily shown to form an orthonormal basis for $L_{2,\omega}^\alpha(\Omega)$

$$E_{mn}^\alpha(r, \theta) = \frac{1}{\omega_{mn}^\alpha} e_{mn}^\alpha(r, \theta) \quad (\text{VI.41})$$

The inner products of $L_2^\alpha(\Omega)$ and $L_{2,\omega}^\alpha(\Omega)$ are related to each other as follows;

$$\langle\langle f, E_{mn}^\alpha \rangle\rangle_{\alpha,\omega} = \omega_{mn}^\alpha \langle\langle f, e_{mn}^\alpha \rangle\rangle_\alpha \quad (\text{VI.42})$$

The same applies to the sine and cosine analogues, for $m, n = 0, 1, 2, \dots$

$$C_{mn}^\alpha(r, \theta) = \frac{1}{\omega_{mn}^\alpha} c_{mn}^\alpha(r, \theta) \quad (\text{VI.43})$$

and for $m \neq 0$

$$S_{mn}^\alpha(r, \theta) = \frac{1}{\omega_{mn}^\alpha} s_{mn}^\alpha(r, \theta) \quad (\text{VI.44})$$

We will now define the inverses of our weakly and hyper-singular operators.

Definition VI.24 For

$$g(r, \theta) = \sum_{m=-\infty}^{\infty} \sum_{n=0}^{\infty} g_{mn} E_{mn}^0(r, \theta) \in L_{2,\omega}^0(\Omega)$$

and

$$f(\rho, \vartheta) = \sum_{m=-\infty}^{\infty} \sum_{n=0}^{\infty} f_{mn} e_{m,n}^1(\rho, \vartheta) \in L_2^1(\Omega)$$

we define the operators

$$\mathbb{F}^0 : L_{2,\omega}^0(0, 1) \rightarrow L_2^0(0, 1) \quad (\text{VI.45})$$

and

$$\mathbb{F}^1 : L_2^1(0, 1) \rightarrow L_{2,\omega}^1(0, 1) \quad (\text{VI.46})$$

by

$$\mathbb{F}^0 [g(r, \theta)](\rho) = \sum_{m=-\infty}^{\infty} \sum_{n=0}^{\infty} g_{mn} e_{mn}^0(\rho, \vartheta) \quad (\text{VI.47})$$

and

$$\mathbb{F}^1 [f(\rho, \vartheta)](r) = \sum_{m=-\infty}^{\infty} \sum_{n=0}^{\infty} f_{mn} E_{mn}^1(r, \theta) \quad (\text{VI.48})$$

We wish to show the completeness of the $L_{2,\omega}^\alpha(\Omega)$ spaces, to do this we first introduce a lemma relating Cauchy sequences in these spaces and in the $L_2^\alpha(\Omega)$ spaces.

Lemma VI.25 If $\{f^{(i)}\}$ is a Cauchy sequence in $L_{2,\omega}^\alpha(\Omega)$ then

1. $\{f^{(i)}\}$ is also a Cauchy sequence in $L_2^\alpha(\Omega)$
2. $\{g^{(i)}\} = \left\{ \begin{array}{ll} \mathbb{F}^0 f^{(i)} & , \alpha = 0 \\ -\Delta_2 \mathbb{B}^1 f^{(i)} & , \alpha = 1 \end{array} \right\}$ is a Cauchy sequence in $L_2^\alpha(\Omega)$.

Proof.

1. For $i = 0, 1, 2, \dots$

$$f^{(i)} = \sum_{m=-\infty}^{\infty} \sum_{n=0}^{\infty} f_{mn}^{(i)} E_{mn}^\alpha = \sum_{m=-\infty}^{\infty} \sum_{n=0}^{\infty} \frac{f_{mn}^{(i)}}{\omega_{mn}^\alpha} e_{mn}^\alpha$$

Now since $\{f^{(i)}\}$ is a Cauchy sequence in $L_{2,\omega}^\alpha(\Omega)$ for any given integer $p \geq 1, \epsilon > 0$ there exists an $M > 0$ such that

$$i > M \implies \left\| \|f^{(i+p)} - f^{(i)}\| \right\|_{\alpha,\omega}^2 < \epsilon$$

or that

$$i > M \implies \sum_{m=-\infty}^{\infty} \sum_{n=0}^{\infty} |f_{mn}^{(i+p)} - f_{mn}^{(i)}|^2 < \epsilon$$

then

$$\left\| \|f^{i+p} - f^i\| \right\|_{\alpha}^2 = \sum_{m=-\infty}^{\infty} \sum_{n=0}^{\infty} \frac{1}{\omega_{mn}^\alpha} |f_{mn}^{(i+p)} - f_{mn}^{(i)}|^2 \leq \sum_{m=-\infty}^{\infty} \sum_{n=0}^{\infty} |f_{mn}^{(i+p)} - f_{mn}^{(i)}|^2 < \epsilon$$

hence $\{f^{(i)}\}$ is a Cauchy sequence in $L_2^\alpha(\Omega)$ ■

2. For $i = 0, 1, 2, \dots$

$$g^{(i)} = \sum_{m=-\infty}^{\infty} \sum_{n=0}^{\infty} f_{mn}^{(i)} e_{mn}^\alpha$$

For any integer $p \geq 1$

$$\left\| \|g^{(i+p)} - g^{(i)}\| \right\|_{\alpha}^2 = \sum_{m=-\infty}^{\infty} \sum_{n=0}^{\infty} |f_{mn}^{(i+p)} - f_{mn}^{(i)}|^2 = \left\| \|f^{(i+p)} - f^{(i)}\| \right\|_{\alpha,\omega}^2 < \epsilon$$

Hence $\{g^{(i)}\}$ is Cauchy in $L_2^\alpha(\Omega)$ ■

Theorem VI.26 Every Cauchy sequence $\{f^{(i)}\}$ in $L_{2,\omega}^\alpha(\Omega)$ converges to a unique limit in $L_{2,\omega}^\alpha(\Omega)$ and hence the space is complete.

Proof. By above Lemma $\{g^{(i)}\} = \left\{ \begin{array}{ll} \mathbb{F}^0 f^{(i)} & , \alpha = 0 \\ -\Delta_2 \mathbb{B}^1 f^{(i)} & , \alpha = 1 \end{array} \right\}$ is a Cauchy sequences in $L_2^\alpha(\Omega)$ so there exists a unique limit

$$g = \sum_{m=-\infty}^{\infty} \sum_{n=0}^{\infty} g_{mn} e_{mn}^\alpha \in L_2^\alpha(\Omega)$$

There will then exists an $M > 0, \epsilon > 0$ such that

$$i > M \implies \left\| \|g - g^{(i)}\| \right\|_{\alpha}^2 = \sum_{m=-\infty}^{\infty} \sum_{n=0}^{\infty} |g_{mn} - f_{mn}^{(i)}|^2 < \epsilon$$

Let us consider

$$f = \sum_{m=0}^{\infty} \sum_{n=0}^{\infty} g_{mn} E_{mn}^{\alpha}$$

then

$$\|f\|_{\alpha, \omega}^2 = \sum_{m=-\infty}^{\infty} \sum_{n=0}^{\infty} |g_{mn}|^2 = \|g\|_{\alpha}^2 < \infty$$

and therefore $f \in L_{2, \omega}^{\alpha}(\Omega)$. Now supposing $i > M$ then

$$\begin{aligned} \|f - f^{(i)}\|_{\alpha, \omega}^2 &= \sum_{m=-\infty}^{\infty} \sum_{n=0}^{\infty} \omega_{mn}^{\alpha} \left| \frac{g_{mn}}{\omega_{mn}^{\alpha}} - \frac{f_{mn}^{(i)}}{\omega_{mn}^{\alpha}} \right|^2 \\ &= \sum_{m=-\infty}^{\infty} \sum_{n=0}^{\infty} |g_{mn} - f_{mn}^{(i)}|^2 < \epsilon \end{aligned}$$

hence the result.

Note also that

$$\begin{aligned} \|f - f^{(i)}\|_{\alpha}^2 &= \sum_{m=-\infty}^{\infty} \sum_{n=0}^{\infty} \frac{1}{\omega_{mn}^{\alpha}} |g_{mn} - f_{mn}^{(i)}|^2 \\ &\leq \sum_{m=-\infty}^{\infty} \sum_{n=0}^{\infty} |g_{mn} - f_{mn}^{(i)}|^2 < \epsilon \end{aligned}$$

and so f is the limit of the Cauchy sequence $\{f^{(i)}\}$ in both the $L_2^{\alpha}(\Omega)$ and $L_{2, \omega}^{\alpha}(\Omega)$ spaces ■

A similar result regarding weakly-convergent sequences now follows.

Lemma VI.27 Let $\{f^{(i)}\}$ be a sequence in $L_{2, \omega}^{\alpha}(\Omega)$ weakly convergent to $f \in L_{2, \omega}^{\alpha}(\Omega)$ then $\{f^{(i)}\}$ is also a weakly convergent sequence in $L_2^{\alpha}(\Omega)$ converging to the same limit $f \in L_2^{\alpha}(\Omega)$.

Proof. Let

$$h = \sum_{m=-\infty}^{\infty} \sum_{n=0}^{\infty} h_{mn} e_{mn}^{\alpha} \in L_2^{\alpha}(\Omega)$$

then

$$g = \sum_{m=-\infty}^{\infty} \sum_{n=0}^{\infty} h_{mn} E_{mn}^{\alpha} \in L_{2, \omega}^{\alpha}(\Omega)$$

then by definition

$$\lim_{i \rightarrow \infty} \langle \langle f^{(i)} - f, g \rangle \rangle_{\alpha, \omega} \rightarrow 0$$

so that

$$\begin{aligned} \langle f^{(i)} - f, h \rangle_{\alpha} &= \sum_{m=-\infty}^{\infty} \sum_{n=0}^{\infty} \langle \langle f^{(i)} - f, e_{mn}^{\alpha} \rangle \rangle_{\alpha} \langle \langle h, e_{mn}^{\alpha} \rangle \rangle_{\alpha} \text{ by Parseval's Formula} \\ &< \sum_{m=-\infty}^{\infty} \sum_{n=0}^{\infty} \omega_{mn}^{\alpha} \langle \langle f^{(i)} - f, e_{mn}^{\alpha} \rangle \rangle_{\alpha} \langle \langle h, e_{mn}^{\alpha} \rangle \rangle_{\alpha} \\ &= \sum_{m=-\infty}^{\infty} \sum_{n=0}^{\infty} (\omega_{mn}^{\alpha})^2 \langle \langle f^{(i)} - f, e_{mn}^{\alpha} \rangle \rangle_{\alpha} \frac{h_n}{\omega_{mn}^{\alpha}} \\ &= \sum_{m=-\infty}^{\infty} \sum_{n=0}^{\infty} (\omega_{mn}^{\alpha})^2 \langle \langle f^{(i)} - f, e_{mn}^{\alpha} \rangle \rangle_{\alpha} \langle \langle g, e_{mn}^{\alpha} \rangle \rangle_{\alpha} \\ &= \langle \langle f^{(i)} - f, g \rangle \rangle_{\alpha, \omega} \rightarrow 0 \text{ as } i \rightarrow \infty \end{aligned}$$

meaning

$$\lim_{i \rightarrow \infty} \langle \langle f^{(i)} - f, h \rangle \rangle_{\alpha} \rightarrow 0, \forall h \in L_2^{\alpha}(\Omega)$$

and hence result ■

Theorem VI.28 *The operator*

$$\mathbb{B}^0 : L_2^0(\Omega) \rightarrow L_{2, \omega}^0(\Omega)$$

is a Hilbert space isomorphism with inverse

$$\mathbb{F}^0 : L_{2, \omega}^0(\Omega) \rightarrow L_2^0(\Omega)$$

Proof. *The sequence $\{e_{mn}^0\}_{m=-\infty, n=0}^{\infty}$ is a basis for $L_2^0(\Omega)$ and the sequence $\{E_{mn}^0\}_{n=0}^{\infty}$ is a basis for $L_{2, \omega}^0(\Omega)$ since*

$$\mathbb{B}^0 e_{mn}^0 = E_{mn}^0$$

it follows that \mathbb{B}^0 is a Hilbert space isomorphism.

We also have

$$\mathbb{F}^0 E_{mn}^0 = e_{mn}^0$$

which implies that \mathbb{F}^0 is not only a Hilbert space isomorphism but the inverse of \mathbb{B}^0 ■

Theorem VI.29 *The operator*

$$-\Delta_2 \mathbb{B}^1 : L_{2,\omega}^1(\Omega) \rightarrow L_2^1(\Omega)$$

is a Hilbert space isomorphism with inverse

$$\mathbb{F}^1 : L_2^1(\Omega) \rightarrow L_{2,\omega}^1(\Omega)$$

Proof. *The sequence $\{e_{mn}^1\}_{m=-\infty, n=0}^{\infty}$ is a basis for $L_2^1(\Omega)$ and the sequence $\{E_{mn}^1\}_{n=0}^{\infty}$ is a basis for $L_{2,\omega}^1(0, 1)$ since*

$$-\Delta_2 \mathbb{B}^1 E_{mn}^1 = e_{mn}^1$$

it follows that $-\Delta_2 \mathbb{B}^1$ is a Hilbert space isomorphism.

We also have that

$$\mathbb{F}^1 e_{mn}^1 = E_{mn}^1$$

which implies that \mathbb{F}^1 is not only a Hilbert space isomorphism but the inverse of $-\Delta_2 \mathbb{B}^1$ ■

The \mathbb{F}^α operators have the obvious analogous relationships with the c_{mn}^α , s_{mn}^α , C_{mn}^α and S_{mn}^α functions.

We can now see that the isomorphism \mathbb{F}^0 has unbounded eigenvalues (λ_{mn}) and will hence be unbounded and not compact, while the isomorphism \mathbb{F}^1 has bounded eigenvalues (μ_{mn}). Since \mathbb{F}^1 has strictly decreasing eigenvalues that are all less than 1 and converge to zero similarly to $\frac{1}{n}$, it will be compact but not Hilbert-Schmidt as the double sum will not be convergent. To establish that it is in fact compact we can readily see it can be written as a diagonal operator with strictly decreasing diagonal entries convergent to zero with compactness following again using the result by Halmos ([15], prob. 132).

CHAPTER VII

A 2-D WEAKLY-SINGULAR INTEGRAL EQUATION

VII.1 INTRODUCTION

In this chapter we will investigate weakly-singular integral equations of the type

$$\int_0^1 \int_{-\pi}^{\pi} \{B(\rho, \vartheta; r, \theta) + R(\rho, \vartheta; r, \theta)\} f(\rho, \vartheta) w^0(\rho) d\vartheta d\rho = g(r, \theta) \quad (\text{VII.1})$$

where $R(\rho, \vartheta; r, \theta) \in L_2^0(\Omega) \times L_2^0(\Omega)$ is a continuous kernel, $0 \leq r \leq 1$, $-\pi < \theta \leq \pi$ and $B(\rho, \vartheta; r, \theta)$ is the Boussinesq kernel discussed in Chapter VI;

$$B(\rho, \vartheta; r, \theta) = \frac{1}{4\pi} \frac{1}{\sqrt{\rho^2 + r^2 - 2r\rho \cos(\theta - \vartheta)}} \quad (\text{VII.2})$$

To write in operator notation we will define the following integral operator \mathbb{R}^0 with continuous $L_2^0(\Omega)$ kernel $R(\rho, \vartheta; r, \theta)$;

$$\mathbb{R}^0 \{f(\rho, \vartheta)\}(r, \theta) = \int_0^1 \int_{-\pi}^{\pi} f(\rho, \vartheta) R(\rho, \vartheta; r, \theta) w^0(\rho) d\vartheta d\rho \quad (\text{VII.3})$$

We will solve these equations with procedures comparable to those in Chapter IV where we will again represent the integral equations as operator equations in the Hilbert spaces discussed in Chapter VI. We will examine the sub-cases where, for specific continuous $L_2^0(\Omega)$ kernels, we can exploit their radial nature by reducing the problem to that of solving the one-dimensional integral equations discussed in Chapter IV. We will also look at solving more general problems for kernels with an unknown or non-radially symmetric expansion.

The operator equation equivalent to (VII.1) is

$$[(\mathbb{B}^0 + \mathbb{R}^0) f(\rho, \vartheta)](r, \theta) = g(r, \theta) \in L_{2,\omega}^0(\Omega) \quad (\text{VII.4})$$

As before, we will first consider the dominant weakly-singular part first

$$[\mathbb{B}^0 f(\rho, \vartheta)](r, \theta) = g(r, \theta) \in L_{2,\omega}^0(\Omega) \quad (\text{VII.5})$$

VII.2 THE DOMINANT WEAKLY SINGULAR EQUATION

We have already looked at the properties of the integral operator \mathbb{B}^0 and have established it is a compact self adjoint operator with eigenvalues λ_{mn}^{-1} and eigenfunctions e_{mn}^0 . The next theorem uses the fact that the

$$\mathbb{B}^0 : L_2^0(\Omega) \rightarrow L_{2,\omega}^0(\Omega)$$

operator is a Hilbert space isomorphism with inverse

$$\mathbb{F}^0 : L_{2,\omega}^0(\Omega) \rightarrow L_2^0(\Omega)$$

to get a unique solution to (VII.5).

Theorem VII.1 *The equation*

$$[\mathbb{B}^0 f(\rho, \vartheta)](r, \theta) = g(r, \theta) = \sum_{m=-\infty}^{\infty} \sum_{n=0}^{\infty} g_{mn} E_{mn}^0(r, \theta) \in L_{2,\omega}^0(\Omega) \quad (\text{VII.6})$$

has a unique solution $f \in L_2^0(\Omega)$ given by

$$f(\rho, \vartheta) = \mathbb{F}^0 g(r, \theta) = \sum_{m=-\infty}^{\infty} \sum_{n=0}^{\infty} g_{mn} e_{mn}^0(r, \theta) \quad (\text{VII.7})$$

Proof. *By applying Thm. VI.28 we get that*

$$\begin{aligned} \mathbb{B}^0 f &= g \Leftrightarrow \mathbb{F}^0 \mathbb{B}^0 f = \mathbb{F}^0 g \Leftrightarrow f = \mathbb{F}^0 g \\ &\Leftrightarrow f(\rho, \vartheta) = \sum_{m=-\infty}^{\infty} \sum_{n=0}^{\infty} g_{mn} e_{mn}^0(\rho, \vartheta) \quad \blacksquare \end{aligned}$$

VII.3 THE GENERAL EQUATION

The set $L_{2,\omega}^0(\Omega)$ represents all possible functions $g(r)$ such that (VII.6) has a solution. To get a solution to the general problem we also need conditions on the

continuous $L_2^0(\Omega)$ integral operator \mathbb{R}^0 as illustrated in the following theorem.

Theorem VII.2 *The weakly-singular integral equation*

$$[(\mathbb{B}^0 + \mathbb{R}^0) f(\rho)](r) = g(r) \in L_{2,\omega}^0(\Omega) \quad (\text{VII.8})$$

has the unique solution

$$f = (\mathbb{I} + \mathbb{F}^0 \mathbb{R}^0)^{-1} \mathbb{F}^0 g \quad (\text{VII.9})$$

provided $\mathbb{F}^0 \mathbb{R}^0$ is compact and the null-space of $(\mathbb{I} + \mathbb{F}^0 \mathbb{R}^0)$ is trivial.

Proof. By Thm. VII.1, (VII.8) is equivalent to

$$(\mathbb{I} + \mathbb{F}^0 \mathbb{R}^0) f = \mathbb{F}^0 g \in L_2^0(\Omega) \quad (\text{VII.10})$$

By the Fredholm Theorems [16], $\mathbb{I} + \mathbb{F}^0 \mathbb{R}^0$ has a unique inverse if $\mathbb{F}^0 \mathbb{R}^0$ is compact and the null-space of $(\mathbb{I} + \mathbb{F}^0 \mathbb{R}^0)$ is trivial ■

We now define a four-dimensional array that can be used to expand a continuous $L_2^0(\Omega)$ kernel in terms of the basis functions.

Definition VII.3 For bounded integral operators \mathbb{R}^0 on $L_2^0(\Omega)$ with kernel $R(\rho, \vartheta; r, \theta)$ we can define the array R_{ij}^{mn} as follows

$$R_{ij}^{mn} = \langle \langle \mathbb{R}^0 e_{mn}^0, e_{ij}^0 \rangle \rangle_0 \quad (\text{VII.11})$$

$$= \int_0^1 \int_0^1 \int_{-\pi}^{\pi} \int_{-\pi}^{\pi} R(\rho, \vartheta; r, \theta) e_{mn}^0(\rho, \vartheta) \overline{e_{ij}^0(r, \theta)} w^0(\rho) w^0(r) d\vartheta d\theta d\rho dr \quad (\text{VII.12})$$

The generalized kernel expansion is then as in the following theorem.

Theorem VII.4 For $m = 0, \pm 1, \pm 2, \pm 3, \dots, n = 0, 1, 2, 3, \dots$ and \mathbb{R}^0 a bounded operator with kernel $R(\rho, \vartheta; r, \theta)$, then

$$R(\rho, \vartheta; r, \theta) = \sum_{i=-\infty}^{\infty} \sum_{j=0}^{\infty} \sum_{m=-\infty}^{\infty} \sum_{n=0}^{\infty} R_{ij}^{mn} \overline{e_{mn}^0(\rho, \vartheta)} e_{ij}^0(r, \theta) \quad (\text{VII.13})$$

and

$$\|\mathbb{R}^0\|_0^2 = \sum_{m=-\infty}^{\infty} \sum_{n=0}^{\infty} \sum_{i=-\infty}^{\infty} \sum_{j=0}^{\infty} |R_{ij}^{mn}|^2 \quad (\text{VII.14})$$

Proof. Since $\mathbb{R}e_{mn}^0 = \langle \langle R, \overline{e_{mn}^0} \rangle \rangle_0$

$$\begin{aligned} R(\rho, \vartheta; r, \theta) &= \sum_{m=-\infty}^{\infty} \sum_{n=0}^{\infty} \langle \langle R, \overline{e_{mn}^0} \rangle \rangle_0 \overline{e_{mn}^0(\rho, \vartheta)} \\ &= \sum_{m=-\infty}^{\infty} \sum_{n=0}^{\infty} \sum_{i=-\infty}^{\infty} \sum_{j=0}^{\infty} \langle \langle \mathbb{R}e_{mn}^0, e_{ij}^0 \rangle \rangle_0 \overline{e_{mn}^0(\rho, \vartheta)} e_{ij}^0(r, \theta) \\ &= \sum_{m=-\infty}^{\infty} \sum_{n=0}^{\infty} \sum_{i=-\infty}^{\infty} \sum_{j=0}^{\infty} R_{ij}^{mn} \overline{e_{mn}^0(\rho, \vartheta)} e_{ij}^0(r, \theta) \end{aligned}$$

hence,

$$\begin{aligned} \|\mathbb{R}^0\|_0^2 &= \int_{-\pi}^{\pi} \int_{-\pi}^{\pi} \int_0^1 \int_0^1 w^0(r) w^0(\rho) |R(\rho, \vartheta; r, \theta)|^2 w^0(\rho) w^0(r) d\rho dr d\vartheta d\theta \\ &= \sum_{m=-\infty}^{\infty} \sum_{n=0}^{\infty} \sum_{i=-\infty}^{\infty} \sum_{j=0}^{\infty} |R_{ij}^{mn}|^2, \text{ by orthogonality } \blacksquare \end{aligned}$$

Theorem VII.5 If \mathbb{R}^0 is an $L_2^0(\Omega)$ integral operator with continuous kernel $R(\rho, \vartheta; r, \theta)$ and

$$f(\rho, \vartheta) = \sum_{k=-\infty}^{\infty} \sum_{l=0}^{\infty} f_{kl} e_{kl}^0(\rho, \vartheta)$$

then

$$[\mathbb{R}^0 f(\rho, \vartheta)](r, \theta) = \sum_{i=-\infty}^{\infty} \sum_{j=0}^{\infty} \sum_{m=-\infty}^{\infty} \sum_{n=0}^{\infty} R_{ij}^{mn} f_{mn} e_{ij}^0(r, \theta) \quad (\text{VII.15})$$

Proof. $[\mathbb{R}^0 f(\rho, \vartheta)](r, \theta)$

$$\begin{aligned} &= \int_{-\pi}^{\pi} \int_0^1 R(\rho, \vartheta; r, \theta) f(\rho, \vartheta) w^0(\rho) d\rho d\vartheta \\ &= \sum_{i=-\infty}^{\infty} \sum_{j=0}^{\infty} \sum_{m=-\infty}^{\infty} \sum_{n=0}^{\infty} \sum_{k=-\infty}^{\infty} \sum_{l=0}^{\infty} f_{kl} R_{ij}^{mn} e_{ij}^0(r, \theta) \int_{-\pi}^{\pi} \int_0^1 \overline{e_{mn}^0(\rho, \vartheta)} e_{kl}^0(\rho, \vartheta) w^0(\rho) d\rho d\vartheta \\ &\quad \text{by (VII.13)} \\ &= \sum_{i=-\infty}^{\infty} \sum_{j=0}^{\infty} \sum_{m=-\infty}^{\infty} \sum_{n=0}^{\infty} R_{ij}^{mn} f_{mn} e_{ij}^0(r, \theta) \blacksquare \end{aligned}$$

To correctly apply the inverse \mathbb{F}^0 to $\mathbb{R}^0 g$, for $g \in L_2^0(\Omega)$, we need to guarantee that $\mathbb{R}^0 g \in L_{2,\omega}^0(\Omega)$. The following theorem provides a condition that will allow us

to be sure of that.

Theorem VII.6 *If \mathbb{R}^0 is an $L_2^0(\Omega)$ integral operator with continuous kernel $R(\rho, \vartheta; r, \theta)$ such that*

$$\sum_{m=-\infty}^{\infty} \sum_{n=0}^{\infty} \sum_{i=-\infty}^{\infty} \sum_{j=0}^{\infty} \lambda_{|ij|}^2 |R_{ij}^{mn}|^2 < \infty \quad (\text{VII.16})$$

and

$$f(\rho, \vartheta) = \sum_{k=-\infty}^{\infty} \sum_{l=0}^{\infty} f_{kl} e_{kl}^0(\rho, \vartheta) \in L_2^0(\Omega)$$

then

$$g(r) = [\mathbb{R}^0 f(\rho, \vartheta)](r, \theta) \in L_{2,\omega}^0(\Omega) \quad (\text{VII.17})$$

Proof.

$$\begin{aligned} [\mathbb{R}^0 f(\rho, \vartheta)](r, \theta) &= \sum_{i=-\infty}^{\infty} \sum_{j=0}^{\infty} \sum_{m=-\infty}^{\infty} \sum_{n=0}^{\infty} R_{ij}^{mn} f_{mn} e_{ij}^0(r, \theta) \text{ by (VII.15)} \\ &= \sum_{i=-\infty}^{\infty} \sum_{j=0}^{\infty} g_{ij} e_{ij}^0(r, \theta) \end{aligned}$$

where

$$g_{ij} = \sum_{m=-\infty}^{\infty} \sum_{n=0}^{\infty} R_{ij}^{mn} f_{mn} \quad (\text{VII.18})$$

then by the Cauchy-Schwartz inequality

$$|g_{ij}|^2 \leq \sum_{m=-\infty}^{\infty} \sum_{n=0}^{\infty} |R_{ij}^{mn}|^2 \cdot \sum_{m=-\infty}^{\infty} \sum_{n=0}^{\infty} |f_{mn}|^2$$

so

$$\begin{aligned} \|g\|_{0,\omega}^2 &= \sum_{i=-\infty}^{\infty} \sum_{j=0}^{\infty} \lambda_{|ij|}^2 |g_{ij}|^2 \\ &\leq \sum_{m=-\infty}^{\infty} \sum_{n=0}^{\infty} \sum_{i=-\infty}^{\infty} \sum_{j=0}^{\infty} \lambda_{|ij|}^2 |R_{ij}^{mn}|^2 \cdot \|f\|_0^2 < \infty \end{aligned}$$

and result follows ■

We will in certain cases, as will be shown in later chapters, have a continuous operator whose kernel has a certain angular symmetry. The next theorem shows that when this is the case then our two-dimensional operator equations can be readily solved as a collection of one-dimensional operator equations.

Theorem VII.7 *If $R(\rho, \vartheta; r, \theta)$ can be expressed as*

$$R(\rho, \vartheta; r, \theta) = \frac{1}{2\pi} \sum_{m=-\infty}^{\infty} K_m(\rho, r) \exp(im(\theta - \vartheta)) \quad (\text{VII.19})$$

then for

$$f(\rho, \vartheta) = \sum_{m=-\infty}^{\infty} f_m(\rho) \frac{\exp(im\vartheta)}{\sqrt{2\pi}}, g(r, \theta) = \sum_{m=-\infty}^{\infty} g_m(r) \frac{\exp(im\theta)}{\sqrt{2\pi}} \quad (\text{VII.20})$$

the equation

$$[(\mathbb{B}^0 + \mathbb{R}^0) f(\rho, \vartheta)](r, \theta) = g(r, \theta) \in L_{2,\omega}^0(\Omega) \quad (\text{VII.21})$$

is equivalent to

$$\{(\mathbb{L}_m^0 + \mathbb{K}_m^0) f_m(\rho)\}(r) = g_m(r) \in L_{2,m}^0(0, 1) \text{ for } m = 0, \pm 1, \pm 2, \pm 3, \dots \quad (\text{VII.22})$$

Proof. $[(\mathbb{B}^0 + \mathbb{R}^0) f(\rho, \vartheta)](r, \theta)$

$$\begin{aligned} &= \int_0^1 \int_{-\pi}^{\pi} \{B(\rho, \vartheta; r, \theta) + R(\rho, \vartheta; r, \theta)\} f(\rho, \vartheta) w^0(\rho) d\vartheta d\rho \\ &= \sum_{m=-\infty}^{\infty} f_m \left\{ \int_0^1 \int_{-\pi}^{\pi} B(\rho, \vartheta; r, \theta) \frac{\exp(im\vartheta)}{\sqrt{2\pi}} d\vartheta f_m(\rho) w^0(\rho) d\rho \right. \\ &\quad \left. + \sum_{p=-\infty}^{\infty} \frac{\exp(ip\theta)}{\sqrt{2\pi}} K_m(\rho, r) \int_0^1 \int_{-\pi}^{\pi} \frac{\exp(im\vartheta) \exp(ip\vartheta)}{2\pi} d\vartheta f_m(\rho) w^0(\rho) d\rho \right\} \\ &= \sum_{m=-\infty}^{\infty} \frac{\exp(im\theta)}{\sqrt{2\pi}} \int_0^1 [l_m(\rho, r) + K_m(\rho, r)] f_m(\rho) w^0(\rho) d\rho \\ &\quad \text{by orthogonality and (VI.19)} \\ &= \sum_{m=-\infty}^{\infty} \frac{\exp(im\theta)}{\sqrt{2\pi}} \{(\mathbb{L}_m^0 + \mathbb{K}_m^0) f_m(\rho)\}(r) \end{aligned}$$

so that

$$\begin{aligned}
& [(\mathbb{B}^0 + \mathbb{R}^0) f(\rho, \vartheta)](r, \theta) = g(r, \theta) \in L_{2, \omega}^0(\Omega) \\
\Leftrightarrow & \sum_{m=-\infty}^{\infty} \frac{\exp(im\theta)}{\sqrt{2\pi}} \{(\mathbb{L}_m^0 + \mathbb{K}_m^0) f_m(\rho)\}(r) = \sum_{m=-\infty}^{\infty} g_m(r) \frac{\exp(im\theta)}{\sqrt{2\pi}} \\
\Leftrightarrow & \{(\mathbb{L}_m^0 + \mathbb{K}_m^0) f_m(\rho)\}(r) = g_m(r) \text{ for } m = 0, \pm 1, \pm 2, \pm 3, \dots \blacksquare
\end{aligned}$$

When we have a continuous kernel that satisfies the properties of the above theorem our problem can be solved by using the numerical techniques and theory of Chapter IV. We now proceed to considering numerical solutions for the more general case.

VII.4 NUMERICAL SOLUTIONS

VII.4.1 Quadrature

We will now identify the quadrature scheme we will use throughout for integrating over the region $[-\pi, \pi]$ or in fact any region of length 2π with only a shift in quadrature points required. The quadrature points are also the points that will be used as collocation points for the collocation method. We start by defining these quadrature points and their associated weight functions which come from the extended Simpson's rule as in ([5], 25.4.6). The radial integration will be performed as in Lem. IV.15 with notation as in Def. IV.14.

Definition VII.8

N : Will use $2N + 1$ Quadrature points for angular integration

h : Step size

$$h = \frac{\pi}{N}$$

θ_p : Quadrature points

$$\theta_p = h \times p, \text{ for } p = 0, 1, 2, 3, \dots, 2N \quad (\text{VII.23})$$

\tilde{w}_p . The Simpson's rule weights

$$\tilde{w}_p = \frac{h}{3} \cdot \begin{cases} 1 & \text{if } p = 0, 2N \\ 2 & \text{if } p \text{ is odd} \\ 4 & \text{otherwise} \end{cases} \quad (\text{VII.24})$$

Our double quadrature scheme will hence be

$$\int_{-\pi}^{\pi} \int_0^1 w^0(r) f(r, \theta) dr \simeq \sum_{p=1}^{2N+1} \sum_{q=1}^M \tilde{w}_p w_q f(r_q, \theta_p) \quad (\text{VII.25})$$

VII.4.2 The Galerkin Method

For the Galerkin method we will solve (VII.10) to get the solution to (VII.8). We will approximate the solution $f \in L_2^0(\Omega)$ with the finite expansion;

$$f^{(M,N)}(\rho, \vartheta) = \sum_{i=-M}^M \sum_{j=0}^N f_{ij} e_{ij}^0(\rho, \vartheta) \quad (\text{VII.26})$$

where the coefficients f_{ij} 's are obtained by requiring that

$$\langle\langle (\mathbb{I} + \mathbb{F}^0 \mathbb{R}^0) f^{(M,N)} - \mathbb{F}^0 g, e_{kl}^0 \rangle\rangle_0 = 0 \text{ for } k = 0, \pm 1, \pm 2, \dots, M, l = 0, 1, 2, \dots, N$$

we then get the following $(2M + N + 2) \times (2M + N + 2)$ system of equations

$$\sum_{m=-M}^M \sum_{n=0}^N f_{mn} \{ \delta_{km} \delta_{ln} + \lambda_{kl} R_{kl}^{mn} \} = \lambda_{kl} g_{kl} \text{ for } k = 0, \pm 1, \pm 2, \dots, \pm M, l = 0, 1, 2, \dots, N \quad (\text{VII.27})$$

where (VII.25) gives us

$$g_{kl} = \int_{-\pi}^{\pi} \int_0^1 w^0(r) g(r, \theta) \overline{e_{kl}^0(r, \theta)} dr d\theta \quad (\text{VII.28})$$

$$\simeq \sum_{p=1}^{2N+1} \sum_{q=1}^M \tilde{w}_p w_q g(r_q, \theta_p) \overline{e_{kl}^0(r_q, \theta_p)} \quad (\text{VII.29})$$

and

$$R_{kl}^{mn}$$

$$= \int_{-\pi}^{\pi} \int_{-\pi}^{\pi} \int_0^1 \int_0^1 w^0(r) w^0(\rho) R(\rho, \vartheta; r, \theta) e_{mn}^0(\rho, \vartheta) \lambda_{kl} \overline{e_{kl}^0(r, \theta)} d\rho dr d\vartheta d\theta \quad (\text{VII.30})$$

$$\simeq \sum_{i=1}^{2N+1} \sum_{j=1}^M \sum_{p=1}^{2N+1} \sum_{q=1}^M \tilde{w}_i w_j \tilde{w}_p w_q R(r_q, \theta_p; r_i, \theta_j) e_{mn}^0(r_q, \theta_p) \overline{e_{kl}^0(r_i, \theta_j)} \quad (\text{VII.31})$$

VII.4.3 The Collocation Method

To solve (VII.8) we will approximate the solution $f(\rho, \vartheta) \in L_2^0(\Omega)$ by the finite expansion

$$f^{(M,N)}(\rho, \vartheta) = \sum_{i=-M}^M \sum_{j=0}^N f_{ij} e_{ij}^0(\rho, \vartheta) \quad (\text{VII.32})$$

then, letting

$$R_{mn}(r, \theta) = \int_{-\pi}^{\pi} \int_0^1 w^0(\rho) e_{mn}^0(\rho, \vartheta) R(\rho, \vartheta; r, \theta) d\rho d\vartheta \quad (\text{VII.33})$$

$$\simeq \sum_{p=1}^{2N+1} \sum_{q=1}^M \tilde{w}_p w_q e_{mn}^0(r_q, \theta_p) R(r_q, \theta_p; r, \theta) \quad (\text{VII.34})$$

we get the $(2M + N + 2) \times (2M + N + 2)$ linear system

$$\sum_{m=-M}^M \sum_{n=0}^N f_{mn} \{E_{mn}^0(r_q, \theta_p) + R_{mn}(r_q, \theta_p)\} = g(r_q, \theta_p), \quad (\text{VII.35})$$

for $p = 0, \pm 1, \pm 2, \dots, \pm M$, $q = 0, 1, 2, \dots, N$ where r_q and θ_p are as in Defns. IV.14 and VII.8.

VII.4.4 Numerical Tests

We are going to illustrate a problem that was created to test the method and the code. We are going to look at an even problem so our solution will be of the form

$$f^{(M,N)}(\rho, \vartheta) = \sum_{i=0}^M \sum_{j=0}^N f_{ij} c_{ij}^0(\rho, \vartheta) \quad (\text{VII.36})$$

If we consider the following functions

$$g(r, \theta) = \sum_{i=0}^M \sum_{j=0}^N g_{ij} c_{ij}^0(r, \theta) \quad (\text{VII.37})$$

$$= C_{00}^0(r, \theta) + c_{01}^0(r, \theta) + C_{11}^0(r, \theta) \quad (\text{VII.38})$$

$$= \frac{1}{\sqrt{2\pi}} \frac{1}{\lambda_{00}} + \frac{1}{\sqrt{2\pi}} t_1^0(r) + \frac{1}{\sqrt{\pi}} \frac{1}{\lambda_{11}} t_1^1(r) \cos \theta \quad (\text{VII.39})$$

$$= \frac{1}{4} \sqrt{\frac{\pi}{2}} + \sqrt{\frac{5}{2\pi}} \left(1 - \frac{3}{2} r^2\right) + \frac{3}{64} \sqrt{\frac{7\pi}{12}} \left(\frac{15}{2} r^3 - 6r\right) \cos \theta \quad (\text{VII.40})$$

and $R(\rho, \vartheta; r, \theta)$

$$= \sum_{i=0}^M \sum_{j=0}^N \sum_{p=0}^M \sum_{q=0}^N R_{ij}^{pq} c_{pq}^0(\rho, \vartheta) c_{ij}^0(r, \theta) \quad (\text{VII.41})$$

$$= c_{00}^0(\rho, \vartheta) c_{01}^0(r, \theta) + c_{00}^0(\rho, \vartheta) c_{10}^0(r, \theta) - c_{11}^0(\rho, \vartheta) c_{10}^0(r, \theta) \quad (\text{VII.42})$$

$$= \frac{1}{2\pi} t_1^0(r) + \frac{1}{\pi\sqrt{2}} t_0^1(r) \cos \theta - \frac{1}{\pi} t_1^1(\rho) t_0^1(r) \cos \vartheta \cos \theta \quad (\text{VII.43})$$

$$= \frac{\sqrt{5}}{4\pi} (2 - 3r^2) - \frac{\sqrt{3}}{2\pi} r \cos \theta + \frac{1}{2\pi} \sqrt{\frac{21}{24}} (15\rho^3 - 12\rho) r \cos \vartheta \cos \theta \quad (\text{VII.44})$$

so that clearly

$$g_{ij} = \begin{cases} \frac{1}{\lambda_{00}} & \text{if } i = j = 0 \\ 1 & \text{if } i = 0, j = 1 \\ \frac{1}{\lambda_{11}} & \text{if } i = j = 1 \\ 0 & \text{otherwise} \end{cases} \quad (\text{VII.45})$$

and

$$R_{ij}^{pq} = \begin{cases} 1 & , \text{ if } i = p = q = 0, j = 1 \\ & \text{ or } i = j = q = 0, p = 1 \\ -1 & , \text{ if } i = j = p = 1, q = 0 \\ 0 & , \text{ otherwise} \end{cases} \quad (\text{VII.46})$$

it should also then be clear that

$$f_{mn} = 0, \text{ for } m, n > 1 \quad (\text{VII.47})$$

so that we can choose $M = N = 1$ without affecting the solution.

If we define the following matrices

$$A = \text{diag}\{a_{[(i-1)(N+1)+j-1]} = \frac{1}{\lambda_{ij}}\} \quad (\text{VII.48})$$

$$B = (b_{[p(N+1)+q+1][i(N+1)+j+1]}) = R_{ij}^{pq} \quad (\text{VII.49})$$

and the vectors

$$\vec{f} = (f_{m(N+1)+n+1}) = f_{mn} \quad (\text{VII.50})$$

$$\vec{g} = (g_{m(N+1)+n+1}) = g_{mn} \quad (\text{VII.51})$$

then our Galerkin problem becomes the following linear system

$$\{A + B\} \vec{f} = \vec{g} \quad (\text{VII.52})$$

or

$$\left\{ \left[\begin{array}{cccc} \frac{1}{\lambda_{00}} & 0 & 0 & 0 \\ 0 & \frac{1}{\lambda_{01}} & 0 & 0 \\ 0 & 0 & \frac{1}{\lambda_{10}} & 0 \\ 0 & 0 & 0 & \frac{1}{\lambda_{11}} \end{array} \right] + \left[\begin{array}{cccc} 0 & 0 & 0 & 0 \\ 1 & 0 & 0 & 0 \\ 1 & 0 & 0 & -1 \\ 0 & 0 & 0 & 0 \end{array} \right] \right\} \begin{pmatrix} f_{00} \\ f_{01} \\ f_{10} \\ f_{11} \end{pmatrix} = \begin{pmatrix} \frac{1}{\lambda_{00}} \\ 1 \\ 0 \\ \frac{1}{\lambda_{11}} \end{pmatrix} \quad (\text{VII.53})$$

equivalently

$$\left\{ \left[\begin{array}{cccc} 1 & 0 & 0 & 0 \\ \lambda_{01} & 1 & 0 & 0 \\ \lambda_{10} & 0 & 1 & -\lambda_{10} \\ 0 & 0 & 0 & 1 \end{array} \right] \right\} \begin{pmatrix} f_{00} \\ f_{01} \\ f_{10} \\ f_{11} \end{pmatrix} = \begin{pmatrix} 1 \\ \lambda_{01} \\ 0 \\ 1 \end{pmatrix} \quad (\text{VII.54})$$

which has the solution

$$\begin{pmatrix} f_{00} \\ f_{01} \\ f_{10} \\ f_{11} \end{pmatrix} = \begin{pmatrix} 1 \\ 0 \\ 0 \\ 1 \end{pmatrix} \quad (\text{VII.55})$$

giving

$$f^{(M,N)}(\rho, \vartheta) = c_{00}^0(\rho, \vartheta) + c_{11}^0(\rho, \vartheta) \quad (\text{VII.56})$$

$$= \frac{1}{\sqrt{2\pi}} + \frac{1}{\sqrt{\pi}} t_1^1(\rho) \cos \vartheta \quad (\text{VII.57})$$

$$= \frac{1}{\sqrt{2\pi}} + \sqrt{\frac{7}{12\pi}} \left(\frac{15}{2} \rho^3 - 6\rho \right) \cos \vartheta \quad (\text{VII.58})$$

This problem can be solved numerically for any values of M and N using both collocation and Galerkin methods with both methods giving accurate solutions every time.

CHAPTER VIII

A 2-D HYPER-SINGULAR INTEGRAL EQUATION

VIII.1 INTRODUCTION

In this chapter we will investigate hyper-singular integral equations of the type (the Hadamard singularity is assumed to exist only in the proper context)

$$\int_0^1 \int_{-\pi}^{\pi} \{(-\Delta_2 + \kappa) B(\rho, \vartheta; r, \theta) + R(\rho, \vartheta; r, \theta)\} f(\rho, \vartheta) w^1(\rho) d\vartheta d\rho = g(r, \theta) \quad (\text{VIII.1})$$

where $R(\rho, \vartheta; r, \theta) \in L_2^1(\Omega) \times L_2^1(\Omega)$ is a continuous kernel, $0 \leq r \leq 1$, $-\pi \leq \theta \leq \pi$, κ is a constant possibly zero and $B(\rho, \vartheta; r, \theta)$ is the Boussinesq kernel discussed in Chapter VI;

$$B(\rho, \vartheta; r, \theta) = \frac{1}{4\pi} \frac{1}{\sqrt{\rho^2 + r^2 - 2r\rho \cos(\theta - \vartheta)}} \quad (\text{VIII.2})$$

To write these in operator notation we will define the following integral operator \mathbb{R}^1 with continuous $L_2^1(\Omega)$ kernel $R(\rho, \vartheta; r, \theta)$;

$$\mathbb{R}^1 \{f(\rho, \vartheta)\}(r, \theta) = \int_0^1 \int_{-\pi}^{\pi} f(\rho, \vartheta) R(\rho, \vartheta; r, \theta) w^1(\rho) d\vartheta d\rho \quad (\text{VIII.3})$$

We will solve these equations with procedures comparable to those in Chapter V where we will again represent the integral equations as operator equations in the Hilbert spaces discussed in Chapter VI. We will examine the sub-cases where, for specific continuous $L_2^1(\Omega)$ kernels, we can exploit their radial nature by reducing them to the solving of the one-dimensional integral equations discussed in Chapter V. We will also look at solving more general problems for kernels with an unknown or non-radially symmetric expansion.

In operator notation our general hyper-singular equation will be

$$[(-\Delta_2 \mathbb{B}^1 + \kappa \mathbb{B}^1 + \mathbb{R}^1) f(\rho, \vartheta)](r, \theta) = g(r, \theta) \quad (\text{VIII.4})$$

Again, we will first consider the dominant hyper-singular part

$$[-\Delta_2 \mathbb{B}^1 f(\rho, \vartheta)](r, \theta) = g(r, \theta) \quad (\text{VIII.5})$$

VIII.2 THE DOMINANT HYPER-SINGULAR EQUATION

We have already looked at the properties of the Integral Operator $-\Delta_2 \mathbb{B}^1$ and have established it is an unbounded self adjoint operator with eigenvalues μ_{mn}^{-1} , eigenfunctions e_{mn}^1 and compact inverse \mathbb{F}^1 .

Theorem VIII.1 *The equation*

$$[-\Delta_2 \mathbb{B}^1 f(\rho, \vartheta)](r, \theta) = g(r, \theta) = \sum_{m=-\infty}^{\infty} \sum_{n=0}^{\infty} g_{mn} e_{mn}^1(r, \theta) \in L_2^1(\Omega) \quad (\text{VIII.6})$$

has a unique solution $f \in L_{2,\omega}^1(\Omega)$ given by

$$f(\rho, \vartheta) = \mathbb{F}^1 \{g(r, \theta)\}(\rho, \vartheta) = \sum_{m=-\infty}^{\infty} \sum_{n=0}^{\infty} g_{mn} E_n^m(r, \theta) \quad (\text{VIII.7})$$

Proof. *By utilizing Thm. VI.28,*

$$\begin{aligned} -\Delta_2 \mathbb{B}^1 f &= g \Leftrightarrow \mathbb{F}^1(-\Delta_2 \mathbb{B}^1) f = \mathbb{F}^1 g \Leftrightarrow f = \mathbb{F}^1 g \\ &\Leftrightarrow f(\rho, \vartheta) = \sum_{m=-\infty}^{\infty} \sum_{n=0}^{\infty} g_{mn} E_{mn}^1(r, \theta) \quad \blacksquare \end{aligned}$$

VIII.3 THE GENERAL EQUATION

We can now go back and look at the general equation. First a result which shows that compactness on $L_2^1(\Omega)$ implies compactness on $L_{2,\omega}^1(\Omega)$.

Lemma VIII.2 *If \mathbb{R}^1 is an $L_2^1(\Omega)$ integral operator then \mathbb{R}^1 is compact when considered on $L_{2,\omega}^1(\Omega)$ such that.*

$$\mathbb{R}^1 : L_{2,\omega}^1(\Omega) \rightarrow L_2^1(\Omega)$$

Proof. *By Lem. VI.27 every weakly convergent sequence in $L_{2,\omega}^1(\Omega)$ is also a weakly convergent sequence in $L_2^1(\Omega)$ with both sequences converging to the same unique*

limit. Since \mathbb{R}^1 is Hilbert-Schmidt it is compact on $L_2^1(\Omega)$ and hence maps weakly convergent sequences in $L_2^1(\Omega)$ (and hence those in $L_{2,m}^1(\Omega)$) into strongly convergent ones in $L_2^1(\Omega)$ so the result follows ■

Theorem VIII.3 *The hyper-singular equation*

$$[\{(-\Delta_2 + \kappa)\mathbb{B}^1 + \mathbb{R}^1\} f(\rho)](r) = g(r) \in L_2^1(\Omega) \quad (\text{VIII.8})$$

has the unique solution

$$f = (\mathbb{I} - \mathbb{F}^1(\kappa\mathbb{B}^1 + \mathbb{R}^1))^{-1} \mathbb{F}^1 g \in L_{2,\omega}^1(\Omega) \quad (\text{VIII.9})$$

provided the null-space of $\mathbb{I} + \mathbb{F}^1(\kappa\mathbb{B}^1 + \mathbb{R}^1)$ is trivial.

Proof. By Thm. VIII.1, (VIII.8) is equivalent to

$$\{\mathbb{I} + \mathbb{F}^1(\kappa\mathbb{B}^1 + \mathbb{R}^1)\} f = \mathbb{F}^1 g \in L_{2,\omega}^1(\Omega) \quad (\text{VIII.10})$$

Since \mathbb{B}^1 , \mathbb{F}^1 and \mathbb{R}^1 are compact, $\mathbb{F}^1(\kappa\mathbb{B}^1 + \mathbb{R}^1)$ is also compact and so $(\mathbb{I} + \mathbb{F}^1(\kappa\mathbb{B}^1 + \mathbb{R}^1))^{-1}$ exists by Fredholm theorems [16], provided the null-space of $\mathbb{I} + \mathbb{F}^1(\kappa\mathbb{B}^1 + \mathbb{R}^1)$ is trivial and the result follows ■

Definition VIII.4 For the $L_2^1(\Omega)$ integral operator \mathbb{R}^1 with kernel $R(\rho, \vartheta; r, \theta)$ we can define the array R_{ij}^{mn} as follows

$$R_{ij}^{mn} = \langle \langle \mathbb{R}^1 e_{mn}^1, e_{ij}^1 \rangle \rangle_1 \quad (\text{VIII.11})$$

$$= \frac{1}{4\pi} \int_0^1 \int_0^1 \int_{-\pi}^{\pi} \int_{-\pi}^{\pi} R(\rho, \vartheta; r, \theta) e_{mn}^1(\rho, \vartheta) \overline{e_{ij}^1(r, \theta)} w^1(\rho) w^1(r) d\vartheta d\theta d\rho dr \quad (\text{VIII.12})$$

Theorem VIII.5 For $m = 0, \pm 1, \pm 2, \pm 3, \dots, n = 0, 1, 2, 3, \dots$ and \mathbb{R}^1 an $L_2^1(\Omega)$ operator with kernel $R(\rho, \vartheta; r, \theta)$, then

$$R(\rho, \vartheta; r, \theta) = \sum_{i=-\infty}^{\infty} \sum_{j=0}^{\infty} \sum_{m=-\infty}^{\infty} \sum_{n=0}^{\infty} R_{ij}^{mn} \overline{e_{mn}^1(\rho, \vartheta)} e_{ij}^1(r, \theta) \quad (\text{VIII.13})$$

and additionally

$$\|\mathbb{R}^1\|_1^2 = \sum_{m=-\infty}^{\infty} \sum_{n=0}^{\infty} \sum_{i=-\infty}^{\infty} \sum_{j=0}^{\infty} |R_{ij}^{mn}|^2 \quad (\text{VIII.14})$$

Proof. Since $\mathbb{R}e_{mn}^1 = \left\langle \left\langle R, \overline{e_{mn}^1} \right\rangle \right\rangle_1$

$$\begin{aligned} R(\rho, \vartheta; r, \theta) &= \sum_{m=-\infty}^{\infty} \sum_{n=0}^{\infty} \left\langle \left\langle R, \overline{e_{mn}^1} \right\rangle \right\rangle_1 \overline{e_{mn}^1(\rho, \vartheta)} \\ &= \sum_{m=-\infty}^{\infty} \sum_{n=0}^{\infty} \sum_{i=-\infty}^{\infty} \sum_{j=0}^{\infty} \left\langle \left\langle \mathbb{R}e_{mn}^1, e_{ij}^1 \right\rangle \right\rangle_1 e_{ij}^1(r, \theta) \overline{e_{mn}^1(\rho, \vartheta)} \\ &= \sum_{i=-\infty}^{\infty} \sum_{j=0}^{\infty} \sum_{m=-\infty}^{\infty} \sum_{n=0}^{\infty} R_{ij}^{mn} \overline{e_{mn}^1(\rho, \vartheta)} e_{ij}^1(r, \theta) \end{aligned}$$

hence,

$$\begin{aligned} \|\mathbb{R}^1\|_1^2 &= \int_{-\pi}^{\pi} \int_{-\pi}^{\pi} \int_0^1 \int_0^1 |R(\rho, \vartheta; r, \theta)|^2 w^1(\rho) w^1(r) \rho dr d\vartheta d\theta \\ &= \sum_{m=-\infty}^{\infty} \sum_{n=0}^{\infty} \sum_{i=-\infty}^{\infty} \sum_{j=0}^{\infty} |R_{ij}^{mn}|^2, \text{ by orthogonality } \blacksquare \end{aligned}$$

Theorem VIII.6 If \mathbb{R}^1 is an $L_2^1(\Omega)$ integral operator with continuous kernel $R(\rho, \vartheta; r, \theta)$ and

$$f(\rho, \vartheta) = \sum_{k=-\infty}^{\infty} \sum_{l=0}^{\infty} f_{kl} e_{kl}^1(\rho, \vartheta)$$

then

$$[\mathbb{R}^1 f(\rho, \vartheta)](r, \theta) = \sum_{i=-\infty}^{\infty} \sum_{j=0}^{\infty} \sum_{m=-\infty}^{\infty} \sum_{n=0}^{\infty} R_{ij}^{mn} f_{mn} e_{ij}^1(r, \theta) \quad (\text{VIII.15})$$

Proof. $[\mathbb{R}^1 f(\rho, \vartheta)](r, \theta)$

$$\begin{aligned} &= \int_{-\pi}^{\pi} \int_0^1 R(\rho, \vartheta; r, \theta) f(\rho, \vartheta) w^1(\rho) \rho d\vartheta \\ &= \sum_{i=-\infty}^{\infty} \sum_{j=0}^{\infty} \sum_{m=-\infty}^{\infty} \sum_{n=0}^{\infty} \sum_{k=-\infty}^{\infty} \sum_{l=0}^{\infty} f_{kl} R_{ij}^{mn} e_{ij}^1(r, \theta) \int_{-\pi}^{\pi} \int_0^1 \overline{e_{mn}^1(\rho, \vartheta)} e_{kl}^1(\rho, \vartheta) w^1(\rho) \rho d\vartheta \\ &\quad \text{by (VIII.13)} \\ &= \sum_{i=-\infty}^{\infty} \sum_{j=0}^{\infty} \sum_{m=-\infty}^{\infty} \sum_{n=0}^{\infty} R_{ij}^{mn} f_{mn} e_{ij}^1(r, \theta) \blacksquare \end{aligned}$$

We will in certain cases, as will be shown in later chapters, have a continuous operator whose kernel has a certain angular symmetry. The next theorem shows that

when this is the case then our two-dimensional operator equations can be readily solved as a collection of one-dimensional operator equations.

Theorem VIII.7 *If $R(\rho, \vartheta; r, \theta)$ can be expressed as*

$$R(\rho, \vartheta; r, \theta) = \frac{1}{2\pi} \sum_{m=-\infty}^{\infty} K_m(\rho, r) \exp(im(\theta - \vartheta)) \quad (\text{VIII.16})$$

then

$$[(-\Delta_2 \mathbb{B}^1 + \kappa \mathbb{B}^1 + \mathbb{R}^1) f(\rho, \vartheta)](r, \theta) = g(r, \theta) \in L_2^1(\Omega) \quad (\text{VIII.17})$$

is equivalent to

$$\{(\mathbb{D}_m \mathbb{L}_m^1 + \kappa \mathbb{L}_m^1 + \mathbb{K}_m^1) f_m(\rho)\}(r) = g_m(r) \in L_2^1(0, 1) \text{ for } m = 0, \pm 1, \pm 2, \pm 3, \dots, \quad (\text{VIII.18})$$

where

$$f(\rho, \vartheta) = \sum_{m=-\infty}^{\infty} f_m(\rho) \frac{\exp(im\vartheta)}{\sqrt{2\pi}}, \quad g(r, \theta) = \sum_{m=-\infty}^{\infty} g_m(r) \frac{\exp(im\theta)}{\sqrt{2\pi}} \quad (\text{VIII.19})$$

and solutions to $f_m(\rho)$ are sought in $L_{2,m}^1(0, 1)$.

Proof. $[(\Delta_2 \mathbb{B}^1 + \kappa \mathbb{B}^1 + \mathbb{R}^1) f(\rho, \vartheta)](r, \theta)$

$$\begin{aligned} &= \int_0^1 \int_{-\pi}^{\pi} \{-\Delta_2 B(\rho, \vartheta; r, \theta) + \kappa B(\rho, \vartheta; r, \theta) + R(\rho, \vartheta; r, \theta)\} f(\rho, \vartheta) w^1(\rho) d\vartheta d\rho \\ &= \sum_{m=-\infty}^{\infty} f_m \left\{ \int_0^1 \int_{-\pi}^{\pi} -\Delta_2 B(\rho, \vartheta; r, \theta) \frac{\exp(im\vartheta)}{\sqrt{2\pi}} d\vartheta f_m(\rho) w^1(\rho) d\rho \right. \\ &\quad + \int_0^1 \int_{-\pi}^{\pi} \kappa B(\rho, \vartheta; r, \theta) \frac{\exp(im\vartheta)}{\sqrt{2\pi}} d\vartheta f_m(\rho) w^1(\rho) d\rho \\ &\quad \left. + \sum_{p=-\infty}^{\infty} \frac{\exp(ip\theta)}{\sqrt{2\pi}} K_m(\rho, r) \int_0^1 \int_{-\pi}^{\pi} \frac{\exp(ip\vartheta) \exp(im\vartheta)}{\pi \sqrt{(1+\delta_{m0})(1+\delta_{p0})}} d\vartheta f_m(\rho) w^1(\rho) d\rho \right\} \\ &= \sum_{m=-\infty}^{\infty} \frac{\exp(im\theta)}{\sqrt{2\pi}} \int_0^1 [\mathbb{D}_m l_m(\rho, r) + \kappa l_m(\rho, r) + K_m(\rho, r)] f_m(\rho) w^0(\rho) d\rho \\ &\quad \text{by orthogonality, (VI.19) and (VI.20)} \\ &= \sum_{m=-\infty}^{\infty} \frac{\exp(im\theta)}{\sqrt{2\pi}} \{(\mathbb{D}_m \mathbb{L}_m^1 + \kappa \mathbb{L}_m^1 + \mathbb{K}_m^1) f_m(\rho)\}(r) \end{aligned}$$

so that

$$\left[(-\Delta_2 \mathbb{B}^1 + \kappa \mathbb{B}^1 + \mathbb{R}^1) f(\rho, \vartheta) \right] (r, \theta) = g(r, \theta) \in L_2^1(\Omega)$$

\Leftrightarrow

$$\sum_{m=-\infty}^{\infty} \frac{\exp(im\theta)}{\sqrt{2\pi}} \left\{ (\mathbb{D}_m \mathbb{L}_m^1 + \kappa \mathbb{L}_m^1 + \mathbb{K}_m^1) f_m(\rho) \right\} (r) = \sum_{m=-\infty}^{\infty} g_m(r) \frac{\exp(im\theta)}{\sqrt{2\pi}}$$

\Leftrightarrow

$$\left\{ (\mathbb{D}_m \mathbb{L}_m^1 + \kappa \mathbb{L}_m^1 + \mathbb{K}_m^1) f_m(\rho) \right\} (r) = g_m(r) \text{ for } m = 0, \pm 1, \pm 2, \pm 3, \dots \blacksquare$$

We finish the section with some results in $L_{2,\omega}^1(\Omega)$ concerning the \mathbb{B}^1 operator, that will be required for our numerical schemes.

Theorem VIII.8 For $m = 0, \pm 1, \pm 2, \dots$ and $n = 0, 1, 2, \dots$

$$\mathbb{F}^1 \mathbb{B}^1 E_{mn}^1 = \mu_{|m|n} \left(\eta_{n-1}^{|m|} E_{m(n-1)}^1 + \gamma_n^{|m|} E_{mn}^1 + \eta_n^{|m|} E_{m(n+1)}^1 \right) \quad (\text{VIII.20})$$

Proof.

$$\begin{aligned} \mathbb{F}^1 \mathbb{B}^1 E_{mn}^1 &= \mu_{|m|n} \mathbb{F}^1 \left(\eta_n^{|m|} e_{m(n-1)}^1 + \gamma_n^{|m|} e_{mn}^1 + \eta_{n-1}^{|m|} e_{m(n-1)}^1 \right) \text{ by (VI.32)} \\ &= \mu_{|m|n} \left(\eta_{n-1}^{|m|} E_{m(n-1)}^1 + \gamma_n^{|m|} E_{mn}^1 + \eta_n^{|m|} E_{m(n+1)}^1 \right) \text{ by (VI.48)} \blacksquare \end{aligned}$$

Theorem VIII.9 For $m, i = 0, \pm 1, \pm 2, \dots$ and $n, j = 0, 1, 2, \dots$

$$\begin{aligned} &\left\langle \left\langle \mathbb{F}^1 \mathbb{B}^1 E_{mn}^1, E_{ij}^1 \right\rangle \right\rangle_{1,\omega} \\ &= \delta_{mi} \left(\delta_{nj} \mu_{|m|n} \gamma_n^{|m|} + \delta_{(n-1)j} \mu_{|m|(n+1)} \eta_{n-1}^{|m|} + \delta_{(n+1)j} \mu_{|m|(n-1)} \eta_n^{|m|} \right) \quad (\text{VIII.21}) \end{aligned}$$

Proof. $\left\langle \left\langle \mathbb{F}^1 \mathbb{B}^1 E_{mn}^1, E_{ij}^1 \right\rangle \right\rangle_{1,\omega}$

$$\begin{aligned} &= \frac{\mu_{|m|n}}{\mu_{|i|j}} \left\langle \left\langle \gamma_n^{|m|} E_{mn}^1, e_{ij}^1 \right\rangle \right\rangle_1 + \frac{\mu_{|m|n}}{\mu_{|i|j}} \left\langle \left\langle \eta_{n-1}^{|m|} E_{m(n-1)}^1, e_{ij}^1 \right\rangle \right\rangle_1 \\ &\quad + \frac{\mu_{|m|n}}{\mu_{|i|j}} \left\langle \left\langle \eta_n^{|m|} E_{m(n+1)}^1, e_{ij}^1 \right\rangle \right\rangle_1, \text{ by (VIII.20)} \\ &= \delta_{mi} \left(\frac{\gamma_n^{|m|} \mu_{|m|n} \mu_{|m|n}}{\mu_{|i|j}} \delta_{nj} + \frac{\eta_{n-1}^{|m|} \mu_{|m|(n-1)} \mu_{|m|n}}{\mu_{|i|j}} \delta_{(n-1)j} + \frac{\eta_n^{|m|} \mu_{|m|(n+1)} \mu_{|m|n}}{\mu_{|i|j}} \delta_{(n+1)j} \right) \\ &= \delta_{mi} \left(\delta_{nj} \mu_{|m|n} \gamma_n^{|m|} + \delta_{(n-1)j} \mu_{|m|(n+1)} \eta_{n-1}^{|m|} + \delta_{(n+1)j} \mu_{|m|(n-1)} \eta_n^{|m|} \right) \blacksquare \end{aligned}$$

VIII.4 NUMERICAL SOLUTIONS

VIII.4.1 Quadrature

We will use the same quadrature scheme for integrating over the region $[-\pi, \pi]$ as before. The radial integration will be performed as in (V.20) with notation as in Def. IV.14.

Our double quadrature scheme will hence be

$$\int_{-\pi}^{\pi} \int_0^1 w^0(r) f(r, \theta) dr \simeq \sum_{p=1}^{2N+1} \sum_{q=1}^M \tilde{w}_p w_q f(r_q, \theta_p) [1 - r_q^2] \quad (\text{VIII.22})$$

VIII.4.2 The Galerkin Method

For the Galerkin method we will solve (VIII.10) to get the solution to (VIII.8)

We will approximate the solution $f \in L_{2,\omega}^1(\Omega)$ by the finite expansion,

$$f^{(M,N)}(\rho, \vartheta) = \sum_{i=-M}^M \sum_{j=0}^N f_{ij} E_{ij}^1(\rho, \vartheta) \quad (\text{VIII.23})$$

where the coefficients f_{ij} 's are obtained by requiring that

$$\langle\langle (\mathbb{I} + \mathbb{F}^1(\kappa \mathbb{B}^1 + \mathbb{R}^1)) f^{(M,N)} - \mathbb{F}^1 g, E_{kl}^1 \rangle\rangle_{1,\omega} = 0 \quad (\text{VIII.24})$$

for $k = 0, \pm 1, \pm 2, \pm 3, \dots, M, l = 0, 1, 2, 3, \dots, N$

We will then get the following $(2M + N + 2) \times (2M + N + 2)$ linear system of equations

$$\begin{aligned} \sum_{m=-M}^M \sum_{n=0}^N f_{mn} \{ \delta_{km} \delta_{ln} [1 + \kappa \mu_{|m|n} \gamma_n^{|m|}] + \delta_{km} \delta_{(n-1)l} \kappa \mu_{|m|(n+1)} \eta_{n-1}^{|m|} \\ + \delta_{km} \delta_{(n+1)l} \kappa \mu_{|m|(n-1)} \eta_n^{|m|} + \mu_{|m|n} R_{kl}^{mn} \} = g_{kl} \end{aligned} \quad (\text{VIII.25})$$

for $k = 0, \pm 1, \pm 2, \pm 3, \dots, M, l = 0, 1, 2, 3, \dots, N$, where (VIII.22) gives us

$$g_{kl} = \int_{-\pi}^{\pi} \int_0^1 w^1(r) g(r, \theta) \overline{e_{kl}^1(r, \theta)} dr d\theta \quad (\text{VIII.26})$$

$$\simeq \sum_{p=1}^{2N+1} \sum_{q=1}^M \tilde{w}_p w_q g(r_q, \theta_p) \overline{e_{kl}^1(r_q, \theta_p)} [1 - r_q^2] \quad (\text{VIII.27})$$

and

$$R_{kl}^{mn} = \int_{-\pi}^{\pi} \int_{-\pi}^{\pi} \int_0^1 \int_0^1 w^1(r) w^1(\rho) R(\rho, \vartheta; r, \theta) e_{mn}^1(\rho, \vartheta) \lambda_{kl} \overline{e_{kl}^1(r, \theta)} d\rho d\vartheta dr d\theta \quad (\text{VIII.28})$$

$$\simeq \sum_{i=1}^{2N+1} \sum_{j=1}^M \sum_{p=1}^{2N+1} \sum_{q=1}^M \tilde{w}_i w_j \tilde{w}_p w_q R(r_q, \theta_p; r_i, \theta_j) e_{mn}^1(r_q, \theta_p) \overline{e_{kl}^1(r_i, \theta_j)} [1 - r_q^2] [1 - r_i^2] \quad (\text{VIII.29})$$

VIII.4.3 The Collocation Method

To solve (VIII.8) we will approximate the solution $f(\rho, \vartheta) \in L_{2,\omega}^1(\Omega)$ by the finite expansion

$$f^{(M,N)}(\rho, \vartheta) = \sum_{i=-M}^M \sum_{j=0}^N f_{ij} E_{ij}^1(\rho, \vartheta) \quad (\text{VIII.30})$$

letting

$$R_{mn}(r, \theta) = \int_{-\pi}^{\pi} \int_0^1 w^1(\rho) E_{mn}^1(\rho, \vartheta) R(\rho, \vartheta; r, \theta) d\rho d\vartheta \quad (\text{VIII.31})$$

$$\simeq \sum_{p=1}^{2N+1} \sum_{q=1}^M \tilde{w}_p w_q E_{mn}^1(r_q, \theta_p) R(r_q, \theta_p; r, \theta) [1 - r_q^2] \quad (\text{VIII.32})$$

leads to the $(2M + N + 2) \times (2M + N + 2)$ linear system

$$\sum_{m=-M}^M \sum_{n=0}^N f_{mn} [e_{mn}^1(r_q, \theta_p) + \mu_{|m|n} R_{mn}(r_q, \theta_p) + \kappa \mu_{|m|n} \left(\frac{\alpha_{n-1}^{|m|}}{\lambda_{|m|(n-1)}} e_{m(n-1)}^0(r_q, \theta_p) + \frac{\beta_n^{|m|}}{\lambda_{|m|n}} e_{mn}^0(r_q, \theta_p) \right)] = g(r_q, \theta_p) \quad (\text{VIII.33})$$

or

$$\begin{aligned} & \sum_{m=-M}^M \sum_{n=0}^N f_{mn} \{ e_{mn}^1(r_q, \theta_p) + \mu_{|m|n} R_{mn}(r_q, \theta_p) \\ & + \kappa \mu_{|m|n} (\eta_n^{|m|} e_{m(n-1)}^1(r, \theta) + \gamma_n^{|m|} e_{mn}^1(r, \theta) + \eta_{n-1}^{|m|} e_{m(n-1)}^1(r, \theta)) \} = g(r_q, \theta_p) \end{aligned} \quad (\text{VIII.34})$$

for $q = 1, 2, \dots, N+1, p = 0, \pm 1, \pm 2, \pm 3, \dots, M$ where r_q and θ_p are as in Defns. IV.14 and VII.8.

VIII.4.4 Numerical Tests

We are going to illustrate a problem that was created to test the method and the code. We are going to look at an odd problem so our solution will be of the form

$$f^{(M,N)}(\rho, \vartheta) = \sum_{i=1}^M \sum_{j=0}^N f_{ij} s_{ij}^1(\rho, \vartheta) \quad (\text{VIII.35})$$

As a test for the weakly-singular part we can use the equation ($\kappa = 1$);

$$\{B^1[f(\rho, \vartheta)]\}(r, \theta) = g(r, \theta), 0 \leq r \leq 1, -\pi < \theta \leq \pi \quad (\text{VIII.36})$$

where for any given m and p values

$$g(r, \theta) = \sum_{i=1}^M \sum_{j=0}^N g_{ij} s_{ij}^1(r, \theta) \quad (\text{VIII.37})$$

$$= \mu_{mp} (\eta_{p-1}^m s_{m(p-1)}^1(r, \theta) + \gamma_p^m s_{mp}^1(r, \theta) + \eta_p^m s_{m(p+1)}^1(r, \theta)) \quad (\text{VIII.38})$$

$$= \mu_{mp} \frac{\sin(m\theta)}{\sqrt{\pi}} (\eta_{p-1}^m u_{p-1}^m(r) + \gamma_p^m u_p^m(r) + \eta_p^m u_{p+1}^m(r)) \quad (\text{VIII.39})$$

$$= \mu_{mp} \left(\frac{\beta_p^m}{\lambda_{mp}} s_{mp}^0(r, \theta) + \frac{\alpha_p^m}{\lambda_{m(p+1)}} s_{m(p+1)}^0(r, \theta) \right) \quad (\text{VIII.40})$$

$$= \mu_{mp} \frac{\sin(m\theta)}{\sqrt{\pi}} \left(\frac{\beta_p^m}{\lambda_{mp}} t_p^m(r) + \frac{\alpha_p^m}{\lambda_{m(p+1)}} t_{p+1}^m(r) \right) \quad (\text{VIII.41})$$

with solution

$$f(\rho) = S_{mp}^1(\rho) \quad (\text{VIII.42})$$

If we define the following matrix

$$D = \left\{ \begin{array}{l} d_{[(i-1)(N+1)+j+1]} = \gamma_j^i \\ d_{[(i-1)(N+1)+j+1][(i-1)(N+1)+j]} = \eta_j^i H(j-1) \\ d_{[(i-1)(N+1)+j][(i-1)(N+1)+j+1]} = \eta_j^i H(j-1) \\ d_{ij} = 0, \text{ otherwise} \end{array} \right\} \quad (\text{VIII.43})$$

and the vectors

$$\vec{f} = (f_{m(N+1)+n+1}) = f_{mn} \quad (\text{VIII.44})$$

$$\vec{g} = (g_{m(N+1)+n+1}) = g_{mn} \quad (\text{VIII.45})$$

then our Galerkin system can be written as

$$D\vec{f} = \vec{g} \quad (\text{VIII.46})$$

where for $m < 3, p < 2$, we can set $M = 2, N = 1$ giving the system

$$\begin{pmatrix} \gamma_0^1 & \eta_0^1 & 0 & 0 \\ \eta_0^1 & \gamma_1^1 & 0 & 0 \\ 0 & 0 & \gamma_0^2 & \eta_0^2 \\ 0 & 0 & \eta_0^2 & \gamma_1^2 \end{pmatrix} \begin{pmatrix} f_{10} \\ f_{11} \\ f_{20} \\ f_{21} \end{pmatrix} = \begin{pmatrix} \mu_{mp} [\delta_{m1} (\delta_{p1}\eta_0^1 + \delta_{p0}\gamma_0^1)] \\ \mu_{mp} [\delta_{m1} (\delta_{p2}\eta_0^1 + \delta_{p1}\gamma_0^1 + \delta_{p0}\eta_0^1)] \\ \mu_{mp} [\delta_{m2} (\delta_{p1}\eta_0^2 + \delta_{p0}\gamma_0^2)] \\ \mu_{mp} [\delta_{m2} (\delta_{p2}\eta_1^2 + \delta_{p1}\gamma_1^2 + \delta_{p0}\eta_0^2)] \end{pmatrix} \quad (\text{VIII.47})$$

which for $m = 2, p = 1$ is

$$\begin{pmatrix} \gamma_0^1 & \eta_0^1 & 0 & 0 \\ \eta_0^1 & \gamma_1^1 & 0 & 0 \\ 0 & 0 & \gamma_0^2 & \eta_0^2 \\ 0 & 0 & \eta_0^2 & \gamma_1^2 \end{pmatrix} \begin{pmatrix} f_{10} \\ f_{11} \\ f_{20} \\ f_{21} \end{pmatrix} = \begin{pmatrix} 0 \\ 0 \\ \mu_{21}\eta_0^2 \\ \mu_{21}\gamma_1^2 \end{pmatrix} \quad (\text{VIII.48})$$

Both methods give accurate and fast solutions for all values of m, p, M and N ($M \geq m, N \geq n$) used.

Now we consider $\kappa = 0$, the problem with no weakly-singular part. If we define

the following functions

$$g(r, \theta) = \sum_{i=1}^M \sum_{j=0}^N g_{ij} s_{ij}^1(r, \theta) \quad (\text{VIII.49})$$

$$= \frac{1}{\mu_{11}} s_{11}^1(r, \theta) + \frac{1}{\mu_{20}} s_{20}^1(r, \theta) \quad (\text{VIII.50})$$

$$= \frac{45\sqrt{\pi}}{64} u_1^1(r) \sin \theta + \frac{15\sqrt{\pi}}{32} u_0^2(r) \sin 2\theta \quad (\text{VIII.51})$$

$$= \frac{675}{256} \sqrt{\frac{\pi}{5}} (7r^3 - 4r) \sin \theta + \frac{225}{64} \sqrt{\frac{7\pi}{30}} r^2 \sin 2\theta \quad (\text{VIII.52})$$

and

$$R(\rho, \vartheta; r, \theta) = \sum_{i=1}^M \sum_{j=0}^N \sum_{p=1}^M \sum_{q=0}^N R_{ij}^{pq} s_{pq}^1(\rho, \vartheta) s_{ij}^1(r, \theta) \quad (\text{VIII.53})$$

$$= s_{10}^1(\rho, \vartheta) s_{10}^1(r, \theta) + s_{11}^1(\rho, \vartheta) s_{21}^1(r, \theta) - s_{20}^1(\rho, \vartheta) s_{21}^1(r, \theta) \quad (\text{VIII.54})$$

$$= \frac{1}{\pi} u_0^1(\rho) u_0^1(r) \sin \vartheta \sin \theta + \frac{1}{\pi} u_1^1(\rho) u_1^2(r) \sin \vartheta \sin 2\theta - \frac{1}{\pi} u_0^2(\rho) u_1^2(r) \sin 2\vartheta \sin 2\theta \quad (\text{VIII.55})$$

$$= \frac{15}{2\pi} \rho r \sin \vartheta \sin \theta - \frac{1575}{8\pi} \sqrt{\frac{11}{1050}} (7\rho^3 - 4\rho) (3r^4 - 2r^2) \sin \vartheta \sin 2\theta + \frac{1575}{8\pi} \sqrt{\frac{77}{6300}} \rho^2 (3r^4 - 2r^2) \sin 2\vartheta \sin 2\theta \quad (\text{VIII.56})$$

so that clearly

$$g_{ij} = \begin{cases} \frac{1}{\mu_{11}} & \text{if } i, j = 1 \\ \frac{1}{\mu_{20}} & \text{if } i = 2, j = 0 \\ 0 & \text{otherwise} \end{cases} \quad (\text{VIII.57})$$

and

$$R_{ij}^{pq} = \begin{cases} 1 & \text{if } i = p = 1, j = q = 0 \\ & \text{or } i, j, q = 1, p = 2 \\ -1 & \text{if } i, p = 2, j = 0, q = 1 \\ 0 & \text{otherwise} \end{cases} \quad (\text{VIII.58})$$

It should also then be clear that

$$f_{mn} = 0, \text{ for } m > 2, n > 1 \quad (\text{VIII.59})$$

so that we can choose $M = 2, N = 1$ without affecting the solution.

If we define the following matrices

$$A = \text{diag} \left(a_{[(i-1)(N+1)+j+1]} = \frac{1}{\mu_{ij}} \right) \quad (\text{VIII.60})$$

$$B = (b_{[(p-1)N+q+1][(i-1)N+j+1]}) = R_{ij}^{pq} \quad (\text{VIII.61})$$

then our Galerkin problem (with $\kappa = 0$), becomes the following linear system

$$\{A + B\} \vec{f} = \vec{g} \quad (\text{VIII.62})$$

or

$$\left\{ \begin{bmatrix} \frac{1}{\mu_{10}} & 0 & 0 & 0 \\ 0 & \frac{1}{\mu_{11}} & 0 & 0 \\ 0 & 0 & \frac{1}{\mu_{20}} & 0 \\ 0 & 0 & 0 & \frac{1}{\mu_{11}} \end{bmatrix} + \begin{bmatrix} 1 & 0 & 0 & 0 \\ 0 & 0 & 0 & 0 \\ 0 & 1 & -1 & 0 \\ 0 & 0 & 0 & 0 \end{bmatrix} \right\} \begin{pmatrix} f_{10} \\ f_{11} \\ f_{20} \\ f_{21} \end{pmatrix} = \begin{pmatrix} 0 \\ \frac{1}{\mu_{11}} \\ \frac{1}{\mu_{20}} \\ 0 \end{pmatrix} \quad (\text{VIII.63})$$

equivalently

$$\left\{ \begin{bmatrix} 1 + \mu_{10} & 0 & 0 & 0 \\ 0 & 1 & 0 & 0 \\ 0 & \mu_{20} & 1 - \mu_{20} & 0 \\ 0 & 0 & \eta_j^i & 1 \end{bmatrix} \right\} \begin{pmatrix} f_{10} \\ f_{11} \\ f_{20} \\ f_{21} \end{pmatrix} = \begin{pmatrix} 0 \\ 1 \\ 1 \\ 0 \end{pmatrix} \quad (\text{VIII.64})$$

which has the solution

$$\begin{pmatrix} f_{10} \\ f_{11} \\ f_{20} \\ f_{21} \end{pmatrix} = \begin{pmatrix} 0 \\ 1 \\ 1 \\ 0 \end{pmatrix} \quad (\text{VIII.65})$$

giving

$$f^{(M,N)}(\rho, \vartheta) = s_{01}^0(\rho, \vartheta) + s_{10}^0(\rho, \vartheta) \quad (\text{VIII.66})$$

$$= \sqrt{\frac{1}{2\pi}} t_1^0(\rho) + \frac{1}{\sqrt{\pi}} t_0^1(\rho) \sin \vartheta \quad (\text{VIII.67})$$

$$= \sqrt{\frac{5}{2\pi}} \left(1 - \frac{3}{2} \rho^2 \right) - \sqrt{\frac{3}{2\pi}} \rho \sin \vartheta \quad (\text{VIII.68})$$

This problem can be solved numerically for any values of M and N using both collocation and Galerkin methods with both methods giving accurate solutions every time.

To test the full equation we will repeat the previous problem with $\kappa = 1$ giving the Galerkin system

$$\{A + D + B\} \vec{f} = \vec{g} \quad (\text{VIII.69})$$

or

$$\begin{pmatrix} 1 + \frac{1}{\mu_{10}} + \gamma_0^1 & \eta_0^1 & 0 & 0 \\ \eta_1^1 & \frac{1}{\mu_{11}} + \gamma_1^1 & 0 & 0 \\ 0 & 1 & \frac{1}{\mu_{20}} + \gamma_0^2 - 1 & \eta_0^2 \\ 0 & 0 & \eta_1^2 & \frac{1}{\mu_{21}} + \gamma_1^2 \end{pmatrix} \begin{pmatrix} f_{10} \\ f_{11} \\ f_{20} \\ f_{21} \end{pmatrix} = \begin{pmatrix} 0 \\ \frac{1}{\mu_{11}} \\ \frac{1}{\mu_{21}} \\ 0 \end{pmatrix} \quad (\text{VIII.70})$$

equivalently

$$\begin{pmatrix} 1 + \mu_{10}(1 + \gamma_0^1) & \mu_{10}\eta_0^1 & 0 & 0 \\ \mu_{11}\eta_0^1 & 1 + \mu_{11}\gamma_1^1 & 0 & 0 \\ 0 & \mu_{20} & 1 - \mu_{20}(\gamma_0^2 - 1) & \mu_{20}\eta_1^2 \\ 0 & 0 & \mu_{21}\eta_0^2 & 1 + \mu_{21}\eta_1^2\gamma_1^2 \end{pmatrix} \begin{pmatrix} f_{10} \\ f_{11} \\ f_{20} \\ f_{21} \end{pmatrix} = \begin{pmatrix} 0 \\ 1 \\ 1 \\ 0 \end{pmatrix} \quad (\text{VIII.71})$$

which has the solution

$$\begin{pmatrix} f_{10} \\ f_{11} \\ f_{20} \\ f_{21} \end{pmatrix} = \begin{pmatrix} 1 + \mu_{10}(1 + \gamma_0^1) & \mu_{10}\eta_0^1 & 0 & 0 \\ \mu_{11}\eta_0^1 & 1 + \mu_{11}\gamma_1^1 & 0 & 0 \\ 0 & \mu_{20} & 1 - \mu_{20}(\gamma_0^2 - 1) & \mu_{20}\eta_1^2 \\ 0 & 0 & \mu_{21}\eta_0^2 & 1 + \mu_{21}\eta_1^2\gamma_1^2 \end{pmatrix}^{-1} \begin{pmatrix} 0 \\ 1 \\ 1 \\ 0 \end{pmatrix} \quad (\text{VIII.72})$$

We solve for both methods with varying M and N values with an example solution set shown in Table (2).

TABLE 2

Comparison of results for two-dimensional hyper-singular test problem. Results are shown for the number of terms and the number of collocation points 6 for both variables, with 30 quadrature points for each variable.

m	n	f_{mn} Galerkin	f_{mn} Collocation	m	n	f_{mn} Galerkin	f_{mn} Collocation
1	0	0.539760	0.539760	4	0	0.000000	0.000000
1	1	1.035361	1.035361	4	1	0.000000	0.000000
1	2	0.007294	0.007294	4	2	0.000000	0.000000
1	3	0.000029	0.000029	4	3	0.000000	0.000000
1	4	0.000000	0.000000	4	4	0.000000	0.000000
1	5	0.000000	0.000000	4	5	0.000000	0.000000
2	0	1.046612	1.046612	5	0	0.000000	0.000000
2	1	0.005751	0.005751	5	1	0.000000	0.000000
2	2	0.000029	0.000029	5	2	0.000000	0.000000
2	3	0.000000	0.000000	5	3	0.000000	0.000000
2	4	0.000000	0.000000	5	4	0.000000	0.000000
2	5	0.000000	0.000000	5	5	0.000000	0.000000
3	0	0.000000	0.000000	6	0	0.000000	0.000000
3	1	0.000000	0.000000	6	1	0.000000	0.000000
3	2	0.000000	0.000000	6	2	0.000000	0.000000
3	3	0.000000	0.000000	6	3	0.000000	0.000000
3	4	0.000000	0.000000	6	4	0.000000	0.000000
3	5	0.000000	0.000000	6	5	0.000000	0.000000

CHAPTER IX

APPLICATIONS I: PROBLEMS IN POTENTIAL THEORY

IX.1 INTRODUCTION

In this chapter we illustrate some applications in Potential Theory and in particular Electrostatics. The problems we will consider will involve charged discs in an infinite medium. The first and simplest problem we will consider involves a single charged disc in an electrostatic field. It is easily identified with the Dirichlet problem of Chapter II and is solved by a single layer potential. The layer potential solution requires the charge density to satisfy a two-dimensional weakly-singular boundary integral equation which fits the criteria of Thm. VII.7 and can therefore be solved as a collection of one-dimensional problems as in Chapter IV. These particular problems have no separate non-singular kernel and were largely motivational in finding the eigenfunctions, eigenvalues and defining the Hilbert spaces we use to solve the other problems.

Other problems we will consider involve two (or more) charged discs. These problems produce simultaneous integral equations with a weakly-singular kernel and a continuous non-singular kernel or kernels. We will generally investigate problems with angular symmetries that reduce to a single equation. Our first multiple disc case exhibits such symmetries, a pair of charged parallel discs and in particular the parallel plate condenser problem. These problems when solved by layer potentials produce two dimensional weakly-singular boundary integral equations with continuous kernels that fit the criteria of Thm. VII.7 allowing us to again solve as a collection of one-dimensional weakly singular integral equations. When the discs are non-coaxial we have to solve the full two dimensional weakly-singular problem as in Chapter VII. We tackle various examples some to illustrate how the method works and others to demonstrate it's use in more sophisticated problems. We will generally look for the Capacitance or Capacitance like properties of these pairs of discs.

IX.2 SINGLE DISC PROBLEMS

IX.2.1 General Problem

Consider a thin Laminar conductor

$$\Omega = \{(r, \theta) : 0 \leq r \leq 1, -\pi < \theta \leq \pi\} \quad (\text{IX.1})$$

that is charged to a potential of V volts, placed in a field

$$\vec{E}_0(\vec{r}) = -\nabla U^0(\vec{r}) \quad (\text{IX.2})$$

where \vec{E}_0 is in volts/meter and $U^0(\vec{r})$ is a potential function that may depend on position.

If the charged density on the positive side is $\sigma^+(\vec{r})$ coulombs/meter² and the charge density on the negative side is $\sigma^-(\vec{r})$ then the total charge density is

$$\sigma(\vec{r}) = \sigma^+(\vec{r}) + \sigma^-(\vec{r}) \quad (\text{IX.3})$$

The potential at a point $\vec{r} \in \mathbb{R}^3$ is then given by

$$\phi(\vec{r}) = U^0(\vec{r}) + \frac{1}{4\pi\epsilon_0} \int_{\Omega} \frac{\sigma(\vec{r}') dS(\vec{s}')}{|\vec{r} - \vec{s}'|} \quad (\text{IX.4})$$

$$= U^0(\vec{r}) + \frac{1}{\epsilon_0} \mathbb{S}[\sigma(\vec{r})](\vec{s}) \quad (\text{IX.5})$$

If \vec{r} approaches Ω , we find that $\sigma(\vec{r})$ is given by the following Boussinesq Equation

$$\frac{1}{4\pi\epsilon_0} \int_{\Omega} \frac{\sigma(\vec{r}') dS(\vec{s}')}{|\vec{r} - \vec{s}'|} = V - U^0(\vec{r}), \text{ for } \vec{r} \in \Omega \quad (\text{IX.6})$$

We can also know that

$$\sigma^+(\vec{r}) - \sigma^-(\vec{r}) = -2 \frac{\partial U^0(\vec{r})}{\partial z} = 2E_z(\vec{r}), \text{ for } \vec{r} \in \Omega$$

from which we can find both σ^+ and σ^- once σ is known.

Since the Laminar conductor is the circular disc as in (IX.1), we get the following Boussinesq type equation

$$\frac{1}{4\pi} \int_0^1 \int_{-\pi}^{\pi} \frac{f(\rho, \vartheta)}{\sqrt{r^2 + \rho^2 - 2r\rho \cos(\vartheta - \theta)}} w^0(\rho) d\rho d\vartheta = g(r, \theta), \text{ for } (r, \theta) \in \Omega \quad (\text{IX.7})$$

where

$$g(r, \theta) = V - U^0(r, \theta) \quad (\text{IX.8})$$

and

$$f(\rho, \vartheta) = \frac{1}{\epsilon_0} \sigma(\rho, \vartheta) \sqrt{1 - \rho^2} \quad (\text{IX.9})$$

The equivalent operator equation in Hilbert space is

$$\mathbb{B}^0[f(\rho, \vartheta)](r, \theta) = g(r, \theta) \in L_{2,\omega}^0(\Omega) \quad (\text{IX.10})$$

which reduces to the one-dimensional weakly-singular operator equation

$$\mathbb{L}_m^0[f_m(\rho)](r) = g_m(r) \in L_{2,m}^0(\Omega), \text{ for } m = 0, 1, 2, \dots \quad (\text{IX.11})$$

where

$$f_m(\rho) = \int_{-\pi}^{\pi} f(\rho, \vartheta) \frac{\exp im\vartheta}{\sqrt{2\pi}} d\vartheta \quad (\text{IX.12})$$

and

$$g_m(r) = \int_{-\pi}^{\pi} g(r, \theta) \frac{\exp im\theta}{\sqrt{2\pi}} d\theta \quad (\text{IX.13})$$

are the Fourier series coefficients of f and g .

IX.2.2 Case 1: Circular Disc Charged to a Constant Potential

In the case where the circular disc Ω , is charged to a constant potential V volts and there is no external field present we see that

$$g(r, \theta) = V = \sum_{m=-\infty}^{\infty} \delta_{m0} V \exp(im\theta) \quad (\text{IX.14})$$

and

$$f(\rho, \vartheta) = f(\rho) = \frac{1}{\epsilon_0} \sigma(\rho) \sqrt{1 - \rho^2} = \sum_{m=-\infty}^{\infty} \delta_{m0} f_m(\rho) \exp(im\vartheta) \quad (\text{IX.15})$$

where $f(\rho)$ is given by the following equation

$$\mathbb{L}_0^0 [f(\rho)](r) = V \quad (\text{IX.16})$$

Clearly (IX.10) has the solution

$$f(\rho) = \lambda_{00} V = \frac{4V}{\pi} \quad (\text{IX.17})$$

giving Weber's well known result for the charge density

$$\sigma(\rho) = \frac{4\epsilon_0 V}{\pi\sqrt{1-\rho^2}} \quad (\text{IX.18})$$

Some solutions are shown in Figure 2 for differing values of V . The key points to note are the proportionality relationship with V and the singularity on the edge of the discs.

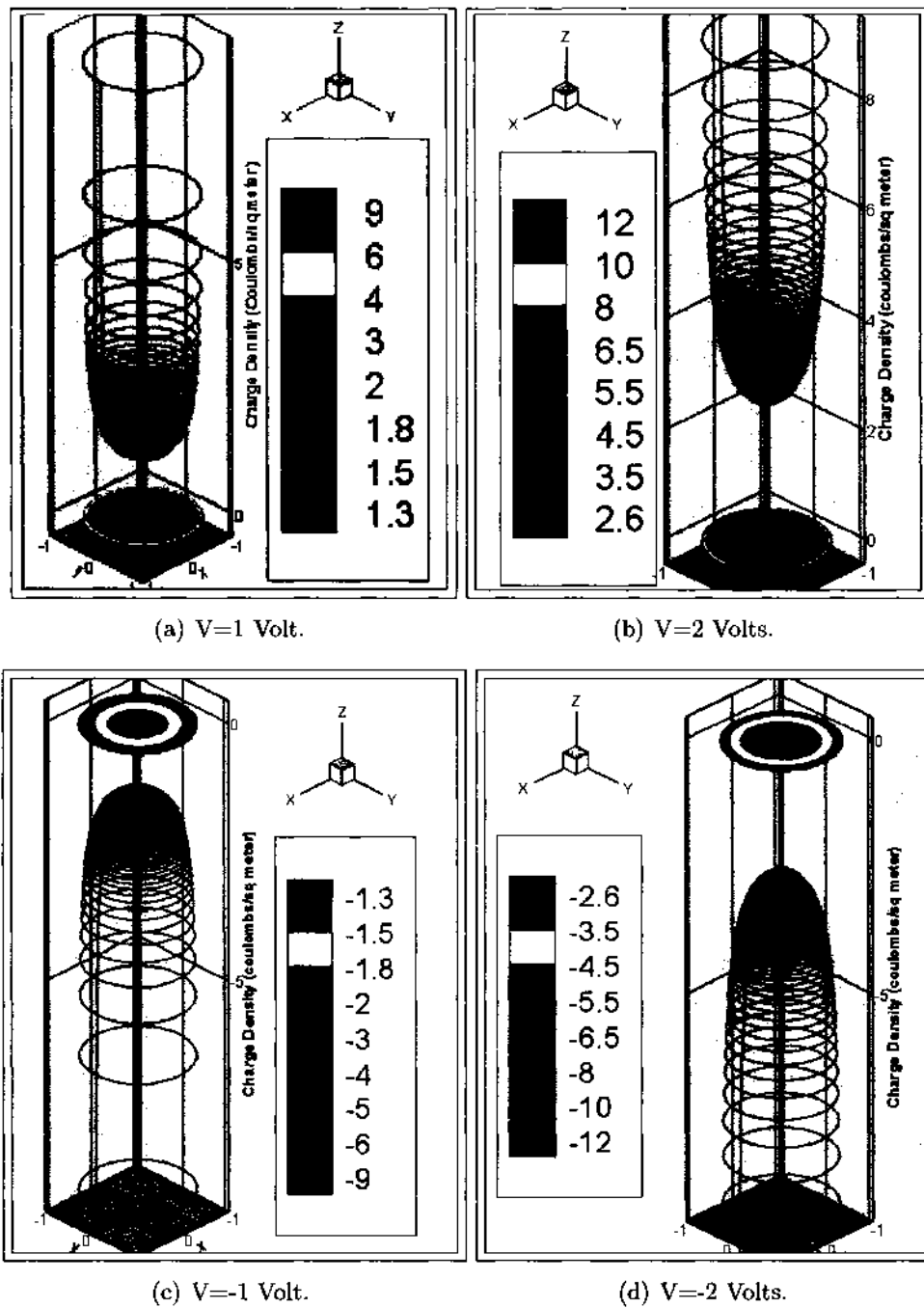


FIG. 2. Some plots of the scaled charge density (σ/ϵ_0) on a lamina disc held to different F potentials.

IX.2.3 Case 2: Earthed Circular Disc in a Parallel Field

Here we insert the circular disc Ω into the field $\vec{E}_0 = E_0 \vec{i}$ and hold it to a zero potential so that $\vec{E}_0 = -\nabla U^0$ where

$$U^0(r, \theta, z) = -E_0 r \cos \theta \quad (\text{IX.19})$$

it follows that

$$g(r, \theta) = E_0 r \cos \theta = \sum_{m=0}^{\infty} -\delta_{m1} E_0 \sqrt{\frac{2}{3}} t_0^1(r) \cos(m\theta) \quad (\text{IX.20})$$

and since we can expand f as the even function

$$f(\rho, \vartheta) = \frac{1}{\epsilon_0} \sigma(\rho, \vartheta) \sqrt{1-\rho^2} = f_1(\rho) \cos(m\vartheta) = \sum_{m=0}^{\infty} \delta_{m1} f_m(\rho) \cos(m\vartheta) \quad (\text{IX.21})$$

where $f_1(\rho)$ is given by the one-dimensional weakly-singular operator equation

$$\mathbb{L}_1^0[f_1(\rho)](r) = E_0 r = \sum_{n=0}^{\infty} -\delta_{n0} E_0 \sqrt{\frac{2}{3}} t_n^1(r), \text{ for } 0 \leq r \leq 1 \quad (\text{IX.22})$$

the solution is then given by

$$f_1(\rho) = \sum_{n=0}^{\infty} -\delta_{n0} \lambda_{1n} E_0 \sqrt{\frac{2}{3}} t_n^1(\rho) = -\frac{8E_0}{\pi} \sqrt{\frac{2}{3}} t_0^1(\rho) = \frac{8E_0}{\pi} \rho$$

yielding the charge density

$$\sigma(\rho, \vartheta) = \frac{-8E_0 \epsilon_0}{\pi \sqrt{1-\rho^2}} \sqrt{\frac{2}{3}} t_0^1(\rho) \cos \vartheta = \frac{8E_0 \epsilon_0}{\pi \sqrt{1-\rho^2}} \rho \cos \vartheta \quad (\text{IX.23})$$

Some graphs of solutions obtained for different E_0 values are shown (Figure 3) illustrating that a positive field attracts the electrons to the negative x side while a negative field repels them to the positive side. The edges of the disc illustrate the $(1-\rho^2)^{-\frac{1}{2}}$ singularity at $\rho = 1$ except when $\vartheta = \pm \frac{\pi}{2}$ where the zero of the cosine dominates.

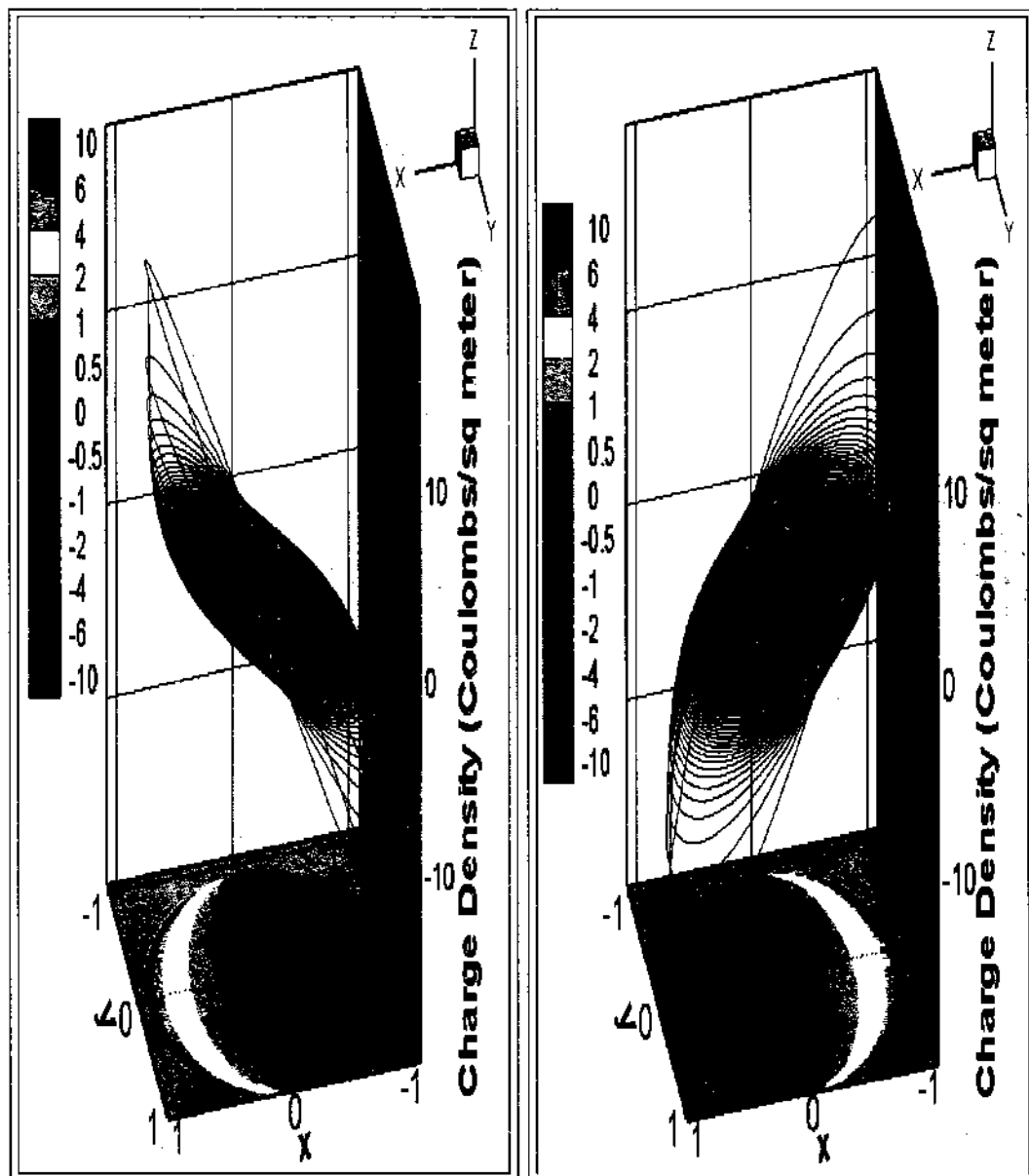
(a) $E_0 = 1$ Volts per Meter.(b) $E_0 = -1$ Volts per Meter.

FIG. 3. The scaled charge density (σ/ϵ_0) on an insulated laminar disc in a parallel field of magnitude 1 oriented in the direction of the x -axis.

IX.2.4 Case 3: Earthed Circular Disc in the Field Generated by a Point Charge

In this case our circular disc Ω , is held to a zero potential but is placed in the field generated by a point charge of strength q coulombs placed at a position $P(a, 0, b)$ near but not on a grounded circular disc Ω . The potential due to the point charge is given by

$$u^0(r, \theta, z) = \frac{q}{4\pi\epsilon_0\sqrt{r^2 + a^2 - 2ra\cos\theta + (z-b)^2}} = \frac{q}{\epsilon_0} B_{\frac{z-b}{2}}(a, 0; r, \theta) \quad (\text{IX.24})$$

so that g takes the form

$$g(r, \theta) = -\frac{q}{\epsilon_0} B_{\frac{z-b}{2}}(a, 0; r, \theta), \text{ for } 0 \leq r \leq 1, -\pi \leq \theta < \pi \quad (\text{IX.25})$$

By virtue of (VI.11) and Fourier's Theorem we can expand $B_{\frac{z-b}{2}}(\rho, \vartheta; r, \theta)$ as

$$B_{\frac{z-b}{2}}(\rho, \vartheta; r, \theta) = \frac{1}{2\pi} \sum_{m=-\infty}^{\infty} L_m(\rho, r; b) \exp(im[\vartheta - \theta]) \quad (\text{IX.26})$$

and write

$$f(\rho, \vartheta) = \sigma(\rho, \vartheta) \sqrt{1 - \rho^2} = \sum_{m=-\infty}^{\infty} f_m(\rho) \exp(im\vartheta) \quad (\text{IX.27})$$

which yields the one dimensional weakly-singular operator equations

$$\mathbb{L}_m^0[f_{\pm m}(\rho)](r) = -\frac{q}{2\pi} L_m(a, r; b), \text{ for } 0 \leq r \leq 1, m = 0, 1, 2, \dots \quad (\text{IX.28})$$

The charge density is then given by

$$\sigma(\rho, \vartheta) = \sum_{m=-\infty}^{\infty} \frac{f_m(\rho)}{\sqrt{1 - \rho^2}} \exp(im\vartheta) \quad (\text{IX.29})$$

and is found by numerically solving (IX.28).

When evaluating the $L_m(\rho, r; b)$ we do so by evaluating it as a ring function as in (VI.8), we need to be careful and avoid the numerical difficulties when r or a are

equal to zero. Using (VI.12) and the fact that

$$J_m(0) = \delta_{m0} \quad (\text{IX.30})$$

we get that

$$-\frac{q}{2\pi} L_m(r, 0; b) = -\frac{q}{4\pi} \frac{\delta_{m0}}{\sqrt{r^2 + b^4}} \quad (\text{IX.31})$$

and

$$-\frac{q}{2\pi} L_m(0, a; b) = -\frac{q}{4\pi} \frac{\delta_{m0}}{\sqrt{a^2 + b^4}} \quad (\text{IX.32})$$

which we use instead of the ring function representation when r and/or a are zero.

We first examine a special case with a known solution. For $P(a, 0, b) = P(0, 0, b)$ the charge densities on the positive and negatives sides are shown by Lebedev et al. [19], to be

$$\sigma^\pm(\rho) = -\frac{qb}{2\pi^3 (b^2 + \rho^2)^{\frac{3}{2}}} \left[\sqrt{\frac{b^2 + \rho^2}{1 - \rho^2}} + \tan^{-1} \left(\sqrt{\frac{1 - \rho^2}{b^2 + \rho^2}} \right) \pm \frac{\pi}{2} \right] \quad (\text{IX.33})$$

so that

$$\sigma(\rho) = \sigma^+(\rho) + \sigma^-(\rho) = -\frac{qb}{\pi^3 (b^2 + \rho^2)^{\frac{3}{2}}} \left[\sqrt{\frac{b^2 + \rho^2}{1 - \rho^2}} + \tan^{-1} \left(\sqrt{\frac{1 - \rho^2}{b^2 + \rho^2}} \right) \right] \quad (\text{IX.34})$$

Since $a = 0$, $f_0(\rho)$ is given by the following one-dimensional weakly-singular operator equation

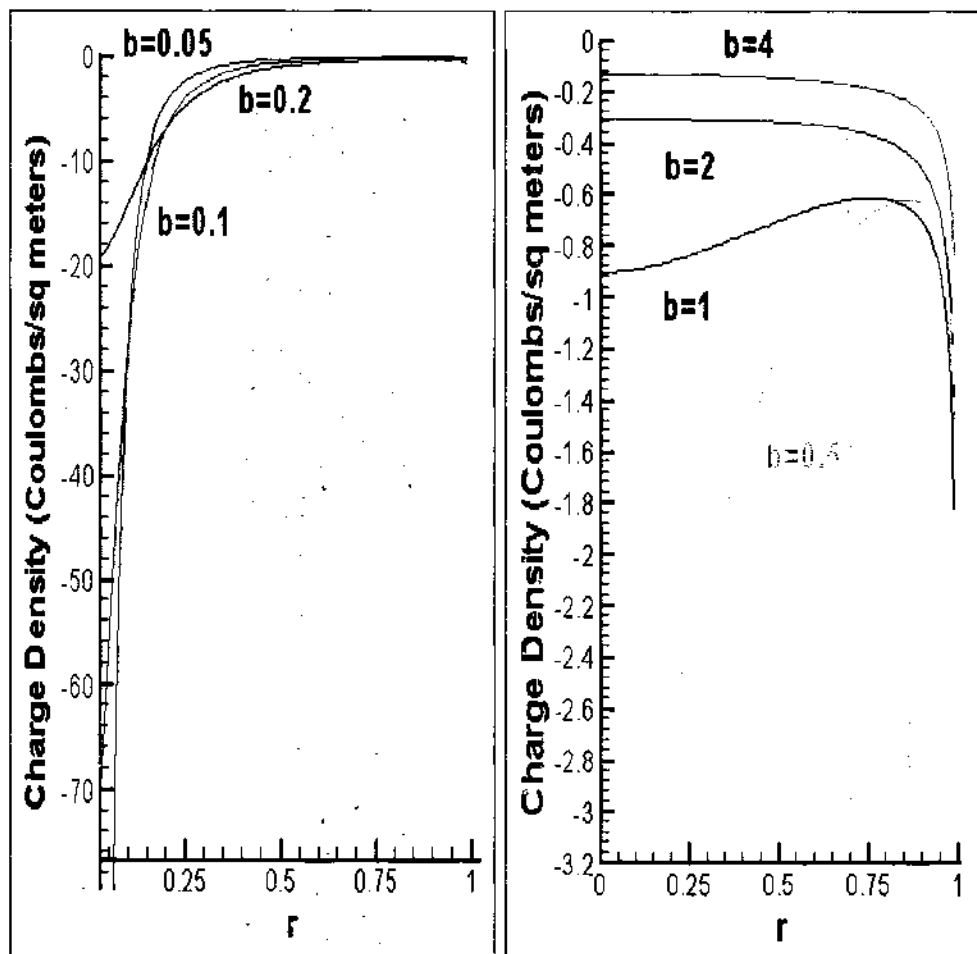
$$\mathbb{L}_0^0[f_0(\rho)](r) = -\frac{q}{4\pi} \frac{1}{\sqrt{r^2 + b^4}}, \text{ for } 0 \leq r \leq 1 \quad (\text{IX.35})$$

and hence

$$\sigma(\rho, \vartheta) = \frac{f_0(\rho)}{\sqrt{1 - \rho^2}} = -\frac{q}{4\pi} \mathbb{S}_0^0 \left[\frac{1}{\sqrt{r^2 + b^4}} \right](r) \quad (\text{IX.36})$$

We now look at some numerical solutions first of all to confirm the result in (IX.34). The computational results are accurate to machine error with those given by IX.34 so we just illustrate some plots for the computed solution to the charge density function in Figs. 4 and 5. When close to the disc the point charge produces a large localized affect on the center which is eliminated by distance. The singularities

at the edge are still obvious but less so as the point charge gets really close to the disc where the local disturbance dominates the charge distribution.



(a) Plot for $b=0.05, 0.1$ and 0.2 .

(b) Plot for $b=0.5, 1.0, 2.0$ and 4.0 .

FIG. 4. The charge density on an insulated laminar disc plotted against the radius of the disc, when a point charge of charge 5 coulombs is placed directly above at varying heights, b , above the disc.

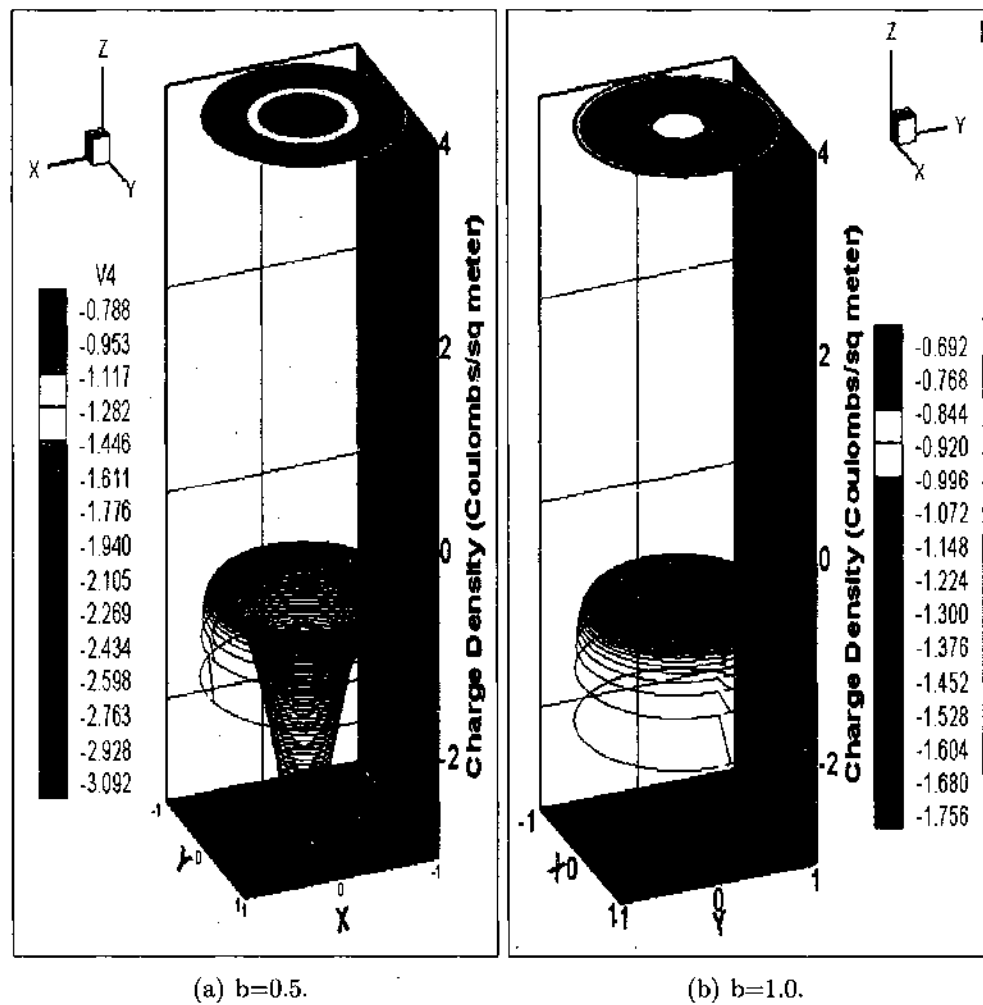


FIG. 5. The charge density on an insulated laminar disc when a point charge of charge 10 coulombs is placed directly above at varying heights, b , above the disc.

In the non-coaxisymmetric case, when $b = 0$ we have some numerical instability problems when $|a|$ is close to 1 but results for $|a| > 1.5$ seem to be fine. Figure 6 shows some solutions for the point charge in the plane of the laminar conductor. The localized affect as in Figure 6(a) is clearly reduced as the point charge is moved further away as in Figure 6(b).

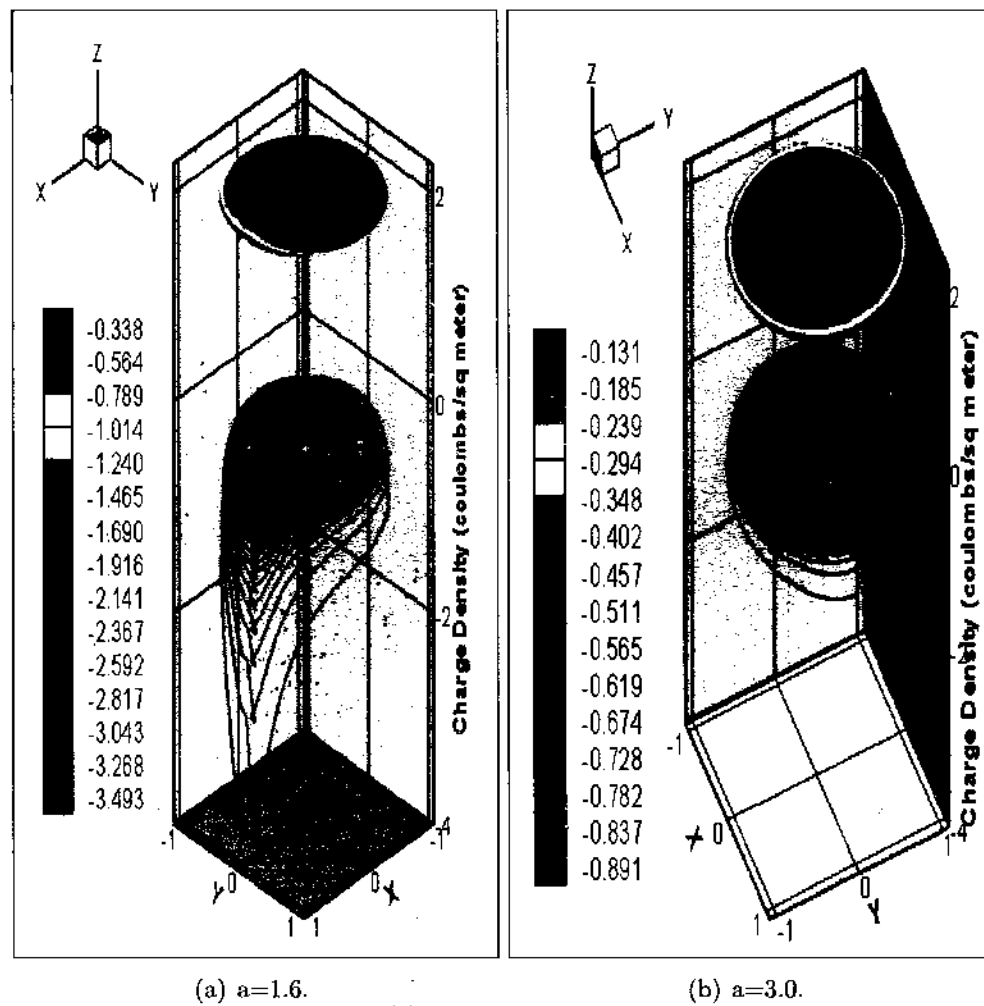


FIG. 6. The charge density on an insulated laminar disc when a point charge 5 coulombs is placed in the same plane.

When a, b are both non-zero we get a combination of the effects as illustrated in Fig 7.

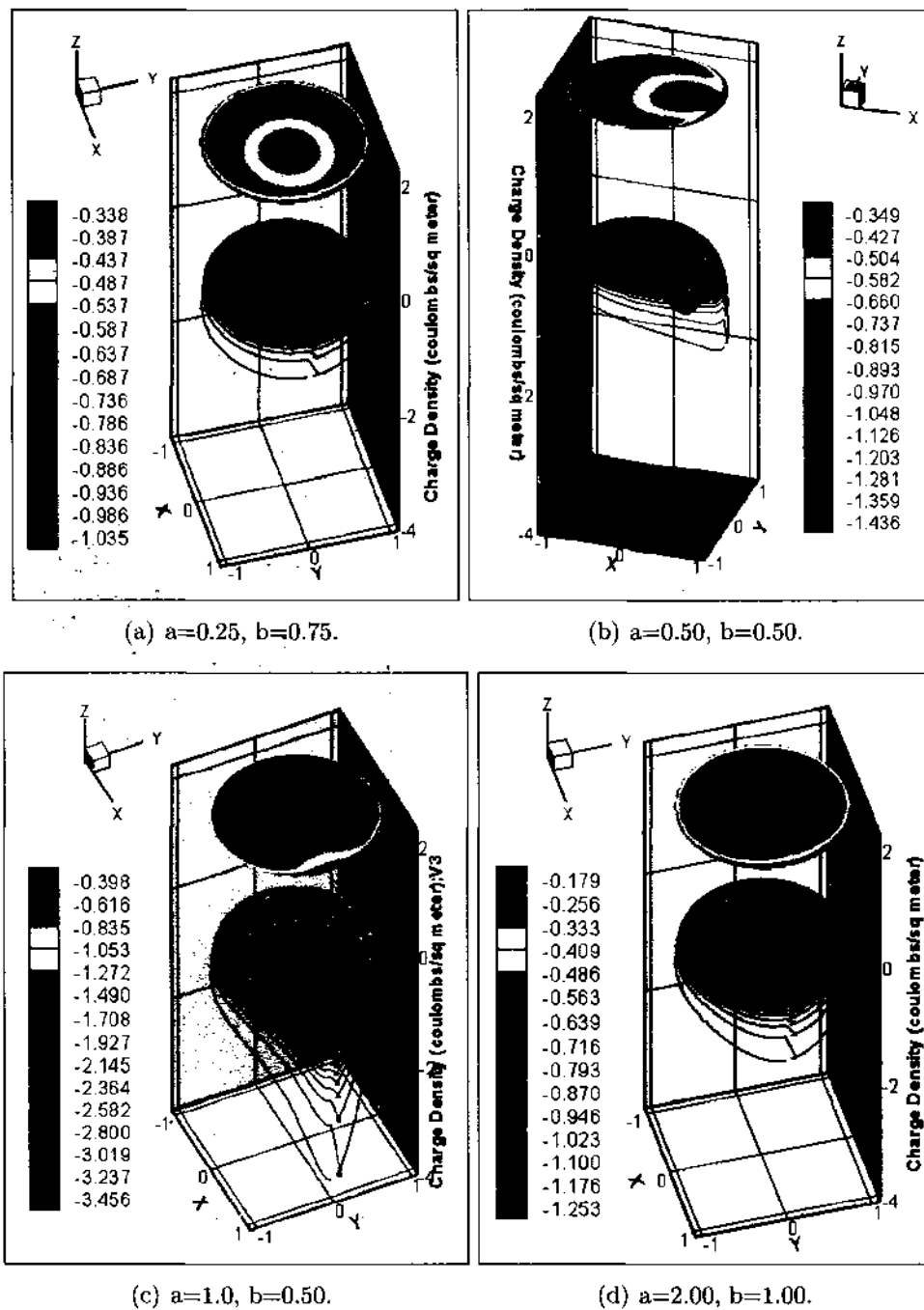


FIG. 7. The charge density on an insulated laminar disc when a point charge of charge 5 coulombs is placed at varying positions.

IX.3 MULTIPLE DISC PROBLEMS

IX.3.1 The Parallel Plate Condenser

Coaxial Discs

Instead of one unit disk we have a pair of circular laminar disks centered on the z -axis at $z = \pm h$. Our solutions will be in the form $V = V_1 + V_2$ where V_1 and V_2 are potentials relating to the individual disks. We will look at the capacitance and capacitance like properties of the two disks which will have different potentials

$$V(r, \theta, +h) = g^+(r, \theta) \quad (\text{IX.37})$$

$$V(r, \theta, -h) = g^-(r, \theta) \quad (\text{IX.38})$$

Let us define the following domains

$$\Omega_0 = [(r, \theta) : 0 \leq r \leq 1, -\pi \leq \theta < \pi] \quad (\text{IX.39})$$

$$\Omega^\pm = [(r, \theta, z) : (r, \theta) \in \Omega_0, z = \pm h] \quad (\text{IX.40})$$

$$\Omega = \Omega^+ \cup \Omega^- \quad (\text{IX.41})$$

The potential $V(r, \theta, z)$ will be given by the following combination of single layer potential functions

$$\begin{aligned} V(r, \theta, z) = & \frac{1}{4\pi} \int_0^1 \int_{-\pi}^{\pi} \frac{\sigma^+(\rho, \vartheta) \rho d\rho d\vartheta}{\sqrt{r^2 + \rho^2 - 2r\rho \cos(\theta - \vartheta) + (z - h)^2}} \\ & + \frac{1}{4\pi} \int_0^1 \int_{-\pi}^{\pi} \frac{\sigma^-(\rho, \vartheta) \rho d\rho d\vartheta}{\sqrt{r^2 + \rho^2 - 2r\rho \cos(\theta - \vartheta) + (z + h)^2}} \quad (\text{IX.42}) \end{aligned}$$

provided the charge density functions $\sigma^+(\rho, \vartheta)$ and $\sigma^-(\rho, \vartheta)$ satisfy the following weakly-singular operator dual equations

$$\left[\left\{ \mathbb{B}^0 \left(\sigma^+ \sqrt{1 - \rho^2} \right) + \mathbb{B}_h^0 \left(\sigma^- \sqrt{1 - \rho^2} \right) \right\} \right] (r, \theta) = g^+(r, \theta), \text{ for } (r, \theta) \in \Omega_0 \quad (\text{IX.43})$$

and

$$\left[\left\{ \mathbb{B}_h^0 \left(\sigma^+ \sqrt{1 - \rho^2} \right) + \mathbb{B}^0 \left(\sigma^- \sqrt{1 - \rho^2} \right) \right\} \right] (r, \theta) = g^- (r, \theta), \text{ for } (r, \theta) \in \Omega_0 \quad (\text{IX.44})$$

The General Case For the general case we expand the functions in (IX.43) and (IX.44) as follows

$$f^\pm (\rho, \vartheta) = \sigma^\pm (\rho, \vartheta) \sqrt{1 - \rho^2} = \sum_{m=-\infty}^{\infty} f_m^\pm (\rho) \exp (im\vartheta)$$

and

$$g^\pm (r, \theta) = \sum_{m=-\infty}^{\infty} g_m^\pm (r) \exp (im\theta) \quad (\text{IX.45})$$

we then exploit (VI.19) to reduce to the following system of one dimensional weakly-singular operator dual equations

$$\left[\left(\mathbb{L}_m^0 f_m^+ + \mathbb{L}_{m,h}^0 f_m^- \right) (\rho) \right] (r) = g_m^+ (r), \text{ for } 0 \leq r \leq 1, m = 0, \pm 1, \pm 2, \dots \quad (\text{IX.46})$$

and

$$\left[\left(\mathbb{L}_{m,h}^0 f_m^+ + \mathbb{L}_m^0 f_m^- \right) (\rho) \right] (r) = g_m^- (r), \text{ for } 0 \leq r \leq 1, m = 0, \pm 1, \pm 2, \dots \quad (\text{IX.47})$$

An arbitrary function $f(z)$ can be decomposed as follows

$$\begin{aligned} f(z) &= \frac{1}{2} [f(z) + f(-z)] + \frac{1}{2} [f(z) - f(-z)] \\ &= f_1(z) + f_2(z) \end{aligned} \quad (\text{IX.48})$$

where $f_1(z)$ is even and $f_2(z)$ is odd, we can therefore have no loss in generality if we consider only the special cases where

$$g^- (r) = \pm g^+ (r) \quad (\text{IX.49})$$

in this case we will also get that

$$\sigma^- (r) = \pm \sigma^+ (r) \quad (\text{IX.50})$$

The problem then reduces to a single Integral Equation.

Equally Charged Discs $g^+ = g^- = g$ By symmetry the charge potentials on each disc will also be equal, $\sigma^+ = \sigma^- = \sigma$, so that (IX.43) and (IX.44) reduce to the single equation

$$[\{\mathbb{B}^0 + \mathbb{B}_h^0\} \sigma(\rho, \vartheta)](r, \theta) = g(r, \theta), \text{ for } (r, \theta) \in \Omega_0 \quad (\text{IX.51})$$

Expanding as follows

$$f(\rho, \vartheta) = \sigma(\rho, \vartheta) \sqrt{1 - \rho^2} = \sum_{m=-\infty}^{\infty} f_m(\rho) \exp(im\vartheta) \quad (\text{IX.52})$$

and

$$g(r, \theta) = \sum_{m=-\infty}^{\infty} g_m(r) \exp(im\theta) \quad (\text{IX.53})$$

(VI.19) then gives us the following system of one dimensional weakly-singular operator equations

$$[(\mathbb{L}_m^0 + \mathbb{L}_{m,h}^0) f_{\pm m}(\rho)](r) = g_{\pm m}(r), \text{ for } 0 \leq r \leq 1, m = 0, 1, 2, \dots \quad (\text{IX.54})$$

Oppositely Charged Discs $g^+ = -g^- = g$ Here by symmetry the charge potentials will also be opposite $\sigma^+ = -\sigma^- = \sigma$ so that (IX.43) and (IX.44) reduce to the single equation

$$[\{\mathbb{B}^0 - \mathbb{B}_h^0\} \sigma(\rho, \vartheta)](r, \theta) = g(r, \theta), \text{ for } (r, \theta) \in \Omega_0 \quad (\text{IX.55})$$

expanding as in (IX.52) and (IX.53), we can exploit (VI.19) to reduce to the following system of one dimensional weakly-singular operator equations

$$[(\mathbb{L}_m^0 - \mathbb{L}_{m,h}^0) f_{\pm m}(\rho)](r) = g_{\pm m}(r), \text{ for } 0 \leq r \leq 1, m = 0, 1, 2, \dots \quad (\text{IX.56})$$

Numerical Results We will check the simple case where the parallel discs are charged to an equal or opposite constant potentials. We can compare these results with those in Sneddon ([2], p238) by looking at the Capacitance. First let us consider

the case where the potential is equal in magnitude and constant on both discs;

$$g^+(r, \theta) = V_0, \text{ for } (r, \theta) \in \Omega_0 \quad (\text{IX.57})$$

$$g^-(r, \theta) = \pm V_0, \text{ for } (r, \theta) \in \Omega_0 \quad (\text{IX.58})$$

the total charge on the upper disc is then given by

$$Q = \int_0^1 \int_0^{2\pi} \sigma(\rho, \vartheta) \rho d\rho d\vartheta = 2\pi f_{00} \quad (\text{IX.59})$$

where since g is even

$$f(\rho, \vartheta) = \sum_{m=-\infty}^{\infty} \sum_{n=0}^{\infty} \delta_{m0} \delta_{n0} f_{mn} t_n^{|m|}(\rho) \cos(m\vartheta) \quad (\text{IX.60})$$

The Capacitance (C) is then given by

$$C = \frac{Q}{2V_0} = \pi f_{00} \quad (\text{IX.61})$$

If we compare these with the results given by Sneddon ([2], p238) which lists πC_{sneddon} where the capacitance C_{sneddon} is in different units, with the conversion as follows;

$$\pi C_{\text{sneddon}} = \frac{C}{4} = \frac{\pi f_{00}}{4} \quad (\text{IX.62})$$

A comparison of results for $V_0 = 1$ and differing distances between the discs ($\kappa = 2h$) is given in Table. 3 showing that the results are equivalent to at least three decimal places with our results possibly more accurate.

TABLE 3

Comparison of Capacitance ($C_{Sneddon}$) results for a pair of parallel plates charged to equal or opposite potentials. Source ([2],p238).

κ	Nomura -Cooke		Galerkin		Collocation	
	Equal	Opposite	Equal	Opposite	Equal	Opposite
0.4	0.6027	3.1029	0.602499	3.102305	0.602499	3.102305
0.6	0.6364	2.3956	0.636407	2.395441	0.636407	2.395441
0.8	0.6656	2.0372	0.665610	2.037267	0.665610	2.037267
1.0	0.6912	1.8208	0.691207	1.820785	0.691207	1.820785
1.2	0.7138	1.676	0.713812	1.676043	0.713812	1.676043
1.5	0.7437	1.5227	0.743020	1.531444	0.743020	1.531444
2.0	0.7817	1.3867	0.781752	1.388027	0.781752	1.388027
2.5	0.8113	1.3034	0.811260	1.303422	0.811259	1.303423
3.0	0.8342	1.2421	0.834216	1.248107	0.834216	1.248107
5.0	0.8896	1.1417	0.889579	1.141723	0.889579	1.141723
10.0	0.9405	1.0675	0.940518	1.067514	0.940518	1.067514
20.0	0.9683	1.0319	0.969201	1.032821	0.969201	1.032821
	Fox-Blake		Galerkin		Collocation	
	Equal		Equal		Equal	
0.1	9.233		9.233081		9.233081	

We now test the limits of the method by examining some limiting cases. In the equal potential case as the distance, κ , goes towards zero it should start acting as if the total charge is split between the two discs and $C_{Sneddon}$ should approach $\frac{1}{2}$ as is illustrated in Table. 4.

TABLE 4

The Capacitance ($C_{Sneddon}$) as the distance between two equally charged parallel discs tends towards zero can be seen to approach 0.5. Results from collocation method. Note numerical singularities appear for smaller kappa values.

κ	Collocation
	Equal
0.2	0.5613624
0.1	0.5358826
0.05	0.5205986
0.02	0.5096676
0.01	0.5053793
0.0005	0.5029637
0.0001	0.5007223

In the oppositely charged case as the distance, κ , between the plates tends to infinity it should start acting like a single disc with all its charge, so $C_{Sneddon}$ should approach 1 as is illustrated in Table. 5.

Non Coaxial Discs

This time the discs will be parallel to the (r, θ) plane and centered at $(a, 0, h)$ and $(-a, 0, -h)$ where $a > 1$ if $h = 0$, so the discs do not touch or overlap. Our solutions will again be in the form $V = V_1 + V_2$ where V_1 and V_2 are potentials relating to the individual discs. We will also look at the capacitance and capacitance like properties of the two disks.

Let us define the following domains

$$\Omega_0 = [(r, \theta) : 0 \leq r \leq 1, -\pi \leq \theta < \pi] \quad (\text{IX.63})$$

$$\Omega^\pm = [(x, y, z) : 0 \leq (x \pm a)^2 + y^2 \leq 1] \quad (\text{IX.64})$$

$$D^\pm = [(x, y, z) : z = \pm h, (x, y) \in \Omega^\pm] \quad (\text{IX.65})$$

TABLE 5

The Capacitance ($C_{Sneddon}$) as the distance between two oppositely charged parallel discs tends towards infinity can be seen to approach 1. Results here are obtained from using the collocation method.

κ	Collocation
	Opposite
100	1.0064070
250	1.0025530
750	1.0008500
1000	1.0006370
10000	1.0000640
50000	1.0000130
100000	1.0000060
1000000	1.0000010
10000000	1.0000000
100000000	1.0000000

Let $\sigma^\pm(x, y)$ be the charge densities on the disks D^\pm and let $g^\pm(x, y)$ be the corresponding potentials. The potential $V(x, y, z)$ will be given by the following combination of single layer potential functions

$$\begin{aligned}
 V(x, y, z) = & \frac{1}{4\pi\epsilon_0} \iint_{\Omega^+} \frac{\sigma^+(s, t) dsdt}{\sqrt{(x-s)^2 + (y-t)^2 + (z-h)^2}} \\
 & + \frac{1}{4\pi\epsilon_0} \iint_{\Omega^-} \frac{\sigma^-(s, t) dsdt}{\sqrt{(x-s)^2 + (y-t)^2 + (z+h)^2}} \quad (\text{IX.66})
 \end{aligned}$$

provided the charge densities satisfy the dual equations

$$\begin{aligned}
 & \frac{1}{4\pi\epsilon_0} \iint_{\Omega^+} \frac{\sigma^+(s, t) dsdt}{\sqrt{(x-s)^2 + (y-t)^2}} \\
 & + \frac{1}{4\pi\epsilon_0} \iint_{\Omega^-} \frac{\sigma^-(s, t) dsdt}{\sqrt{(x-s)^2 + (y-t)^2 + 4h^2}} = g^-(x, y), \quad (x, y) \in \Omega^+ \quad (\text{IX.67})
 \end{aligned}$$

and

$$\begin{aligned} & \frac{1}{4\pi\epsilon_0} \iint_{\Omega^+} \frac{\sigma^+(s, t) dsdt}{\sqrt{(x-s)^2 + (y-t)^2 + 4h^2}} \\ & + \frac{1}{4\pi\epsilon_0} \iint_{\Omega^-} \frac{\sigma^-(s, t) dsdt}{\sqrt{(x-s)^2 + (y-t)^2}} = g^-(x, y), \quad (x, y) \in \Omega^- \end{aligned} \quad (\text{IX.68})$$

or equivalently

$$\begin{aligned} & \frac{1}{4\pi\epsilon_0} \iint_{\Omega^+} \frac{\sigma^+(s, t) dsdt}{\sqrt{(x-s)^2 + (y-t)^2}} \\ & + \frac{1}{4\pi\epsilon_0} \iint_{\Omega^+} \frac{\sigma^-(-s, -t) dsdt}{\sqrt{(x+s)^2 + (y+t)^2 + 4h^2}} = g^+(x, y), \quad (x, y) \in \Omega^+ \end{aligned} \quad (\text{IX.69})$$

and

$$\begin{aligned} & \frac{1}{4\pi\epsilon_0} \iint_{\Omega^-} \frac{\sigma^+(-s, -t) dsdt}{\sqrt{(x+s)^2 + (y+t)^2 + 4h^2}} \\ & + \frac{1}{4\pi\epsilon_0} \iint_{\Omega^-} \frac{\sigma^-(s, t) dsdt}{\sqrt{(x-s)^2 + (y-t)^2}} = g^-(x, y), \quad (x, y) \in \Omega^- \end{aligned} \quad (\text{IX.70})$$

Since an arbitrary function $f(x, y)$ of two variables can be decomposed as follows

$$\begin{aligned} f(x, y) &= \frac{1}{2} [f(x, y) + f(-x, -y)] + \frac{1}{2} [f(x, y) - f(-x, -y)] \\ &= f_1(x, y) + f_2(x, y) \end{aligned} \quad (\text{IX.71})$$

where $f_1(x, y)$ is even in both x and y while $f_2(x, y)$ is odd in both, we can therefore have no loss in generality if we take only the special cases where

$$g^-(-x, -y) = \pm g^+(x, y) \quad (\text{IX.72})$$

and we will also get that

$$\sigma^-(-x, -y) = \pm \sigma^+(x, y) \quad (\text{IX.73})$$

so we can reduce (IX.69) and (IX.70) to the single equation

$$\frac{1}{4\pi\epsilon_0} \iint_{\Omega^+} \left\{ \frac{1}{\sqrt{(x-s)^2+(y-t)^2}} \pm \frac{1}{\sqrt{(x+s)^2+(y+t)^2+4h^2}} \right\} \sigma^+(s,t) dsdt = g^+(x,y), \quad (x,y) \in \Omega^+ \quad (\text{IX.74})$$

If we introduce the polar coordinates

$$\begin{aligned} s - a &= \rho \cos \vartheta, & t &= \rho \sin \vartheta \\ x - a &= r \cos \theta, & y &= r \sin \theta \end{aligned} \quad (\text{IX.75})$$

and write

$$\sigma^+(s,t) = \sigma(\rho, \vartheta), \quad g^+(x,y) = g(r, \theta) \quad (\text{IX.76})$$

we find that if

$$g^-(r, -\theta) = \pm g^+(r, \theta) = g(r, \theta) \quad (\text{IX.77})$$

we will also get that

$$\sigma^-(r, -\theta) = \pm \sigma^+(r, \theta) = \sigma(\rho, \vartheta) \quad (\text{IX.78})$$

so that we will then get the following two dimensional operator equation

$$[\{\mathbb{B}^0 \pm \mathbb{K}_{h,a}^0\} f(\rho, \vartheta)](r, \theta) = g(r, \theta), \quad \text{for } (r, \theta) \in \Omega_0 \quad (\text{IX.79})$$

where

$$f(\rho, \vartheta) = \sigma(\rho, \vartheta) \sqrt{1 - \rho^2} \quad (\text{IX.80})$$

and the non-singular operator $\mathbb{K}_{h,a}^0$ is defined as follows

$$[\mathbb{K}_{h,a}^0 f(\rho, \vartheta)](r, \theta) = \int_0^1 \int_0^{2\pi} f(\rho, \vartheta) K_{h,a}(\rho, \vartheta; r, \theta) w^0(\rho) d\rho d\vartheta \quad (\text{IX.81})$$

with kernel

$$K_{h,a}(\rho, \vartheta; r, \theta) = \frac{1}{\sqrt{r^2 + \rho^2 + 2r\rho \cos(\vartheta - \theta) + 4a\rho \cos \vartheta + 4ar \cos \theta + 4a^2 + 4h^2}}$$

Numerical Results We will consider the simple case where the discs are charged to an equal or opposite constant charge and hence we deal with just even cosine expansions. Tables. 6 and 7 show the Capacitance ($C_{Sneddon}$) given by both the Collocation and Galerkin methods for the equally charged discs . We show the

collocation method results for oppositely charged discs in Table. 8. The results for $a = 0$ can be compared with those in Table. 3 to confirm that the accuracy of the two-dimensional methods.

TABLE 6

Capacitance ($C_{Sneddon}$) for offset discs equally charged to a constant potential, centered at $(a,0,h)$ and $(-a,0,-h)$. Results from collocation method.

M = 3 θ, r quad points = 20
 N = 5 θ_{coll}, r_{coll} points = 3,5

h	a	0	0.2	0.4	0.6	0.8
0.2		0.6025	0.6282	0.6732	0.7152	0.7508
0.4		0.6656	0.6769	0.7034	0.7340	0.7629
0.6		0.7138	0.7200	0.7362	0.7572	0.7791
0.8		0.7517	0.7555	0.7658	0.7803	0.7964
1		0.7818	0.7842	0.7912	0.8013	0.8132
2		0.8672	0.8677	0.8693	0.8717	0.8748
3		0.9056	0.9058	0.9063	0.9072	0.9084
5		0.9405	0.9406	0.9407	0.9409	0.9412
10		0.9692	0.9692	0.9692	0.9693	0.9693
h	a	1	2	3	5	10
0		0.7773	0.8659	0.9051	0.9404	0.9692
0.2		0.7803	0.8664	0.9053	0.9404	0.9692
0.4		0.7883	0.8681	0.9059	0.9406	0.9692
0.6		0.7996	0.8706	0.9068	0.9408	0.9692
0.8		0.8125	0.8740	0.9080	0.9411	0.9693
1		0.8257	0.8779	0.9095	0.9415	0.9693
2		0.8786	0.9004	0.9196	0.9444	0.9698
3		0.9098	0.9197	0.9307	0.9484	0.9704
5		0.9416	0.9445	0.9485	0.9570	0.9723
10		0.9694	0.9698	0.9705	0.9724	0.9780

TABLE 7

Capacitance ($C_{Sneddon}$) for offset discs equally charged to a constant potential, centered at $(a,0,h)$ and $(-a,0,-h)$. Results from Galerkin method.

M,N =		3 θ,r quad points = 20				
h	a	0	0.2	0.4	0.6	0.8
0.2		0.6025	0.6281	0.6731	0.7152	0.7509
0.4		0.6656	0.6769	0.7034	0.7340	0.7630
0.6		0.7138	0.7200	0.7362	0.7572	0.7791
0.8		0.7517	0.7555	0.7658	0.7803	0.7965
1		0.7818	0.7842	0.7912	0.8013	0.8133
2		0.8672	0.8677	0.8693	0.8717	0.8748
3		0.9056	0.9058	0.9063	0.9072	0.9084
5		0.9405	0.9406	0.9407	0.9409	0.9412
10		0.9692	0.9692	0.9692	0.9693	0.9693
h	a	1	2	3	5	10
0		0.7775	0.8659	0.9051	0.9404	0.9692
0.2		0.7804	0.8665	0.9053	0.9404	0.9692
0.4		0.7884	0.8681	0.9059	0.9406	0.9692
0.6		0.7997	0.8707	0.9068	0.9408	0.9692
0.8		0.8126	0.8740	0.9080	0.9411	0.9693
1		0.8257	0.8780	0.9095	0.9415	0.9693
2		0.8786	0.9004	0.9196	0.9444	0.9698
3		0.9098	0.9197	0.9307	0.9484	0.9704
5		0.9416	0.9445	0.9485	0.9570	0.9723
10		0.9694	0.9698	0.9705	0.9724	0.9780

TABLE 8

Capacitance results, $C_{Sneddon}$, for offset discs oppositely charged to a constant potential, centered at $(a,0,h)$ and $(-a,0,-h)$. Results from collocation method.

M = 3 θ, r quad points = 20
 N = 5 θ_{coll}, r_{coll} points = 3,5

h	a	0	0.2	0.4	0.6	0.8
0.2		3.1023	2.5605	1.9940	1.6849	1.5082
0.4		2.0373	1.9390	1.7488	1.5812	1.4587
0.6		1.6760	1.6433	1.5656	1.4780	1.4002
0.8		1.4954	1.4809	1.4431	1.3946	1.3457
1		1.3880	1.3804	1.3596	1.3309	1.2993
2		1.1808	1.1798	1.1771	1.1727	1.1670
3		1.1164	1.1161	1.1153	1.1140	1.1122
5		1.0675	1.0675	1.0673	1.0670	1.0666
10		1.0328	1.0328	1.0328	1.0328	1.0327
h	a	1	2	3	5	10
0		1.4082	1.1839	1.1173	1.0677	1.0328
0.2		1.3982	1.1828	1.1170	1.0676	1.0328
0.4		1.3718	1.1798	1.1161	1.0675	1.0328
0.6		1.3374	1.1749	1.1147	1.0672	1.0328
0.8		1.3017	1.1688	1.1129	1.0668	1.0327
1		1.2687	1.1618	1.1106	1.0663	1.0327
2		1.1605	1.1245	1.0959	1.0626	1.0322
3		1.1100	1.0957	1.0805	1.0575	1.0314
5		1.0661	1.0625	1.0575	1.0470	1.0293
10		1.0327	1.0322	1.0314	1.0293	1.0230

CHAPTER X

APPLICATIONS II: 3-D CRACK PROBLEMS

X.1 INTRODUCTION

In order to illustrate the use of the hyper-singular integral equations discussed in Chapters V and VIII we will investigate a number of problems arising in the theory of linear elastic fracture mechanics. We will begin by determining the stress intensity factors for a penny-shaped crack under a variety of loading conditions and then go on to consider problems involving more than one such crack. Before doing so however, it will be necessary to introduce some additional notation and terminology in order to set up the problems appropriately.

It is well known that, in the absence of body forces, the equilibrium displacement, $\mathbf{u} = (u_1, u_2, u_3)$, of a three dimensional linear elastic solid is given by Navier's Equations

$$(1 - 2\nu) u_{i,jj} + u_{j,ji} = 0, \text{ for } i = 1, 2, 3 \quad (\text{X.1})$$

and that the corresponding stresses are given by the constitutive equations

$$\sigma_{ij} = \frac{E\nu}{(1 + \nu)(1 - 2\nu)} u_{k,k} \delta_{ij} + \mu (u_{i,j} + u_{j,i}), \text{ for } i, j = 1, 2, 3 \quad (\text{X.2})$$

where E is Young's modulus, μ is the shear modulus and ν is Poisson's ratio [20].

Papkovich and Neuber ([21] and [22]) have shown that the general solution of the equilibrium equation, (X.1) may be expressed in the form

$$2\mu u_i = -4(1 - \nu) \psi_i + (x_j \psi_j + \phi)_{,i} \quad (\text{X.3})$$

where ϕ is a harmonic scalar and $\boldsymbol{\psi} = (\psi_1, \psi_2, \psi_3)$ is an harmonic vector.

It follows that many problems in the theory of elasticity can be reduced to boundary value problems in potential theory and are therefore amenable to treatment by integral equations of the type discussed in previous chapters. For the purpose of illustration we will restrict our interest to the following special case of the Papkovitch-Neuber Solution as described by Barber ([20], p205 solution F).

In Cartesian Coordinates this solution takes the form shown in Table 9 while Table 10 shows the solution in Cylindrical Polar Coordinates.

TABLE 9

A special case of the Papkovitch-Neuber solution in Cartesian Coordinates.

$2\mu u_x = z \frac{\partial^2 \varphi}{\partial x \partial z} + (1 - 2\nu) \frac{\partial \varphi}{\partial x}$	$\sigma_{xx} = z \frac{\partial^3 \varphi}{\partial x^2 \partial z} + \frac{\partial^2 \varphi}{\partial x^2} + 2\nu \frac{\partial^2 \varphi}{\partial y^2}$	$\sigma_{xz} = z \frac{\partial^3 \varphi}{\partial x \partial z^2}$
$2\mu u_y = z \frac{\partial^2 \varphi}{\partial y \partial z} + (1 - 2\nu) \frac{\partial \varphi}{\partial y}$	$\sigma_{xy} = z \frac{\partial^3 \varphi}{\partial x \partial y \partial z} + (1 - 2\nu) \frac{\partial^2 \varphi}{\partial x \partial y}$	$\sigma_{yz} = z \frac{\partial^3 \varphi}{\partial y \partial z^2}$
$2\mu u_z = z \frac{\partial^2 \varphi}{\partial z^2} - 2(1 - \nu) \frac{\partial \varphi}{\partial z}$	$\sigma_{yy} = z \frac{\partial^3 \varphi}{\partial y^2 \partial z} + \frac{\partial^2 \varphi}{\partial y^2} + 2\nu \frac{\partial^2 \varphi}{\partial x^2}$	$\sigma_{zz} = z \frac{\partial^3 \varphi}{\partial z^3} - \frac{\partial^2 \varphi}{\partial z^2}$

TABLE 10

A special case of the Papkovitch-Neuber solution in Cylindrical Coordinates.

$2\mu u_r = z \frac{\partial^2 \varphi}{\partial r \partial z} + (1 - 2\nu) \frac{\partial \varphi}{\partial r}$	$\sigma_{rz} = z \frac{\partial^3 \varphi}{\partial r \partial z^2}$
$2\mu u_\theta = \frac{z}{r} \frac{\partial^2 \varphi}{\partial \theta \partial z} + \frac{(1-2\nu)}{r} \frac{\partial \varphi}{\partial \theta}$	$\sigma_{\theta z} = \frac{z}{r} \frac{\partial^3 \varphi}{\partial \theta \partial z^2}$
$2\mu u_z = z \frac{\partial^2 \varphi}{\partial z^2} - 2(1 - \nu) \frac{\partial \varphi}{\partial z}$	$\sigma_{zz} = z \frac{\partial^3 \varphi}{\partial z^3} - \frac{\partial^2 \varphi}{\partial z^2}$
$\sigma_{rr} = z \frac{\partial^3 \varphi}{\partial r^2 \partial z} + \frac{\partial^2 \varphi}{\partial r^2} - 2\nu \left(\frac{\partial^2 \varphi}{\partial r^2} + \frac{\partial^2 \varphi}{\partial z^2} \right)$	
$\sigma_{r\theta} = \frac{z}{r} \frac{\partial^3 \varphi}{\partial r \partial \theta \partial z} - \frac{z}{r^2} \frac{\partial^2 \varphi}{\partial r \partial z} + \frac{(1-2\nu)}{r} \left(\frac{\partial^2 \varphi}{\partial r \partial \theta} - \frac{1}{r} \frac{\partial \varphi}{\partial \theta} \right)$	
$\sigma_{\theta\theta} = -(1 - 2\nu) \frac{\partial^2 \varphi}{\partial r^2} - \frac{\partial^2 \varphi}{\partial z^2} - z \frac{\partial^3 \varphi}{\partial r^2 \partial z} - z \frac{\partial^3 \varphi}{\partial z^3}$	

X.2 SINGLE CRACK PROBLEMS

X.2.1 A General Problem

Let Ω be a bounded region of the xy -plane with smooth boundary $\partial\Omega$. Then, we consider the problem of determining the stresses and displacements in the vicinity of a crack that occupies the domain Ω and is opened by a symmetric pressure distribution

$$\sigma_{zz} = -P(x, y), \text{ for } (x, y) \in \Omega \quad (\text{X.4})$$

In order to address this problem we need to find a solution of the equations of three dimensional linear elasticity in the domain $\{(x, y, z) \in \mathbb{R}^3 : |z| > 0\}$, subject to the boundary conditions;

$$\sigma_{ij} \rightarrow 0 \text{ as } \sqrt{x^2 + y^2 + z^2} \rightarrow \infty \quad (\text{X.5})$$

$$\begin{aligned} u_i(x, y, 0^+) - u_i(x, y, 0^-) &= 0 \text{ for } i = 1, 2, 3, (x, y) \in \Omega^c \\ \sigma_{ij}(x, y, 0^+) - \sigma_{ij}(x, y, 0^-) &= 0 \text{ for } i, j = 1, 2, 3, (x, y) \in \Omega^c \end{aligned} \quad (\text{X.6})$$

and

$$\begin{aligned} \sigma_{zx}(x, y, 0^\pm) &= \sigma_{zy}(x, y, 0^\pm) = 0 \text{ for } (x, y) \in \Omega \\ \sigma_{zz}(x, y, 0^\pm) &= -P(x, y) \text{ for } (x, y) \in \Omega \end{aligned} \quad (\text{X.7})$$

By virtue of Table 9 we see that these conditions are satisfied trivially if $\varphi(x, y, z)$ is given by the following harmonic boundary value problem;

Solve the partial differential equation

$$\frac{\partial^2 \varphi}{\partial x^2} + \frac{\partial^2 \varphi}{\partial y^2} + \frac{\partial^2 \varphi}{\partial z^2} = 0, \text{ for } |z| > 0, (x, y, z) \in \mathbb{R}^3 \quad (\text{X.8})$$

with boundary conditions

$$\varphi(x, y, z) \rightarrow 0 \text{ as } \sqrt{x^2 + y^2 + z^2} \rightarrow \infty \quad (\text{X.9})$$

$$\begin{aligned} \varphi(x, y, 0^+) - \varphi(x, y, 0^-) &= 0, \text{ for } (x, y) \in \Omega^c \\ \varphi_z(x, y, 0^+) - \varphi_z(x, y, 0^-) &= 0, \text{ for } (x, y) \in \Omega^c \\ \varphi_{zz}(x, y, 0^+) - \varphi_{zz}(x, y, 0^-) &= 0, \text{ for } (x, y) \in \Omega^c \end{aligned} \quad (\text{X.10})$$

$$\varphi_{zz}(x, y, 0^\pm) = P(x, y), \text{ for } (x, y) \in \Omega \quad (\text{X.11})$$

If we now express $\varphi_z(x, y, z)$ in terms of the double layer potential

$$\varphi_z = \mathfrak{D}[w(s, t)](x, y, z) \quad (\text{X.12})$$

we find that

$$\varphi_z(x, y, 0^+) - \varphi_z(x, y, 0^-) = w(x, y), \text{ for } (x, y) \in \Omega \quad (\text{X.13})$$

and that the harmonic boundary problem is solved if $w(x, y)$ is given by the hyper-singular integral equation

$$\frac{\Delta_2}{4\pi} \iint_{\Omega} \frac{w(s, t) ds dt}{\sqrt{(x-s)^2 + (y-t)^2}} = P(x, y), \text{ for } (x, y) \in \Omega \quad (\text{X.14})$$

Observe that the crack opening displacement is then given by

$$\Delta u_z = u_z(x, y, 0^+) - u_z(x, y, 0^-) = -\frac{1-\nu}{\mu} w(x, y) \text{ for } (x, y) \in \Omega \quad (\text{X.15})$$

Now let \mathbf{n} be the unit outward normal at any point $P \in \partial\Omega$. Then, if we move a distance d in the direction of \mathbf{n} it is found ([24], p149) that the normal stress is given asymptotically by

$$\sigma_{zz} \sim \frac{k_1(P)}{\sqrt{2d}} + \mathcal{O}(d) \quad (\text{X.16})$$

Similarly, if we move a distance d in the direction of $-\mathbf{n}$ it is found that the crack opening displacement is given asymptotically by

$$\Delta u_z \sim \frac{2(1-\nu)}{\mu} \sqrt{2d} k_1(P) + \mathcal{O}(d^{3/2}) \quad (\text{X.17})$$

The quantity k_1 appearing in these expressions is called the opening mode stress intensity factor and is of interest to workers in fracture mechanics because it may be used to predict the onset of crack propagation. Clearly the opening mode stress intensity factor can be obtained directly from the solution of (X.14) via the limit

$$k_1 = \frac{-1}{2} \lim_{d \rightarrow 0} \frac{w}{\sqrt{2d}} \quad (\text{X.18})$$

which can often be evaluated in closed form.

A Penny Shaped Crack Problem

We begin by considering a circular or penny shaped disc of radius $a > 0$ which occupies the region

$$\Omega = \{(r, \theta) : 0 \leq r \leq a, -\pi \leq \theta \leq \pi\} \quad (\text{X.19})$$

of the z - plane and is opened by the symmetric pressure loading

$$\sigma_{zz} = -P(\dot{r}, \theta), \text{ for } (\dot{r}, \theta) \in \Omega \quad (\text{X.20})$$

which leads us to the layer potential solution

$$\begin{aligned} \varphi_z &= \mathfrak{D}[w(\dot{\rho}, \vartheta)](\dot{r}, \theta, z) \\ &= \Delta_2 \frac{1}{4\pi} \int_{-\pi}^{\pi} \int_0^a \frac{w(\dot{\rho}, \vartheta) \dot{\rho} d\dot{\rho} d\vartheta}{\sqrt{\dot{r}^2 + \dot{\rho}^2 - 2\dot{r}\dot{\rho} \cos(\theta - \vartheta) + z^2}} \end{aligned} \quad (\text{X.21})$$

where $w(\dot{\rho}, \vartheta)$ satisfies the hyper-singular integral equation

$$-\Delta_2 \int_{-\pi}^{\pi} \int_0^a w(\dot{\rho}, \vartheta) B(\dot{\rho}, \vartheta; \dot{r}, \theta) \dot{\rho} d\dot{\rho} d\vartheta = -P(\dot{r}, \theta), \quad (\text{X.22})$$

for $0 \leq \dot{r} \leq a$, $-\pi \leq \theta \leq \pi$ or equivalently, the operator equation

$$-\Delta_2 \mathbb{B}^1[f(\rho, \vartheta)](r, \theta) = -p(r, \theta) \in L_2^1(\Omega_0) \quad (\text{X.23})$$

which is obtained by making the simple change of variables; $\dot{r} = ra$, $\dot{\rho} = \rho a$,

$$f(\rho, \vartheta) = \frac{w(\rho a, \vartheta)}{a\sqrt{1-\rho^2}} = \frac{w(\dot{\rho}, \vartheta)}{a\sqrt{1-(\frac{\dot{\rho}}{a})^2}}, \quad (\text{X.24})$$

$$p(r, \theta) = P(ra, \theta) = P(\dot{r}, \theta), \quad (\text{X.25})$$

and

$$\Delta_2 = \frac{\partial^2}{\partial r^2} + \frac{1}{r} \frac{\partial}{\partial r} + \frac{1}{r^2} \frac{\partial^2}{\partial \theta^2} = a^2 \left[\frac{\partial^2}{\partial \dot{r}^2} + \frac{1}{\dot{r}} \frac{\partial}{\partial \dot{r}} + \frac{1}{\dot{r}^2} \frac{\partial^2}{\partial \theta^2} \right] = a^2 \Delta_2 \quad (\text{X.26})$$

The crack opening displacement is then related to w and f by

$$\Delta u_z = -\frac{1-\nu}{\mu} w(\dot{r}, \theta) = -\frac{1-\nu}{\mu} f\left(\frac{\dot{r}}{a}, \theta\right) \sqrt{a^2 - \dot{r}^2} \quad (\text{X.27})$$

and the stress intensity factor takes the form

$$k_1 = \frac{-1}{2} \lim_{\dot{r} \rightarrow a^-} \frac{f\left(\frac{\dot{r}}{a}, \theta\right) \sqrt{a^2 - \dot{r}^2}}{\sqrt{2(a - \dot{r})}} = -\frac{1}{2} f(1, \theta) \sqrt{a} \quad (\text{X.28})$$

X.2.2 Case 1: Constant Pressure

In the case of a constant pressure loading

$$P(r, \theta) = P = P \sqrt{\frac{2\pi}{3}} c_{00}^1 \left(\frac{r}{a}, \theta \right) \quad (\text{X.29})$$

the solution, (X.27), yields the crack opening displacement

$$\Delta u_z = \frac{1-\nu}{\mu} P \sqrt{\frac{2\pi}{3}} C_{00}^1 \left(\frac{r}{a}, \theta \right) \sqrt{a^2 - r^2} = \frac{1-\nu}{\mu} \frac{4P \sqrt{a^2 - r^2}}{\pi} \quad (\text{X.30})$$

and hence the stress intensity factor

$$k_1 = \lim_{r \rightarrow a} \frac{\mu}{2(1-\nu)} \frac{\Delta u_z}{\sqrt{2(a-r)}} = \frac{2P}{\pi} \lim_{r \rightarrow a} \sqrt{\frac{a+r}{2}} = \frac{2P}{\pi} \sqrt{a} \quad (\text{X.31})$$

which is readily verified computationally.

X.2.3 Case 2: Bending Load

Next we consider the case in which the crack is opened by a bending load M about the axis, $z = 0$, $x = b > a$. To find the effective pressure we observe that, in the absence of a crack, the stress on the z -plane is given by

$$\sigma_{zz}(r, \theta, 0^\pm) = M(b - r \cos \theta), \quad (\text{X.32})$$

$$\sigma_{rz}(r, \theta, 0^\pm) = \sigma_{\theta z}(r, \theta, 0^\pm) = 0 \quad (\text{X.33})$$

by the principle of superposition it now follows that the effective pressure on the Penny shaped crack takes the form

$$P(r, \theta) = -M(b - r \cos \theta) = -Mb \sqrt{\frac{2\pi}{3}} c_{00}^1(r, \theta) + M \sqrt{\frac{2\pi}{15}} c_{10}^1(r, \theta), \quad (\text{X.34})$$

as before, the crack opening displacement is given by

$$\Delta u_z = -\frac{1-\nu}{\mu} w(r, \theta) \quad (\text{X.35})$$

where the w satisfies the hyper-singular integral equation

$$-\Delta_2 \int_{-\pi}^{\pi} \int_0^a w(\rho, \vartheta) B(\rho, \vartheta; \dot{r}, \theta) \rho d\rho d\vartheta = -P(\dot{r}, \theta), \text{ for } 0 \leq \dot{r} \leq a, -\pi \leq \theta \leq \pi \quad (\text{X.36})$$

or equivalently f satisfies the operator equation

$$-\Delta_2 \mathbb{B}^1 [f(\rho, \vartheta)](r, \theta) = -p(r, \theta) \in L_2^1(\Omega_0) \quad (\text{X.37})$$

which is obtained by making the simple change of variables; $\dot{r} = ra$, $\rho = \rho a$ and $\dot{b} = ba$ where

$$f(\rho, \vartheta) = \frac{w(\rho a, \vartheta)}{Ma^2 \sqrt{1 - \rho^2}} = \frac{w(\dot{\rho}, \vartheta)}{Ma \sqrt{a^2 - \dot{\rho}^2}}, \quad (\text{X.38})$$

$$p(r, \theta) = \frac{1}{aM} P(ra, \theta) = \frac{1}{aM} P(\dot{r}, \theta) = b - r \cos \theta = \frac{\dot{b}}{a} - \frac{\dot{r}}{a} \cos \theta \quad (\text{X.39})$$

and

$$\Delta_2 = \frac{\partial^2}{\partial r^2} + \frac{1}{r} \frac{\partial}{\partial r} + \frac{1}{r^2} \frac{\partial^2}{\partial \theta^2} = a^2 \left[\frac{\partial^2}{\partial \dot{r}^2} + \frac{1}{\dot{r}} \frac{\partial}{\partial \dot{r}} + \frac{1}{\dot{r}^2} \frac{\partial^2}{\partial \theta^2} \right] = a^2 \dot{\Delta}_2 \quad (\text{X.40})$$

The stress intensity factor for this problem is then

$$k_1 = - \lim_{\dot{r} \rightarrow a^-} \frac{1}{2} \frac{w(\dot{r}, \theta)}{\sqrt{2(a - \dot{r})}} = -\frac{1}{2} Ma^{\frac{3}{2}} f(1, \theta) \quad (\text{X.41})$$

or

$$\frac{k_1}{k_0} = -\frac{\pi}{4} f(1, \vartheta) \quad (\text{X.42})$$

where we have introduced the scaling factor

$$k_0 = \frac{2}{\pi} Ma^{\frac{3}{2}} \quad (\text{X.43})$$

For $0 \leq \theta < 2\pi$ the exact solution for this quantity is given by

$$\frac{k_1}{k_0} = \frac{\dot{b}}{a} - \frac{2}{3} \cos \vartheta \quad (\text{X.44})$$

which has its maximum value when $\vartheta = \pi$ and in that case

$$\left(\frac{k_1}{k_0}\right)_{\max} = \frac{b}{a} + \frac{2}{3} \quad (\text{X.45})$$

Figure 8 illustrates the nature of the stress intensity at different points on the edge of the crack for differing crack radii and positions of bending loads.

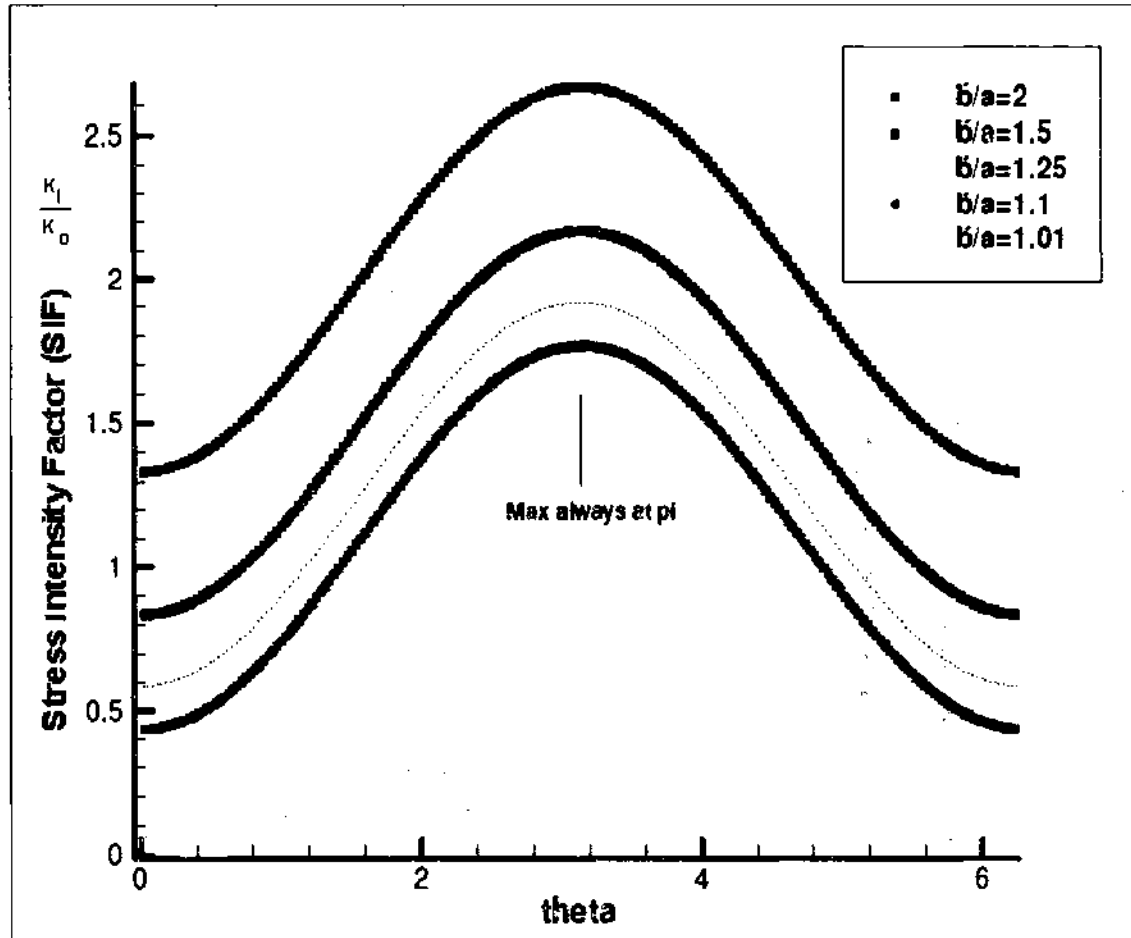


FIG. 8. A penny shaped crack of radius a , centered at $(0,0,0)$ and opened by a bending force about the line $x = b > a$. Plots show how the scaled stress intensity factor varies with θ for several values of $b = b/a$.

X.2.4 Case 3: Equal and Opposite Point Forces

Case 3a: The Axisymmetric Loading Case

We now consider the problem in which a penny shaped crack is opened by equal and opposite point forces $\pm P\vec{k}$ at the positions $(0, 0, \pm h)$. First we need to determine the effective pressure. From Kelvin's Solution ([20], page 219) for a point force of magnitude P acting in the positive z direction at the origin;

$$\begin{aligned}\sigma_{zz}(\dot{r}, z) &= -\frac{P}{8\pi(1-\nu)} \left[(1-2\nu) \frac{z}{R^3} + \frac{3z^3}{R^5} \right] \\ \sigma_{rz}(\dot{r}, z) &= -\frac{P}{8\pi(1-\nu)} \left[(1-2\nu) \frac{\dot{r}}{R^3} + \frac{3\dot{r}z^2}{R^5} \right] \\ \sigma_{\theta z}(\dot{r}, z) &= 0\end{aligned}\tag{X.46}$$

where $R = \sqrt{\dot{r}^2 + z^2}$

Using this solution, the principle of superposition and the notation $R_z = \sqrt{\dot{r}^2 + (z-h)^2}$, we find that the two point loading yields the stresses

$$\sigma_{zz}(\dot{r}, z) = \frac{-P}{8\pi(1-\nu)} \left[(1-2\nu) \frac{(z-h)}{R_z^3} + \frac{3(z-h)^3}{R_z^5} - (1-2\nu) \frac{(z+h)}{R_{-z}^3} - \frac{3(z+h)^3}{R_{-z}^5} \right]\tag{X.47}$$

$$\sigma_{rz}(\dot{r}, z) = \frac{-P}{8\pi(1-\nu)} \left[(1-2\nu) \frac{\dot{r}}{R_z^3} + \frac{3\dot{r}(z-h)^2}{R_z^5} - (1-2\nu) \frac{\dot{r}}{R_{-z}^3} - \frac{3\dot{r}(z+h)^2}{R_{-z}^5} \right]\tag{X.48}$$

$$\sigma_{\theta z}(\dot{r}, z) = 0\tag{X.49}$$

so that

$$\sigma_{\theta z}(\dot{r}, 0) = \sigma_{rz}(\dot{r}, 0) = 0\tag{X.50}$$

and

$$\sigma_{zz}(\dot{r}, 0) = \frac{P\dot{h}}{4\pi} \left[\frac{2}{R_0^3} + \frac{1}{1-\nu} \frac{3\dot{h}^2 - R_0^2}{R_0^5} \right]\tag{X.51}$$

hence the effective pressure loading can be written in the form

$$P(\dot{r}) = P_1(\dot{r}) + \frac{1}{1-\nu} P_2(\dot{r})\tag{X.52}$$

where

$$P_1(\dot{r}) = \frac{P\dot{h}}{4\pi R_0^3} \quad (X.53)$$

$$P_2(\dot{r}) = \frac{P\dot{h}}{4\pi} \frac{3\dot{h}^2 - R_0^2}{R_0^5} \quad (X.54)$$

The crack opening displacement is then given by

$$\Delta u_z = -\frac{1-\nu}{\mu} w(\dot{r}) = -\frac{1}{\mu} [(1-\nu)w_1(\dot{r}) + w_2(\dot{r})] \quad (X.55)$$

where the w_k satisfy the integral equations

$$-\Delta_2 \int_{-\pi}^{\pi} \int_0^a w_k(\dot{\rho}) B(\dot{\rho}, \vartheta; \dot{r}, \theta) \dot{\rho} d\dot{\rho} d\vartheta = -P_k(\dot{r}), \quad (X.56)$$

for $0 \leq \dot{r} \leq a$, $-\pi \leq \theta \leq \pi$, $k = 1, 2$ or equivalently; as operator equations in f

$$-\Delta_2 \mathbb{B}^1[f(\rho)](r, \theta) = -p_k(r) \in L_2^1(\Omega_0) \quad (X.57)$$

obtained by making the change of variables; $\dot{r} = ra$, $\dot{\rho} = \rho a$ and $\dot{h} = ha$ where

$$f_k(\rho) = \frac{4\pi a w_k(\rho a)}{P\sqrt{1-\rho^2}} = \frac{4\pi a^2 w_k(\dot{\rho})}{P\sqrt{a^2-\dot{\rho}^2}}, \quad (X.58)$$

$$p_k(r) = \frac{4\pi a^2}{P} P_k(ra) = \frac{4\pi a^2}{P} P_k(\dot{r}) \quad (X.59)$$

and

$$\Delta_2 = \frac{\partial^2}{\partial r^2} + \frac{1}{r} \frac{\partial}{\partial r} + \frac{1}{r^2} \frac{\partial^2}{\partial \theta^2} = a^2 \left[\frac{\partial^2}{\partial \dot{r}^2} + \frac{1}{\dot{r}} \frac{\partial}{\partial \dot{r}} + \frac{1}{\dot{r}^2} \frac{\partial^2}{\partial \theta^2} \right] = a^2 \dot{\Delta}_2 \quad (X.60)$$

Since (X.56) exhibits axial symmetry it is easily converted to a one dimensional integral equation as discussed in Thm. (VIII.7). This leads to the one dimensional operator equations

$$\mathbb{D}_0 \mathbb{L}_0^1[f_k(\rho)](r) = p_k(r) \in L_{2,0}^1(0,1), \text{ for } 0 \leq r \leq 1, k = 1, 2 \quad (X.61)$$

where

$$p_k(r) = \left\{ \begin{array}{l} \frac{2h}{(r^2 + h^2)^{\frac{3}{2}}}, \quad k = 1 \\ \frac{h^3 - hr^2}{(r^2 + h^2)^{\frac{3}{2}}}, \quad k = 2 \end{array} \right\} \quad (\text{X.62})$$

In this case the scaled stress intensity factor may be expressed by

$$\frac{k_1}{k_0} = \frac{k_1^{(1)}}{k_0} + \frac{1}{1 - \nu} \frac{k_1^{(2)}}{k_0}, \quad (\text{X.63})$$

where

$$k_1^{(k)} = -\frac{1}{2} \lim_{r \rightarrow a^-} \frac{w_k(r)}{\sqrt{2(a-r)}} = \frac{-P}{8\pi a^{\frac{3}{2}}} f_k(1), \quad \text{for } k = 1, 2 \quad (\text{X.64})$$

and the scaling factor chosen,

$$k_0 = \frac{P}{\pi^2 a^{\frac{3}{2}}} \quad (\text{X.65})$$

is the stress intensity factor for a plane circular crack with symmetrical and opposing point forces at the center [23].

It now follows that

$$\frac{k_1}{k_0} = -\frac{\pi}{8} \left[f_1(1) + \frac{1}{1 - \nu} f_2(1) \right] \quad (\text{X.66})$$

which can be computed and compared with the exact solution as found in [23]

$$\frac{k_1}{k_0} = \frac{1}{1 + h^2} + \frac{1}{1 - \nu} \frac{h^2}{(1 + h^2)^2} \quad (\text{X.67})$$

A plot of the results obtained for certain ν values is shown next (Figure 9) and compares favorably with the known result.

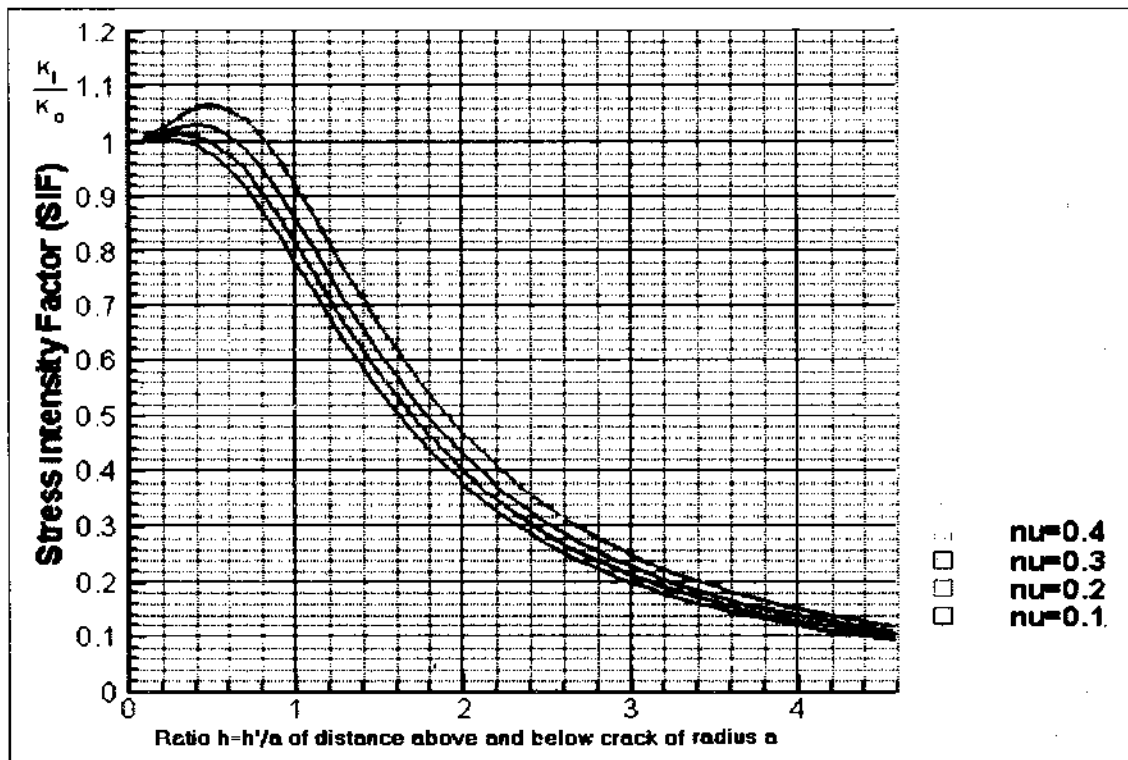


FIG. 9. A penny shaped crack of radius a , centered at $(0,0,0)$ and opened by point forces $\pm Pk$ centered above and below the cracks at $(0,0,\pm h')$. Plots show how the scaled stress intensity factor varies with $h = h'/a$ for several values of ν .

Case 3b: The Non-Axisymmetric Loading Case

This time we are going to have the point forces centered at $(b, 0, \pm h)$. If we let R be as follows

$$R = \sqrt{(x - b)^2 + y^2 + h^2}$$

then by virtue of Kelvin's solution ([20], page 219) it is readily seen that

$$P(r, \theta) = P_1(r, \theta) + \frac{1}{1 - \nu} P_2(r, \theta) \quad (\text{X.68})$$

where

$$P_1(\dot{r}, \theta) = \frac{Ph}{2\pi R_1^3}, \quad (\text{X.69})$$

$$P_2(\dot{r}, \theta) = \frac{Ph(2h^2 - R_1^2)}{4\pi R_1^5} \quad (\text{X.70})$$

and

$$R_1(\dot{r}, \theta) = \sqrt{\dot{r}^2 - 2\dot{r}b \cos \theta + b^2 + h^2}$$

The crack opening displacement is then given by

$$\Delta u_z = -\frac{1-\nu}{\mu} w(\dot{r}) = -\frac{1}{\mu} [(1-\nu) w_1(\dot{r}) + w_2(\dot{r})] \quad (\text{X.71})$$

where the w_k are solutions of the integral equations

$$-\Delta_2 \int_{-\pi}^{\pi} \int_0^a w_k(\dot{\rho}) B(\dot{\rho}, \vartheta; \dot{r}, \theta) \dot{\rho} d\dot{\rho} d\vartheta = -P_k(\dot{r}), \quad (\text{X.72})$$

for $0 \leq \dot{r} \leq a$, $-\pi < \theta \leq \pi$, $k = 1, 2$ or equivalently; f_k are solutions of the operator equations

$$-\Delta_2 \mathbb{B}^1 [f_k(\rho, \vartheta)](r, \theta) = -p_k(r, \theta) \in L_2^1(\Omega_0) \quad (\text{X.73})$$

obtained by making the change of variables; $\dot{r} = ra$, $\dot{\rho} = \rho a$, $b = \beta a$ and $h = \gamma a$ where

$$f_k(\rho, \vartheta) = \frac{4\pi a w_k(\rho a, \vartheta)}{P\sqrt{1-\rho^2}} = \frac{4\pi a^2 w_k(\dot{\rho}, \vartheta)}{P\sqrt{a^2 - \dot{\rho}^2}}, \quad (\text{X.74})$$

$$p_k(r, \theta) = \frac{4\pi a^2}{P} P_k(ra, \theta) = \frac{4\pi a^2}{P} P(\dot{r}, \theta), \quad (\text{X.75})$$

$$\Delta_2 = \frac{\partial^2}{\partial r^2} + \frac{1}{r} \frac{\partial}{\partial r} + \frac{1}{r^2} \frac{\partial^2}{\partial \theta^2} = a^2 \left[\frac{\partial^2}{\partial \dot{r}^2} + \frac{1}{\dot{r}} \frac{\partial}{\partial \dot{r}} + \frac{1}{\dot{r}^2} \frac{\partial^2}{\partial \theta^2} \right] = a^2 \Delta_2, \quad (\text{X.76})$$

$$R^2 = \dot{r}^2 - 2\dot{r}b \cos \theta + b^2 + h^2 = a^2 [r^2 - 2r\beta \cos \theta + \beta^2 + \gamma^2] = a^2 R_1(r, \theta) \quad (\text{X.77})$$

and noting that

$$\begin{aligned} P(\dot{r}, \theta) &= \frac{Ph}{4\pi} \left[\frac{2}{R^3} + \frac{1}{1-\nu} \frac{2h^2 - R^2}{R^5} \right] = \frac{P}{4\pi a^2} \left[\frac{2\gamma}{R_1^3} + \frac{1}{1-\nu} \frac{\gamma(2\gamma^2 - R_1^2)}{R^5} \right] \\ &= \frac{P}{4\pi a^2} \left[p_1(r, \theta) + \frac{1}{1-\nu} p_2(r, \theta) \right] \end{aligned} \quad (\text{X.78})$$

We must solve (X.73) as a full two dimensional equation. The scaled stress intensity factor for this problem has no known closed form solution but will be of the form

$$\frac{k_1}{k_0} = \frac{k_1^{(1)}}{k_0} + \frac{1}{(1-\nu)} \frac{k_1^{(2)}}{k_0} \quad (\text{X.79})$$

where for

$$k_1^{(k)} = -\frac{1}{2} \lim_{r \rightarrow a^-} \frac{w_k(r, \theta)}{\sqrt{2(a-r)}} = \frac{-P}{8\pi a^{\frac{3}{2}}} f_k(1, \theta), \text{ for } k = 1, 2 \quad (\text{X.80})$$

the scaling factor needed is given by (X.65).

It is now apparent that

$$\frac{k_1}{k_0} = -\frac{\pi}{8} \left[f_1(1, \theta) + \frac{1}{1-\nu} f_2(1, \theta) \right] \quad (\text{X.81})$$

and it is clear, from physical considerations, that the maximum stress intensity factor will occur when $\theta = 0$.

We now exhibit the stress intensity factor with a few graphs illustrating some results. Firstly a plot showing the stress intensity factor for a set ratio $\gamma = \frac{b}{a} = 1$, and various $\beta = \frac{b}{a}$ and ν values (Figure 10). We can see clearly that in Figure 10 the stress decreases as both ν decreases and β increases. β increasing means the forces are moved further away from the crack reducing the effect.

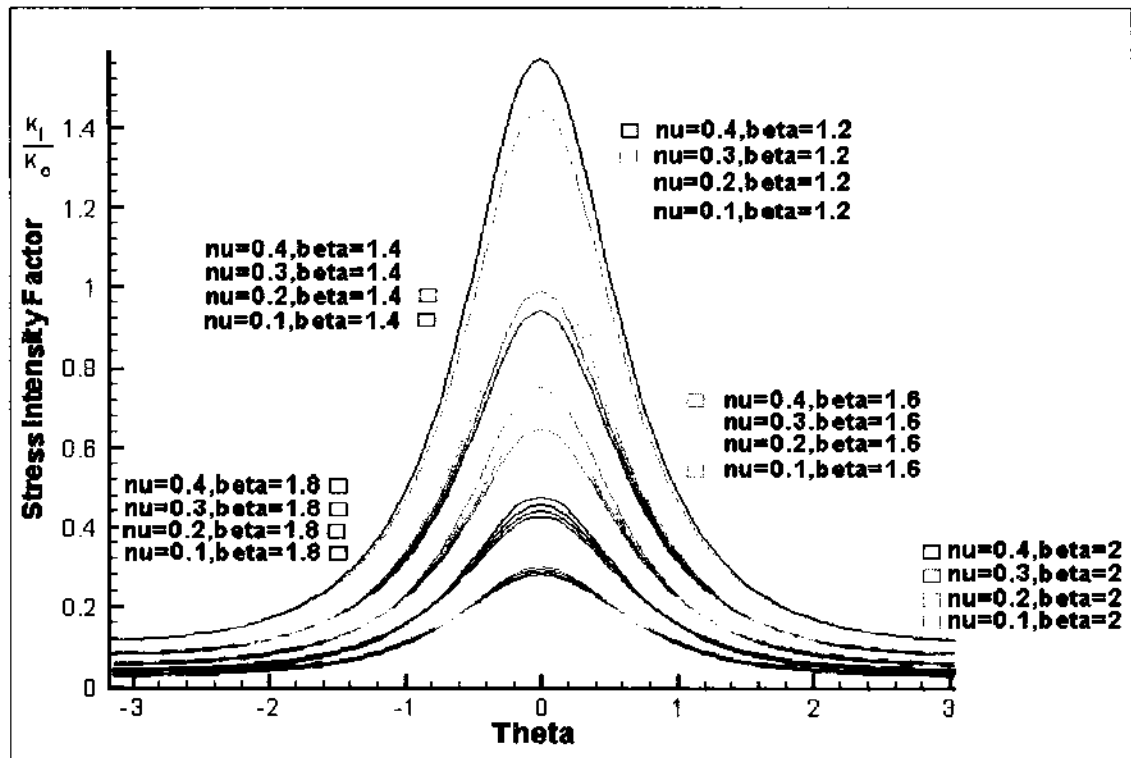


FIG. 10. A penny shaped crack of radius a , centered at $(0,0,0)$ and opened by point forces $\pm P\mathbf{k}$ at $(b,0,\pm h')$. Plots show how the scaled stress intensity factor varies with θ for different values of $\beta = b/a$ for several values of ν with $\gamma = h/a = 1$.

The next two plots (Figures 11 and 12) have set values of both $\beta = 2$ and $\nu = 0.4$ and show the effect of varying γ . In Figure 11 it can be clearly seen that the stress increases as γ increases for very small γ values. This phenomenon is due to the fact that when the height is very small the point forces partially cancel and do not exert their full force on the crack edges. Figure 12 shows that when γ gets bigger (in this case bigger than 1) the stress intensity drops as the height gets higher and hence further away from the cracks.

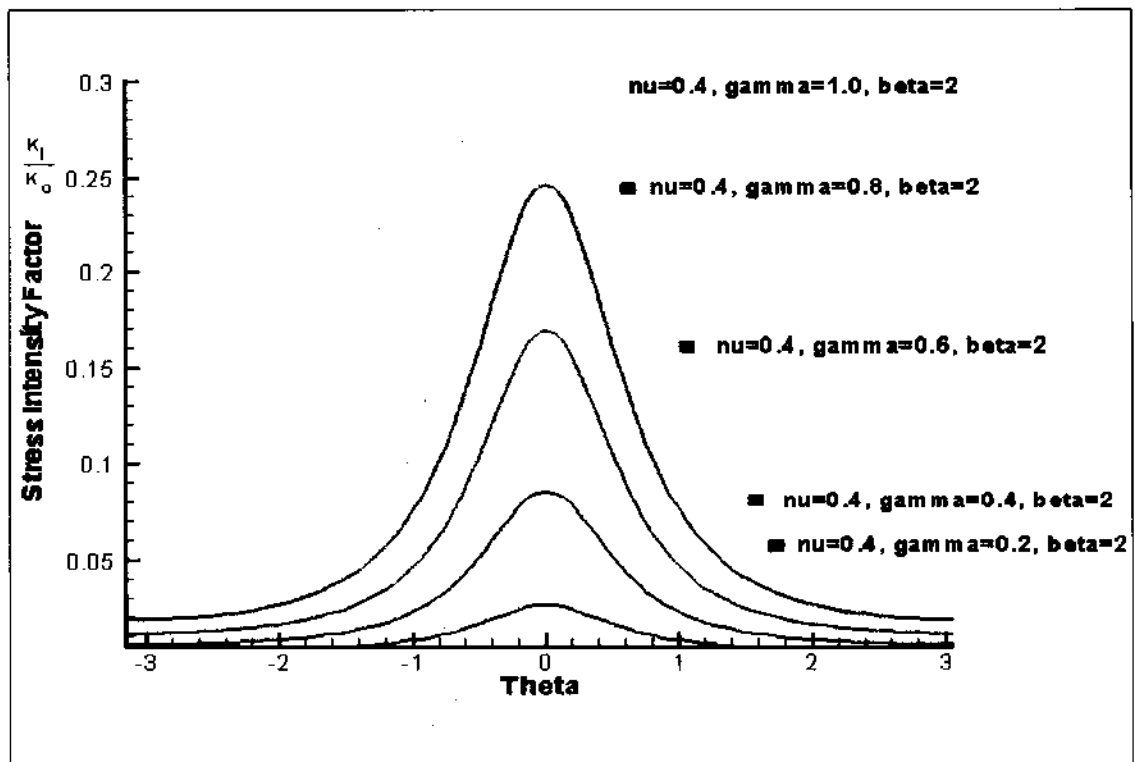


FIG. 11. A penny shaped crack of radius a , centered at $(0, 0, 0)$ and opened by point forces $\pm P\mathbf{k}$ at $(b, 0, \pm h')$. Plots show how the scaled stress intensity factor varies with θ for different small values of $\gamma = h/a$ for $\nu = 0.4$ and $\beta = b/a = 2$.

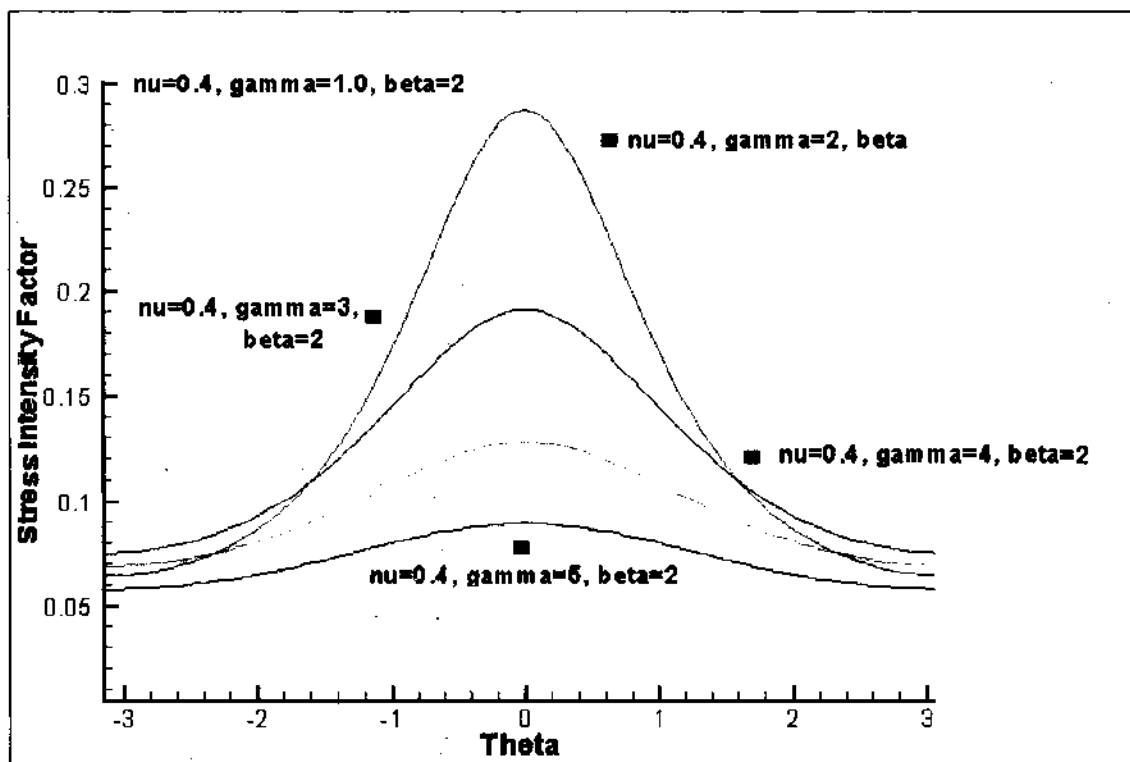


FIG. 12. A penny shaped crack of radius a , centered at $(0,0,0)$ and opened by point forces $\pm P\mathbf{k}$ at $(b,0,\pm h')$. Plots show how the scaled stress intensity factor varies with θ for different medium to large values of $\gamma = h/a$ for $\nu = 0.4$ and $\beta = b/a = 2$.

All these plots indicate the same profile of graph with differing magnitudes. The maximum stress is the most important consideration when considering crack propagation and Figures 13 and 14 illustrate the maximum stress intensity factor for various γ and β values, first as a three dimensional plot and then as a contour plot. Loads directly above the crack and near to the edge clearly produce significantly more stress than those further away from the crack. Close to the center of the crack would appear to be a point where the stresses are partially balanced.

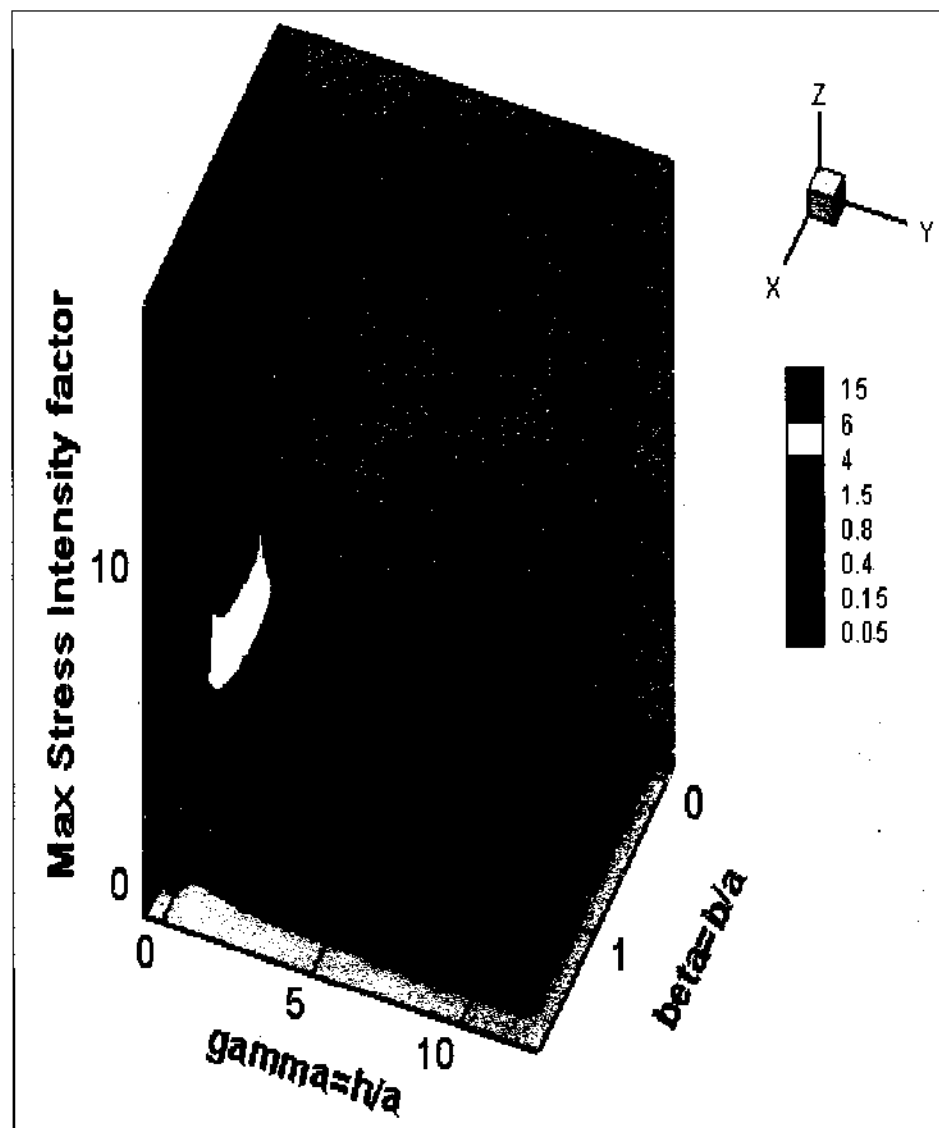


FIG. 13. A penny shaped crack of radius a , centered at $(0,0,0)$ and opened by point forces $\pm Pk$ at $(b,0,\pm h')$. Plot shows how the scaled maximum stress intensity factor varies with $\gamma = h/a$ and $\beta = b/a$ for $\nu = 0.4$.

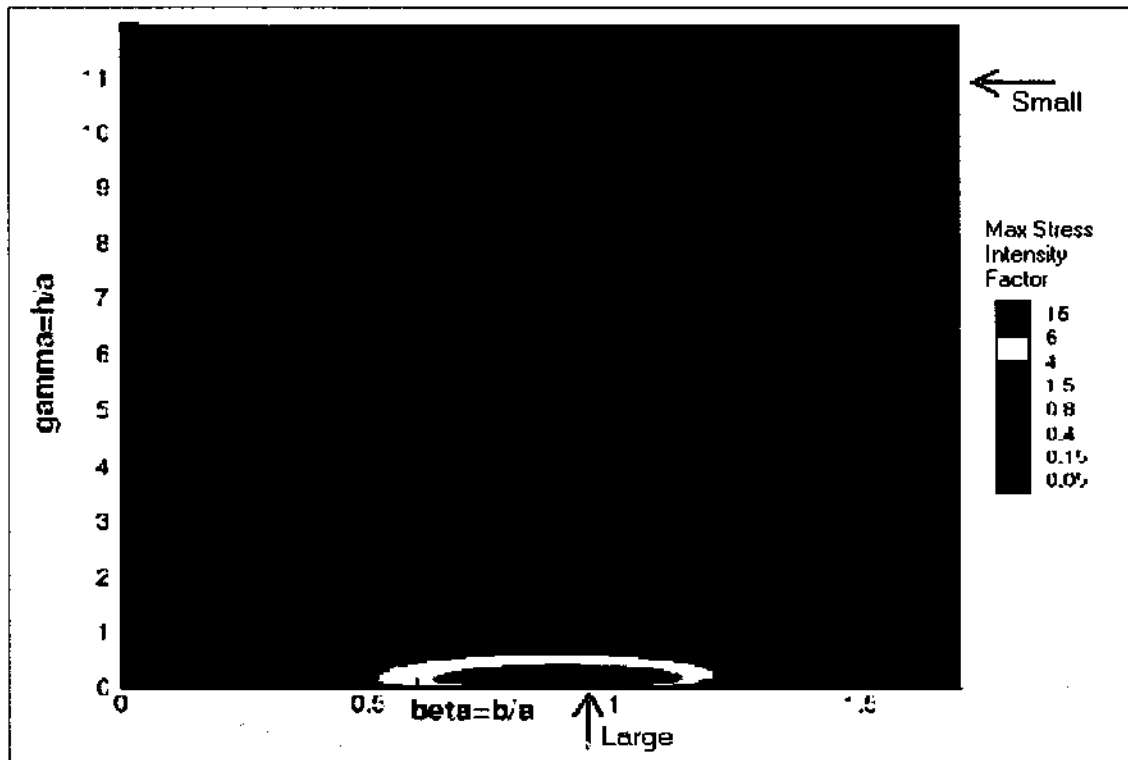


FIG. 14. A penny shaped crack of radius a , centered at $(0,0,0)$ and opened by point forces $\pm Pk$ at $(b,0,\pm h')$. Contour plot shows how the scaled maximum stress intensity factor varies with $\gamma = h/a$ and $\beta = b/a$ for $\nu = 0.4$.

X.3 MULTIPLE CRACK PROBLEMS

X.3.1 General Problem

This time we will examine a pair of coplanar penny shaped cracks of radius a centered on $(\pm \epsilon, 0, 0)$, $\epsilon > a$, given by $\Omega^\pm = \{(x, y) : (x \mp \epsilon)^2 + y^2 \leq a^2\}$. These cracks will be opened by the loading pressure

$$\sigma_{zz}(x, y, 0) = -P(x, y), \text{ for } (x, y) \in \Omega \quad (\text{X.82})$$

where

$$P(x, y) = \begin{cases} P^+(x, y) & , \text{ for } (x, y) \in \Omega^+ \\ P^-(x, y) & , \text{ for } (x, y) \in \Omega^- \end{cases} \quad (\text{X.83})$$

and $\Omega = \Omega^+ \cup \Omega^-$.

The crack opening displacement will then be given by

$$\begin{aligned}\Delta u_z &= u_z(x, y, 0^+) - u_z(x, y, 0^-) \\ &= \frac{-1}{\mu(1-\nu)} w(x, y), \text{ for } (x, y) \in \Omega\end{aligned}\quad (\text{X.84})$$

where the potential function is such that

$$w(x, y) = \begin{cases} w^+(x, y) & , \text{ for } (x, y) \in \Omega^+ \\ w^-(x, y) & , \text{ for } (x, y) \in \Omega^- \end{cases}\quad (\text{X.85})$$

and is given by the pair of hyper-singular equations

$$\frac{\Delta_2}{4\pi} \int \int_{\Omega^+} \frac{w^+(s, t) ds dt}{\sqrt{(x-s)^2 + (y-t)^2}} + \frac{\Delta_2}{4\pi} \int \int_{\Omega^-} \frac{w^-(s, t) ds dt}{\sqrt{(x-s)^2 + (y-t)^2}} = P^+(x, y),\quad (\text{X.86})$$

for $(x, y) \in \Omega^+$ and

$$\frac{\Delta_2}{4\pi} \int \int_{\Omega^+} \frac{w^+(s, t) ds dt}{\sqrt{(x-s)^2 + (y-t)^2}} + \frac{\Delta_2}{4\pi} \int \int_{\Omega^-} \frac{w^-(s, t) ds dt}{\sqrt{(x-s)^2 + (y-t)^2}} = P^-(x, y),\quad (\text{X.87})$$

for $(x, y) \in \Omega^-$

We will solve these type of problems by splitting (when necessary) the pressure function into even and odd components and then exploiting the symmetries these individual parts exhibit. We will choose for generality symmetry about the origin so that we can assume that;

$$P^-(x, y) = \pm P^+(x, y), \text{ for } (x, y) \in \Omega^+ \quad (\text{X.88})$$

and it can then be shown that the potential function exhibits similar symmetries

$$w^-(x, y) = \pm w^+(x, y), \text{ for } (x, y) \in \Omega^+ \quad (\text{X.89})$$

so that on making the correct change of variables we can reduce (X.86) and (X.87)

to the one equation

$$\frac{\Delta_2}{4\pi} \iint_{\Omega^+} \left\{ \frac{1}{\sqrt{(x-s)^2 + (y-t)^2}} \pm \frac{1}{\sqrt{(x+s)^2 + (y+t)^2}} \right\} w^+(s, t) ds dt = P^+(x, y), \quad (\text{X.90})$$

for $(x, y) \in \Omega^+$

Introducing polar coordinates (with $\acute{c} = ac$, $\acute{r} = ar$, $\acute{\rho} = a\rho$)

$$\begin{aligned} x - \acute{c} &= \acute{r} \cos \theta, & y &= \acute{r} \sin \theta \\ s - \acute{c} &= \acute{\rho} \cos \vartheta, & t &= \acute{\rho} \sin \vartheta \end{aligned} \quad (\text{X.91})$$

and letting

$$\begin{aligned} w^+(\acute{\rho}, \vartheta) &= aP\sqrt{1-\rho^2}f(\rho, \theta) \\ P^+(\acute{r}, \theta) &= -P.p(r, \theta) \end{aligned} \quad (\text{X.92})$$

where

$$\Delta_2 = \frac{\partial^2}{\partial r^2} + \frac{1}{r} \frac{\partial}{\partial r} + \frac{1}{r^2} \frac{\partial^2}{\partial \theta^2} = a^2 \left[\frac{\partial^2}{\partial \acute{r}^2} + \frac{1}{\acute{r}} \frac{\partial}{\partial \acute{r}} + \frac{1}{\acute{r}^2} \frac{\partial^2}{\partial \theta^2} \right] = a^2 \acute{\Delta}_2 \quad (\text{X.93})$$

we then obtain the integral equation

$$\int_{-\pi}^{\pi} \int_0^1 w_1(\rho) f(\rho, \theta) \left\{ \frac{-\Delta_2}{4\pi} B(\rho, \vartheta; r, \theta) + K_c^\pm(\rho, \vartheta; r, \theta) \right\} d\rho d\vartheta = p(r, \theta) \quad (\text{X.94})$$

for $0 \leq r \leq 1$, $-\pi < \theta \leq \pi$, where

$$K_c^\pm(\rho, \vartheta; r, \theta) = \Delta_2 \frac{\mp 1}{4\pi \sqrt{r^2 + \rho^2 + 2r\rho \cos(\theta - \vartheta) + 4c(\rho \cos \vartheta + r \cos \theta) + 4c^2}} \quad (\text{X.95})$$

or in operator form

$$\{-\Delta_2 \mathbb{B}^1 + \mathbb{K}_{\pm, c}^1\} [f(\rho, \vartheta)](r, \theta) = p(r, \theta), \text{ for } 0 \leq r \leq 1, -\pi < \theta \leq \pi \quad (\text{X.96})$$

where

$$\mathbb{K}_{\pm, c}^1 [f(\rho, \vartheta)](r, \theta) = \int_{-\pi}^{\pi} \int_0^1 w^1(\rho) f(\rho, \theta) K_c^\pm(\rho, \vartheta; r, \theta) d\rho d\vartheta. \quad (\text{X.97})$$

The crack opening displacement is then given by

$$\Delta u_z = -\frac{1-\nu}{\mu} w(r, \theta) = -\frac{(1-\nu)P}{\mu} f\left(\frac{r}{a}, \theta\right) \sqrt{a^2 - r^2} \quad (\text{X.98})$$

and the stress intensity factor by

$$k_1 = -\frac{1}{2} \lim_{r \rightarrow a^-} \frac{w^+(r, \theta)}{\sqrt{2(a-r)}} = \frac{-P\sqrt{a}}{2} f(1, \theta) \quad (\text{X.99})$$

The stress intensity factor will be scaled with respect to that for a single disc

$$k_0 = \frac{2P}{\pi} \sqrt{a} \quad (\text{X.100})$$

which then gives

$$\frac{k_1}{k_0} = -\frac{\pi}{4} f(1, \theta) \quad (\text{X.101})$$

X.3.2 Case 1: Constant Pressure

In the case of a constant pressure loading

$$P(r, \theta) = P \quad (\text{X.102})$$

which is of even type, we need only solve the operator equation

$$\{-\Delta_2 \mathbb{B}^1 + \mathbb{K}_{+,c}^1\} [f(\rho, \vartheta)](r, \theta) = 1, \text{ for } 0 \leq r \leq 1, -\pi < \theta \leq \pi \quad (\text{X.103})$$

where

$$w(\rho, \vartheta) = -P\sqrt{a^2 - \rho^2} f\left(\frac{\rho}{a}, \vartheta\right) \quad (\text{X.104})$$

The crack opening displacement and the stress intensity factor are then given by

$$\Delta u_z = -\frac{1-\nu}{\mu} w(r, \theta) = \frac{(1-\nu)P}{\mu} f\left(\frac{r}{a}, \theta\right) \sqrt{a^2 - r^2} \quad (\text{X.105})$$

and

$$\frac{k_1}{k_0} = \frac{\pi}{4} f(1, \theta) \quad (\text{X.106})$$

Figure 15 illustrates the stress intensity for various c values. It can be clearly

seen that as the cracks become further apart (c increases) the stress will become increasingly similar to the single disk problem and hence as $c \rightarrow \infty$, $\frac{k_1}{k_0} \rightarrow 1$. When c is small we see that the stress intensity becomes larger particularly at points nearer the other crack ($\theta > \frac{\pi}{2}$ or $\theta < -\frac{\pi}{2}$). The maximum stress intensity is clearly shown to be at $\theta = \pm\pi$ as would be expected since the crack propagation would most likely be initiated here.

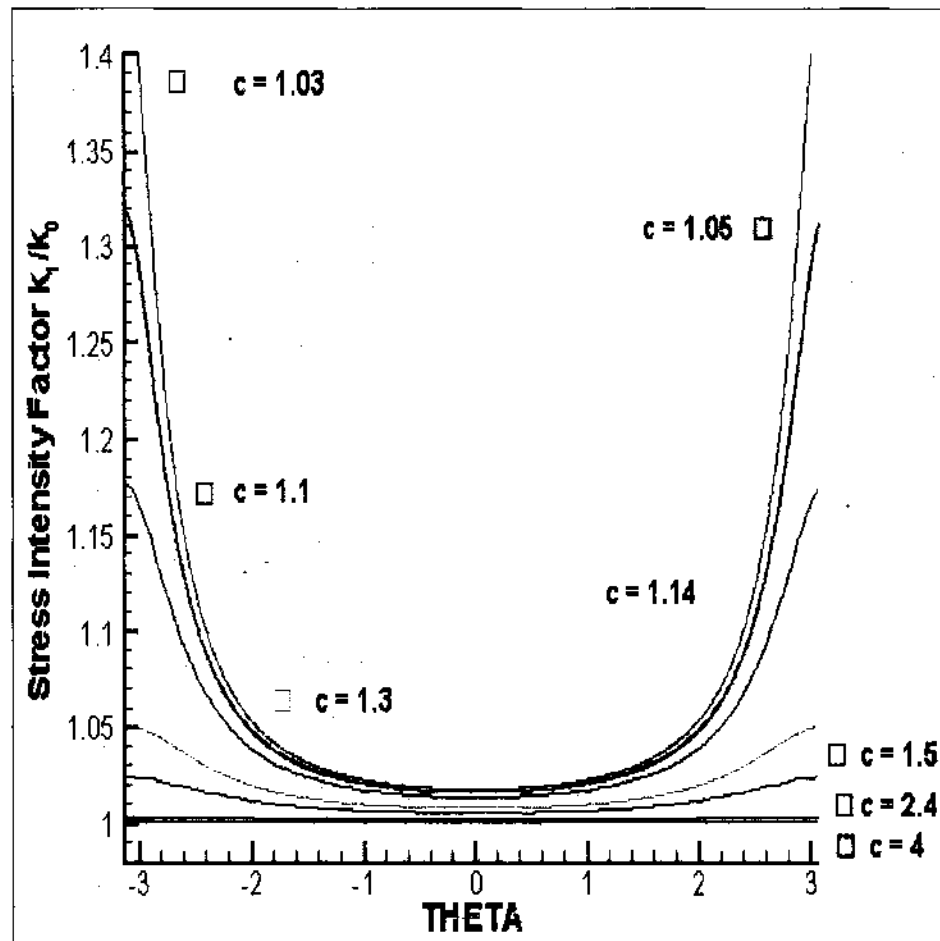


FIG. 15. Coplanar penny shaped cracks of radius a , centered at $(\pm c', 0, 0)$ and opened by a constant pressure load. Plots show how the scaled stress intensity factor varies with θ for several values of $c = c'/a$.

X.3.3 Case 2: Bending Load

Here we consider the case where the cracks are opened by a bending force about the line $y = \acute{b} > a$. In the absence of the cracks the tractions on the xy -plane are given by

$$\sigma_{zz}(x, y, 0) = M(\acute{b} - y), \sigma_{xz}(x, y, 0) = \sigma_{yz}(x, y, 0) = 0 \quad (\text{X.107})$$

therefore by the principle of superposition the crack load will be

$$\sigma_{zz}(x, y, 0) = -M(\acute{b} - y), \sigma_{xz}(x, y, 0) = \sigma_{yz}(x, y, 0) = 0 \quad (\text{X.108})$$

in this case our pressure function is given by

$$P(x, y) = M(\acute{b} - y) \quad (\text{X.109})$$

which is neither even or odd so we can split it up and consider

$$P_o(x, y) = -My = -Mr \sin \theta \quad (\text{X.110})$$

which is odd and

$$P_e(x, y) = M\acute{b} \quad (\text{X.111})$$

which is even.

The corresponding layer densities $w_o(\acute{\rho}, \vartheta)$ and $w_e(\acute{\rho}, \vartheta)$ are then related to the solutions of the integral equations

$$\{-\Delta_2 \mathbb{B}^1 + \mathbb{K}_{-,c}^1\} [f_o(\rho, \vartheta)](r, \theta) = r \sin \theta, \text{ for } 0 \leq r \leq 1, -\pi < \theta \leq \pi \quad (\text{X.112})$$

and

$$\{-\Delta_2 \mathbb{B}^1 + \mathbb{K}_{+,c}^1\} [f_e(\rho, \vartheta)](r, \theta) = 1, \text{ for } 0 \leq r \leq 1, -\pi < \theta \leq \pi \quad (\text{X.113})$$

via the relationships

$$w_o(\acute{\rho}, \vartheta) = Ma \sqrt{a^2 - \acute{\rho}^2} f_o\left(\frac{\acute{\rho}}{a}, \theta\right) \quad (\text{X.114})$$

and

$$w_e(\acute{\rho}, \vartheta) = -Mba \sqrt{a^2 - \acute{\rho}^2} f_e\left(\frac{\acute{\rho}}{a}, \theta\right) \quad (\text{X.115})$$

The crack opening displacement is then given by

$$\begin{aligned}\Delta u_z &= -\frac{1-\nu}{\mu} [w_e(\dot{r}, \vartheta) + w_o(\dot{r}, \vartheta)] \\ &= \frac{(1-\nu)Ma}{\mu} \sqrt{a^2 - \dot{r}^2} \left[f_o\left(\frac{\dot{r}}{a}, \theta\right) - bf_e\left(\frac{\dot{r}}{a}, \theta\right) \right]\end{aligned}\quad (\text{X.116})$$

This time we scale the stress intensity factor with the stress intensity factor for a single crack centered on the origin subject to a bending load about the line $y = b'$ which can be obtained from X.44 and X.43,

$$k_0 = \frac{2M}{\pi} a^{\frac{3}{2}} \left(b - \frac{2}{3} \sin \theta \right). \quad (\text{X.117})$$

therefore, since

$$k_1 = k_1^o + k_1^e = -\frac{1}{2} \lim_{\dot{r} \rightarrow a^-} \frac{[w_e(\dot{r}, \vartheta) + w_o(\dot{r}, \vartheta)]}{\sqrt{2(a - \dot{r})}} = \frac{Ma^{\frac{3}{2}}}{2} (bf_e(1, \theta) - f_o(1, \theta)) \quad (\text{X.118})$$

we find that

$$\frac{k_1}{k_0} = -\frac{3\pi [bf_e(1, \theta) - f_o(1, \theta)]}{4(3b - 2 \sin \theta)}. \quad (\text{X.119})$$

Figure 16 illustrates that the non-symmetrical nature of the stress intensity factor which is due to the bending line and the presence of the other disc having competing effects on the nature of the stress. The bending causes the stress to be highest at $x = -\frac{\pi}{2}$, lowest at $\frac{\pi}{2}$ and symmetrical about the line $y = 0$. The presence of the other disc increases the stress most at points close to it (at $x = \pi$) and least at points further away (at $x = 0$) while being symmetrical about the line $x = c'$. The maximum increase does not occur at the closest point but some point near to it's vicinity.

In Figure 17 we change the value of c and it can clearly be seen as the discs become further apart that the effect of the other crack on the stresses tends towards zero and the scaled stress intensity factor approaches one.

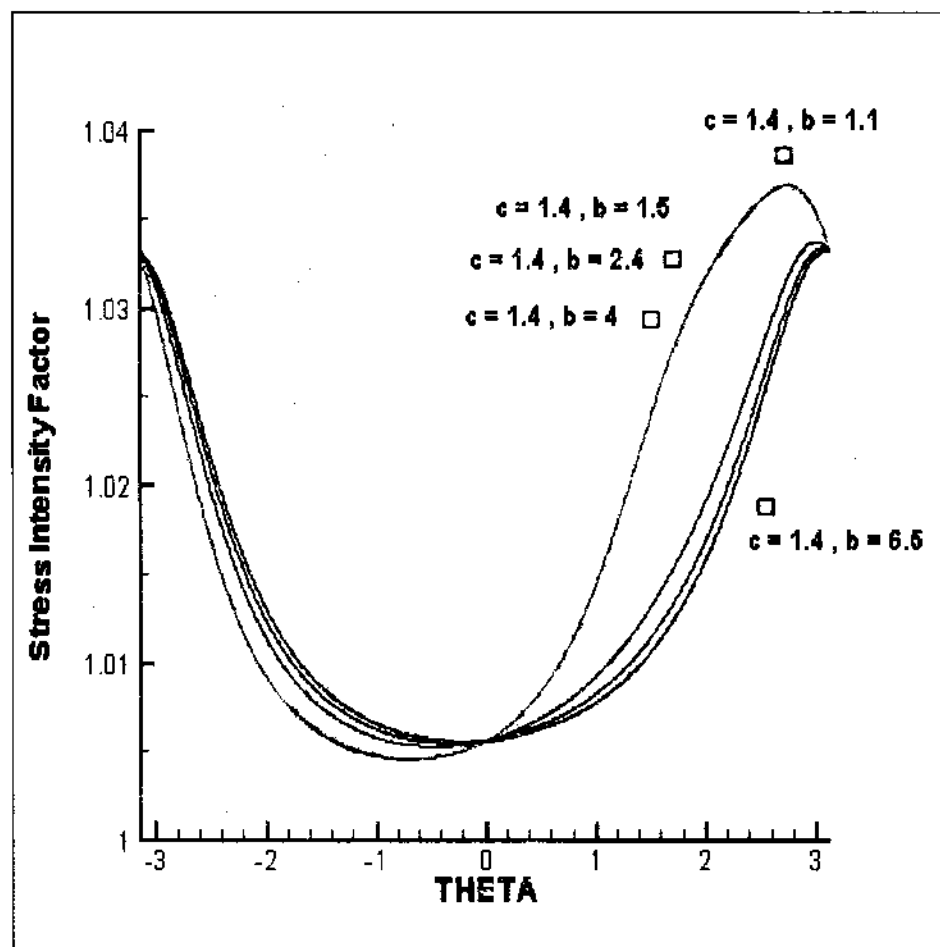


FIG. 16. Coplanar penny shaped cracks of radius a , centered at $(\pm c', 0, 0)$ and opened by a bending force about the line $y = b'$. Plots show how the scaled stress intensity factor varies with θ for $c = c'/a = 1.4$ and several values of $b = b'/a$.

Since the maximum is not this time obvious we will re-scale with the stress intensity factor for a bending load on a single crack (X.43),

$$k_0 = \frac{2M}{\pi} a^{\frac{3}{2}}$$

so that

$$\frac{k_1}{k_0} = -\frac{\pi}{4} [bf_e(1, \theta) - f_o(1, \theta)] \quad (\text{X.120})$$

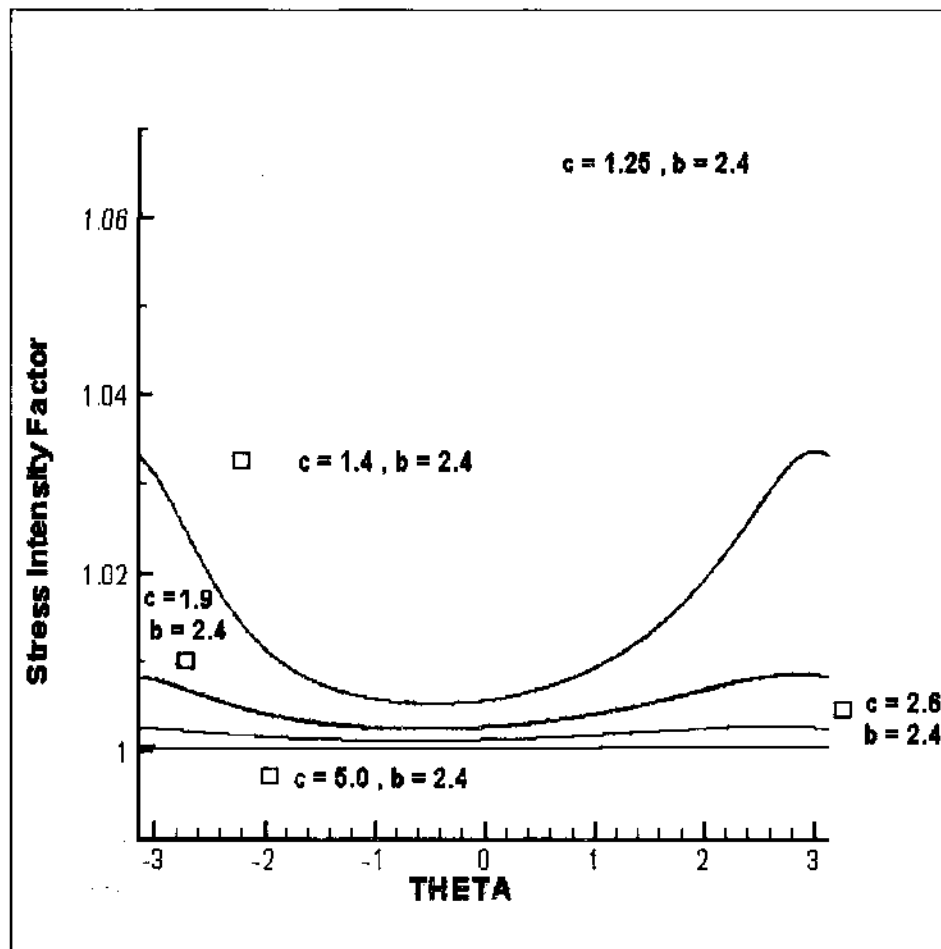


FIG. 17. Coplanar penny shaped cracks of radius a , centered at $(\pm c', 0, 0)$ and opened by a bending force about the line $y = b'$. Plots show how the scaled stress intensity factor varies with θ for $b = b'/a = 2.4$ and several values of $c = c'/a$.

Figure 18 indicates that although the maximum stress intensity factor may this time not be at exactly $\theta = -\frac{\pi}{2}$ it will be close enough for us to assume that it is the maximum.

We will now go back to our original scaling and look at

$$\frac{(k_1)_{\max}}{(k_0)_{\max}} = \frac{3\pi [bf_e(1, -\frac{\pi}{2}) - f_o(1, -\frac{\pi}{2})]}{4(3b+2)} \quad (\text{X.121})$$

firstly for different b values as we vary c as in Figure 19 and then for varying b and c values as a contour plot in Figure 20.

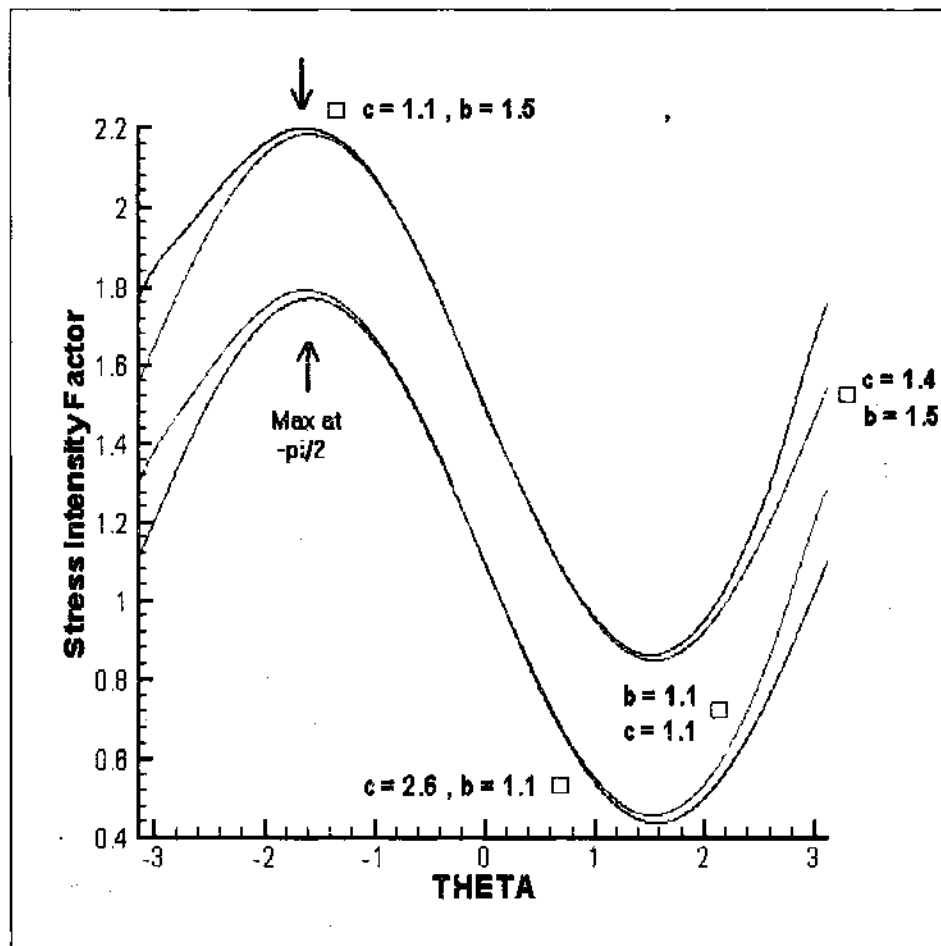


FIG. 18. Coplanar penny shaped cracks of radius a , centered at $(\pm c', 0, 0)$ and opened by a bending force about the line $y = b'$. Plots show how the alternatively scaled stress intensity factor varies with θ for several values of $c = c'/a$ and $b = b'/a$.

We can see clearly that as the distance between the cracks increases the scaled maximum stress tends towards one indicating the cracks stop affecting each other. Figure 19 shows that the stress increases as the bending line is moved further from the crack, while Figure 20 indicates this effect slows down as b gets big, visible since the contour lines are becoming straight vertical lines.

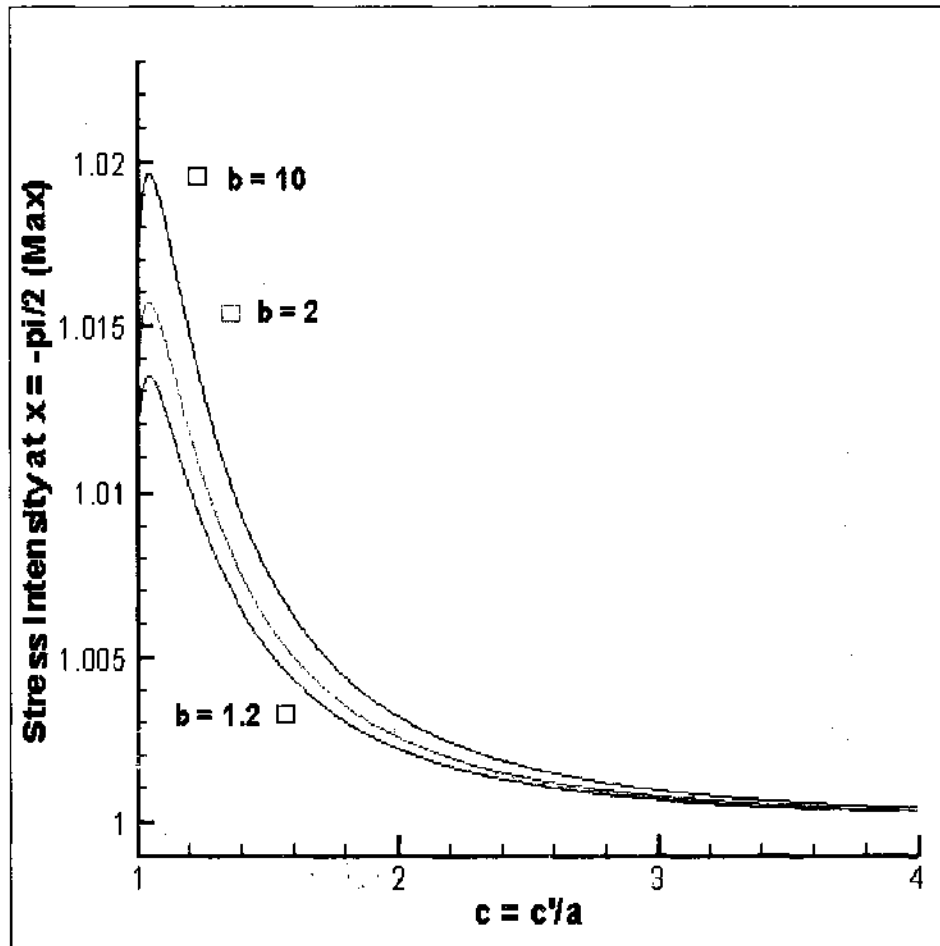


FIG. 19. Coplanar penny shaped cracks of radius a , centered at $(\pm c', 0, 0)$ and opened by a bending force about the line $y = b'$. Plots show how the scaled maximum stress intensity factor varies with $c = c'/a$ for several values of $b = b'/a$.

X.3.4 Case 3: Equal and Opposite Point Forces

Case 3a: Point Loads on the z-axis In this case we consider two equal and opposite point forces symmetrically placed with respect to the crack surfaces and the cracks themselves. Let the point forces $\pm P\mathbf{k}$ and be placed at $(0, 0, \pm h)$, then Kelvin's solution shows that in the absence of cracks,

$$\sigma_{zz}(r, \theta, 0) = \frac{Ph}{4\pi} \left[\frac{2}{R^3} + \frac{1}{1-\nu} \frac{[3h^2 - R^2]}{R^5} \right]$$

$$\sigma_{rz}(r, \theta, 0) = \sigma_{\theta z}(r, \theta, 0) = 0$$

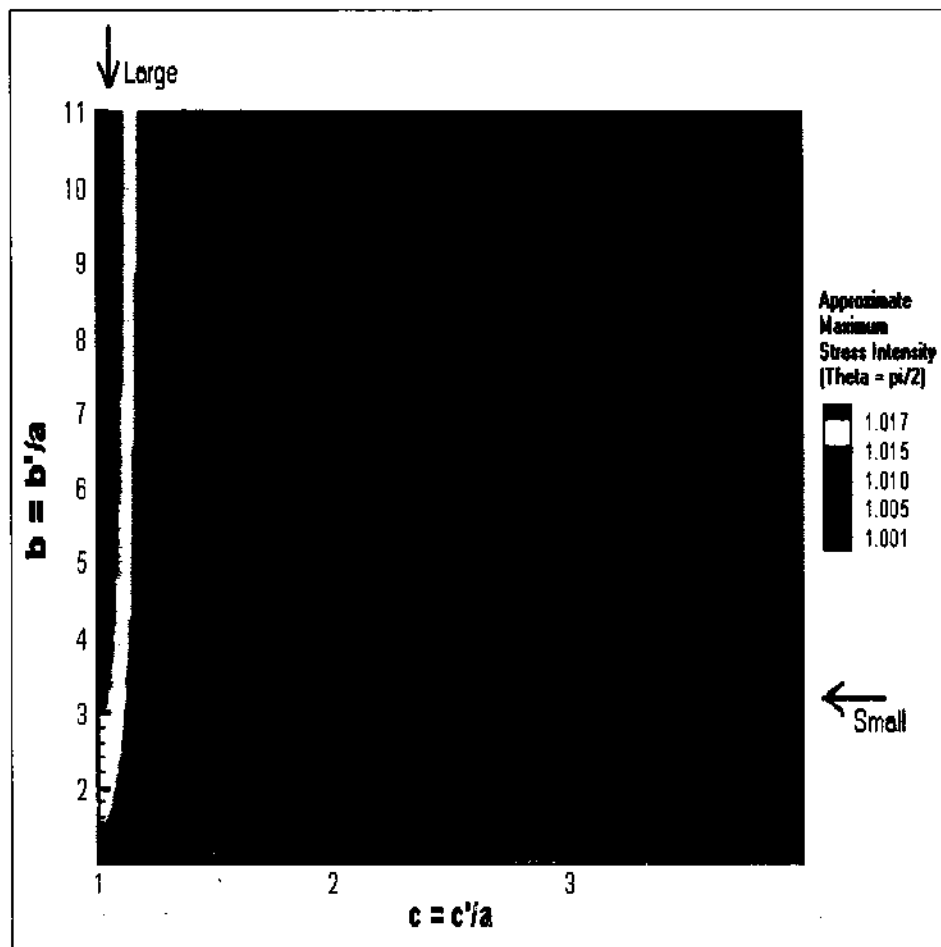


FIG. 20. Coplanar penny shaped cracks of radius a , centered at $(\pm c', 0, 0)$ and opened by a bending force about the line $y = b'$. Contour plot show how the scaled maximum stress intensity factor varies with $c = c'/a$ and $b = b'/a$.

where

$$R = \sqrt{x^2 + y^2 + h^2} = \sqrt{r^2 + 2rc \cos \theta + c^2 + h^2}$$

and

$$x = r \cos \theta + c = a(r \cos \theta + c), y = r \sin \theta = ar \sin \theta$$

therefore by the principle of superposition, our problem is equivalent to the pressurized penny shaped problem with load

$$\sigma_{zz}(\dot{r}, \theta, 0^\pm) = -\frac{P\dot{h}}{2\pi R^3} - \frac{1}{1-\nu} \frac{P\dot{h} [3\dot{h} - R^2]}{R^5} \quad (\text{X.122})$$

$$= -P_1(\dot{r}, \theta) - \frac{1}{1-\nu} P_2(\dot{r}, \theta) \quad (\text{X.123})$$

in which P_1 and P_2 are both even.

The crack opening displacement is then given by

$$\Delta u_z = -\frac{1-\nu}{\mu} w(\dot{r}, \vartheta) = -\frac{1-\nu}{\mu} \left[w_1(\dot{r}, \vartheta) + \frac{1}{1-\nu} w_2(\dot{r}, \vartheta) \right] \quad (\text{X.124})$$

where the $w_k(\dot{r}, \vartheta)$, for $k = 1, 2$, can be obtained from the relationship

$$f_k(\rho, \theta) = \frac{4\pi a}{P\sqrt{1-\rho^2}} w_k(a\rho, \vartheta), \text{ for } k = 1, 2 \quad (\text{X.125})$$

the $f_k(\rho, \vartheta)$ being solutions of

$$\{-\Delta_2 \mathbb{B}^1 + \mathbb{K}_+^1\} [f_k(\rho, \vartheta)](r, \theta) = p_k(r, \theta), \text{ for } 0 \leq r \leq 1, -\pi < \theta \leq \pi, k = 1, 2 \quad (\text{X.126})$$

where $\dot{r} = ar$, $\dot{\rho} = a\rho$, $\dot{h} = ah$, $\dot{c} = ac$ and

$$p_k(r, \theta) = \frac{4\pi a^2}{P} P_k(ra, \theta) = \begin{cases} \frac{2h}{R_1^3}, & k = 1 \\ \frac{h(3h^2 - R_1^2)}{R_1^5}, & k = 2 \end{cases}$$

with $R_1 = \sqrt{r^2 + 2cr \cos \theta + c^2 + h^2}$

The stress intensity factor for this problem will be in the form

$$k_1 = k_1^{(1)} + \frac{1}{1-\nu} k_1^{(2)} \quad (\text{X.127})$$

where

$$k_1^{(k)} = -\frac{1}{2} \lim_{\dot{r} \rightarrow a^-} \frac{w_k(\dot{r}, \vartheta)}{\sqrt{2(a-\dot{r})}} = \frac{-P}{8\pi a^{\frac{3}{2}}} f_k(1, \theta) \quad (\text{X.128})$$

If we again scale with (X.65)

$$k_0 = \frac{P}{\pi^2 a^{\frac{3}{2}}}$$

we will obtain

$$\frac{k_1^{(k)}}{k_0} = -\frac{\pi}{8} f_k(1, \theta) \quad (\text{X.129})$$

or

$$\frac{k_1}{k_0} = -\frac{\pi}{8} \left[f_1(1, \theta) + \frac{1}{1-\nu} f_2(1, \theta) \right] \quad (\text{X.130})$$

The stress intensity factor will depend on the four parameters; ν , c , h and θ . In the figures that follow we will set ν ($\nu = 0.4$) and vary the other parameters. Firstly, in Figure 21 we look at $\frac{k_1}{k_0}$ plotted against θ , we set $h = 0.5$ and look at a few different values of c . In Figures 22 and 23 we set $c = 1.5$ and this time look at different values of h . In Figure 24 we look at the maximum stress intensity factor (set $\theta = \pi$) plotted against h for some different values of c , while in Figure 25 we see a contour plot where h is plotted against c with maximum stress intensity the contour variable.

The c value represents not just the distance between the cracks but the distance the cracks are from the axis upon which the point forces lie. Figure 21 illustrates that as c gets larger the stress intensity drops towards zero particularly on the side of the crack furthest from both the other crack and the point forces. Large values of the stress intensity factor occur almost entirely in the area around the maximum.

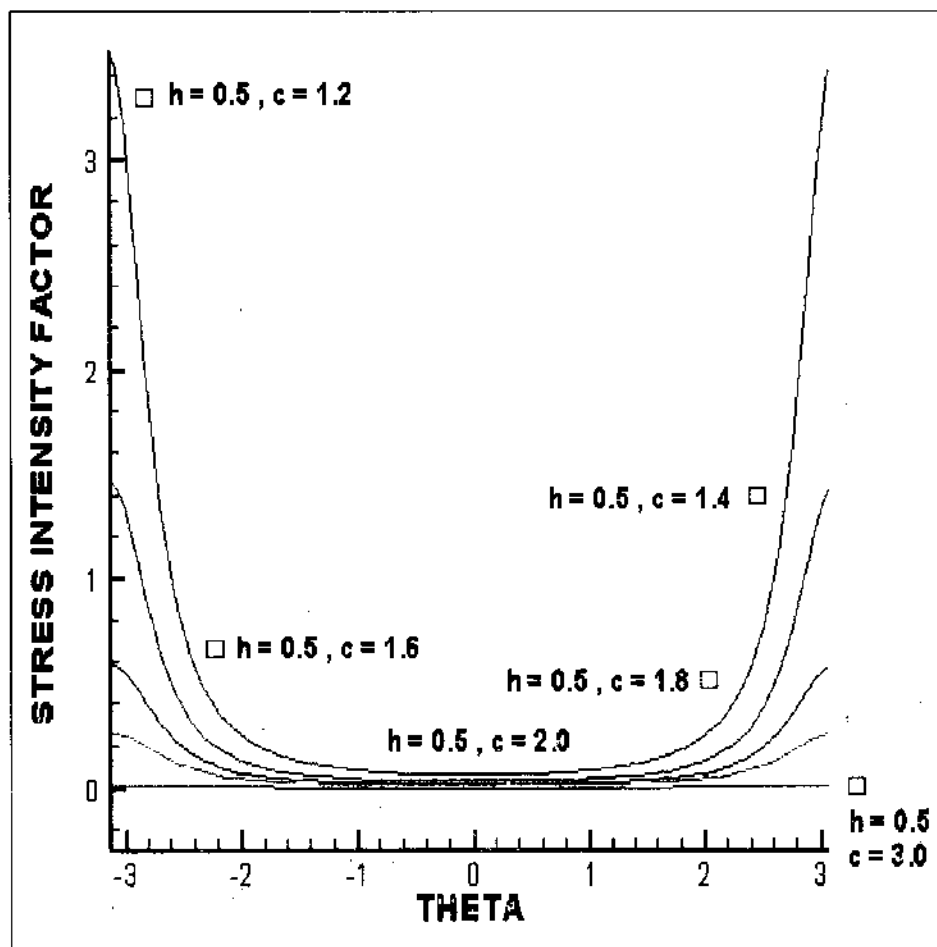


FIG. 21. Coplanar penny shaped cracks of radius a , centered at $(\pm c', 0, 0)$ and opened by point forces $\pm P\mathbf{k}$ at $(0, 0, \pm h')$. Plots show how the scaled stress intensity factor varies with θ for several values of $c = c'/a$ and $h = h'/a = 0.5$ when $\nu = 0.4$.

In Figure 22 we show that for small values of h , increasing h increases the stress intensity, while Figure 23 illustrates that when h gets large enough the stress intensity starts decreasing again. This phenomenon is the same as was discussed in reference to Figures 11 and 12.

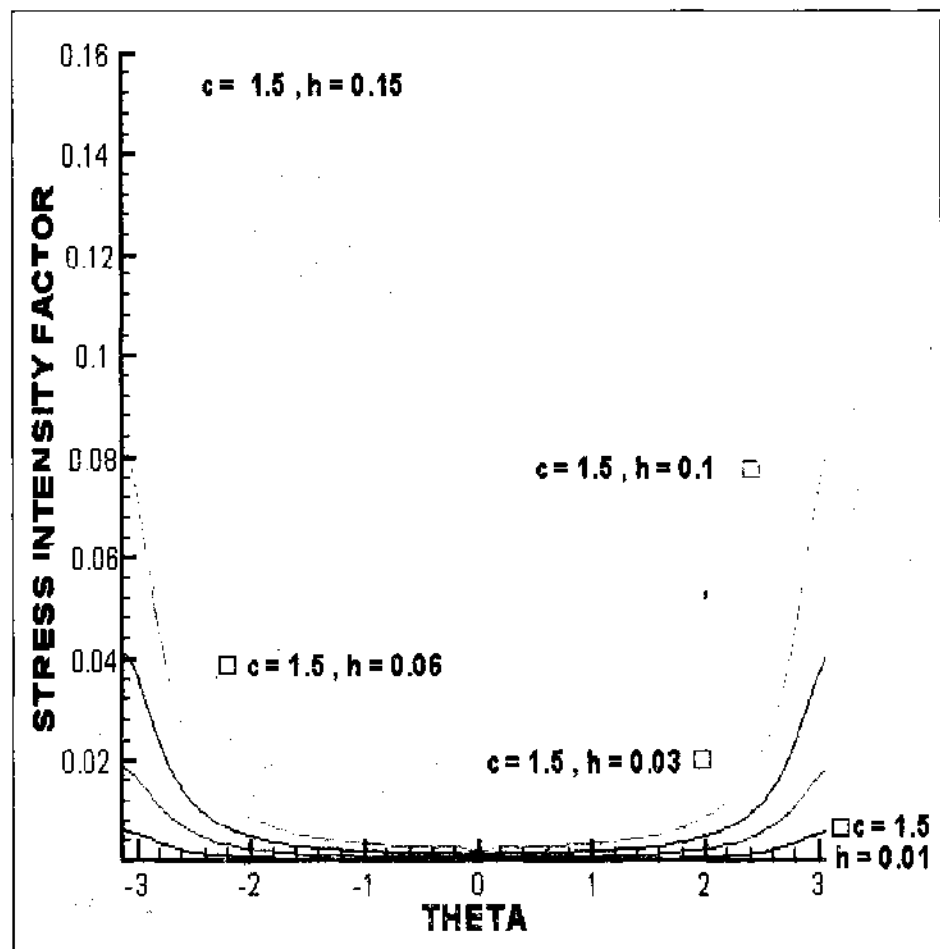


FIG. 22. Coplanar penny shaped cracks of radius a , centered at $(\pm c', 0, 0)$ and opened by point forces $\pm Pk$ at $(0, 0, \pm h')$. Plots show how the scaled stress intensity factor varies with θ for several small values of $h = h'/a$ and $c = c'/a = 1.5$ when $\nu = 0.4$.

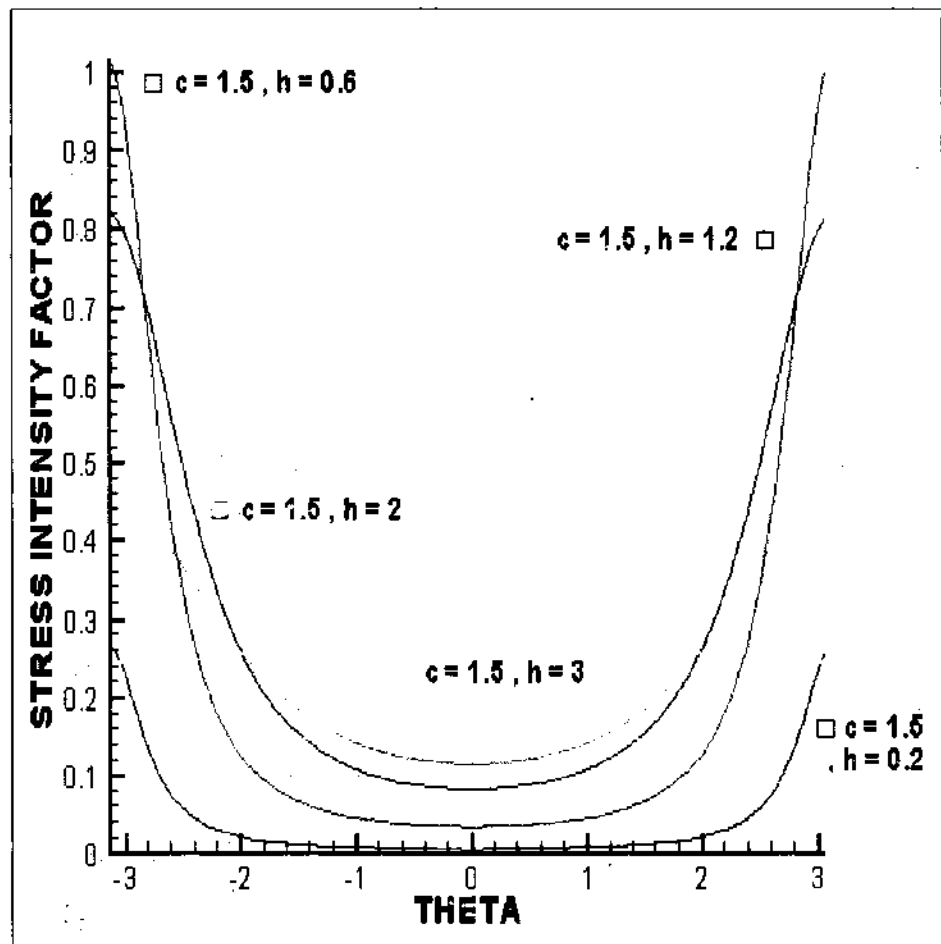


FIG. 23. Coplanar penny shaped cracks of radius a , centered at $(\pm c', 0, 0)$ and opened by point forces $\pm Pk$ at $(0, 0, \pm h')$. Plots show how the scaled stress intensity factor varies with θ for several medium to large values of $h = h'/a$ and $c = c'/a = 1.5$ when $\nu = 0.4$.

In Figure 24 we illustrate for different c values how the maximum stress changes as h increases. When h is zero we get the stress to be zero but as h increases the stress grows, the growth being both more rapid and greater when c is smaller, then rapidly dying away towards zero. Figure 25 shows a contour plot which illustrates the effect of varying both c and h .

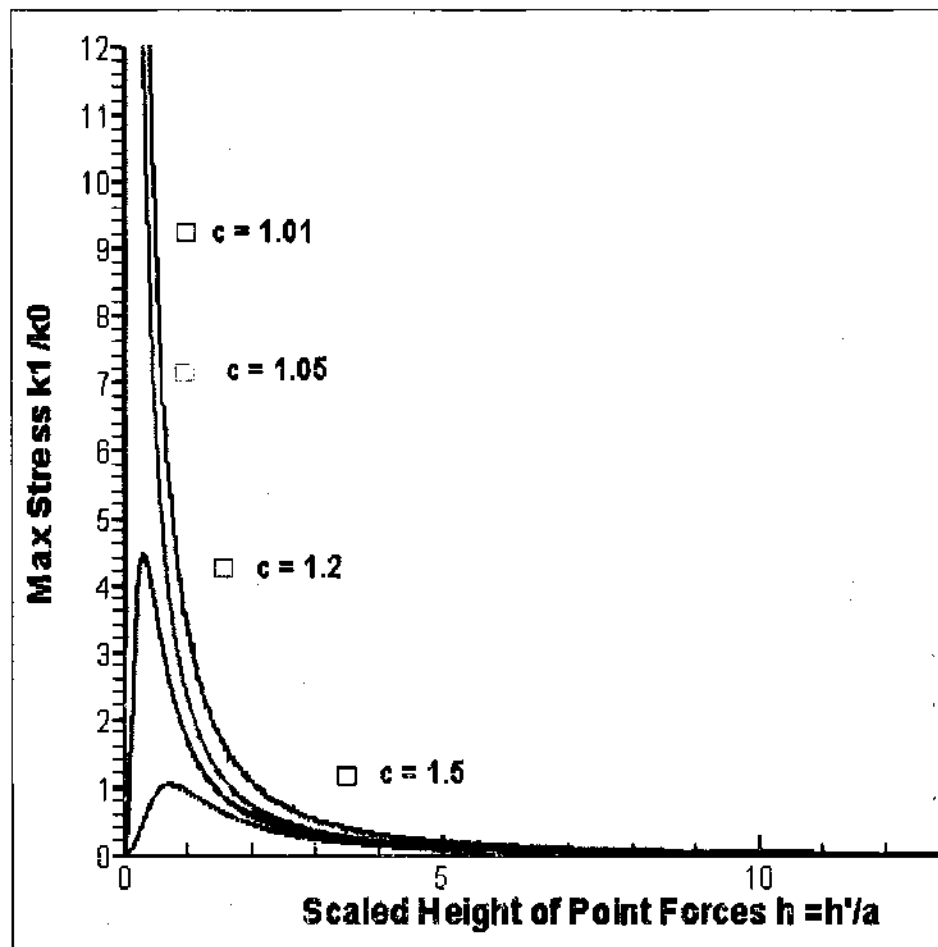


FIG. 24. Coplanar penny shaped cracks of radius a , centered at $(\pm c', 0, 0)$ and opened by point forces $\pm Pk$ at $(0, 0, \pm h')$. Plots show how the scaled maximum stress intensity factor varies with $h = h'/a$ for several values of $c = c'/a$ when $\nu = 0.4$.

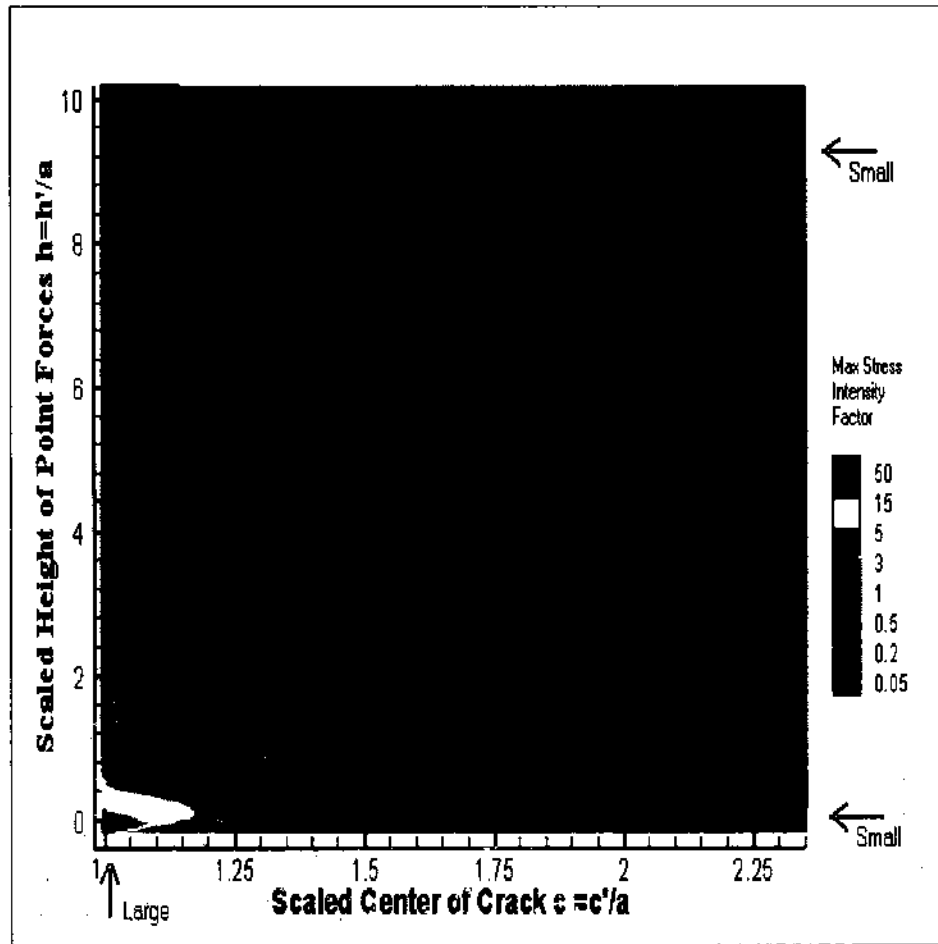


FIG. 25. Coplanar penny shaped cracks of radius a , centered at $(\pm c', 0, 0)$ and opened by point forces $\pm P\mathbf{k}$ at $(0, 0, \pm h')$. Contour plot shows how the scaled maximum stress intensity factor varies with $h = h'/a$ and $c = c'/a$ when $\nu = 0.4$.

Case 3b: Loading Above and Below the Center of Each Disc In this case we will have two equal and opposite point forces above and below the center of each crack surface. Let the point forces $\pm P\mathbf{k}$ be placed at $(-c', 0, \pm h')$ and $(c', 0, \pm h')$, then in the absence of cracks, Kelvin's solution shows that

$$\begin{aligned}\sigma_{zz}(r, \theta, 0) &= \frac{P\dot{h}}{4\pi} \left[\frac{2}{R_1^3} + \frac{2}{R_2^3} + \frac{1}{1-\nu} \left\{ \frac{[3\dot{h}^2 - R_1^2]}{R_1^5} + \frac{[3\dot{h}^2 - R_2^2]}{R_2^5} \right\} \right] \\ \sigma_{\theta z}(r, \theta, 0) &= \sigma_{rz}(r, \theta, 0) = 0\end{aligned}\quad (\text{X.131})$$

where

$$R_1 = \sqrt{(x - \dot{c})^2 + y^2 + \dot{h}^2} = \sqrt{r^2 + \dot{h}^2}, \quad (\text{X.132})$$

$$R_2 = \sqrt{(x + \hat{c})^2 + y^2 + \hat{h}^2} = \sqrt{r^2 + 4r\hat{c}\cos\theta + 4\hat{c}^2 + \hat{h}^2} \quad (\text{X.133})$$

and

$$x = \hat{r}\cos\theta + \hat{c} = a(r\cos\theta + c), y = \hat{r}\sin\theta = ar\sin\theta$$

by the principle of superposition, our problem is equivalent to the pressurized penny shaped problem with load

$$\begin{aligned} \sigma_{zz}(\hat{r}, \theta, 0^\pm) &= -P_1(\hat{r}, \theta) - \frac{1}{1-\nu}P_2(\hat{r}, \theta) \end{aligned} \quad (\text{X.134})$$

$$= -\frac{P\hat{h}}{2\pi} \left(\frac{1}{R_1^3} + \frac{1}{R_2^3} \right) - \frac{P\hat{h}}{1-\nu} \left\{ \frac{[3\hat{h} - R_1^2]}{R_1^5} + \frac{[3\hat{h} - R_2^2]}{R_2^5} \right\} \quad (\text{X.135})$$

in which P_1 and P_2 are both even.

The crack opening displacement is then given by

$$\Delta u_z = -\frac{1-\nu}{\mu}w(\hat{r}, \vartheta) = -\frac{1-\nu}{\mu} \left[w_1(\hat{r}, \vartheta) + \frac{1}{1-\nu}w_2(\hat{r}, \vartheta) \right] \quad (\text{X.136})$$

where the $w_k(\hat{r}, \vartheta)$, for $k = 1, 2$, are obtained from the equations

$$\{-\Delta_2\mathbb{B}^1 + \mathbb{K}_+^1\} [f_k(\rho, \vartheta)](r, \theta) = p_k(r, \theta), \text{ for } 0 \leq r \leq 1, -\pi < \theta \leq \pi, k = 1, 2 \quad (\text{X.137})$$

in which $\hat{r} = ar$, $\hat{\rho} = a\rho$, $\hat{h} = ah$, $\hat{c} = ac$

$$w_k(a\rho, \vartheta) = \frac{P}{4\pi a} \sqrt{1 - \rho^2} f_k(\rho, \theta), \text{ for } k = 1, 2 \quad (\text{X.138})$$

and

$$p_k(r, \theta) = \frac{4\pi a^2}{P} P_k(ra, \theta) = \begin{cases} 2h \left(\frac{1}{R_1^3} + \frac{1}{R_2^3} \right), & k = 1 \\ h \left\{ \frac{[3\hat{h} - R_1^2]}{R_1^5} + \frac{[3\hat{h} - R_2^2]}{R_2^5} \right\}, & k = 2 \end{cases} \quad (\text{X.139})$$

where $R_1 = \sqrt{r^2 + \hat{h}^2}$, $R_2 = \sqrt{r^2 + 4cr\cos\theta + 4c^2 + \hat{h}^2}$

This time we scale with respect to the stress intensity factor for a plane circular

crack acted on by equal and opposite axisymmetric point forces (see (X.67))

$$k_0 = \frac{P}{\pi^2 a^{\frac{3}{2}}} \left(\frac{1}{1+h^2} + \frac{1}{1-\nu} \frac{h^2}{(1+h^2)^2} \right) \quad (\text{X.140})$$

then since

$$k_1 = k_1^{(1)} + \frac{1}{1-\nu} k_1^{(1)} \quad (\text{X.141})$$

where

$$k_1^{(k)} = -\frac{1}{2} \lim_{r \rightarrow a^-} \frac{w_k(r, \vartheta)}{\sqrt{2(a-r)}} = \frac{-P}{8\pi a^{\frac{3}{2}}} f_k(1, \theta) \quad (\text{X.142})$$

we have

$$\frac{k_1}{k_0} = -\frac{\pi}{8} [(1-\nu) f_1(1, \theta) + f_2(1, \theta)] \frac{(1+h^2)^2}{[(1-\nu)(1+h^2) + h^2]} \quad (\text{X.143})$$

We finish the chapter by presenting some figures that illustrate a number of results for the case in which ν is again fixed at 0.4. Firstly we fix h and look at the stress intensity factor for various distances between the cracks as in Figure 26. We can clearly see that as c increases the effect of the second crack on the stresses decreases towards *zero* and when the cracks are close the stress increases drastically at the points closest to the other crack.

In Figure 27 we fix c and vary the heights of the point loads. We can see that as h increases the effect of the second crack increases as the loads focus on the area between the two cracks. The reader should remember that we are scaling with the result from a single crack so that although the actual stress will decrease as we increase h enough, it will decrease much slower when there are *two* cracks close together so that the scaled intensity will continue to increase as we increase h . This phenomenon is again illustrated when we examine the maximum stress intensity in Figures 28 and 29 as is the decrease in the effects of the second crack as they move apart.

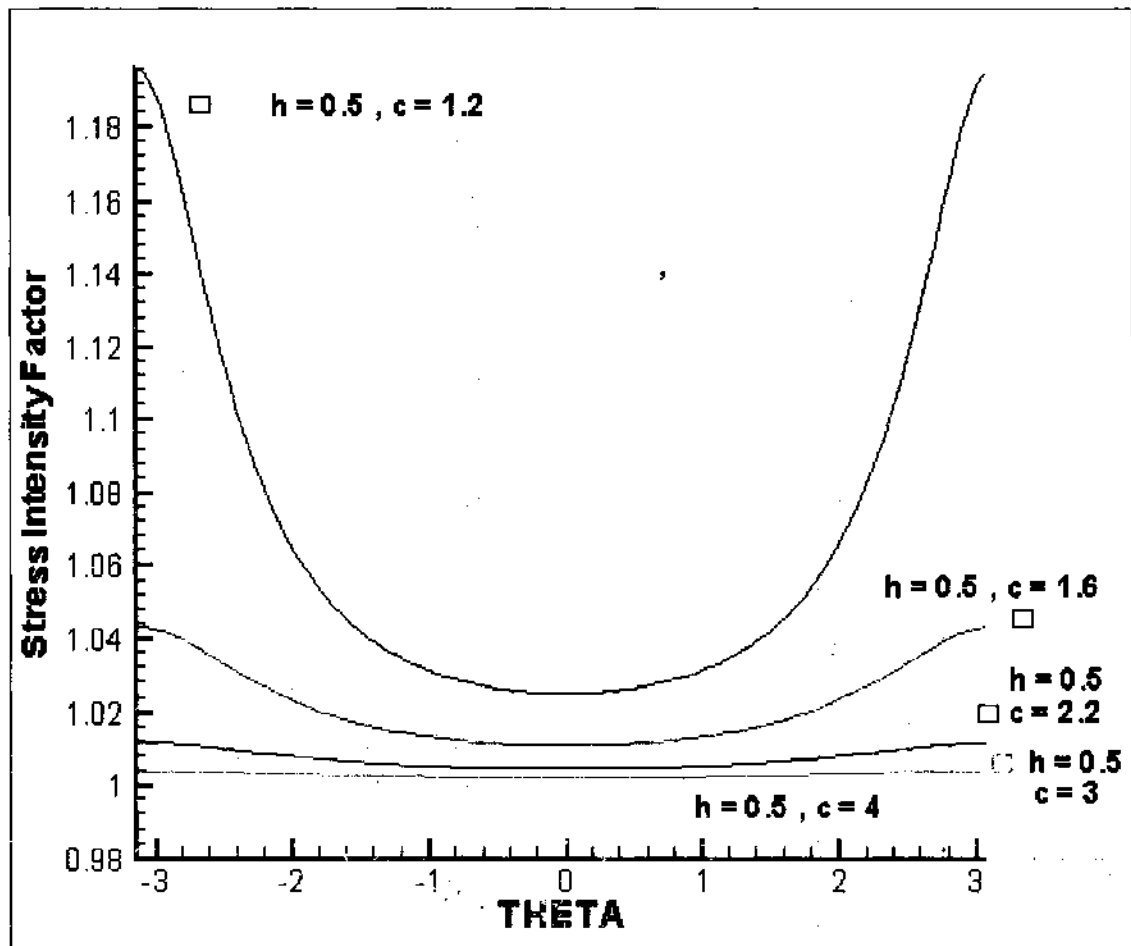


FIG. 26. Coplanar penny shaped cracks of radius a , centered at $(\pm c', 0, 0)$ and opened by point forces $\pm Pk$ centered above and below the cracks at $(\pm c', 0, \pm h')$. Plots show how the scaled stress intensity factor varies with θ for $h = h'/a = 0.5$, $\nu = 0.4$ and several values of $c = c'/a$.

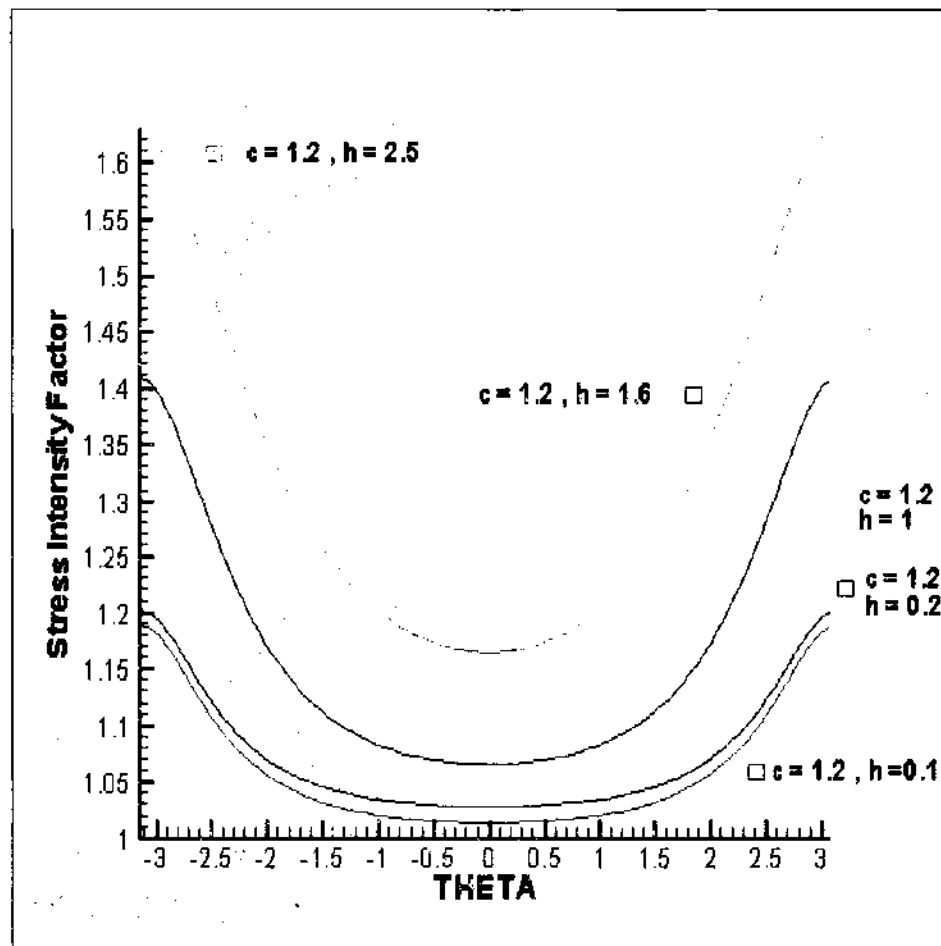


FIG. 27. Coplanar penny shaped cracks of radius a , centered at $(\pm c', 0, 0)$ and opened by point forces $\pm Pk$ centered above and below the cracks at $(\pm c', 0, \pm h')$. Plots show how the scaled stress intensity factor varies with θ for $c = c'/a = 1.2$, $\nu = 0.4$ and several values of $h = h'/a$.

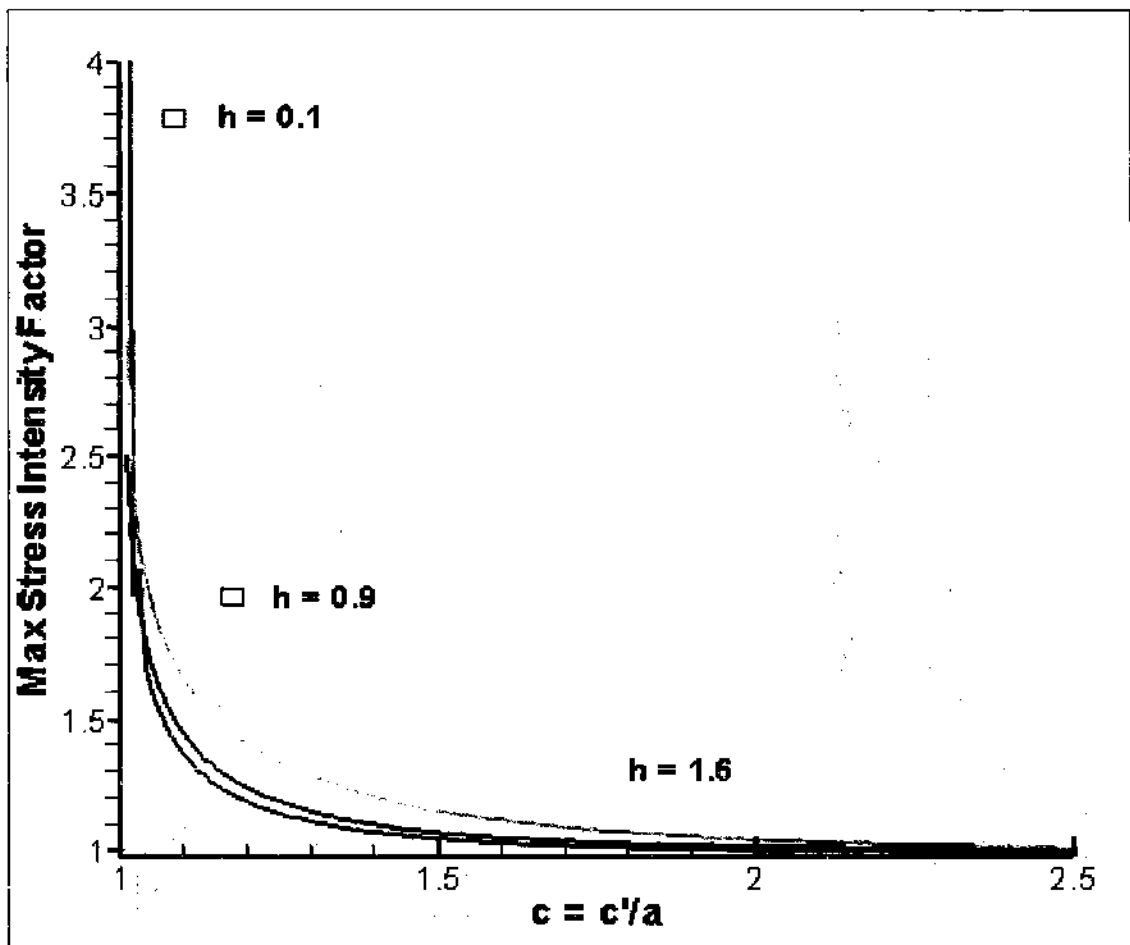


FIG. 28. Coplanar penny shaped cracks of radius a , centered at $(\pm c', 0, 0)$ and opened by point forces $\pm P\mathbf{k}$ centered above and below the cracks at $(\pm c', 0, \pm h')$. Plots show how the scaled maximum stress intensity factor (for $\nu = 0.4$) varies with $h = h'/a$ for several values of $c = c'/a$.

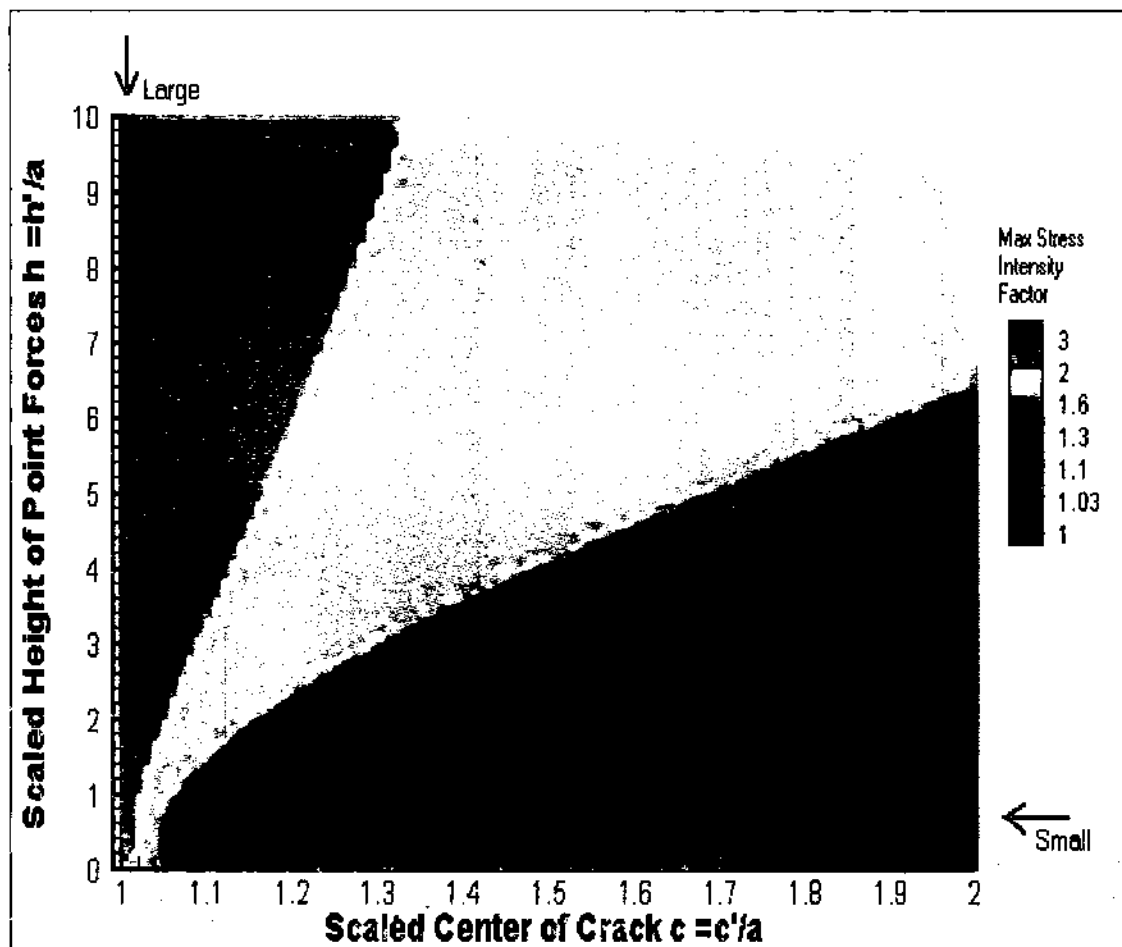


FIG. 29. Coplanar penny shaped cracks of radius a , centered at $(\pm c', 0, 0)$ and opened by point forces $\pm P\mathbf{k}$ centered above and below the cracks at $(\pm c', 0, \pm h')$. Contour plot show how the scaled maximum stress intensity factor (for $\nu = 0.4$) varies with both $h = h'/a$ and $c = c'/a$.

CHAPTER XI

SUMMARY AND FUTURE WORK

In this chapter we do a brief summary of those achievements documented earlier in the thesis. That is followed by a discussion on some possible future developments and related applications of the work.

XI.1 SUMMARY

The work documented herein draws upon a variety of ideas from both classical and contemporary mathematics and is motivated by the desire to understand and solve the singular integral equations of potential theory. While the intent was to produce tools and techniques for the solution of physical problems, we believe that much of the analysis presented is worthy of investigation in its own right. It is hoped that the Hilbert spaces and operators introduced will be of interest to others and that the numerical procedures developed will prove useful to many.

For both classes of boundary integral equations considered, numerical schemes were developed using both collocation and Galerkin methods. The Convergence of the Galerkin methods was proven analytically while the convergence of the collocation methods was verified experimentally. Since the Galerkin methods are computationally expensive particularly when double or quadruple numerical integration is involved, it was correctly anticipated that collocation would be the faster method. No analytical analysis of convergence rates was undertaken but experimentally it would appear that collocation methods converge as quickly if not quicker than the Galerkin for the chosen collocation points. Convergence rates are an aspect to be considered for future analysis and were not considered vital for this thesis.

Once we had established the numerical methods for each type of problem we were then able to apply the techniques to solve problems in both Potential Theory and Fracture Mechanics. Our problems were restricted to those involving single or multiple circular domains. First of all we examined charged circular discs placed in various electrical fields, problems that could be solved via weakly singular integral equations. The methods were first applied to simple problems with a previously

known solution. Comparison with known solutions allowed us to illustrate the effectiveness, efficiency and accuracy of the technique. We then tackled some more difficult, previously unsolved problems to illustrate further capabilities for our methods. Some problems involving penny shaped cracks in an elastic medium subject to various external loads, were examined next. These type of problems can be solved via our class of hyper-singular integral equations. We showed how problems can be solved for multiple circular domains and how symmetries can be exploited to apply our methods efficiently. We were able to show how the special functions, Hilbert space theory and the algorithms we had developed could be applied in a practical sense.

There is plenty of scope for future development of this present work and for expanding the range of future applications. Some of these ideas for future development will be discussed in the next section.

XI.2 EXTENSION OF LAPLACIAN BASED BOUNDARY VALUE PROBLEMS

The most obvious restriction we have placed on all the problems we have examined is that we have only looked at circular domains. Some preliminary work on conformal mappings has indicated that Boussinesq's Equation on a circular domain can be conformally mapped onto other domains. Using conformal mappings we could then look at a much broader range of problems with the ultimate goal being to use numerical conformal mappings to map problems on any type of domain into the unit circle (or some other domain with previously discovered solution algorithm), solve the Integral Equations using our techniques and then map back into the original domain to get the final solution. This is a broad area with much potential and in what follows we illustrate the effect general mappings have on the Boussinesq Equation and provide a basic illustrative example to show how to apply the theory to a real problem.

XI.2.1 Conformal Mapping of Boussinesq's Equation

If we consider the following arbitrary Boussinesq Equation

$$\iint_D \frac{\phi(\xi, \eta) d\xi d\eta}{\sqrt{(x - \xi)^2 + (y - \eta)^2}} = g(x, y), (x, y) \in D \quad (\text{XI.1})$$

and take the conformal mapping

$$p: D \rightarrow \Omega \quad (\text{XI.2})$$

with inverse

$$q: \Omega \rightarrow D$$

such that

$$\begin{aligned} w &= p(z) = u(x, y) + iv(x, y), z = q(w) = x(u, v) + iy(u, v) \\ \tau &= p(\zeta) = s(\xi, \eta) + it(\xi, \eta), \zeta = q(\tau) = \xi(s, t) + i\eta(s, t) \end{aligned} \quad (\text{XI.3})$$

then

$$\frac{\partial(\xi, \eta)}{\partial(s, t)} = \left| \frac{d\zeta}{d\tau} \right|^2 = |q'(\tau)|^2 \quad (\text{XI.4})$$

and

$$\frac{1}{\sqrt{(x-\xi)^2 + (y-\eta)^2}} = \frac{1}{|z-\zeta|} = \left| \frac{w-\tau}{q(w)-q(\tau)} \right| \frac{1}{\sqrt{(u-s)^2 + (v-t)^2}} \quad (\text{XI.5})$$

The Integral Equation (XI.1) thus becomes

$$\int \int_{\Omega} \frac{\phi[\xi(s, t), \eta(s, t)] \left| \frac{w-\tau}{q(w)-q(\tau)} \right| |q'(\tau)|^2}{\sqrt{(u-s)^2 + (v-t)^2}} ds dt = g[x(u, v), y(u, v)], (u, v) \in \Omega \quad (\text{XI.6})$$

Since we can expand $q(w)$ in a Taylor Series about τ as follows

$$q(w) = q(\tau) + q'(\tau)(w-\tau) + \epsilon(w-\tau) \quad (\text{XI.7})$$

where $\epsilon \rightarrow 0$ as $|w-\tau| \rightarrow 0$, we can hence write that

$$\left| \frac{w-\tau}{q(w)-q(\tau)} \right| |q'(\tau)| = \left| \frac{q'(\tau)}{q'(\tau) + \epsilon} \right| \quad (\text{XI.8})$$

$$= [1 + |w-\tau| K(w, \tau)] \quad (\text{XI.9})$$

for some $K(w, \tau)$ non-singular at $w = \tau$.

The integral equation (XI.6) can then be written in the form

$$\int \int_{\Omega} \left\{ \frac{1}{\sqrt{(u-s)^2 + (v-t)^2}} + K(u, v; s, t) \right\} \Phi(s, t) ds dt = G(u, v), (u, v) \in \Omega \quad (\text{XI.10})$$

where

$$\Phi(s, t) = |q'(\tau)| \sigma[\xi(s, t), \eta(s, t)] \quad (\text{XI.11})$$

$$G(u, v) = g[x(u, v), y(u, v)] \quad (\text{XI.12})$$

The behavior of K will predominantly depend on $q'(\tau)$ which for sufficiently smooth mappings should be non-singular giving us the desired type of integral equation.

The Bilinear Mapping

If we look at the special case where $p(z)$ is the bilinear mapping

$$p(z) = \frac{az + b}{cz + d}, ad - bc \neq 0 \quad (\text{XI.13})$$

then

$$\left| \frac{w - \tau}{q(w) - q(\tau)} \right| |q'(\tau)|^2 = \frac{|ad - bc| |cw - d|}{|c\tau - d|} \quad (\text{XI.14})$$

and we get the following integral equation

$$\int \int_{\Omega} \frac{1}{\sqrt{(u-s)^2 + (v-t)^2}} \Phi(s, t) ds dt = G(u, v), (u, v) \in \Omega \quad (\text{XI.15})$$

where

$$\Phi(s, t) = \frac{|ad - bc|}{|cs - d + ict|} \sigma[\xi(s, t), \eta(s, t)] \quad (\text{XI.16})$$

$$G(u, v) = \frac{g[x(u, v), y(u, v)]}{|cu - d + icv|} \quad (\text{XI.17})$$

It is now clear that the weakly singular equation of interest is structurally invariant under a wide class of conformal mappings opening up the possibility that

equations with general domains can be mapped to equations with circular domains. Moreover, since

$$\nabla^2 \phi [p(z)] = |p'(z)|^2 \nabla^2 \phi [w] \quad (\text{XI.18})$$

it is clear that the hyper-singular equation exhibits a similar structural invariance.

We now provide a basic illustrative example to show how this theory can be applied in a practical sense.

Example: Boussinesq's Equation on the Exterior of the Unit Disk If we consider the Dirichlet Problem from Chapter II on the outside of the unit disc

$$S = \{(r, \theta, 0) : 1 \leq r < \infty, -\pi < \theta \leq \pi\} \quad (\text{XI.19})$$

with boundary condition (II.39) given by

$$V(r, \theta, 0) = g(r, \theta), \text{ for } (r, \theta, 0) \in S \quad (\text{XI.20})$$

then V will be given by the single layer potential

$$V(r, \theta, z) = \int_1^\infty \int_{-\pi}^\pi \frac{\sigma(\rho, \vartheta) \rho d\rho d\vartheta}{\sqrt{r^2 + \rho^2 - 2r\rho \cos(\theta - \vartheta) + z^2}} \quad (\text{XI.21})$$

provided the density function $\sigma(\rho, \vartheta)$ satisfies the boundary integral equation

$$\int_1^\infty \int_{-\pi}^\pi \frac{\sigma(\rho, \vartheta) \rho d\rho d\vartheta}{\sqrt{r^2 + \rho^2 - 2r\rho \cos(\theta - \vartheta)}} = g(r, \theta), \text{ for } (r, \theta, 0) \in S \quad (\text{XI.22})$$

If we consider the Boussinesq like operator

$$\mathbb{F}[f(\rho, \vartheta)](r, \theta) = \int_1^\infty \int_{-\pi}^\pi \frac{f(\rho, \vartheta) \varpi(\rho)}{\sqrt{r^2 + \rho^2 - 2r\rho \cos(\theta - \vartheta)}} d\rho d\vartheta \quad (\text{XI.23})$$

where $1 \leq r < \infty, -\pi \leq \theta \leq \pi$ and the weight function $\varpi(\rho)$ is given as follows

$$\varpi(\rho) = \frac{1}{\sqrt{\rho^2 - 1}} \quad (\text{XI.24})$$

we can show using the simple self-inverting conformal mapping $z = \frac{1}{w}$ (which maps the unit circle inside to out) that it has eigenvectors

$$\varepsilon_{mn}^0(\rho, \vartheta) = \frac{1}{\rho} e_{mn}^0\left(\frac{1}{\rho}, \vartheta\right) \quad (\text{XI.25})$$

corresponding to the eigenvalues $\frac{1}{\lambda_{mn}}$ as stated in the following theorem.

Theorem XI.1

$$\lambda_{|m|n} \mathbb{F}[\varepsilon_{mn}^0(\rho, \vartheta)](r, \theta) = \varepsilon_{mn}^0(\rho, \vartheta), \quad m = 0, \pm 1, \pm 2, \dots, n = 0, 1, 2, \dots \quad (\text{XI.26})$$

Proof. Consider the map $r = \frac{1}{\rho}$ applied to

$$\begin{aligned} \mathbb{F}[\varepsilon_{mn}^0(\rho_0, \vartheta_0)](\rho, \vartheta) &= \int_1^\infty \int_{-\pi}^\pi \frac{\frac{1}{\rho_0} e_{mn}^0\left(\frac{1}{\rho_0}, \vartheta_0\right) \frac{1}{\sqrt{\rho_0^2 - 1}}}{\sqrt{\rho^2 + \rho_0^2 - 2\rho\rho_0 \cos(\vartheta_0 - \vartheta)}} d\rho_0 d\vartheta_0 \\ &= \int_1^0 \int_\pi^{-\pi} \frac{r_0 e_{mn}^0(r_0, \theta_0) \frac{r_0}{\sqrt{1-r_0^2}}}{\frac{1}{rr_0} \sqrt{r^2 + r_0^2 - 2rr_0 \cos(\theta - \theta_0)}} \left(\frac{-1}{r_0^2} dr_0\right) (-d\theta_0) \\ &= r \int_0^1 \int_{-\pi}^\pi \frac{e_{mn}^0(r_0, \theta_0) \frac{r_0}{\sqrt{1-r_0^2}}}{\sqrt{r^2 + r_0^2 - 2rr_0 \cos(\theta - \theta_0)}} dr_0 d\theta_0 \\ &= \frac{r}{\lambda_{|m|n}} e_{mn}^0(r, \vartheta), \quad \text{by (VI.21)} \\ &= \frac{1}{\lambda_{|m|n}} \frac{1}{\rho} e_{mn}^0\left(\frac{1}{\rho}, \vartheta\right) \\ &= \frac{1}{\lambda_{|m|n}} \varepsilon_{mn}^0(\rho, \vartheta) \quad \blacksquare \end{aligned}$$

We can therefore solve (XI.22) by expanding as follows

$$\sigma(\rho, \vartheta) \rho \sqrt{\rho^2 - 1} = f(\rho, \vartheta) = \sum_{m=-\infty}^{\infty} \sum_{n=0}^{\infty} f_{mn} \varepsilon_{mn}^0(\rho, \vartheta) \quad (\text{XI.27})$$

and

$$g(r, \theta) = \sum_{m=-\infty}^{\infty} \sum_{n=0}^{\infty} g_{mn} \varepsilon_{mn}^0(r, \theta) \quad (\text{XI.28})$$

to obtain the solution

$$\sigma(\rho, \vartheta) = \frac{1}{\rho\sqrt{\rho^2-1}} \sum_{m=-\infty}^{\infty} \sum_{n=0}^{\infty} \frac{g_{mn}}{\lambda_{|m|n}} \varepsilon_{mn}^0(\rho, \vartheta) \quad (\text{XI.29})$$

We have hence illustrated in this simple example how the use of conformal mappings could lead to solving a much greater range of problems.

XI.3 EXTENSIONS TO THE HELMHOLTZ EQUATION AND ACOUSTICS

Throughout this dissertation we have looked at the Integral Equations resulting from Laplace's Equation on a circular domain. The natural extension is to consider the Helmholtz Equation

$$(\nabla^2 + k^2) \Phi = 0 \quad (\text{XI.30})$$

which admits the free space Green's function

$$G(\vec{r}, \vec{\rho}) = \frac{e^{ik|\vec{r}-\vec{\rho}|}}{4\pi|\vec{r}-\vec{\rho}|} \quad (\text{XI.31})$$

and reduces to Laplace's Equation when $k = 0$.

Without going into any details when we replace Laplace's Equation in our work with the Helmholtz Equation, we can ultimately produce the weakly singular equations

$$\frac{1}{4\pi} \int \int_{\Omega} \left[\frac{e^{ik|\vec{r}-\vec{\rho}|}}{4\pi|\vec{r}-\vec{\rho}|} + K(\vec{r}, \vec{\rho}) \right] f(\vec{\rho}) d\vec{\rho} = g(\vec{r}), \text{ for } \vec{r} \in \Omega \quad (\text{XI.32})$$

and the hyper-singular integral equations

$$(\nabla^2 + k^2) \frac{1}{4\pi} \int \int_{\Omega} \left[\frac{e^{ik|\vec{r}-\vec{\rho}|}}{4\pi|\vec{r}-\vec{\rho}|} + K(\vec{r}, \vec{\rho}) \right] f(\vec{\rho}) d\vec{\rho} = g(\vec{r}), \text{ for } \vec{r} \in \Omega \quad (\text{XI.33})$$

where $K(\vec{r}, \vec{\rho})$ is a non-singular kernel.

It is our belief that with some work similar results can be produced that could

be of great significance in the field of Acoustics. Since,

$$\frac{e^{ik|\vec{r}-\vec{\rho}|}}{4\pi|\vec{r}-\vec{\rho}|} = \frac{1}{4\pi|\vec{r}-\vec{\rho}|} + k(\vec{r}, \vec{\rho}) \quad (\text{XI.34})$$

where

$$k(\vec{r}, \vec{\rho}) = \frac{1 - e^{ik|\vec{r}-\vec{\rho}|}}{4\pi|\vec{r}-\vec{\rho}|} \quad (\text{XI.35})$$

is non-singular the previously discussed methods can be applied to solve these equations. The techniques developed may therefore prove to be useful in fields such as Acoustics and Electromagnetics.

REFERENCES

- [1] E. W. HOBSON, *The Theory of Spherical and Ellipsoidal Harmonics*, Chelsea Publishing Company, New York, 1955.
- [2] I. N. SNEDDON, *Mixed Boundary Value Problems in Potential Theory*, North-Holland Pub. Co, Amsterdam, 1966.
- [3] I. N. SNEDDON AND M. Lowengrub, *Crack Problems in the Classical Theory of Elasticity*, John Wiley & Sons, Inc, New York, 1969.
- [4] G. N. WATSON, *A Treatise on the Theory of Bessel Functions*, Cambridge University Press, Cambridge, 1966.
- [5] M. ABRAMOWITZ AND I. A. STEGAN, *Handbook of Mathematical Functions with Formulas, Graphs, and Mathematical Tables*, Dover Publications, Inc, New York, 1965.
- [6] M. A. JASWON AND G.T. SYMM, *Integral Equations Methods in Potential Theory and Elastostatics*, Academic Pres, New York, 1977.
- [7] O. D. KELLOGG, *Foundations of Potential Theory*, Dover Books, New York, 1953.
- [8] V. I. SMIRNOV, *Integral Equations and Partial Differential Equations: A course in Higher Mathematics*, Vol IV, Pergamon Press, Oxford, 1964.
- [9] R. E. KLEINMAN AND G. F. ROACH, *Boundary Integral Equations for the Three-Dimensional Helmholtz Equation*, SIAM Review, 16, 2 (1974).
- [10] J. R. HIGGINS, *Completeness and Basis Properties of Sets of Special Functions*, Cambridge Univ. Press, Cambridge, 1977.
- [11] E.T. COPSON, *On the problem of the electrified disc*, Proc. Edinburgh. Math. Soc., 8 (1947), pp. 14-19.
- [12] P. F. BYRD AND M. D. FRIEDMAN, *Handbook of Elliptic Integrals for Engineers and Scientists*, Springer-Verlag New York, 1971.
- [13] N. I. AKHIEZER AND I. M. GLAZEMAN, *Theory of Linear Operators in Hilbert Space*, Dover Publications Inc., New York, 1993.

- [14] W. MAGNUS, F. OBERHEITTINGER AND R.P. SONI, *Formulas and Theorems for the Special Functions of Mathematical Physics*, Springer-Verlag, New York Inc., New York, 1966.
- [15] P. R. HALMOS, *A Hilbert Space Problem Book*, D. Van Nostrand Company, Inc., New Jersey, 1967.
- [16] H. HOCHSTADT, *Integral Equations*, Wiley, New York, 1973.
- [17] H. BATEMAN AND A. ERDÉLYI et. al., *Higher Transcendental Functions*, Vol 1, Kreiger, Florida, 1981.
- [18] R. KRESS, *Linear Integral Equations*, Springer-Verlag, Berlin, 1989.
- [19] N. N. LEBEDEV, L. P. SKALSKAYA AND Y. S. UFLYAND, *Worked Problems in Applied Mathematics*, Dover, 1965.
- [20] J. R. BARBER, *Elasticity*, Kluwer Academic Publishers, The Netherlands, 1992.
- [21] P. F. PAPKOVICH, *The Representation of the General Integral of the Fundamental Equations of Elasticity Theory in Terms of Harmonic Functions*, Izv. Akad. Nauk S.S.S.R. Phys-Math. Ser. 10, 1425 (1932).
- [22] H. NEUBER, *Ein neuer Ansatz zur Lösung Räumlicher Probleme der Elastizitätstheorie*, Z. Angew. Math. u. Mech. 14, 203 (1934).
- [23] I. N. SNEDDON AND J. TWEED, *The Stress Intensity factor for a Penny Shaped Crack in an Elastic Body under the Action of Symmetric Body Forces*, International Journal of Fracture Mechanics, 3, 4 (1967).
- [24] H. LIEBOWITZ, Ed., *Fracture: An Advance Treatise Vol II*, Academic Press, New York, 1968.
- [25] B. L. MOISEWITSCH, *Integral Equations*, Longman, London, 1977.
- [26] N. N. LEBEDEV, *Special Functions and their Applications*, Dover, New York, 1972.
- [27] C. D. GREEN, *Integral Equation Methods*, Nelson, New York, 1969.

- [28] A. FRENKEL, *A Chebyshev Expansion of Singular Integral Equations with a Logarithmic Kernel*, Journal of Computational Physics, 51 (1983), pp. 326-334.
- [29] A. FRENKEL, *A Chebyshev Expansion of Singular Integral Equations with a $\partial^2 \ln |s - t| / \partial s \partial t$ Kernel*, Journal of Computational Physics, 51 (1983), pp. 335-342.
- [30] J. FROMME AND M.A. GOLBERG, *Numerical Solutions of a class of Integral Equations Arising in Two-Dimensional Aerodynamics*, Solution Methods for Integral Equations: Theory and Applications, Plenum, New York, 1979.
- [31] M. A. GOLBERG, *The Convergence of Several Algorithms for Solving Integral Equations with Finite-Part Integrals*, Journal of Integral Equations, 5 (1983), pp. 329-340.
- [32] M. A. GOLBERG, *The Convergence of Several Algorithms for Solving Integral Equations with Finite-Part Integrals II*, Applied Math and Comp., 21 (1987), pp. 283-293.
- [33] G. Y. POPOV, *The Contact problem of the Theory of Elasticity for the case of a circular Area of Contact*, Journal of Applied Mathematical Mechanics, 26 (1962), pp. 207-225.
- [34] R. MUKI, *Asymmetric Problems of the Theory of Elasticity for a semi-infinite solid and a thick plate*, Chapter VIII of I.N. Sneddon and R. Hill et. al, *Progress in Solid Mechanics*, Holland Publishing Company, Amsterdam, 1960.
- [35] S. G. MIKHLIN, *Integral Equations*, Pergamon Press, London, 1957.
- [36] L. V. KANTORVICH AND G. P. AKILIOV, *Functional Analysis in Normed Spaces*, Pergamon Press, Oxford, 1964.
- [37] R. SCHINZINGER, P. A. A. LAURA, *Conformal Mapping Methods and Applications*, Dover Publications, Inc, Mineola, New York, 2003.

VITA

Brian George Burns
 Department of Mathematics and Statistics
 Old Dominion University
 Norfolk, VA 23529

Education

2007 - Ph.D. Computational and Applied Mathematics, Old Dominion University
 2005 - M.S. Computational and Applied Mathematics, Old Dominion University
 1999 - M.Sc. Information Systems Management, University of Stirling
 1998 - M.Sci. Honours in the First Class, Mathematics, University of Glasgow

Presentations and Publications

“Solving a Class of Weakly-Singular Integral Equations” -: March 2006, Old Dominion University Math and Stat Club Guest speaker

“Stock Control Management of Burns Pet Nutrition (Scotland)” -: 1999, Masters Thesis for M.Sc. in Information Systems Management, Department of Management & Organization, University of Stirling

Research Interests

- Singular Integral Equations
- Functional Analysis
- Hilbert Space and Operator Theory
- Boundary Value Problems
- Partial Differential Equations
- Potential Theory
- Fracture Mechanics
- Acoustics
- Conformal Mappings
- Numerical Analysis
- Algorithm Development
- Programming
- Operations and Logistics
- Stock Control Management

Typeset using \LaTeX .